

FAULT DIAGNOSIS OF SINGLE POINT CUTTING TOOL THROUGH ONLINE AND OFFLINE MONITORING TECHNIQUES

Thesis

Submitted in partial fulfillment of the requirements for the degree of

DOCTOR OF PHILOSOPHY

by

GANGADHAR N.



DEPARTMENT OF MECHANICAL ENGINEERING
NATIONAL INSTITUTE OF TECHNOLOGY KARNATAKA,
SURATHKAL, MANGALORE – 575025

July, 2016

DECLARATION

I hereby *declare* that the Research Thesis entitled “**FALUT DIAGNOSIS OF SINGLE POINT CUTTING TOOL THROUGH ONLINE AND OF FLINEMONITORING**

TECHNIQUES” which is being submitted to the **National Institute of Technology Karnataka, Surathkal** in partial fulfillment of the requirements for the award of the Degree of **Doctor of Philosophy in Department of Mechanical Engineering** is a bona fide report of the research work carried out by me. The material contained in this Research Thesis has not been submitted to any University or Institution for the award of any degree.

Register Number : **123045ME12FO9**

Name of the Research Scholar : **GANGADHAR N.**

Signature of the Research Scholar :

Department of Mechanical Engineering

Place : **NITK-Surathkal**

Date :

CERTIFICATE

This is to *certify* that the Research Thesis titled “**FALUT DIAGNOSIS OF SINGLE POINT CUTTING TOOL THROUGH ONLINE AND OFFLINE MONITORING TECHNIQUES**” submitted by **Mr. GANGADHARN. (Register Number: 123045ME1 2F09)** as the record of the research work carried out by him, is accepted as the *Research Thesis submission* in partial fulfillment of the requirements for the award of degree of **Doctor of Philosophy.**

Research Guide(s)

Prof. Narendranath S.

Professor

Department of Mechanical Engineering

NITK, Surathkal

Dr. Hemantha Kumar

Assistant Professor

Department of Mechanical Engineering

NITK, Surathkal

Chairman-DRPC

Date:

ACKNOWLEDGEMENTS

With a deep sense of gratitude, I wish to express my sincere thanks to my supervisors **Prof. Narendranath S.** and **Dr. Hemantha Kumar**, Department of Mechanical Engineering, National Institute of Technology Karnataka (N.I.T.K), Surathkal, for their excellent guidance and support throughout the work. I received very useful, encouraging and excellent academic feedback from them, which has stood in good stead while writing this thesis. Their constant encouragement, help and review of the entire work during the course of the investigation were invaluable. I profoundly thank them.

I take this opportunity to thank **Prof. K. V. Gangadharan**, Professor and Head, Department of Mechanical Engineering for his continuous and timely suggestions.

I gratefully acknowledge the help received from **Dr. V. Sugumaran**, Associate Professor, VIT University for making me to understand the advanced concepts of machine learning techniques. I also acknowledge help rendered by **Dr. Umashankar K. S.** Professor, Department of Mechanical Engineering, K V G College of Engineering, Sullia, Karnataka.

I am grateful to **The Managing Trustee**, Panchajanya Vidya Peetha Welfare Trust (R), Dr. A.I.T. Bangalore for permitting me to carry out this research work and extending the support whenever I required it.

I would like to thank **Dr. T. N. Raju**, Associate Professor and **Dr. S. Sathish**, Associate Professor, Department of Mechanical Engineering, Dr. A.I.T. Bangalore, for their kind help and encouragement for successful completion of this research work.

I acknowledge the support from SOLVE: The Virtual Lab @ NITK and experimental facility provided by Centre for System Design (CSD): A Centre of excellence at NITK-Surathkal.

I wish to thank all the members of the Research Program Assessment Committee including **Dr. K. S. Ravishankar**, Assistant Professor, Department of Metallurgical and Materials Engineering and **Dr. M. R. Ramesh**, Assistant professor, Department of Mechanical Engineering for their appreciation and criticism all through this research work.

I wish to express my sincere gratitude to all the faculty members of the Department of Mechanical Engineering, N.I.T.K Surathkal for their help, encouragement and support all through this research work.

I owe my deepest gratitude to Mr. Jaya Davadiga (Senior Technical Assistant), Mr. C. A. Verghese (Technical Assistant) and Mr. Pradeep (Technical Helper), Machine shop, NITK, for permitting me to carry out the experiment work.

My sincere thanks to all mylab mates Dr. Muralidhar A., Dr. M. Manjaiah, Mr. Kiran Vernekar, Mr. Hemanth K., Mr. Madhusudana C. K., Mr. Gurubasavaraju T. M., Mr. J. VipinAlien, Mr. Priyaranjan Sharma, Mr. HargovindSoniand Mr. A.Ganeshafor their help and support to carry out this dissertation work.

I am indebted to myroommates Mr. Nivish George, Mr. V. Shamanth, Mr. Hemanth K., Mr. H. S. Nithin, Mr. Rakesh K Rajan and Mr. H. S. Ashrith for their constant help and encouragement during the entire this research work.

Finally, I would like to thank my parents who have trusted me throughout my life. I would like to share this moment of happiness with my parents, Jayamma S. and Nanjundaiah; my Brothers, Mr. Mukunda, Mr. Sunil Kumar and Mr. Raghavendra for their constant encouragement.

The list goes on and there are many others I should mention. There are people who have helped me all the way and provided me support when I didn't even realize I needed it, or needed it now, or needed it constantly. Listing all of them would fill a book itself, so I merely will have to limit myself to a few words: I THANK YOU ALL.....!

(Gangadhar N.)

ABSTRACT

Tool condition monitoring plays a crucial role in automated industry to monitor the state of cutting tool. It prevents any hazards occurring to the machine, avoid deterioration of the surface finish on end product and it helps to introduce a new tool in an instant at which the existing tool has worn out to ensure safety, productivity and optimum performance of the metal cutting process.

In the present research work, fault diagnosis of single point cutting tool is investigated based on the vibration signals and cutting force signals on an engine lathe. Vibration signals and cutting force signals corresponding to a healthy insert (baseline) and different types of industrial practical worn out inserts were recorded. The research work is carried out in three phases.

The first phase investigates fault diagnosis of cutting tool using signal processing techniques such as time domain, spectrum, cepstrum, continuous wavelet transform (CWT), recurrence plots (RPs) and recurrence quantification analysis (RQA). The result shows that recurrence plots and recurrence quantification analysis were useful for revealing post fault detection and diagnosis of worn states of the inserts.

The second phase of research work presents fault diagnosis of cutting tool using machine learning approach based on vibration signals. From the vibration signals, statistical features, histogram features, discrete wavelet transform (DWT) features and empirical mode decomposition (EMD) features were extracted. Principle component analysis (PCA) and J48 algorithm (decision tree) were used for important feature selection/reduction. Artificial neural network (ANN), Naïve Bayes, Bayes net, support vector machine (SVM), K-star and J48 algorithm classifiers have been used to classify the different fault conditions. Classification accuracy is found to be reasonably good with J48 algorithm feature selection compared to PCA.

The third phase presents the results of investigations undertaken to find suitability of vibration signals and cutting forces to detect the condition of tungsten carbide cutting tool insert, surface roughness and type of chip formation. The results show that there is an increase in the level of acceleration and cutting force at faulty tool condition as

compared with the healthy condition of the tool. Based on this finding, cutting tool acceleration and cutting forces can be used to predict the cutting tool condition, surface roughness and chip formation type. Qualitative comparisons of the computational predicted forces are drawn by plotting the trends of the predicted forces together with the measured forces. The Deform-3D has correctly predicted this trend which is consistent with the experimental trends of the cutting forces components. Tool wear analysis has been carried out on the worn tungsten carbide insert cutting tools to find the tool wear mechanisms. Based on SEM micrographs of worn surface of the cutting tool, micro-abrasion, micro-attrition, adhesion and micro-fatigue behaviors are identified as the dominant kinds of wear mechanisms.

Keywords: *Tool condition monitoring; Recurrence plots; Recurrence quantification analysis; Machine learning approach; Cutting forces; Surface roughness; Chip formation.*

CONTENTS

Page No.

Declaration	
Certificate	
Acknowledgements	
Abstract	
Contents.....	i
List of figures.....	viii
List of tables.....	xii
Abbreviations.....	xv
1. INTRODUCTION.....	1
1.1. OVERVIEW.....	1
1.2. NEED FOR TOOL CONDITION MONITORING SYSTEM.....	1
1.3. SENSORS FOR PROCESS MONITORING.....	2
1.4. APPLICATIONS OF MONITORING SYSTEMS.....	3
1.5. TOOL FAILURE MODES.....	3
1.5.1. Flank wear.....	4
1.5.2. Crater wear.....	4
1.5.3. Notch wear.....	5
1.5.4. Chipping.....	5
1.5.5. Thermal cracks.....	5
1.5.6. Breakage.....	5
1.6. TOOL CONDITION MONITORING TECHNIQUES.....	5
1.6.1. Vibration signal based condition monitoring.....	6
1.7. OFFLINE TOOL WEAR MONITORING.....	7
1.7.1. Signal processing techniques.....	7
1.7.2. Cutting forces analysis.....	8
1.7.3. Surface roughness analysis.....	8
1.7.4. Chip morphology studies.....	8

1.7.5. Computational approach.....	8
1.8. ONLINE TOOL WEAR MONITORING.....	9
1.8.1. Machine learning approach.....	9
1.9. SALIENT FEATURES OF THE PRESENT WORK.....	10
1.10. THESIS OUTLINE.....	11
2. LITERATURE REVIEW.....	13
2.1. INTRODUCTION.....	13
2.2. SENSORS USED IN TOOL CONDITION MONITORING SYSTEMS...	13
2.3. TOOL CONDITION MONITORING TECHNIQUES.....	14
2.3.1. Direct condition monitoring methods.....	15
2.3.2. Indirect condition monitoring methods.....	16
2.3.2.1. Tool tip temperature.....	16
2.3.2.2. Acoustic emission technique.....	18
2.3.2.3. Cutting forces.....	19
2.3.2.4. Vibrational analysis.....	23
2.3.2.5. Ultrasonic methods.....	24
2.3.2.6. Spindle motor current.....	25
2.4. ONLINE AND OFFLINE MONITORING TECHNIQUES.....	25
2.4.1. Online monitoring using machine learning approach.....	26
2.4.1.1. Feature extraction methods.....	26
2.4.1.1.1. Statistical features.....	26
2.4.1.1.2. Histogram features.....	27
2.4.1.1.3. Discrete wavelet transform (DWT) features.....	27
2.4.1.1.4. Empirical mode decomposition (EMD) features...	27
2.4.1.2. Feature reduction algorithm.....	29
2.4.1.2.1. Decision tree technique.....	29
2.4.1.2.2. Principle component analysis.....	29
2.4.1.3. Feature classification.....	30
2.4.1.3.1. Support vector machine.....	30
2.4.1.3.2. Artificial neural network (ANN).....	30
2.4.1.3.3. Decision tree algorithm.....	31

2.4.1.3.4. Naive Bayes algorithm.....	32
2.4.2. Offline tool monitoring techniques.....	32
2.4.2.1. Signal processing techniques.....	32
2.4.2.1.1. Time domain analysis.....	33
2.4.2.1.2. Spectrum analysis.....	33
2.4.2.1.3. Cepstrum analysis.....	33
2.4.2.1.4. Wavelet analysis.....	34
2.4.2.1.5. Recurrence quantification analysis.....	34
2.4.2.2. Tribological studies.....	36
2.4.2.2.1. Tool wear analysis.....	39
2.4.2.2.2. Chip formation mechanism.....	41
2.4.2.2.3. Surface roughness analysis.....	42
2.4.2.2.3.1. Surface roughness and tool wear.....	43
2.4.2.2.3.2. Vibration monitoring and surface roughness.....	44
2.5. MODEL BASED APPROACH.....	45
2.5.1. Mathematical model based approach.....	45
2.5.2. Computational model based approach.....	46
2.6. MOTIVATION FROM LITERATURE REVIEW.....	47
2.7. SCOPE OF THE RESEARCH WORK.....	48
2.8. OBJECTIVES OF THE RESEARCH WORK.....	50
2.9. SUMMARY.....	50
3. EXPERIMENTAL APPROACH AND METHODOLOGY.....	51
3.1. INTRODUCTION.....	51
3.2. EXPERIMENTAL SETUP.....	51
3.2.1. Work material.....	53
3.2.2. Tool material.....	53
3.3. DATA ACQUISITION USING LAB-VIEW.....	54
3.3.1. Sensors used in the experiments.....	54
3.3.1.1. Accelerometer.....	54
3.3.1.2. Lathe tool dynamometer.....	55
3.3.2. NI-DAQ system.....	56

3.3.3. Software interface.....	57
3.4. EXPERIMENTAL PROCEDURE.....	58
3.5. METHODOLOGY.....	59
3.5.1. Online monitoring.....	60
3.5.1.1. Vibration measurement setup.....	60
3.5.1.2. Data acquisition.....	60
3.5.1.3. Feature extraction.....	61
3.5.1.4. Feature selection / reduction.....	61
3.5.1.5. Fault classification.....	61
3.5.2. Offline monitoring.....	62
3.5.2.1. Vibration and cutting forces measurement.....	62
3.5.2.2. Data acquisition.....	62
3.5.2.3. Signal processing techniques.....	63
3.5.2.4. Cutting forces analysis.....	63
3.5.2.5. Machining process simulation with finite element method...	63
3.5.2.6. Surface roughness measurement of workpiece.....	63
3.5.2.7. Chip morphology studies.....	64
3.5.2.8. Tool wear analysis.....	64
3.6. SUMMARY.....	64
4. FAULT DIAGNOSIS USING SIGNAL PROCESSING TECHNIQUES...	65
4.1. INTRODUCTION.....	65
4.2. TIME AND FREQUENCY DOMAIN ANALYSIS.....	65
4.3. CEPSTRUM ANALYSIS.....	68
4.4. WAVELET ANALYSIS.....	70
4.4.1. Continuous wavelet transform.....	71
4.5. DEMERITS OF SPECTRUM, CEPSTRUM AND WAVELET ANALYSIS.....	73
4.6. RECURRENCE QUANTIFICATION ANALYSIS.....	74
4.6.1. Recurrence plot (RP).....	75
4.6.2. Recurrence quantification analysis parameters.....	77
4.6.3. Qualitative investigation.....	82
4.6.4. Quantitative investigation.....	83

4.6.4.1. Influence of different tool conditions on RQA parameters...	84
4.7. SUMMARY.....	86
5. FAULT DIAGNOSIS USING MACHINE LEARNING TECHNIQUE...	87
5.1. INTRODUCTION.....	87
5.2. NEED FOR MACHINE LEARNING TECHNIQUES.....	87
5.3. MACHINE LEARNING APPROACH.....	88
5.4. FEATURE EXTRACTION.....	90
5.4.1. Statistical features.....	90
5.4.2. Histogram features.....	92
5.4.3. Discrete wavelet transform features.....	94
5.4.4. Empirical mode decomposition features.....	97
5.5. FEATURE SELECTION.....	99
5.5.1. Principal component analysis (PCA).....	99
5.5.2. Decision tree technique.....	100
5.5.2.1. Information gain and entropy reduction.....	101
5.6. FAULT CLASSIFICATION METHODS.....	102
5.6.1. Artificial neural network.....	102
5.6.1.1. Multi-layer perceptron (MLP).....	104
5.6.2. Naive Bayes classifier.....	106
5.6.3. Bayes net algorithm.....	107
5.6.4. Support vector machine.....	107
5.6.5. K-star algorithm.....	109
5.7. RESULTS AND DISCUSSIONS.....	109
5.7.1. Classification based on statistical features.....	109
5.7.2. Feature selection (Statistical features).....	111
5.7.2.1. Principal component analysis (PCA).....	111
5.7.2.2. Decision tree (J48 algorithm).....	112
5.7.2.2.1. Features suggested by J48 algorithm.....	112
5.7.3. Classification.....	114
5.7.3.1. Artificial neural network.....	114
5.7.3.2. Naïve Bayes algorithm.....	115
5.7.3.3. Bayes net algorithm.....	116

5.7.3.4. Support vector machine.....	117
5.7.3.5. K-star algorithm.....	118
5.7.3.6. J48 algorithm.....	118
5.7.4. Classification with discrete wavelet features.....	120
5.7.5. Feature selection (DWT features).....	121
5.7.6. Classification.....	122
5.7.6.1. Artificial neural network.....	122
5.7.6.2. Naïve Bayes algorithm.....	123
5.7.6.3. Bayes net algorithm.....	123
5.7.6.4. Support vector machine.....	124
5.7.6.5. K-star algorithm.....	125
5.7.6.6. J48 algorithm.....	126
5.7.7. Classification with EMD features.....	127
5.7.8. Feature selection (EMD features).....	132
5.7.9. Classification.....	133
5.7.9.1. Artificial neural network.....	133
5.7.9.2. Naïve Bayes algorithm.....	134
5.7.9.3. Bayes net algorithm.....	134
5.7.9.4. Support vector machine.....	135
5.7.9.5. K-star algorithm.....	136
5.7.9.6. J48 algorithm.....	137
5.7.10. Classification with histogram features.....	138
5.7.11. Feature selection (histogram features).....	141
5.7.12. Classification.....	141
5.7.12.1. Artificial neural network.....	141
5.7.12.2. Naïve Bayes algorithm.....	142
5.7.12.3. Bayes net algorithm.....	143
5.7.12.4. Support vector machine.....	144
5.7.12.5. K-star algorithm.....	144
5.7.12.6. J48 algorithm.....	145
5.8. SUMMARY.....	148

6. ANALYSIS OF CUTTING FORCES, SURFACE ROUGHNESS, CHIP MORPHOLOGY AND COMPUTATIONAL APPROACH FOR FAULT DIAGNOSIS OF CUTTING TOOL.....	149
6.1. INTRODUCTION.....	149
6.2. CUTTING FORCES ANALYSIS.....	149
6.2.1. Experimental approach.....	150
6.2.2. Computational approach.....	155
6.2.3. Validation of computational cutting forces.....	156
6.2.4. Effect of depth of cut on cutting forces.....	157
6.2.5. Effect of cutting speed on cutting forces.....	158
6.3. SURFACE ROUGHNESS (Ra) ANALYSIS.....	160
6.3.1. Surface roughness (Ra) and vibration signal (RMS).....	160
6.3.1.1. Surface roughness (Ra).....	161
6.3.1.2. Vibration signal (RMS).....	163
6.4. CHIP MORPHOLOGY STUDIES.....	165
6.4.1. Chip morphology.....	165
6.5. SEM micrographs of tool wear.....	168
6.6. SUMMARY.....	172
7. CONCLUSION AND SCOPE FOR FUTURE WORK	173
7.1. CONCLUSION.....	173
7.2. SCOPE FOR FUTURE WORK.....	175
7.3. KEY CONTRIBUTIONS.....	175
REFERENCES.....	177

TECHNICAL PAPERS PUBLISHED

BIODATA

LIST OF FIGURES

Figure No.	Description	Page No.
Figure 1.1	Different tool failure modes (a-c)	4
Figure 2.1	Reconfigurable multi-sensor monitoring systems	14
Figure 2.2	Temperature measurements in machining	17
Figure 2.3	Cutting force components on a single point cutting tool during turning	20
Figure 2.4	Cutting force (a) and feed force (b) as functions of cutting speed	21
Figure 2.5	Depth of crater as a function of cutting speed	22
Figure 2.6	Cutting forces vs. flank wear surface area	22
Figure 2.7	Prototype of the implemented FPGA-based system	24
Figure 2.8	Recurrence plots of the MIP time series for different speeds (a-f) (n = 1000, 1200, 1400, 1600, 1800 and 2000 rpm)	36
Figure 2.9	SEM image of the flank and crater wear of cutting tool	38
Figure 2.10	Profile of cutting edge. (a) Catastrophic wear viewed from rake face, (b) tip breakage	39
Figure 2.11	SEM micrograph of the free face of chip	39
Figure 2.12	Ridges imprinted on (a) the chip surface by (b) the fracture wear of cutting edge	40
Figure 2.13	Different types of chip formation	41
Figure 2.14	(a) Stable chips, (b) chatter chips, (c) critical chips and (d) severe chips under different cutting conditions	42
Figure 3.1	Schematic line diagram of experimental setup	52
Figure 3.2	Condition monitoring test setup	52

Figure 3.3	Piezoelectric triaxial accelerometer	54
Figure 3.4	Experimental configurations for measuring the components of cutting force	55
Figure 3.5	NI USB-9234 with NI USB carrier	56
Figure 3.6	VI Block diagram for the data acquisition	57
Figure 3.7	Front panel to represent the acquired data	57
Figure 3.8	Five different tungsten carbide tool insert tip conditions	59
Figure 3.9	Online tool condition monitoring using machine learning approach	60
Figure 3.10	Fault diagnosis of cutting tool through offline monitoring techniques	62
Figure 4.1	Acceleration with healthy and faulty cutting tool inserts in time domain (a-e) and (i) to (v) represents corresponding spectrum	67
Figure 4.2	Relationship between spectrum and cepstrum	69
Figure 4.3	Vibration responses in quefreny-domain for different tool conditions (a-e)	70
Figure 4.4	CWT plots for different tool conditions (a-e)	73
Figure 4.5	Nonlinear recurrence quantification analysis	75
Figure 4.6	AMI plot for healthy insert condition	80
Figure 4.7	FNN plot for healthy insert condition	81
Figure 4.8	Recurrence plots for different conditions of tool (a-e)	83
Figure 5.1	Flow chart of fault diagnosis of cutting tool with machine learning approach	89
Figure 5.2	Sample histogram of a rectangular distribution	93
Figure 5.3	Histogram of signals	94
Figure 5.4	Wavelet decomposition tree	97

Figure 5.5	PCA visualization	100
Figure 5.6	Artificial neuron used in the neural network	103
Figure 5.7	Multi-layer network	103
Figure 5.8	Histogram of a hypothetical two-class problem	106
Figure 5.9	Illustration of support vector machine classifier	108
Figure 5.10	Decision tree for statistical features	113
Figure 5.11	Classification efficiencies of different classifiers for statistical features	119
Figure 5.12	Decision tree for DWT features	121
Figure 5.13	Classification efficiencies of different classifiers for DWT features	127
Figure 5.14	Intrinsic mode functions of cutting tool vibration signal with a healthy insert	129
Figure 5.15	Intrinsic mode functions of breakage and thermally cracked tool insert	130
Figure 5.16	Intrinsic mode functions of notch wear and rake face chipping tool insert	131
Figure 5.17	Decision tree for EMD features	132
Figure 5.18	Classification efficiencies of different classifiers for EMD features	138
Figure 5.19	Decision tree for histogram features	140
Figure 5.20	Classification efficiencies of different classifiers for histogram features	146
Figure 6.1	Influence of the cutting speed on the thrust force (F_y) for depth of cut ' d ' = 0.1 mm	150

Figure 6.2	Influence of the cutting speed on the cutting force (F_z) for depth of cut ' d ' = 0.1 mm	151
Figure 6.3	Influence of the depth of cut on the thrust force (F_y) for cutting speed ' v ' = 236 m/min	152
Figure 6.4	Influence of the depth of cut on the cutting force (F_z) for cutting speed ' v ' = 236 m/min	153
Figure 6.5	Basic components of turning and relation to analysis domain	155
Figure 6.6	Simulation model and basic cutting parameters	156
Figure 6.7	Predicted and experimental thrust force (F_y) vs. depth of cut	157
Figure 6.8	Predicted and experimental cutting force (F_z) vs. depth of cut	158
Figure 6.9	Predicted and experimental thrust force (F_y) vs. cutting speed	159
Figure 6.10	Predicted and experimental cutting force (F_z) vs. cutting speed	159
Figure 6.11	Effect of tool condition on surface roughness of the workpiece	161
Figure 6.12	Fluctuation of vibration signal (RMS) components at different tool conditions	163
Figure 6.13	Variation in surface roughness of workpiece and vibration signal (RMS) component ' a_y ' at different tool conditions	164
Figure 6.14	SEM micrographs of healthy insert and different worn out inserts (a-e) after machining AISI H13 steel (die steel) under dry condition	169
Figure 6.15	SEM image showing (a) edge chipping (b) micro-thermal cracks	170
Figure 6.16	SEM image showing (a) adhesion (b) micro-abrasion	171
Figure 6.17	SEM image showing (a) micro-thermal-fatigue. (b) micro-attrition	171

LIST OF TABLES

Table No.	Description	Page No.
Table 3.1	Physical and mechanical properties of AISI H13 steel	53
Table 3.2	Chemical compositions of the work material	53
Table 3.3	Physical and mechanical properties of the tungsten carbide tool insert	54
Table 3.4	Specification of the accelerometer	55
Table 3.5	Specification of NI USB-9234	56
Table 3.6	Experimental parameters	58
Table 4.1	Embedding dimension, time delay and threshold radius	81
Table 4.2	RQA analysis for different tool conditions	84
Table 5.1	Extracted statistical features	110
Table 5.2	ANN results with statistical features	114
Table 5.3	Confusion matrix of ANN with statistical features	114
Table 5.4	Naive Bayes algorithm results with statistical features	115
Table 5.5	Confusion matrix of Naive Bayes algorithm with statistical features	116
Table 5.6	Bayes net algorithm results with statistical features	116
Table 5.7	Confusion matrix of Bayes net algorithm with statistical features	116
Table 5.8	SVM results with statistical features	117
Table 5.9	Confusion matrix of SVM with statistical features	117
Table 5.10	K-star algorithm results with statistical features	118
Table 5.11	Confusion matrix of K-star algorithm with statistical features	118
Table 5.12	J48 algorithm results with statistical features	119

Table 5.13	Confusion matrix of J48 algorithm with statistical features	119
Table 5.14	Extracted features using DWT method	120
Table 5.15	ANN results with DWT features	122
Table 5.16	Confusion matrix of ANN with DWT features	122
Table 5.17	Naive Bayes algorithm results with DWT features	123
Table 5.18	Confusion matrix of Naive Bayes algorithm with DWT features	123
Table 5.19	Bayes net algorithm results with DWT features	124
Table 5.20	Confusion matrix of Bayes net algorithm with DWT features	124
Table 5.21	SVM results with DWT features	124
Table 5.22	Confusion matrix of SVM with DWT features	125
Table 5.23	K-star algorithm results with DWT features	125
Table 5.24	Confusion matrix of K-star algorithm with DWT features	126
Table 5.25	J48 algorithm results with DWT features	126
Table 5.26	Confusion matrix of J48 algorithm with DWT features	126
Table 5.27	Feature vector based on EMD method	128
Table 5.28	ANN results with EMD features	133
Table 5.29	Confusion matrix of ANN with EMD features	133
Table 5.30	Naive Bayes algorithm results with EMD features	134
Table 5.31	Confusion matrix of Naive Bayes algorithm with EMD features	134
Table 5.32	Bayes net algorithm results with EMD features	135
Table 5.33	Confusion matrix of Bayes net algorithm with EMD features	135
Table 5.34	SVM results with EMD features	135
Table 5.35	Confusion matrix of SVM with EMD features	136
Table 5.36	K-star algorithm results with EMD features	136

Table 5.37	Confusion matrix of K-star algorithm with EMD features	136
Table 5.38	J48 algorithm results with EMD features	137
Table 5.39	Confusion matrix of J48 algorithm with EMD features	137
Table 5.40	Histogram features extracted from vibration signals for different tool conditions	139
Table 5.41	ANN results with histogram features	142
Table 5.42	Confusion matrix of ANN with histogram features	142
Table 5.43	Naive Bayes algorithm results with histogram features	142
Table 5.44	Confusion matrix of Naive Bayes algorithm with histogram features	143
Table 5.45	Bayes net algorithm results with histogram features	143
Table 5.46	Confusion matrix of Bayes net algorithm with histogram features	143
Table 5.47	SVM results with histogram features	144
Table 5.48	Confusion matrix of SVM with histogram features	144
Table 5.49	K-star algorithm results with histogram features	145
Table 5.50	Confusion matrix of K-star algorithm with histogram features	145
Table 5.51	J48 algorithm results with histogram features	145
Table 5.52	Confusion matrix of J48 algorithm with histogram features	146
Table 5.53	Summary of classification accuracies	147
Table 6.1	Influence of the depth of cut and cutting speed on the cutting forces for different tool conditions	154
Table 6.2	Surface roughness (R_a), a_x , a_y , and a_z for different tool conditions	160
Table 6.3	Chips formed while machining at different tool conditions	166

ABBREVIATIONS

AE	: Acoustic emission
AISI	: American iron and steel institute
AMI	: Average mutual information
ANN	: Artificial neural network
ANOVA	: Analysis of variance
AR	: Autoregressive
ART	: Adaptive resonance theory
BNC	: Bayonet Neill–Concelman
BPNN	: Back propagation neural network
BSS	: Blind source separation
BUE	: Built-up-edge
CAD	: Computer aided drafting
CBM	: Condition based maintenance
CBN	: Cubic boron nitride
CCD	: Charge coupled device
CNC	: Computerized numerical control
CWT	: Continuous wavelet transform
DAG	: Directed acyclic graph
DAQ	: Data acquisition system
DET	: Percent determinism
DFT	: Discrete Fourier transform
DHMM	: Discrete hidden Markov model
DOF	: Degree of freedom
DWT	: Discrete wavelet transform
EBP	: Error back propagation
EDS	: Energy dispersive spectrometer
EDX	: Energy-dispersive X-ray spectroscopy
EEMD	: Ensemble empirical mode decomposition
EMD	: Empirical mode decomposition

EMF	: Electro motive force
ENT	: Entropy
FE	: Finite element
FEA	: Finite element analysis
FEM	: Finite element method
FFT	: Fast Fourier transform
FL	: Fuzzy logic
FNN	: False nearest neighbors
FP	: False positive
FPGA	: Field-programmable gate array
FRFT	: Fractional Fourier transform
FT	: Fourier transform
GA	: Genetic algorithm
GFRP	: Glass fiber-reinforced polymers
HHT	: Hilbert–Huang transform
HMMs	: Hidden Markov models
HR	: Hot rolled
HRC	: Rockwell hardness
HSM	: High-speed machining
HSS	: High speed steel
HSV	: Hue saturation value
HT	: Hard turning
ICA	: Independent component analysis
IGES	: Initial graphical exchange specification
IIR	: Infinite impulse response
I-kaz	: Integrated kurtosis based algorithm for Z filter technique
IMF	: Intrinsic mode function
IP	: Internet protocol
JIS	: Japanese industrial standard
LabVIEW	: Laboratory virtual instrumentation engineering workbench
LAM	: Percent laminarity

LR	: Linear regression
MATLAB	: Matrix laboratory
MIP	: Mean indicated pressure
MMC	: Metal matrix composites
MSE	: Mean square error
MVC	: Minimum variance cepstrum
NI	: National instruments
OM	: Optical microscope
PCA	: Principal component analysis
PSO	: Particle swarm optimization
PSVM	: Proximal support vector machine
REC	: Percent recurrence
RMS	: Root mean square
RP	: Recurrence plot
RQA	: Recurrence quantification analysis
SAW	: Surface acoustic wave
SEM	: Scanning electron microscope
SLP	: Single layer perceptron
SOM	: Self-organizing map
SRS	: Surface roughness and straightness
STFT	: Short-time Fourier transforms
SVC	: Support vector classifier
SVM	: Support vector machine
TCM	: Tool condition monitoring
TCMS	: Tool condition monitoring system
TiC	: Titanium carbide
TiCN	: Titanium carbo nitride
TiN	: Titanium nitride
TP	: True positive
TT	: Trapping time
TV	: Television

UHP	: Ultra-high pressure
UPRM	: Ultra-precision raster milling
USB	: Universal serial bus
VI	: Virtual instrumentation
VRA	: Visual recurrence analysis
WC	: Tungsten carbide
WPD	: Wavelet packet decomposition
WT	: Wavelet transform

CHAPTER 1

INTRODUCTION

1.1 OVERVIEW

Modern manufacturing industries are aiming to produce components at lower cost and at a higher production rate with less manpower, therefore automation has been introduced in manufacturing systems (Groover 2007). Tool condition monitoring system (TCMS) is one of the main element of automated manufacturing systems. To monitor the cutting edge of the tool used in the machine tool, the replacement of the healthy tool with worn out/defect tool will prevent the occurrence of the damage to the work surface. Hence it reduces waste, reduction in idle time and increased productivity. Tool wear is the major cause of increase in cutting force and vibration levels in the cutting tool, which results in poor surface quality. Before tool cutting edge fails, a cutting tool must be replaced or grounded for the prevention of further damage in production. This is directly have an effect on productivity and monitoring of cutting tool wear and thus it is of great importance for better manufacturing.

1.2 NEED FOR TOOL CONDITION MONITORING SYSTEM

The need for monitoring in machining process includes monitoring the machine as well as cutting process dynamics, workpiece and cutting tools to ensure optimum performance of the cutting process. The lack of TCMS may leads to excessive power consumption, inaccurate tolerances, serrations, poor surface finish and finally leading to machine peripheral damage or machine tool damage incurring additional costs. Automated tool condition monitoring system improves overall product quality, reduces defects and also results in increased productivity. The failure of cutting tool causes severe loss in terms of defective products, labor cost, problems with inventory, cost associated with the downtime etc. Thus automated tool condition monitoring system prevents abrupt failure of the cutting tool and ensures the better product with in time. This can be achieved by adopting the sensor technologies with in the machine tool (Saglam and Unuvar 2003; Ertunc et al. 2001).

1.3 SENSORS FOR PROCESS MONITORING

A wide variety of sensors for process monitoring are available today. The most common sensors using in the industry are listed as below (Pfeifer and Thrum 1996):

- Flame detector
- Smoke sensor
- Sound level sensor
- Image sensor
- Lubrication oil detector
- Temperature sensor
- Touch sensor
- Tool wear sensor
- Edge position sensor
- Accelerometer (vibration)
- Limit sensor
- Seismic sensor
- Clamping force sensor
- Tool damage sensor
- Speed sensor
- Current sensor
- Torque sensor
- Acoustic emission (AE) sensor
- pH sensor
- Machined surface roughness sensor
- Level meter
- Coolant temperature sensor
- Thermal distribution sensor
- Chip monitoring sensor
- Temperature distribution sensor
- Dust sensor
- Humidity sensor
- Pressure sensor
- CO₂ gas sensor
- Cutting tool dynamometer

These sensors and many more have found their rightful place in the manufacturing industry. Most of them are only used for a specific monitoring objective. The focus of monitoring may fall on one or more of the following areas:

1. The machine (diagnostics and performance).
2. The tools for machining (wear, lubrication and alignment).
3. Workpiece (surface roughness, tolerance, geometry).
4. Process (chip formation, energy consumption, temperature).

The development of smart sensor technology also presents new and exciting developments for the manufacturing industry. With smart sensors, the time needed for signal processing is reduced significantly, thus enabling faster response for an on-line control scheme. These sensors can also possess abilities such as self-calibration, self-

diagnostics, signal conditioning and decision making. This development, together with sophisticated signal processing software, makes measurements accurate, inexpensive and fast in the manufacturing systems.

1.4 APPLICATIONS OF MONITORING SYSTEMS

Applications of tool wear and surface roughness monitoring systems are found in a wide range of modern manufacturing industries. The online monitoring of tool wear allows timely tool replacement with minimum down time. Applications of condition monitoring system found in the following, they are:

- The automotive industry.
- Manufacturing of machine components.
- Mass production of household items.
- Computerized numerical control (CNC) machining optimization.
- Electrical / Mechanical product manufacture.

Byrne et al. (1995) shown that monitoring systems are most often used in turning, drilling, milling and grinding. They also suggested 100% reliability cannot be expected in any of the monitoring system. Further, they found that in most cases the demand for monitoring scheme is to monitor tool breakage, tool wear and collision. They concluded that reliable operation of the manufacturing process is more important than quality monitoring.

1.5 TOOL FAILURE MODES

It is important to identify the different tool failure modes in order to select appropriate operating conditions for machining. The most widely studied tool failure modes are flank wear, breakage (fracture), crater wear and plastic deformation (Lever et al. 1997). Only a few researchers reported tool failure because of notching (groove wear), cracking and chipping. Notching and chipping changes the tool nose curvature. Figure 1.1, shows the tool failure modes, as depicted by Rao et al. (1986). Flank and crater wear are generally accepted as the normal tool failure modes, because the other failure modes can be avoided by selecting the proper machining parameters. The growth of flank and crater wear are directly related to the cutting time (or length of

cut), unlike some of the other failure modes such as notching (groove wear), cracking and chipping which can occur unexpectedly, even with a new tool.

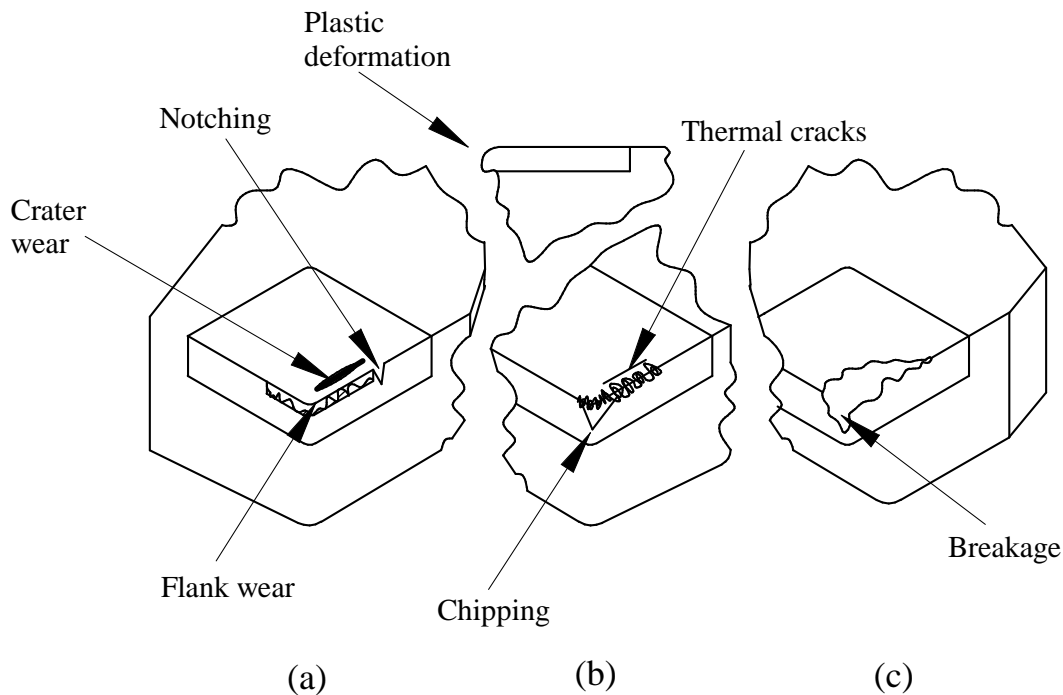


Figure 1.1 Different tool failure modes (a-c) (Rao et al. 1986)

1.5.1 Flank wear

Flank wear is mainly caused by the friction between the newly machined work piece surface and the tool flank face. Flank wear is marked on the cutting tool and it is shown in figure 1.1 (a). It is responsible for a poor surface finish, a decrease in the dimension accuracy of the tool and an increase in cutting force, temperature and vibration. Hence the width of the flank wear land is usually taken as a measure of the amount of wear and a threshold value of the width is defined as tool reshape criterion.

1.5.2 Crater wear

Crater wear normally forms on rake face. It conforms to the shape of the chip underside and reaches the maximum depth at a distance away from the cutting edge, where highest temperature occurs. At high cutting speed, crater wear is the main factor that determines the life of the cutting tool, due to weakened tool edge which results in severe cratering and eventually fractures. Crater wear is improved by

selecting suitable cutting parameters and using coated tool or ultra-hard material tool. Crater wear and flank wear shown in figure 1.1 (a) and they are the most common wear types.

1.5.3 Notch wear

Notch wear is a single groove formation that occurs simultaneously on the face and flank of the tool at the depth of cut. Machining parts with severe (hard or oxidized) surfaces will cause notch wear. Figure 1.1 (a) shows the depth of cut notch wear.

1.5.4 Chipping

Figure 1.1 (b) shows the chipping on cutting edge. Chipping is the result of an overload of mechanical tensile stresses. These stresses can be due to a number of reasons, such as chip hammering, depth of cut or high feed rate, sand inclusions in the workpiece material, built-up edge, vibrations or excessive wear on the insert.

1.5.5 Thermal cracks

Thermal cracks appear on the rake face that is perpendicular to the cutting edge as shown in figure 1.1 (b). Thermal cracking occurs when inserts go through rapid heating and cooling cycles. This failure mode is caused by interrupted cutting and poor application of cutting fluids.

1.5.6 Breakage

Breakage is a mode of failure characterized by breakaway of material on the tool edge. Breakage occurs when the feed-rate is too high, or when a tool is used with too low fracture strength. The usual pattern or geometry of wear of turning inserts is typically shown in figure 1.1 (c).

1.6 TOOL CONDITION MONITORING TECHNIQUES

The primary concern in automated machining system is to recognize irregularities in the cutting process. The implemented system must identify the abnormalities before tool failure arises. Therefore, a suitable monitoring technique must be chosen to fulfill these requirements. The monitoring techniques are divided into two categories, direct

and indirect. These categories are defined by the different approaches applied in their measuring methods. The tool condition monitoring techniques that various researchers have studied are.

- Acoustic emission technique
- Tool temperature monitoring
- Cutting force analysis
- Vibration signal based condition monitoring
- Vision based (Direct method) monitoring

1.6.1 Vibration signal based condition monitoring

The fault diagnosis is a significant process in condition based maintenance that involves two steps, data acquisition and its technical interpretation. The fault can be diagnosed by continuously or periodically recording the variables for further processing, analyzing and then interpreting the results. Tracking the amount of change and rate of change of measured or calculated variables reveals the faulty condition of the cutting tool. Vibration monitoring, cutting force, acoustic emission, wear debris analysis, infrared thermography, ultrasonic monitoring etc. are some of the fault diagnosis techniques currently used in the industry. Each technique has its own advantages and it can be used in various industrial applications. Among this, vibration and cutting force monitoring is extensively used as a successful technique in identification of faults in the cutting tool (Sakthivel et al. 2010).

In modern tool condition monitoring techniques one of the most important and being informative is the vibration signal based monitoring. Vibration generated from the cutting tool contains vital information of the cutting tool state and it can be used to identify developing problems. Regular vibration monitoring can help to detect deterioration or defective tools. Based on literature review almost 70% of real time applications of tool condition monitoring system are based on vibration signal driven systems. Majority of tool condition monitoring systems can be classified as

- Offline monitoring techniques
- Online monitoring techniques

1.7 OFFLINE TOOL WEAR MONITORING

Offline tool wear monitoring pertains to providing information on the condition of cutting tool so that worn out cutting tool can be replaced or changed properly. By having such knowledge of cutting tool condition, one can predict failures and stop the machining operation for maintenance in a planned manner.

1.7.1 Signal processing techniques

Vibrations are produced by cyclic variation in the dynamic components of the cutting forces. Mechanical vibrations generally results from periodic wave motions. The nature of the vibration signal arising from the metal cutting process is such that it incorporates facets of free, forced, periodic and random types of vibration. Direct measurement of vibration is difficult to achieve. Because of its determining characteristic feature, the vibration mode is frequency dependent. Hence, related parameters such as the rate at which dynamic force changes per unit time (acceleration) are measured and the characteristics of the vibrations are derived from the vibration patterns obtained. Each component has its own frequency which can be determined from its dimensions, rotating speed etc. With the help of components character frequency, faulty conditions can be identified. This type of vibration analysis is called as frequency domain or spectral analysis which relates frequency to its components and is widely used as basic approach. Here the acquired time domain signal is transformed into frequency domain signal using fast Fourier transform (FFT) (Jardine et al. 2006). Cepstral analysis can be used to find addition fault diagnostic information in quefrequency domain. Further wavelet analysis will be able to provide information regarding fault condition in time-frequency domain. But turning operation mostly generates a highly non-stationary and complex vibration signature for which the spectral analysis approach is not very useful. To overcome this shortcoming, fault diagnosis can be automated using pattern recognition techniques (online monitoring using machine learning method). The technique of recurrence plot (RP) and recurrence quantification analysis (RQA) is well suited for the analysis of nonlinear and chaotic systems and can basically be used for signal processing without

denoising. The technique reveals lot of information hidden in the time series data from a dynamic system about the system characterization.

1.7.2 Cutting forces analysis

Systems based on cutting forces measurement are seen as promising option for tool condition monitoring due to their non-intrusive nature in process measurement capabilities. Also force measurements are easily attainable and reliable. Generally, cutting force signals in the turning process correlate well with the tool wear. In continuous turning operations, cutting force measurement yield the best performance because of the constant principle cutting force applied to the work material (Gupta and Gill 2012; Fnides et al. 2011).

1.7.3 Surface roughness analysis

Surface roughness is a widely used index of product quality and in most cases a technical requirement for mechanical products (Benardos and Vosniakos 2003). In the field of manufacturing, degree of roughness can be of considerable importance affecting the functioning of a component and its cost. Therefore, it is important to predict surface roughness. It may be possible to use contact vibration as a means for assessing or monitoring surface roughness parameters (Abouelatta and Madl 2001).

1.7.4 Chip morphology studies

The purpose of metal cutting with machine tool is the generation of a new surface having a required geometry. However, the metal cutting process is actually a process of chip formation, in which almost all of the cutting energy is consumed for chip formation and most of the information for the evaluation of cutting process such as surface finish, cutting temperature, tool life and cutting forces are closely related to the chip morphology (Kovac and Sidjanin 1997).

1.7.5 Computational approach

This is one of the model based tool condition monitoring technique. Finite element method (FEM) has been successfully applied to simulate various cutting processes

(Ceretti et al. 1996; Jawahir et al. 1998). It has been shown that the FEM machining simulation can be used to estimate the process variables that are not directly measurable or very difficult to measure during a cutting operation, such as normal stress and temperature on the tool face, chip temperature, and chip sliding velocity along the tool rake face. The knowledge of these process variables provides a better understanding of the fundamental cutting mechanics and enables the engineering analysis of tool wear.

1.8 ONLINE TOOL WEAR MONITORING

The monitoring of cutting tool wear is a more complex phenomenon than expected, because tool wear induces very small changes in the process with a very wide dynamic range. Furthermore, it is difficult to identify whether a change in a signal is caused by tool wear or a change in the cutting conditions. The task of tool wear monitoring can be subdivided into a number of stages (Silva et al. 1998):

- Sensor selection and deployment.
- Generation of a set of features indicative of tool condition.
- Classification of the collected and processed information as to determine the amount of tool wear.

It is necessary to detect the cutting tool condition to avoid poor surface finish, productivity loss and to reduce the maintenance cost. So monitoring the cutting tool and timely identification of the faulty cutting tool, for maintenance decision making is significant in the industrial era. This type of maintenance strategy is called condition based maintenance (CBM) or predictive maintenance. This strategy has emerged over recent years as an important technology in maintenance practices.

1.8.1 Machine learning approach

Machine learning method is used to recognize the signal pattern or the corresponding fault using the classification process. Automatic fault diagnosis system can be achieved by the machine learning process (Saimurugan et al. 2011; Vernekar et al. 2014). The fault identification using machine learning techniques has three phases. They are feature extraction, feature selection/reduction and feature classification. In feature extraction, statistical features, histogram features, discrete wavelet transform

(DWT) features and empirical mode decomposition (EMD) features are extracted from the collected vibration signals.

Feature reduction and feature selection are the two types of data reduction techniques. The existing features are transformed into higher dimensional space in the feature reduction techniques. In the feature selection technique, a subset of the existing features is selected without any transformation. The principal component analysis and independent component analysis are feature reduction techniques and decision tree is a feature selection technique. Machine learning process has two stages in the third phase. In the first stage, the classification algorithm is trained with the help of selected features from the training data of various fault signals. In the second stage, the trained algorithm is tested with the help of selected features from the test data. The classification phase identifies the faulty cutting tool (Widodo and Yang 2007).

Extensive research work has been carried out to identify the capability of machine learning methods to perform fault diagnosis (Ravikumar et al. 2011; Jegadeeshwaran and Sugumaran 2013). Most of works have considered one or two cutting tool fault conditions. The number of fault classes depends on the number of cutting tools and its faults. It is essential to check the classification ability of machine learning methods for multi-class fault diagnosis. It is also important to find out the influence of the number of components of fault diagnosis. Because, the increase in number of fault classes increases the possibility of resemblance in signal pattern and it cause difficulty in classification process.

1.9 SALIENT FEATURES OF THE PRESENT WORK

- The present work is aimed to develop a real – time efficient tool condition monitoring system (TCMS).
- To explore the possibilities of using vibration analysis and cutting force dynamics to improve fault detection system.
- In this study, the fault diagnosis of single point cutting tool is modeled as a machine learning problem to identify the best feature-classifier combination for automated fault diagnosis.

- Cutting forces analysis, tool wear analysis, measurement of workpiece surface roughness, chip morphology studies and computational approach will also be carried out as an offline monitoring to explore additional information.
- The present work is aimed for fault detection of single point cutting tool using signal processing techniques in the time domain, frequency domain, wavelet domain, recurrence quantification analysis (RQA) and cepstrum.
- This research work concerns with fault diagnosis of single point cutting tool using online and offline condition monitoring techniques in conjunction with advanced signal processing approaches.

1.10 THESIS OUTLINE

This thesis has been structured, which contains eight chapters, the contents of which are outlined in the following paragraphs;

Chapter 1 is titled as '*Introduction*' and commences with overview on tool condition monitoring and highlights of the work.

Chapter 2 is titled as '*Literature review*', deals with the detailed literature survey and review of previous work on tool condition monitoring. It also provides motivation to work on common tool condition monitoring and their diagnostic techniques scope and objectives of research work.

Chapter 3 is titled as '*Experimental approach and methodology*', starts by briefly detailing experimental set up used for this research work. It also explains the data acquisition, experimental procedure and methodology involved in the present research work.

Chapter 4 is titled as '*Fault diagnosis using signal processing techniques*', which proposes the investigation of fault detection of cutting tool using signal processing methods in the time domain, frequency domain, cepstrum, RQA and wavelet transform plots. Results of investigation using signal processing techniques are also presented.

Chapter 5 is titled as '*Fault diagnosis using machine learning technique*', which describes the machine learning methods, which include feature extraction, feature selection and classification techniques are discussed.

Chapter 6 is titled as '*Analysis of cutting forces, surface roughness, chip morphology and computational approach for fault diagnosis of cutting tool*', describes dynamic force analysis using cutting forces, average surface roughness measurement of the workpiece with different tool conditions, chip formation type while machining with different tool condition and computational approach to predict cutting forces. SEM micrographs of worn out tungsten carbide cutting tool inserts to determine the tool wear mechanisms.

Chapter 7 is titled as '*Conclusion and scope for future work*', presents the summary and conclusions on the investigations carried out in this research work and also included further recommendations addressing various issues for the future work.

CHAPTER 2

LITERATURE REVIEW

2.1 INTRODUCTION

Manufacturing industry plays a major role in building the economy of the developing countries. Traditional machining like turning, milling, drilling, grinding etc. play enormous role in production systems (Rehorn et al. 2005). The quality of the surface finish of the machined parts is directly influence the healthy condition of the cutting edge and failure of the cutting edge is the major cause of the unplanned interruption in a machining environment, which results in larger down time (Jantunen 2002). Numerical methods and analytical models are generally accepted for tool wear estimation with limited accuracy in comparison with modern online condition monitoring methods (Scheffer et al. 2005). A lot of research has been carried out regarding the development of a reliable TCMS. Teti et al. (2010) have reviewed the methodologies used in modern tool condition monitoring. They have reported that the advanced signal processing and machine learning techniques are extensively used in monitoring the conditions of a cutting tool in both on-line and off-line modes.

2.2 SENSORS USED IN TOOL CONDITION MONITORING SYSTEMS

Monitoring usually takes place in very hostile environments. Subsequently, sensors used for tool wear monitoring should be robust and simple to operate. The use of multiple sensors as shown in figure 2.1 can enhance the performance of tool wear monitoring (Teti et al. 2010).

Sensors used for TCMS must meet certain requirements, such as (Pfeifer and Thrum 1996):

- Measurement as close to the machining point as possible.
- No reduction in the static and dynamic stiffness of the machine tool.
- No restriction of working space and cutting parameters.
- Wear and maintenance free
- Low cost and easy to replace.

- Resistant to dirt, chips and mechanical influence.
- Resistance to electromagnetic and thermal influences.
- Function independent of tool and workpiece.
- Adequate metrological characteristics.
- Reliable signal transmission, e.g. from rotating to fixed machine components.

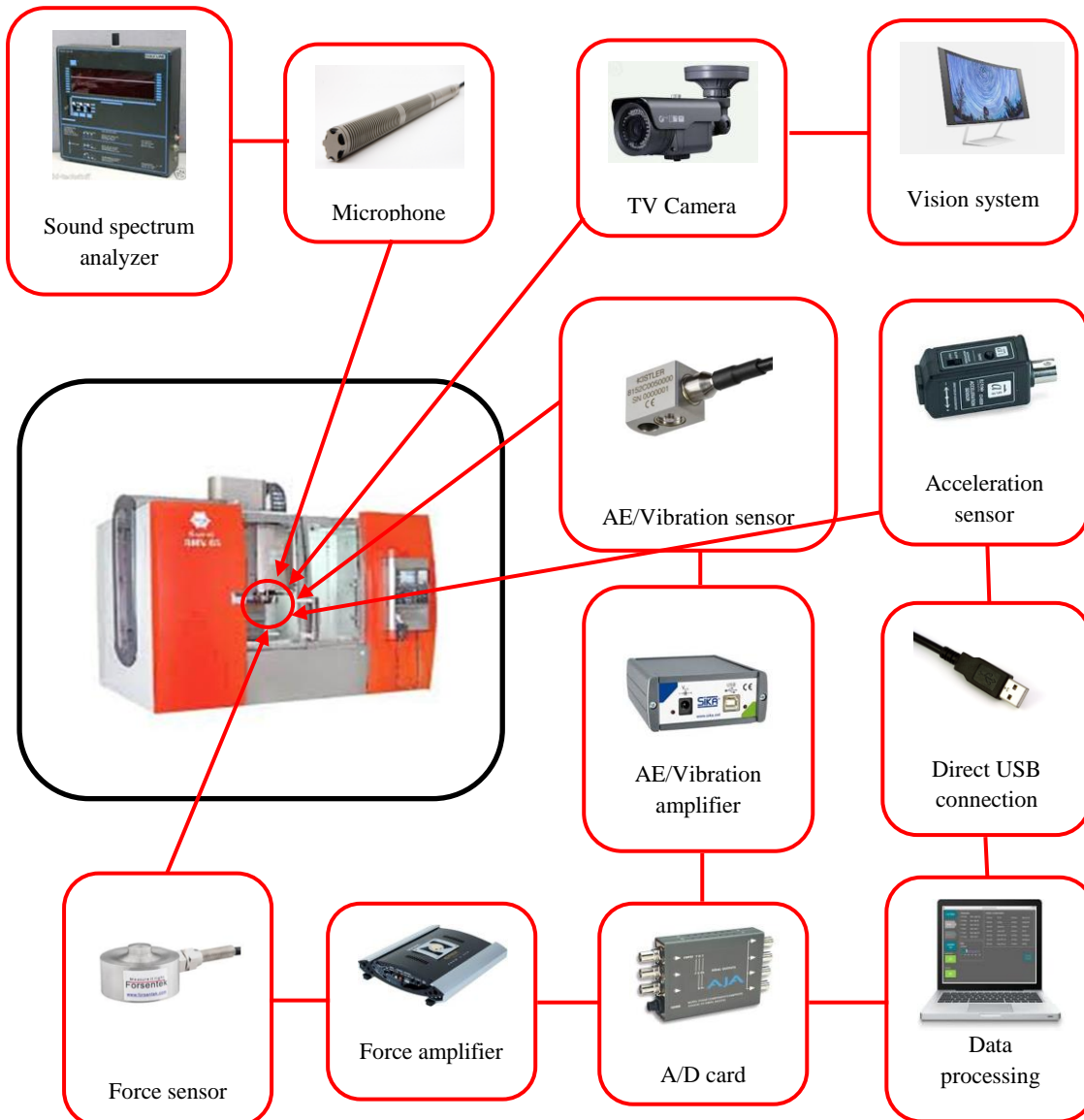


Figure 2.1 Reconfigurable multi-sensor monitoring systems (Teti et al. 2010)

2.3 TOOL CONDITION MONITORING TECHNIQUES

A number of approaches exist to monitor tool wear and are used in manufacturing industries. These techniques can be divided into two categories, namely direct and

indirect. Direct methods always deal with a measurement of volumetric loss at the tool tip, while indirect methods seek a pattern in sensor data from the process to detect a failure mode (Byrne et al. 1995). In general, direct methods are sensitive to dirt and chips, and therefore they are not commonly accepted in manufacturing industries.

2.3.1 Direct condition monitoring methods

Since many years tool wear monitoring is carried out by using image processing techniques. To identify tool wear, the image of the tool is captured while machining by using camera and observed on display unit to identify the wear pattern from captured images to analyze tool wear. Kurada and Bradley (1997) reviewed instrumentation and various image processing systems involved in the advancement of a vision based TCMS. Bradley and Wong (2001) extracted the surface texture signature component due to tool wear from the other texture components using three different image processing techniques and employed it as an indicator for tool condition. They concluded that change in the surface texture can be used for progressive tool wear monitoring. Karthik et al. (1997) proposed a non-contact method that provides visualization of the tool wear geometry using a pair of stereo images and generates the volume of crater wear as a new parameter for inspection. The results showed that the volume of crater wear can be effectively used to measure the amount of the tool wear. Kassim et al. (2000) have analyzed the images of workpiece surfaces while machining and they found the tool-wear patterns by correlating images of the workpiece surfaces. They have identified that the conditions of a cutting tool (sharp, semi-dull, and dull) can be successfully detected by analyzing the respective image data of the machined surfaces. Jurkovic et al. (2005) found a new technique to measure tool wear using a charge coupled device (CCD) vision system consisting of a CCD camera, light source to brighten the tool, a laser diode with linear projector, a grabber for capturing the picture and a computer. Yeo et al. (2000) presented different approaches for the evaluation of tool wear using back propagation neural network and reflectance of cutting chip surface. Results showed that the prediction was in full agreement with the flank wear measured experimentally. They found that the major problem faced in that method was the enmity of the cutting environment. The dust and chip particles accumulated on the optical instrument

results in false indication of tool wear. Kerr et al. (2006) discussed the implementation of digital image processing approaches in the evaluation of worn cutting tool images in order to estimate their amount of wear and thus the remaining useful life. They concluded that textural analysis can be used for direct assessment of the tool wear condition. Wong et al. (1997) devised a vision-based TCMS using a laser scatter pattern of reflected laser ray from the machined workpiece surface finish. The arrangement consisted of a laser source concentrated on the finished workpiece such that its reflected ray is recorded through a digital camera. The recorded image was processed and characterized using the intensity of the optical parameters, the standard deviation and mean of the scatter pattern and their distribution was compared with surface roughness. They concluded that it was very difficult to find tool wear by observing machined surface roughness. Nevertheless, the study revealed a good interrelationship between tool wear and the intensity of the scattered light pattern.

2.3.2 Indirect condition monitoring methods

Indirect methods are less accurate than direct methods, but have found more acceptance in the industry, due to the fact that the most indirect methods are easily interpreted, cost-effective, and in some instances more reliable than direct methods. Also for some applications, it might not be possible to use a direct monitoring method due to the nature of the process.

2.3.2.1 Tool tip temperature

Much research has been undertaken into measuring the temperature generated during cutting operations. Investigators have attempted to measure this cutting temperature with various techniques. Figure 2.2 shows the various methods used for temperature measurement in machining. Metal cutting operations generate a significant amount of heat between workpiece and the tool. The high temperature over the cutting tool edges has an open controlling consequence on the mode and rate of cutting tool wear, due to the friction between cutting tool and chip, and also between the newly formed surface and the cutting tool. Huda et al. (2002) developed a method for measuring temperature between cutting tool and chip interface. A two-color pyrometer with combined fiber coupler was applied to the interface temperature measurement of tool-

chip in wet and dry turning. They measured temperature with pyrometer for a very small object which was not affected with emissivity values. They found temperature distributions on the work material and the cutting tool using the finite element method (FEM). They achieved good agreement between the experimental results and FEM model.

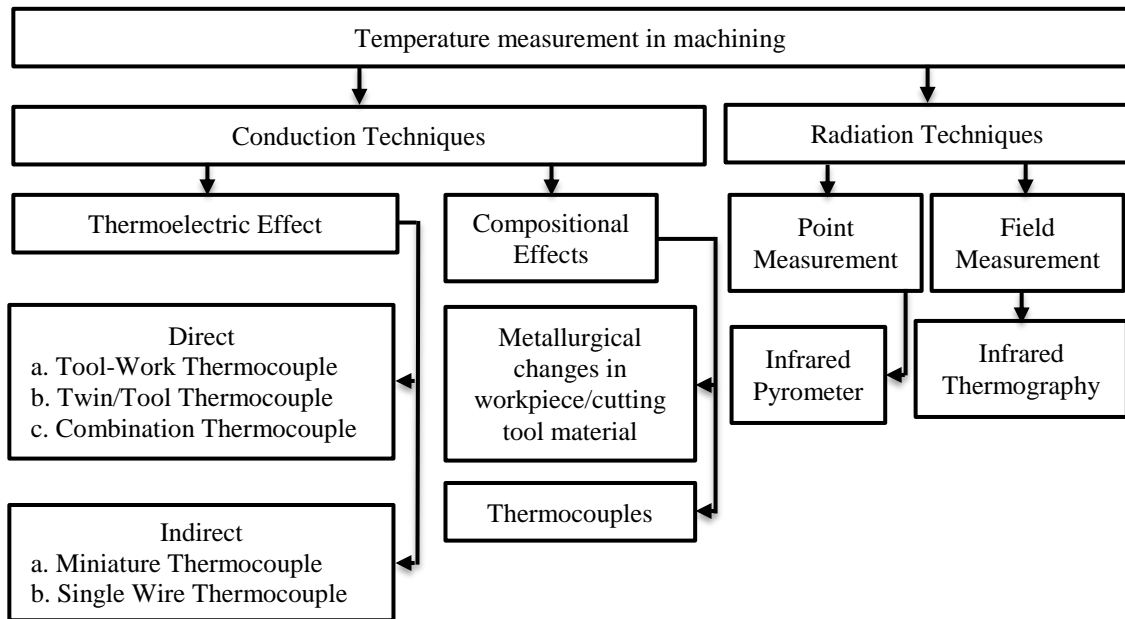


Figure 2.2 Temperature measurements in machining (Sullivan and Cotterell 2001)

Leshock and Shin (1997) depicted the temperature measurement results of tool chip interface by the thermocouple technique. Interface temperature were investigated under a wide range of machining mode during turning of Inconel 718 nickel based alloys and 4140 steel alloys with tungsten carbide tools. They compared experimental results obtained with the Loewen and Shaw's model. They developed an empirical model for the tool face temperature distribution in terms of different cutting parameters. Luo et al. (2005) have developed a new flank wear model for carbide tool insert in turning. The new model was based on the cutting tool temperature simulation, an empirical model and cutting force. The new tool wear model was validated by machining tests. From the experimental results, they found that cutting speed has more effect on tool life compared to feed rate. The comparison of predicted and measured flank wear land width shows that the developed flank wear model can accurately predict the tool flank wear land width to some extent. Murata et al. (2012)

have developed an in process tool-wear detection system. The system senses the thermo-electromotive force generated in the vicinity of cutting tool and workpiece. They have found that the electric resistance and tool-wear are correlated, i.e., a decrease in the electric resistance means an increase in the flank wear. This trend helps to detect the progress of tool-wear during the intermittent machining (e.g., face milling) in a reliable manner. Sullivan and Cotterell (2001) demonstrated different methods used to measure the temperature of a single point cutting tool. They measured simultaneously cutting force and temperature to monitor tool wear. They used embedded thermocouples and infrared camera to measure temperature and monitor the machining process to measure tool wear. Wanigarathne et al. (2005) conducted experimental studies of orthogonal machining of AISI 1045 steel with coated TiN/TiCN/TiC grooved tools and analysed tool-wear progression under dry machining conditions. They measured cutting force components and recorded tool-chip interface temperature using Therma Cam PM695 infrared camera. In addition to the above, they also established the interrelationships between the progressive tool-wear, cutting temperature and the cutting forces. Boothroyd (1988) suggested the use of thermocouple technique to measure interface temperature between cutting tool and work piece using the electro motive force (EMF) generated. But it failed to provide measure of temperature distribution in the tool. Author concluded that remote thermocouple sensor or instruments can only measure the cutting workpiece-tool interface or some other irrelevant area temperature, rather than the tool tip temperature. This process parameter, though an appropriate tool wear indicator, is extremely difficult to measure accurately for online purpose as in TCMS due to the distance of the cutting area rendering it inefficient.

2.3.2.2 Acoustic emission technique

Acoustic emission (AE) is a phenomenon which occurs for different reasons. A small surface displacement of material is formed due to stress waves developed when there is an accelerated liberation of energy either in material, or on its surface. Hence, the AE signal appears to be a promising candidate for tool wear monitoring. Li (2002) have reviewed the methodologies used in tool condition monitoring using AE sensor and observed that the major advantage of using AE to monitor tool condition is that

the frequency range of the AE signal is much higher than that of the machine vibrations and environmental noises, and does not interfere with the machining operation. Ramesh and Siong (2011) established the appropriate ball nose end mill geometry for machining titanium and predicted the performance behavior of a production run ball nose end mill through correlation with RMS value of AE signal to wear behavior. Ren et al. (2014) presented a fuzzy logic TCMS based on AE signals in micro milling. They have analyzed the AE signal features and chosen the best features and integrated to estimate the cutting tool condition through its life. Stoney et al. (2013) developed surface acoustic wave (SAW) sensors for process monitoring operations. Single-axis continuous and interrupted machining investigations were carried out using the SAW technology installed on cutting tool holders demonstrating high dynamic bandwidth strain measurement. Jemielniak and Otman (1998) treated statistical signal processing algorithm to find the kurtosis, root mean square (RMS) and skewness of the AE signal to find catastrophic tool failure. Failure in tool material was identified using cutting force as a reference signal. They reported that the kurtosis and skewness value can be used as an indicator for tool failure rather than RMS values. Similar work carried out by Choi et al. (1999) combined AE and cutting forces in their endeavor to establish an efficient TCMS for turning operations. They observed a sudden decrease in cutting force with tool wear and noticed large burst of AE at the breakage of the tool. They also developed an algorithm for pattern recognition using AE and cutting force signals, and implemented online monitoring tungsten carbide tool in CNC lathe. They found that the drawback of AE signals were more sensitive to variation in cutting conditions and noise. Using only AE to detect the condition of a cutting tool is a difficult task. So AE is suitable with an additional sensing method for increased accuracy for TCMS.

2.3.2.3 Cutting forces

Torque, drift and feed force together with strain measurement are all different ways of measurement of cutting forces and are strongly correlated with the tool wear. The idea behind monitoring torque and feed forces is based on the fact that these dynamic parameters generally increase as the tool gradually wears due to the increasing friction between tool and workpiece. Experiments have shown that the three components of

the cutting force respond differently to the various wear forms occurring on the tool. For example, the feed (F_x or F_f) force is insensitive to crater wear, whereas the feed and radial (F_y or F_r) forces may be influenced more by tool wear than the main cutting (F_z or F_t) force (Yaldiz and Unsaçar 2006; Souza et al. 2009; Lee et al. 1998). Figure 2.3 shows the nomenclature of the cutting force components involved in single point cutting tool operations.

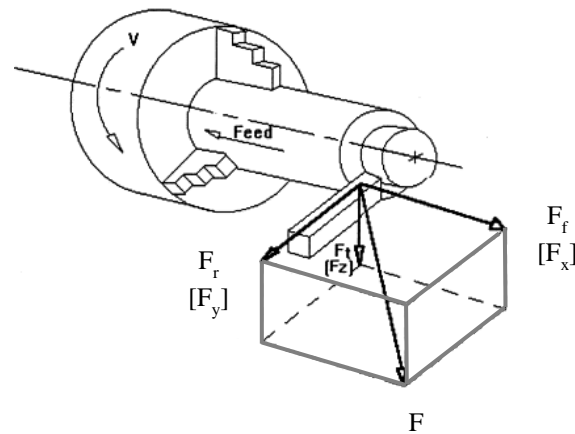


Figure 2.3 Cutting force components on a single point cutting tool during turning (Dimla 2000)

Liu et al. (2003) investigated CBN tool wear in ductile machining of tungsten carbide using high speed milling machine tool. They measured cutting forces using dynamometer and also examined tool wear with scanning electron microscope (SEM) with energy dispersive spectrometer (EDS) and also using optical measurement inspection system. They investigated different wear mechanisms and depicted diffusion, adhesion and abrasion as main causes of wear. Also, they reported that higher cutting speed results in larger tool wear and shorter tool life, increase in cutting distance and flank wear will increase cutting forces. In addition to the above, they also conducted studies on the surface roughness and concluded that increased flank wear will have less influence on roughness parameters. Zhou et al. (2003) monitored the flank wear on the cubic boron nitride (CBN) tool in hard turning process using force dynamometer and estimated tool flank wear with the help of parameters such as normalized passive force, frequency energy and accumulated machining time. Also they carried out investigations to identify the reasons for part geometry inaccuracy, instability in the tool motion and increase in cutting forces due to flank wear.

Devillez et al. (2004) conducted basic orthogonal machining tests under dry conditions. They used CNC lathe which was equipped with a platform dynamometer KISTLER 9265B and used white light interferometry for measurement of wear craters on cutting tool inserts. They monitored machining parameters and generated three dimensional (3D) images of the wear surfaces using Wyko NT1100 optical profiler. They found that decrease in cutting forces, increased depth of crater wear was due to increased cutting speeds as shown in figure 2.4 and figure 2.5.

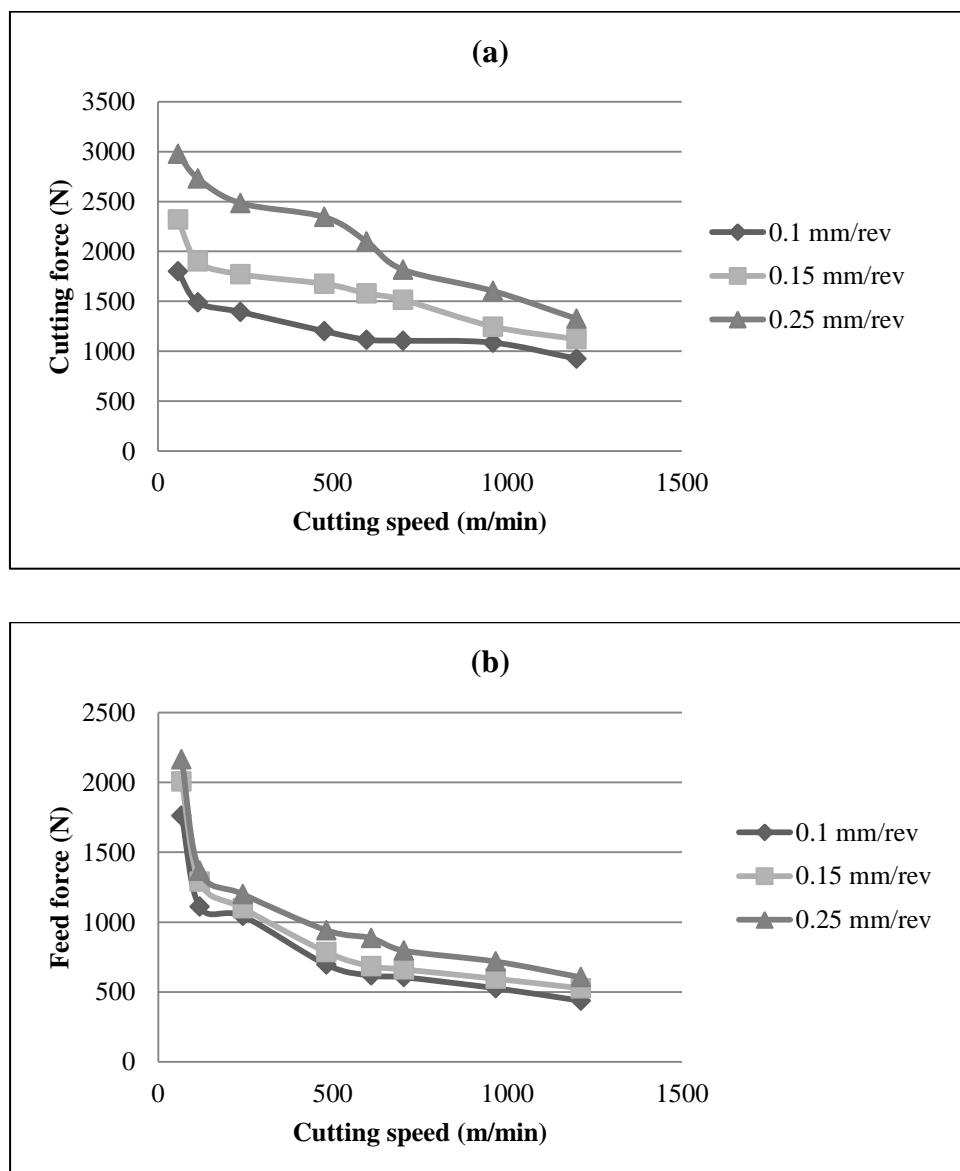


Figure 2.4 Cutting force (a) and feed force (b) as functions of cutting speed (Devillez et al. 2004)

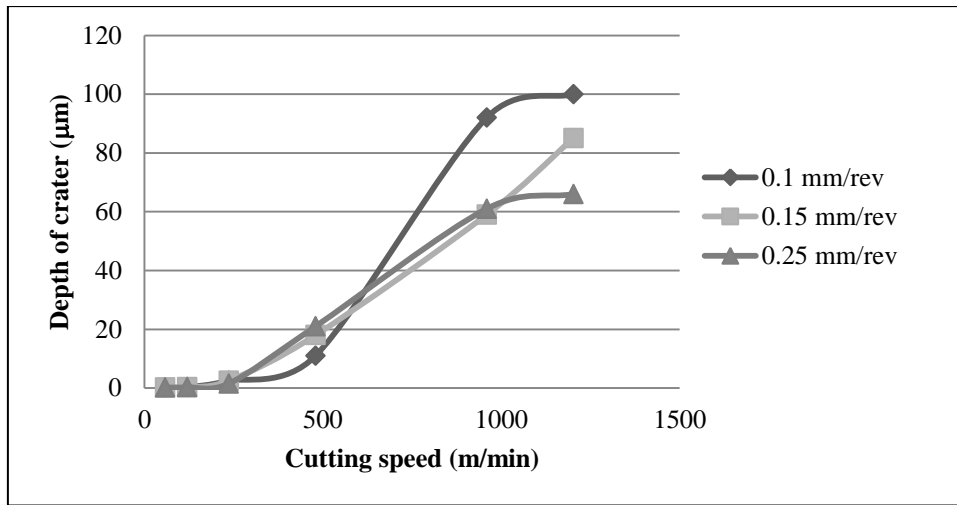


Figure 2.5 Depth of crater as a function of cutting speed (Devillez et al. 2004)

They found increase in friction coefficient due to erosion of cutting tool edge. Further they even observed reduced tool wear in high speed machining with high feed rate. Sikdar and Chen (2002) conducted machining experiments on CNC lathe. They identified the cause for flank wear and were due to abrasive and adhesive actions between the cutting tool and the machined surface. They observed that the cutting force is increasing with the increase in surface area of flank wear as shown in figure 2.6. Among the three cutting forces measured, they found tangential force (F_t) was the largest and radial cutting force (F_r) was the least. They set up a relationship between the cutting forces and the flank wear surface area.

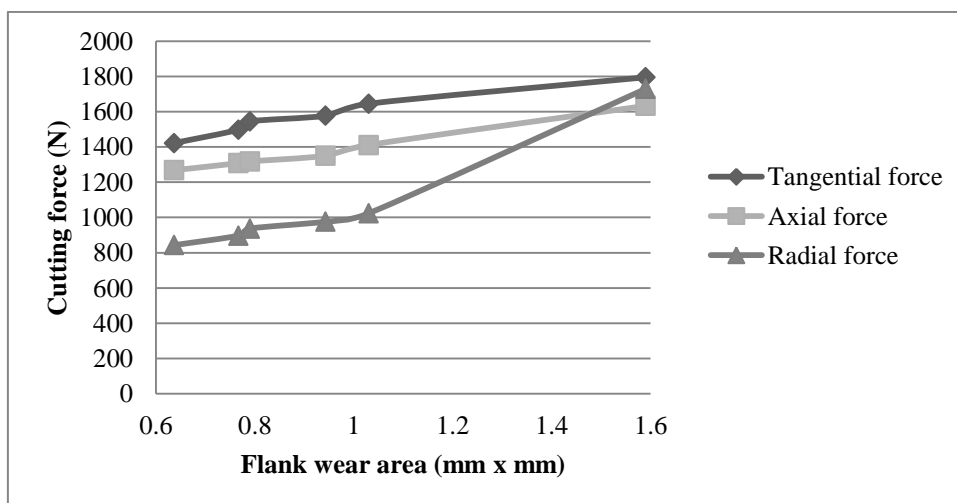


Figure 2.6 Cutting forces vs. flank wear surface area (Sikdar and Chen 2002)

Nouri et al. (2015) developed a new method to monitor end milling tool wear and detect tool failure based on real-time tracking of force model coefficients, which were shown to be independent from the machining conditions and correlated with tool wear. Chen et al. (2014) developed a smart turning tool with piezoelectric film sensors as sensing elements integrated within the tool shank, to measure cutting force and feed force in process with a high resolution and accuracy. Karim et al. (2013) developed condition monitoring system by using a low-cost piezoelectric sensor to monitor the flank wear progression on the cutting tool.

2.3.2.4 Vibrational analysis

Due to the cyclic imbalance in the changing factor of the cutting force, vibrations are produced. Normally, these vibrational motions begin as small chatter produces the serrations on the finished surface and advances in uneven chip thickness. Mechanical vibrations normally result from periodic wave motions. Direct measurement of the vibration is difficult to achieve because of its conclusive predictable feature, and frequency dependent vibration mode. Hence, associated variables such as the rate at which the dynamic forces change per unit time (acceleration) are calculated and the patterns are obtained from the extracted vibration signals. Bhuiyan et al. (2014) have investigated tool wear, chip formation and surface roughness of workpiece under different machining conditions while machining using acoustic emission (AE) and vibration signature analysis in turning. They found that the AE and vibration components can effectively respond to the different occurrences in tool wear and surface roughness. Elangovan et al. (2011) acquired vibration signals while machining with CNC turning center and applied data mining approach to extract hidden information which was available in tool vibration signals. They have studied fault classification using pattern recognition techniques and used decision tree algorithm (C4.5) for selecting features. Gong et al. (2004) discussed an action method in which the damping ratio of the tool vibration and its behavior with tool wear development in the feed direction after impact excitation. They concluded that the tool wear state can be quantitatively estimated in machining at any time. Lim (1995) presented the changes that can be detected in the vibration signatures during machine turning operations. It was found that at various machining speeds, the vibration amplitudes

consistently produce two peaks throughout the life of the tool. Sevilla et al. (2015) presented a reconfigurable system for tool condition monitoring in the high-speed machining (HSM) process. They conclude that the proposed system was compact, economical, fast and reliable in detecting several tool condition types using different cutting parameters under high-speed face milling. Figure 2.7 shows the prototype of the implemented FPGA-based reconfigurable system for the TCMS.

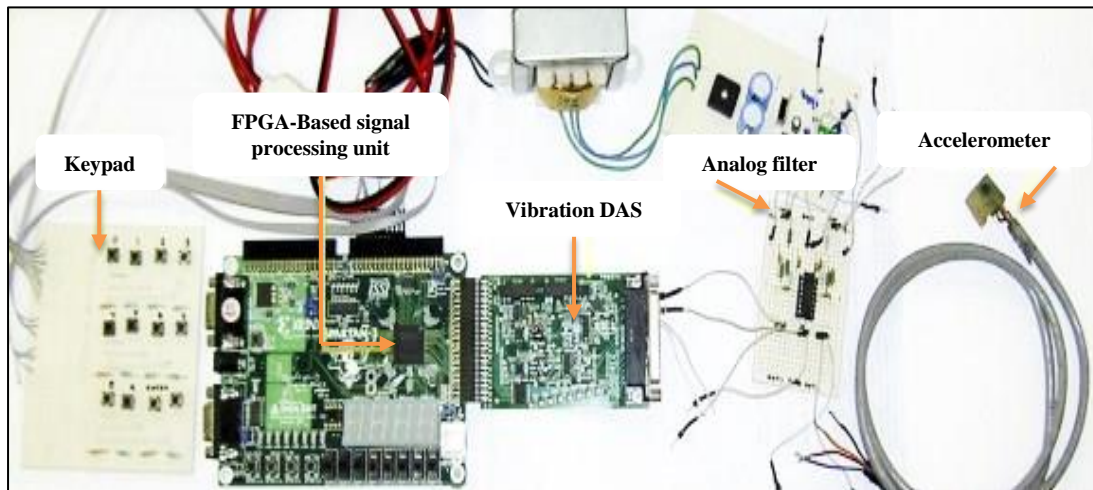


Figure 2.7 Prototype of the implemented FPGA-based system (Sevilla et al. 2015)

Elangovan et al. (2011) monitored the condition of a single point cutting tool using vibration signals and classified using support vector machine (SVM) and compared the classification efficiencies of C-support vector classifier (C-SVC) and v-support vector classifier (v-SVC). They found that v-SVC provided better classification efficiency comparison with other classifiers like decision tree, Naive Bayes and Bayes net and concluded that SVM as a preferred classifier for the prediction of the carbide tipped tool than other classifiers. The static behavior is controlled entirely by the momentum and cutting forces. The dynamic behavior shows vibration and positive aspects of the changing cutting force. The integration of parts of the vibration signals and the cutting forces fused in building multiple sensor-based TCMS would turn out absolutely necessary in the industries.

2.3.2.5 Ultrasonic methods

Nayfeh et al. (1995) used ultrasonic method for online monitoring of tool wear. They used the change in the amount of the reflected energy and related with tool wear and

found a correlation between ultrasonic measurements and gradual wear. Abu and Yu (2003) measured the gradual wear of tungsten carbide inserts during turning operations using discrete wavelet transform of ultrasound waves. They acquired tool wear image by machine vision and counted the number of pixels inside the wear boundary and along the two peaks of the wear using MATLAB. They used three-layer multilayer perceptron (MLP) artificial neural network (ANN) and estimated tool wear and validated with measured wear results.

2.3.2.6 Spindle motor current

Spindle motor current monitoring features have similar characteristics, advantages and drawbacks to that of cutting force signals. Lee et al. (2007) investigated a hybrid approach to find tool wear using cutting force and spindle motor current variation, which have been proved a successful for monitoring of gradual tool wear. Franco et al. (2006) concluded that spindle motor current can be related to the dynamics of drilling process and to monitor the cutting tool condition. Pal et al. (2011) have employed wavelet packet tree and principal component analysis to extract tool wear sensitive features from turning operations. They have built an artificial neural network to correlate machining conditions with tool-wear features so that the amount of tool-wear can be predicted based on the machining conditions applied.

2.4 ONLINE AND OFFLINE MONITORING TECHNIQUES

The second important distinction, possible made with tool condition monitoring techniques is between online and offline monitoring techniques. In the case of online monitoring, the measurement variable is available throughout the machining process. This enables the on-line classification of the process, and ensures that sudden changes can be reacted upon in time (Byrne et al. 1995).

In offline monitoring the variable is only recorded during the machining process and then recorded variables are further analyzed using various offline monitoring techniques. This method has many obvious disadvantages, which includes time losses and high cost.

2.4.1 Online monitoring using machine learning approach

In machine learning technique, computer makes prediction based on feature of past training data sets. Computer algorithm program will build the model and optimize parameters based on the past data sets provided. Many researchers carried out investigations on fault diagnosis of machinery system using machine learning techniques.

2.4.1.1 Features extraction methods

Most decision making techniques for process monitoring are based on features. Information from the force, vibration or AE signal acquired during machining can be used for the monitoring of the cutting tool. Features can be extracted from these signals that show effective and consistent trends towards tool wear. Once these features are extracted through preliminary processing of the signal, the cutting tool state can be predicted with pattern recognition or other classification techniques (Kumar et al. 1997). These features can be derived from time and / or frequency domain data. For example: mean, variance, skewness, kurtosis, powers in a specific frequency band etc. When the signal change during the machining operation as a result of tool wear, the model coefficients also change and this can be utilized to monitor the tool wear.

2.4.1.1.1 Statistical features

Statistical features of the signal provide various parameters which is useful in discriminating the faults in the machinery system. Numerous investigations have been carried out in different area of fault detection using statistical feature for feature selection. Amarnath et al. (2013) investigated on fault diagnosis of bearings by extracting statistical features from sound signals. Girish et al. (2014) adopted the statistical feature extraction method to fault diagnosis of welded joints through vibration signals. Jegadeeshwaran and Sugumaran (2015) proposed a method, where statistical features were used for fault diagnosis of automobile hydraulic brake system.

2.4.1.1.2 Histogram features

A difference in the range of amplitude for different classes could be viewed when the magnitude of the signals were measured in time domain. Variation in the vibration amplitude could be shown by using one of the best methods namely histogram plot. This histogram plot provides some valuable information for classification and this information would serve as histogram features for fault diagnosis of cutting tools. Sakthivel et al. (2011) reported the use of histogram features for decision tree-based fault diagnosis of monoblock centrifugal pump. Sugumaran and Ramachandran (2011) carried out fault diagnosis of roller bearing using fuzzy classifier and histogram features with focus on automatic rule learning. Indira et al. (2011) found a method for calculation of optimum data size and bin size of histogram features in fault diagnosis of mono-block centrifugal pump.

2.4.1.1.3 Discrete wavelet transform (DWT) features

Discrete wavelet transform theory was proposed by Mori et al. (1996) for early identification of defects. DWT decompose the signals into two frequency sub bands such as low frequency band (approximate coefficients) and high frequency band (detailed coefficients) through high pass filter and low pass filters. It is suggested that wavelets might be the perfect tool for many applications requiring automated monitoring of manufacturing operations. However, not enough comparison to FFT or statistical parameters has been explored so far. Franco et al. (2006) analyzed the obtained driving motor current signal to estimate the tool condition by using the discrete wavelet transform (DWT), without the aid of any sensors. The DWT was found helpful and the whole method provided an accurate estimation of drill wear under different drilling conditions.

2.4.1.1.4 Empirical mode decomposition (EMD) features

Peng (2006) presented robust methods for the detection of tool breakage in the end milling operations, based on investigating the characteristic of intrinsic mode functions (IMF) components of cutting force using EMD technique. Wang et al. (2014) proposed a new method combined ensemble empirical mode decomposition

(EEMD) with independent component analysis (ICA) technique to effectively extract compound fault features of the rolling bearing. Their results shown that compound faults, such as the bearing outer-race defect, the roller defect and the unbalance fault of experimental system were effectively separated by their new proposed method.

Junsheng et al. (2006) developed a method for the extraction of fault characteristics of roller bearings using an autoregressive (AR) model based on EMD. Grasso et al. (2014) investigated the suitability of the water pressure signal as a source of information to detect different kinds of fault that may affect both the cutting head and the ultra-high pressure (UHP) pump components using EMD with principal component analysis (PCA). Yang et al. (2011) has developed a new wind turbine condition monitoring technique using the bivariate empirical mode decomposition.

Cao et al. (2015) used an alternative method based on EEMD and nonlinear dimensionless indicators for chatter identification. From EEMD, the vibration signals were decomposed into a set of IMFs, and then IMFs containing rich chatter information were selected for feature extraction. Liu et al. (2015) proposed an effective feature selection and extraction method which gives better modeling accuracy to estimate mill load parameters based on EMD and PCA.

Bin et al. (2012) proposed a new approach based on combined wavelet packet decomposition (WPD) and EMD to extract fault feature frequency and neural network for rotating machinery for early fault diagnosis. Bakker et al. (2015) have discussed the linear friction weld process monitoring of fixture cassette deformations using EMD.

Georgoulas et al. (2014) presented an automatic pattern identification based on the complex empirical mode decomposition of the startup current for the diagnosis of rotor asymmetries in asynchronous machines. Amiri and Darvishan (2015) proposed a methodology to detect damage and its severity in moment frames with nonlinear behavior under earthquake excitation based on combination of a time-series method and data mining approach to overcome the limitations of time-frequency methods for damage detection of nonlinear structures.

2.4.1.2 Feature reduction algorithm

All extracted features from the measured data, may not be required to extract the diagnostic information. Dimensionality reduction techniques remove the redundant information to reduce the original higher dimension for the ease of processing and computation. Recently, the use of feature reduction and feature selection for data preparation before feeding into classifier has received considerable attention (Cao et al. 2003). The details of the dimensionality reduction techniques are discussed in the following sections.

2.4.1.2.1 Decision tree technique

There are many techniques available for feature selection. The commonly used technique for selection of feature is decision tree (Samanta and Al-Balushi 2003). The decision tree selects a subset of the existing features without any transformation by representing the signal information in the form of tree. The decision tree can also be served as a classifier. Sun et al. (2007) proposed new method based on C4.5 decision tree and principal component analysis (PCA) for fault diagnosis. They used PCA to reduce features after data collection, preprocessing and feature extraction. They trained C4.5 by using samples to generate a decision tree model with diagnosis knowledge and used decision tree for diagnosis analysis. Sugumaran and Ramachandran (2007) carried out an experimental study for fault diagnosis of roller bearing in which decision tree has been used to identify the best feature under the various fault condition of bearing.

2.4.1.2.2 Principal component analysis

Principal component analysis (PCA) is one of the widely used multi-dimensional features reduction tool. PCA is the preferred choice because it is a simple and non-parametric method of extracting relevant information from complex data sets. The goal of PCA is to reduce the dimensionality of the data while retaining as much as possible of the variation in the original data sets. Elangovan et al. (2011) discuss the use of PCA with various classifiers mainly to reduce the data dimensionality and reports improvement in classifier efficiency. Sun et al. (2007) proposed a new method

based on C4.5 decision tree and principal component analysis (PCA) in the area of fault diagnosis. They achieved high classification accuracy using feature selection tool as C4.5 decision tree algorithm.

2.4.1.3 Feature classification

Feature classification is the last phase of the machine learning approach. In the classification process, the classification algorithm develops a model with the help of training data and the trained model is used to classify the data belonging to various classes of faults. There are various classification techniques to classify the cutting tool conditions. The following subsections provide the detail about the use of classification algorithms for online tool wear monitoring.

2.4.1.3.1 Support vector machine

Support vector machine has emerged as a pattern classifier that can learn even from a small training data set for each class (Saimurugan et al. 2011). Saravanan et al. (2008) have demonstrated the effectiveness of wavelet-based features for fault diagnosis using SVM and proximal support vector machines (PSVM). Sun et al. (2006) proposed effective usage of training data in tool condition monitoring system. They have used SVM for decision making method and generalization error for performance evaluation criterion. They have divided the original training data set into three subsets $T_{o\text{-flat}}$, $T_{o\text{-peak}}$, $T_{o\text{-fuzzy}}$ for samples from flat, peak and fuzzy regions respectively. They have compared the performance of original training data set T_o with selected training data set T_s and found former need shorter training time and decision making time. Chen et al. (2013) carried out an investigation on gearbox fault diagnosis using empirical mode decomposition (EMD) method to extract features from vibration signal, they used immune genetic algorithm for important features selection out of extracted features and SVM has been used for fault classification.

2.4.1.3.2 Artificial neural network (ANN)

Artificial neural network is modeled on the basis of biological neurons and nervous systems. They have the ability to learn, and has the processing elements known as neurons, which perform their operations in parallel. ANN's are characterized by their

topology, weight vector and activation functions. Dimla et al. (1998) have used multilayer perceptron (MLP) neural network and identified cutting tool state in metal turning operation. They used feed-forward multi-layer perceptron with 12 inputs, 1 binary output and a single hidden layer with 20 and 5 nodes. They classified the tool state with two classes such as worn or sharp and the results were successful between 83 to 96%. Wang et al. (2007) have developed a self-organizing map (neural network) and trained it in a batch mode after each cutting passes against the flank-wear-relevant features of cutting forces obtained from a sensor-based analysis and measured the degree of wear obtained by interpolating the vision based measurement. They have shown that the trained neural network is effective for online tool condition monitoring in milling and independent of the cutting conditions used. Yu et al. (2006) investigated fault diagnosis of roller bearing using EMD method and artificial neural network (ANN) as a classifier. Patra et al. (2010) have developed a tool condition (flank wear) monitoring system using the vibration signals of machining process. They have shown that the fuzzy radial basis function based neural network can recognize the features extracted from the time domain by applying the wavelet packet approach underlying the vibration signals more effectively than other methods (back propagation neural network, radial basis function network, and normalized radial basis function network). Dimla (1999) investigated the application of perceptron-type neural network to tool-state classification during a metal-turning operation. They used both single layer perceptron (SLP) and MLP to train and test for depicting tool state as worn or sharp. They found the MLP system performed better than SLP and the number of hidden nodes in an MLP has not shown significant improvement in classification accuracy. Ali et al. (2015) characterized and classified seven different bearing classes depending on statistical features, EMD energy entropy and artificial neural network (ANN). They have shown that the potential application of ANN for automatic bearing performance degradation assessment without human intervention.

2.4.1.3.3 Decision tree algorithm

A decision tree consists of a number of branches, one root, a number of nodes and a number of leaves. One branch is a chain of nodes from root to a leaf and each node

involves an attribute. The occurrence of an attribute in a tree provides the information about the importance of the associated attribute.

Kilundu et al. (2011) integrated signal processing methodology and different machine learning methodologies (decision trees, Bayesian networks, k-nearest neighbor, and neural network) to handle the computational complexities in monitoring the tool-wear using the cutting vibration signals. A comparison of the tool-wear detection performance has also been presented, showing which machine learning methodology is good for recognizing tool-wear pattern.

2.4.1.3.4 Naive Bayes algorithm

Many researchers implemented Naïve Bayes as a fault classifier in the area of damage detection in engineering materials (Addin et al. 2007), centrifugal pump (Muralidharan and Sugumaran, 2012) and mechanical rotary machine component faults diagnosis such as gears (Sharma et al. 2015) and bearing (Addin et al. 2011). Kumar et al. (2014) employed Naive Bayes classifier to perform fault diagnosis of bearing through vibration signals.

2.4.2 Offline tool monitoring techniques

Offline tool wear monitoring pertains to providing information on the condition of cutting tool so that worn out cutting tool can be replaced or changed properly. By having such knowledge of cutting tool condition, one can predict failures and stop the machining operation for maintenance in a planned manner.

2.4.2.1 Signal processing techniques

There are many different signal processing analysis techniques that extract meaningful information from an acquired vibration signal. Diagnostic parameters can be identified through careful processing of data. The importance of signal processing is to get the meaningful information from the obtained signal. Statistical parameters, time domain, Fourier transform and wavelet analysis appears to be the most prevalent signal processing techniques amongst the researchers (Jantunen 2002).

2.4.2.1.1 Time domain analysis

A time domain signal is not very informative as such. Especially, force sensor signals in the time domain do not show any correlation with tool wear. Utilization of statistical parameters along with time domain signal can be proved promising. Jemielniak et al. (2012) have studied the force, vibration, and acoustic emission signals, while turning a specific material and extracted some features from the time, frequency and time-frequency domains of the signals for detecting the tool wear.

2.4.2.1.2 Spectrum analysis

Fourier transforms (FT), including fast Fourier transforms (FFT), short-time Fourier transforms (STFT) and discrete Fourier transforms (DFT), provide a means to determine the frequency content of a measured signal. In particular, the power spectrum of the drift force changes from a band limited process to a wide band process when the tool is worn. The power content of the high frequencies of the cutting forces increases as tool fails, thus providing a useful indicator to detect the failure of the cutting tool (Jantunen 2002). The bearing faults using the FFT method were investigated by Yang et al. (2009) based on vibration and the current measurements. Amarnath et al. (2009) carried out experimental investigations on back-to-back gear box to measure the change in stiffness along with other parameters such as film thickness, specific film thickness and the vibration levels. They found that RMS vibration levels as well as amplitudes of gear mesh harmonic frequencies provide good diagnostic information to estimate the wear severity in conjunction with film thickness analysis.

2.4.2.1.3 Cepstrum analysis

Cepstrum analysis is a signal processing technique with a variety of applications in areas such as speech and image processing. This approach can be used in the area of machine fault diagnosis. Park et al. (2013) carried out an investigation on early fault diagnosis of ball bearings using the minimum variance cepstrum (MVC), experimental results shows that the MVC could be an efficient way to detect periodic fault signals. Liang et al. (2013) investigated application of power spectrum,

cepstrum, higher order spectrum and neural network analyses for induction motor fault diagnosis. They mentioned that cepstrum analysis is a very useful tool for detection families of harmonics with uniform spacing or the families of sidebands commonly found in gearbox, bearing and engine vibration fault spectra. Borghesani et al. (2013) fault diagnostic analysis of rolling element bearings using cepstrum analysis. Different bearing damages in various operating conditions were considered in their study. Morsy and Achtenova (2014) conducted damage detection study of a gearbox using cepstrum analysis.

2.4.2.1.4 Wavelet analysis

It is suggested that wavelets might be the perfect tool for many applications requiring automated monitoring of manufacturing operations. However, not enough comparison to FFT or statistical parameters has been explored so far. Xu et al. (2014) have developed a methodology to detect the tool wear in drilling. They have used the wavelet transform to identify the features in the static and dynamic components of drilling torque and thrust force signals. They have employed a back propagation neural network for the feature recognition, and found that the features extracted from the low-frequency band in the dynamic component of the signals are effective in detecting the drilling tool-wear. Scheffer and Heyns (2001) reported the simultaneous use of vibration and strain measurement for wear monitoring in turning operation. They extracted features from time and frequency domains, time series model coefficient and from the wavelet analysis. Faults classified using self-organizing map and claims near 100% classification accuracy. The features were chosen using a correlation coefficient approach.

2.4.2.1.5 Recurrence quantification analysis

Recurrence quantification analysis (RQA) is a nonlinear technique developed by Eckmann et al. (1987). The technique has been successfully applied to different fields ranging from physiology to economics (Webber and Zbilut 2005). Recently it has made forays into engineering field. One of the first application of recurrence plots (RPs) to time series generated by models of the Twin-T, Wien-bridge and other chaos generating electronic oscillator circuits (Elwakil and Soliman 1999). Through visual

inspection of the RPs, the chaotic behaviors of the model results were confirmed. RPs has been used to estimate optimal embedding parameters and vicinity threshold. (Matassini and Manfredi 2002). Litak et al. (2008) investigated the time series of a torque applied to the ripping head in the process of a cutting concrete rock with sharp and blunt tools, with application of nonlinear embedding methods and the recurrence plots technique. They proposed this technique for testing the ripping machine efficiency and a method to monitor the state of tools. Nichols et al. (2006) have reported that RQA is a useful tool for detecting subtle, non-stationarities and/or changes in time series. They have applied RQA to detect damage induced changes in the structural dynamics. Masugi (2006) has presented recurrence plot scheme approach to analyze nonstationary transition patterns of internet protocol (IP) network traffic. Acuna et al. (2008) analyzed the electrochemical current oscillations generated during the early stages of corrosion fatigue damage using RPs and RQA. Tahmasebpoor et al. (2015) studied nonlinear time series analysis techniques based on RP and RQA. They used RP and RQA to characterize the hydrodynamics of bubbling gas–solid fluidized beds using measured pressure fluctuation signals. Rafal et al. (2015) investigated the stability of milling process of titanium alloy Ti6242 on the basis of experimental time series of cutting forces. They employed recurrence quantification analysis and the Hilbert–Huang transform (HHT) to identify self-excited vibrations in an active chatter control system.

Jessy et al. (2015) used RQA to assess the drilling of glass fiber-reinforced polymers (GFRP) composites and to determine the influence of machining condition on drill-bit wear. They identified the suitable machining condition that minimizes drill-bit wear during GFRP drilling by monitoring vibration signals. Norouzi et al. (2015) applied nonlinear time-series analysis techniques based on the RP and RQA combined with multi-scale analyses to investigate the effect of the insertion of horizontal tubes on the flow structures in bubbling gas–solid fluidized beds.

Sen et al. (2008) studied the fluctuations of mean indicated pressure (MIP) in a diesel engine using RPs, recurrence quantification analysis and continuous wavelet transform. Figure 2.8 depict the RPs of the MIP. They also proposed the use of results

of their study in developing effective control strategies for efficient engine performance.

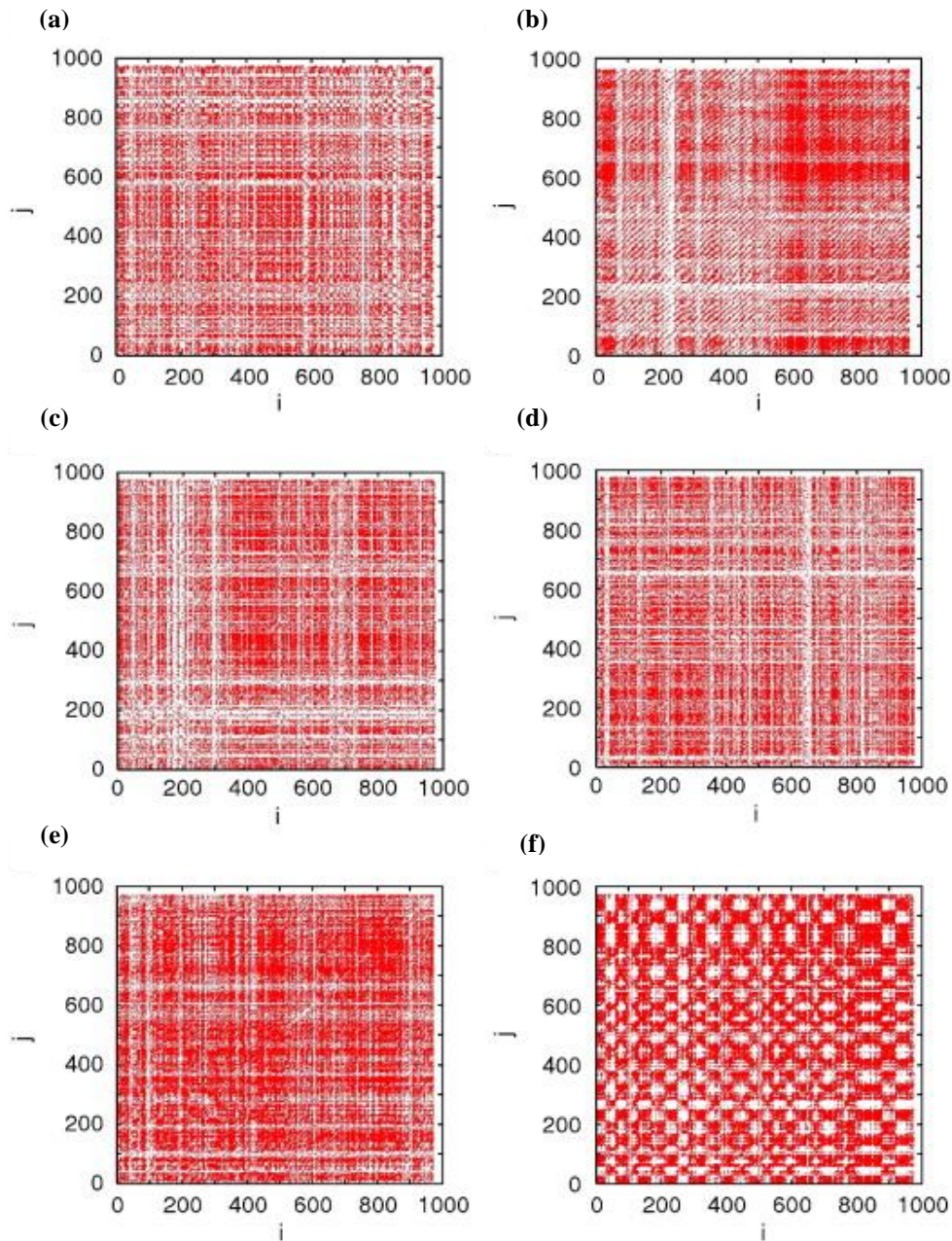


Figure 2.8 Recurrence plots of the MIP time series for different speeds (a-f) ($n = 1000, 1200, 1400, 1600, 1800$ and 2000 rpm) of the crankshaft (Sen et al. 2008)

2.4.2.2 Tribological studies

The data from direct measurement of tool wear (flank wear, breakage, etc.), surface roughness and chip formation occurrences are utilized to correlate with the signals

response (vibration, cutting force, AE signal, etc.). This helps to investigate the tool condition even more accurately. In this section the most recent and significant contributions of the tribological studies (tool wear, surface roughness and chip formation) related to fault detection and diagnostics of machining process are reported. Luo et al. (1999) have studied the wear characteristics in turning high hardness alloy steel by ceramic and CBN tools. Experimental results showed that the main wear mechanism for the CBN tools was the abrasion of the binder material by the hard carbide particles of the workpiece. For ceramic tools, adhesive and abrasive wear were significant. Lin and Chen (1995) studied various cutting characteristics of a CBN tool in cutting hardened steel. CBN tool inserts were used to cut 52100 bearing steel (HRC 64) in the machining studies. Based on the experimental results, certain machining characteristics, such as tool life, cutting forces, surface roughness and tool wear were analysed. Ezugwu et al. (2001) developed polynomial and exponential wear model based on the joint effect of different combination of component forces. They found the highest statistical significance with wear rate based on analysis of variance and correlation coefficient for both polynomial and exponential models. In addition to the above, wear map was established using an exponential wear model based on the force ratios. Chen (2000) found cutting forces while machining steel being hardened to 45–55 HRC with CBN tools. They found that radial thrust cutting force was the largest among the three cutting force components and also most sensitive to the changes of cutting edge geometry and tool wear. Asilturk and Akkuş (2011) have determined the effect of cutting parameters on surface roughness in hard turning using the Taguchi method. Aouici et al. (2012) carried out an analysis of surface roughness and cutting force components in hard turning with cubic boron nitride (CBN) tool and optimized the cutting parameters using a developed model. Kaymakci et al. (2012) developed a unified cutting force model for turning, boring, drilling and milling operations. Xie et al. (2013) conducted experimental studies on cutting temperature and cutting force in dry turning of titanium alloy using a non-coated micro-grooved tool. Ozel et al. (2007) investigated surface finishing and tool flank wear in finish turning of AISI D2 steels (60 HRC) using ceramic wiper (multi-radii) design inserts. Multiple linear regression models and neural network models are developed for predicting surface roughness and tool flank wear. Figure 2.9 shows the

crater and flank wear of ceramic tool observed with scanning electron microscopy (SEM) after tests. They found that tool flank wear reaches to a tool life criterion value of $VB_C = 0.15\text{mm}$ around 15 min of cutting time at high cutting speeds due to elevated temperature.

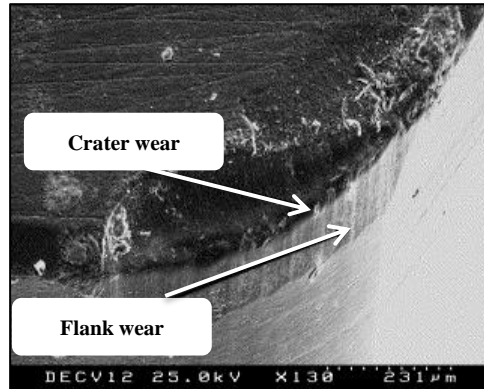


Figure 2.9 SEM image of the flank and crater wear of cutting tool (Ozel et al. 2007)

Lalwani et al. (2008) investigated experimentally the cutting parameters which influences on cutting forces and surface roughness in hard turning of maraging (MDN250) steel. Haddag et al. (2014) analyzed the tribological behavior and tool wear in rough turning of a large-scale part of nuclear power plants using grooved coated insert. Kumar et al. (2013) reviewed the advancement and current status of wear debris analysis for machine condition monitoring. Saini et al. (2012) found the influence of machining parameters on tool wear and surface roughness in hard turning of AISI H11 tool steel using ceramic tools. Makadia and Nanavati (2013) developed the surface roughness prediction model of AISI 410 steel with the aid of statistical method under various cutting conditions based on response surface methodology. Rao et al (2013) analyzed the workpiece roughness, vibration of workpiece and volume of metal removal rate through a laser Doppler vibrometer and a high speed FFT analyzer in boring process. They optimized the cutting parameters using Taguchi method and multiple regression analysis used to express the empirical relation of tool life with volume of metal removed and amplitude of workpiece vibrations and roughness of machined surface. They observed that amplitude of vibration increases as the tool wear increases and feed rate is the significant parameter for affecting surface roughness.

2.4.2.2.1 Tool wear analysis

During machining process, cutting tool will undergo different condition (flank wear, tool chipping, tip breakage, etc.) which makes the process unstable and results in poor surface finish and inaccurate dimension of the product. Wang et al. (2012) investigated the wear behavior and chip formation in drilling of forged steel S48CS1V. Figure 2.10 shows the catastrophic tool breakage.

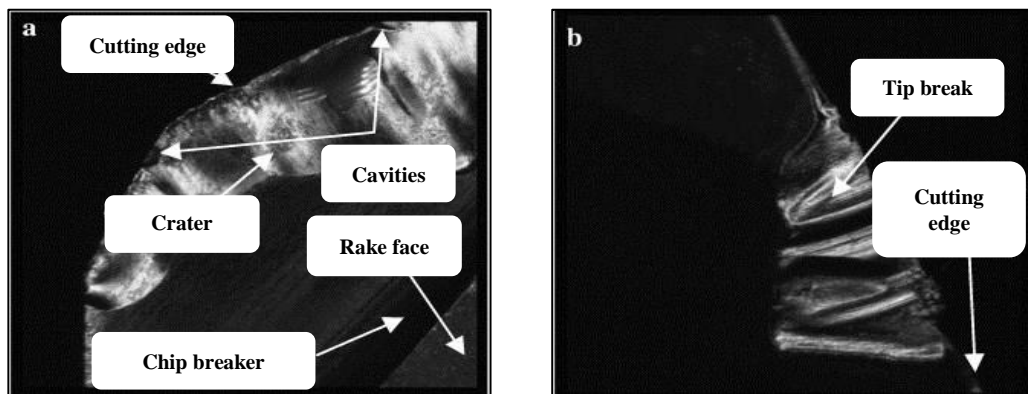


Figure 2.10 Profile of cutting edge. (a) Catastrophic wear viewed from rake face, (b) tip breakage (Wang et al. 2012)

They analyzed wear mechanisms and chip morphology in different machining conditions. They found that the gun drill with TiAlN coating suffered from adhesive wear, which can be seen on the wear pad and chemical diffusion wear on flank face due to the high temperature and stress. Figure 2.11 shows the chip formation during drilling. The plastic deformation occurred due to high alternative stress and cold welding for the atomic absorption.

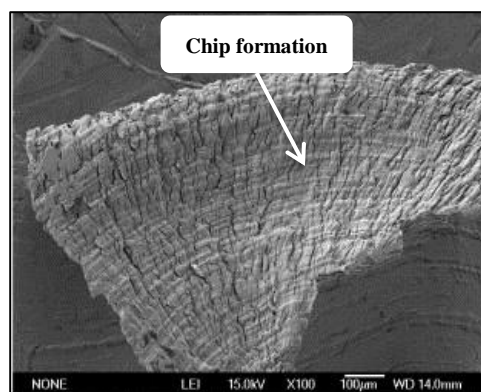


Figure 2.11 SEM micrograph of the free face of chip (Wang et al. 2012)

Grzesik (2008) reported an extensive characterization of the surface roughness generated during hard turning (HT) operations performed with conventional and wiper ceramic tools at variable feed rate and its changes originated from tool wear. Author observed similar trends showing the increase of both Ra and Rz height surface roughness parameters for both tested tools. Comparable values of these parameters were recorded for conventional ceramic tools and wiper tools but working with twice feed rate.

Ning et al (2008) studied flank wear, crater wear and chip formation mechanism in end milling of steel H13 through SEM and EDX analyses. They analyzed the continuous, sawtooth chips and tool wear during milling under different cutting length and also they correlated the flank wear to the measured cutting forces. They reported for tool with TiAlCrN/NbN coating, tool wear rate has been reduced due to combination of protective oxide layer and the fine grain tough substrate was formed on the tool. Zhang et al. (2014) investigated fracture tool wear characteristics and machined surface quality measurement with the help of cutting chips. Figure 2.12(b) shows the fracture tool wear and the corresponding chip formation with imprinted ridges as shown in figure 2.12(a). They proposed a novel tool wear monitoring in ultra-precision raster milling based on mathematical modeling and geometric characteristics of cutting chips.

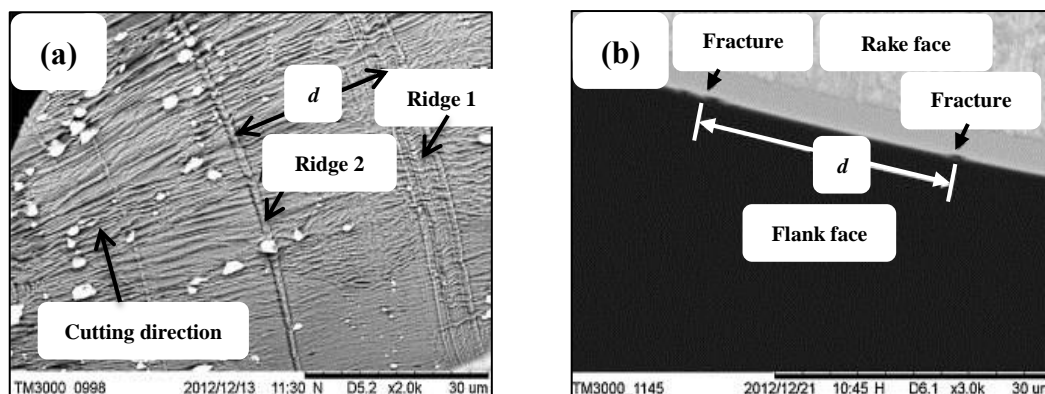


Figure 2.12 Ridges imprinted on (a) the chip surface by (b) the fracture wear of cutting edge (Zhang et al. 2014).

2.4.2.2.2 Chip formation mechanism

Occurrence of different chip formation (upward curling chips, cross curling chips, etc.) represents the condition of the tool. Wang et al (2014) studied the mechanism of chip formation (upward curling and cross curling) as shown in figure 2.13, during high speed milling of hardened steel. They studied the formation of continuous and sawtooth chips under different machining parameters such as axial depth of cut, feed rate and cutting speed. They found that the chip of workpiece with different hardness could be controlled as a continuous chip by optimizing the different combination of depth of cut, feed rate and cutting speed. Also they developed geometric model for sawtooth chip formation to compute shear strain and strain rate during chip formation.

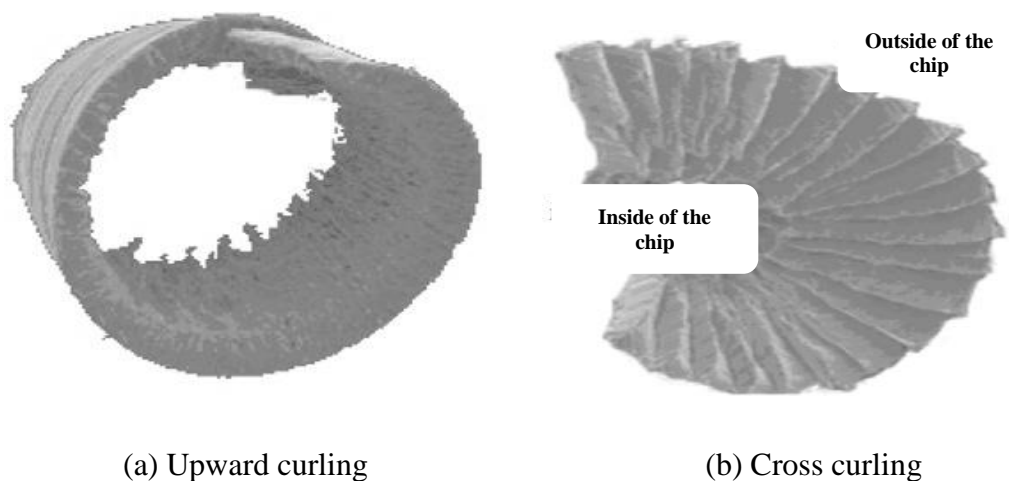
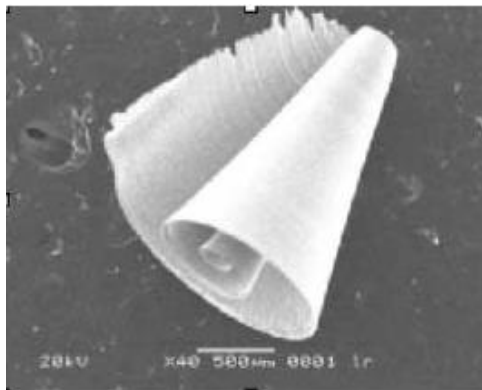


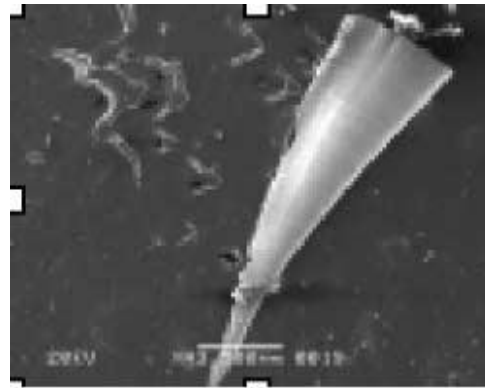
Figure 2.13 Different types of chip formation (Wang et al 2014)

Kovac and Sidjanin (1997) studied the chip formation and surface integrity during milling process using light microscope and SEM. They found that the reason for crack propagation and built-up edge (BUE) formation. Prakash and Kanthababu (2013) have established the relationships among the tool-wear (flank wear), acoustic emission signals, surface roughness, and chip morphology in order to develop a methodology for online detection of tool-wear in micro-end-milling for several metallic materials. Further, Ning et al (2001) investigated the mechanism of chip formation and corresponding surface finish in high speed milling of steel H13 using SEM and energy dispersive X-ray (EDX) spectroscopy methods to analyze the interaction between cutting edge and chip formation. They analyzed four types of chip

formation such as stable chips, chatter chips, critical chips and severe chips as shown in figure 2.14 (a-d), under different cutting conditions. They found that flank wear is the dominant tool wear during process and also chip analysis provides a simple and cost efficient way to determine and optimize the machining process.



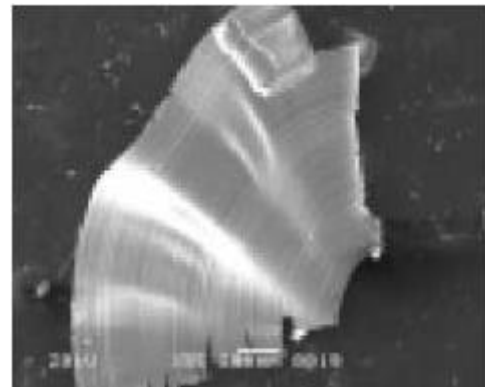
(a) Stable chips



(b) Chatter chips



(c) Critical chips



(d) Severe chips

Figure 2.14 (a) Stable chips, (b) chatter chips, (c) critical chips and (d) severe chips under different cutting conditions (Ning et al. 2001)

2.4.2.3 Surface roughness analysis

Surface roughness is one of the most important factors in evaluating the quality of the machining operation. Because it is sometimes easier to measure the surface roughness of the machined component than to measure the amount of wear on the tool, surface roughness estimation can be utilized to monitor the tool wear (Jang et al. 1996). Machining conditions, such as cutting speed, feed rate, depth of cut, tool geometry and material properties of the tool and workpiece, significantly influence the surface

finish of the workpiece material. If these factors are known and set correctly, an in-process surface roughness measurement system can also indicate a tool condition (Wilkinson et al. 1997; Coker and Shin 1996). Surface inspections in industry have been measured typically as a post-process operation, which is both time consuming and uneconomical since a number of non-conforming parts can be produced prior to inspection. This underlines the importance of devices to monitor surface finish continuously without interrupting the machining process.

Several methods have been used to estimate surface roughness on-line in flexible manufacturing systems (Benardos and Vosniakos 2003; Ozel and Karpaz 2005; Azouzi and Guillot 1997). Some of the methods are as follows

- Correlation between surface roughness and machining vibration to develop an online roughness measuring technique.
- Image processing, stray light and laser focus methods.
- Roughness measurement with non-contacting inductance pick-up.
- Direct measurement with a stylus (contacting sensor or profilometer).
- Ultrasonic sensing approach.

As with TCMS, roughness monitoring systems can also be divided into direct and indirect approaches. This section concentrates on the tool wear and vibration monitoring with relevance to surface roughness monitoring.

2.4.2.3.1 Surface roughness and tool wear

The surface roughness of machined components holds direct correlation with the amount of wear on the cutting tool (Chou and Evans 1997). A logical next step is to use the roughness information to control the machining operation as the tool wear progresses. To maintain a certain roughness, the feed and depth of cutting must either be increased or decreased to maintain the workpiece surface quality. For this, relatively simple geometric control systems can be developed, that measures the roughness and calculates an error value, further change in machining parameters proportionately. Scandiffio et al. (2015) investigated the influence of toolpath direction and tool-workpiece surface contact on machining force, surface roughness,

tool wear, and tool life in free-form milling with a ball-end cutting tool when milling hard quenched and tempered AISI D6 steel. They identified the most influential factor for tool life was tool vibration. Bonifacio and Diniz (1994) found that vibration of the tool is a reliable way to monitor the growth of surface roughness in finish turning, and can be used to establish the tool life. Flank and groove wear mostly influence surface roughness. Some researchers (Abouelatta and Madl 2001; Risbood et al. 2003) found that there is increased amplitude of roughness at the beginning stages of cut, a lesser tendency in the middle and again an increasing tendency at the end of tool life. In finish turning, it is important to monitor the surface roughness in order to establish the moment to change the tool.

2.4.2.3.2 Vibration monitoring and surface roughness

The average surface roughness of a machined part can be assumed to be the result of the super positioning of a theoretical profile computed from cutting kinematics, and of the oscillatory profile determined by the relative vibration between the cutting edge and the workpiece (Thomas et al. 1996). The machining kinematics are influenced by parameters like speed and feed rate, while the relative vibration between the tool and workpiece are caused by the random resistance against machining, which causes a stick-slip process between the chip and the tool. The ideal or theoretical surface profile can be easily calculated from the machining kinematics. The actual surface profile can be measured, or it can be estimated by measuring the relative vibration between the tool and the workpiece. This makes it possible to determine the surface roughness on-line without interrupting the machining process. However, there are lots of practical problems involved, when working in a realistic machining environment. One such problem is that chatter between the tool and workpiece results large vibrations that cannot be superimposed on the surface roughness. Another problem is that loose metal parts and other external factors easily distort signals from the sensors. However, the method has been successfully implemented in dry turning with ferrous metals (Jang et al. 1996). Bonifacio and Diniz (1994) conducted experiments with coated carbide tools in finish turning, measuring in the range of 0 to 8 kHz. The vibration was measured on the two channels, one in the machining direction and other in the feed direction. The root mean square (RMS) value was used to compare set of

measurements. They also varied the feed and cutting speeds with different experiments. They observed that cutting speed had a much larger influence on the tool life than the feed. They also found that both vibration and roughness measurements corresponds to a certain amount of tool wear at a given time. They also discovered that an increase of flank wear causes an increase in vibration in a large frequency range (0-8 kHz).

2.5 MODEL BASED APPROACH

Model based approach (Analytical and computational) can be used for monitoring the cutting tool conditions. In mathematical model based approach analytical models can be built using Taylor's tool life equations to analyze the cutting tool state with different cutting conditions. Whereas in many literatures reported usage of finite element method (computational approach) in analyzing/simulating machining operations for different cutting parameters to monitor the machining process without conducting the experiments.

2.5.1 Mathematical model based approach

Analytical models are very useful to study the effects of tool geometry on the various machining parameters, but these models are too complex in a real-time TCMS. The non-linear, stochastic and time invariant nature of machining process, makes modelling very complex and difficult (Silva et al. 1998). A transformation between the signal characteristics and the physical law representing the process is necessary to establish such a model. Since the machining process is complex, to build analytical models in most instances are difficult. The only remaining option is empirical modelling which can be performed parametrically or non-parametrically. Parametric modelling usually represents only an adaptation of the analytical model and is of limited capability. This method also requires the inputs from mechanisms to translate into simple rules (Lever et al. 1997). Non-parametric modelling methods are based on a statistical description of natural phenomena. Empirical models have been used with great success for describing many manufacturing processes. Grabec et al. (1998) used empirical modelling for estimating tool sharpness on a lathe, for the determination of surface roughness in a grinding process.

A common mathematical model in the case of tool wear can be generated by Taylor's tool life equation. The equation is:

$$VT^n = C \quad (2.1)$$

The equation provides a relationship between cutting speed V (m/min), and tool life T (minutes), and two parameters, n and C depending on tool and workpiece material. The Taylor's parameters are generally determined empirically, if they are unknown. This method is useful in establishing a tentative value for the expected tool life. It was found from experiments that the Taylor's equation could yield estimates within ± 35 percent of the actual tool life. This equation is common in the literature and various versions have been adapted to enhance the equation's performance (Lever et al. 1997; Dos et al. 1999; Silva et al. 1998; Vagnorius et al. 2010; Karandikar et al. 2014; Lalbondre et al. 2014). The use of an analytical model for force reconstruction for wear identification was proposed by Braun et al. (1999). This model can be used for the prediction of chatter onset. Ravindra et al. (1993) proposed a mathematical model based on multiple regression analysis. The model describes the wear-time and wear-force relationships for turning operations. They observed that the good correlation was found between the cutting force and progressive tool wear.

2.5.2 Computational model based approach

The new challenge is the implementation of effective models in a finite element environment in order to perform a reliable prediction of tool wear. In fact, the development of finite element (FE) techniques offered a new testing concept exalting the role of the numerical simulation, since both time and costs can be reduced. For this reason, the introduction of the finite element codes and their computational improvements that make this tool able to approach machining process simulation represents a break point in the past and opens a new scenario (Filice et al. 2007). Yen et al. (2002) used FEM technique for estimating tool wear of carbide tool in orthogonal cutting using new methodology based on measuring stresses and temperature on the tool face. They found tool wear by applying an empirical wear model and also by using FEM simulation using Deform 2D. A lagrangian based analysis was carried out using the LS-DYNA software. They simulated cutting forces

and compared with forces measured by experiments. They observed that the chip formation was realistically modelled, but the output of forces from the analysis was overestimated when compared with forces measured during orthogonal machining experiments (Villumsen and Fauerholdt 2008). Lungu and Borzan (2012) analyzed the influence of cutting speed and feed rate on tool geometry, temperature and cutting forces in machining AISI 1045 carbon steel using tungsten carbide coated with a TiCN. They used Deform-2D software for FEM simulation of machining. They found that increasing the cutting speed increases the temperature but the cutting forces were decreasing. Ceretti et al. (1996) conducted simulations of orthogonal plane strain cutting process using FE software Deform-2D. They have used damage criteria for predicting, when the material starts to separate at the initiation of cutting for simulating the segmented chip formation. Further, they also studied the influence of machining parameters such as cutting speed, rake angle and depth of cut. Subsequently, they compared computed cutting force, temperature, deformations and chip geometry with experimental results. Jaharah et al. (2009) developed an orthogonal metal cutting model and studied the effect on tool geometries with various rake angles, clearance angle and cutting parameters using finite element (FE) software Deform-2D. They found that the change in cutting tool geometries had high influence on stress and temperature generation.

2.6 MOTIVATION FROM LITERATURE REVIEW

Considerable research work has been carried out in TCMS, and there are a number of approaches that can be used for condition monitoring of single point cutting tool. Predominant approach is vibration analysis, which enables to identify healthy and faulty cutting tool. Conventional vibration analysis involves prediction of natural frequencies and mode shapes. Response studies in time domain or frequency domain can only be able to give information about post damage of the cutting tool. This concept can be extended with a machine learning approach for online tool condition monitoring studies to identify different tool conditions. The performance of TCMS depends on classifiers used for diagnosis. Still many investigations are possible in finding best classifier and in building on-line fault diagnosis system using combined vibration signal and cutting forces with data mining approach. Literature review

shows that recurrence analysis techniques have been sparsely used in engineering application, though it is capable of detecting subtle changes in dynamic behavior. Tribological studies are very limited in TCMS. Attempt can be made with tribological studies in conjunction with online monitoring system. Nowadays finite element method (FEM) is applied widely for computing cutting forces and tool wear. Virtual simulations can give better insight regarding stresses induced, temperature variation, sliding velocity etc., all of which are difficult to capture experimentally and are most required information's in tool wear monitoring. In this proposal, vibration signals and cutting force will be acquired under healthy and simulated faulty conditions which will be used for online monitoring of a cutting tool. Along with online monitoring studies, tribological studies will also be carried out as an offline monitoring to explore additional information.

2.7 SCOPE OF THE RESEARCH WORK

Tool condition monitoring systems consist of many concepts that can be combined in numerous ways. Some of the methods were developed three decades ago, and have been implemented in industry. Other methods are fairly new, and still in the development stage. The aim of the present work to develop a real-time efficient tool condition monitoring system (TCMS) using vibration signals acquired while machining. The sensing technologies applied in turning operation of tool condition monitoring research cover most of the available methods, although there is a bias towards the use of AE and tool tip temperature measurements. To determine the state of tool wear, visual inspection of cutting tool is often undertaken. However, this is not applicable in real-time either. It is worth noting that there is little interest in using cutting forces, vibrational analysis and accelerometers with turning, when compared to other machining operations. So this study aims to explore the possibilities of using vibration analysis and cutting force dynamics to improve fault detection system. It is also interesting to note that limited research work has been considered the use of chip formation type as a source of tool condition monitoring information. In addition, the use of surface roughness parameters of workpiece for TCM in machining operations in turning is quite rare. Because of the complexity of the cutting process, work on computational methods is largely incomplete, and thus always a focus for research.

The combination of chip formation type or surface roughness parameters analysis does improve this situation significantly, and additional research on computational approach in this area may produce a more flexible and adaptive type of system. In the development of TCM for turning operation, several important trends have been observed. Advanced signal processing and statistical analysis methods are not widely used in the past. For this reason, this research work concerns with fault diagnosis of single point cutting tool are using online and offline condition monitoring techniques in conjunction with advanced signal processing approaches.

In the past few decades, significant research has been carried out, leading to the development of a large variety of techniques to detect cutting tool failure in machining. From the literature review problem areas where more focus is needed are as follows.

- Better performance of tool condition monitoring system (TCMS) depends on classifiers used for diagnosis. Still many investigations are possible in finding best classifier.
- Many investigations are possible in building on-line fault diagnosis system using vibration signals.
- Tribological studies are limited in the literature of TCMS, attempt can be made with tribological studies in conjunction with on line monitoring system.
- The vibration signal based condition monitoring often require signal processing techniques, like spectral, cepstral and wavelet analysis which results in a hindrance to real time application due to the computation time. The technique of RP and RQA is well suited for the analysis of nonlinear and chaotic systems and can basically be used for signal processing without denoising.
- Nowadays finite element method (FEM) is used widely for computing cutting forces and tool wear measurement. Virtual simulations can give better insight regarding stresses induced, temperature variation, sliding velocity etc., all of which are difficult to capture experimentally and are much required information in tool wear monitoring.

In this research work, the above mentioned issues will be addressed to develop a real time efficient tool condition monitoring system (TCMS).

2.8 OBJECTIVES OF THE RESEARCH WORK

Looking at the ongoing developments in the area of tool condition monitoring and scope for further improvements, the following broad objectives have been derived from the literature review gap of the present research study,

1. Fault diagnosis of single point cutting tool based on data mining approach using vibration signals acquired during machining with healthy and faulty cutting tools.
2. Fault diagnosis of single point cutting tool with advanced signal processing techniques such as cepstrum analysis and continuous wavelet technique.
3. To analyze the vibration signals using a nonlinear time series analyzing technique called recurrence quantification analysis (RQA), which captures the underlying dynamics of turning process qualitatively and quantitatively.
4. Condition monitoring of tool based on cutting forces analysis, computational studies, chip morphology studies and surface profile measurement of workpiece.

2.9 SUMMARY

This chapter presented elaborated review of existing tool condition monitoring techniques. Literature was basically categorized based on direct and indirect methods for tool condition monitoring, online and offline monitoring techniques, signal processing technique, model based approach and machine learning technique. Along with the above, an overview of applications of each method is also discussed citing various researchers who have successfully implemented these techniques for their applications of interest. Experimental approach and methodology involved in this research work is described in chapter 3.

CHAPTER 3

EXPERIMENTAL APPROACH AND METHODOLOGY

3.1 INTRODUCTION

Machining with a worn tool increases the fluctuation of forces on the cutting tool. Due to these force fluctuations, vibrations occur in the system. Therefore by monitoring the level of vibration and cutting force, tool wear can be assessed. Present work, reports investigations to predict the tool condition using machine learning approach, recurrence quantification analysis, surface roughness measurement of workpiece, tool wear and chip morphological studies through acceleration and cutting force measurement, while machining with optimized cutting parameters. This chapter is related to the experimental setup and methodology involved in the research work and also provides description to data acquisition and experimental procedures followed to investigate the fault detection of single point cutting tool.

3.2 EXPERIMENTAL SETUP

Experiments were carried out on engine lathe. It is driven by the motor which is having a power of 3.73 kW and it has a machining speed range from 150 rpm to 830 rpm and feed rate from 0.015 mm/min to 0.5 mm/min. All experiments were conducted under dry cutting conditions. The work piece was clamped to the four jaw chuck and few initial turning pass were carried to remove oxide layer on workpiece surface that is formed due to heat treatment and also due to the presence of any unevenness on the workpiece. The piezoelectric tri-axial accelerometer is mounted on tool holder using magnetic mount and attached to the upper surface of the cutting tool holder, as close as possible to the cutting edge. The dynamic forces of cutting tool were measured with lathe tool dynamometer. The figures 3.1 and 3.2 show the schematic line diagram and experimental test setup used for fault diagnosis of cutting tool condition.

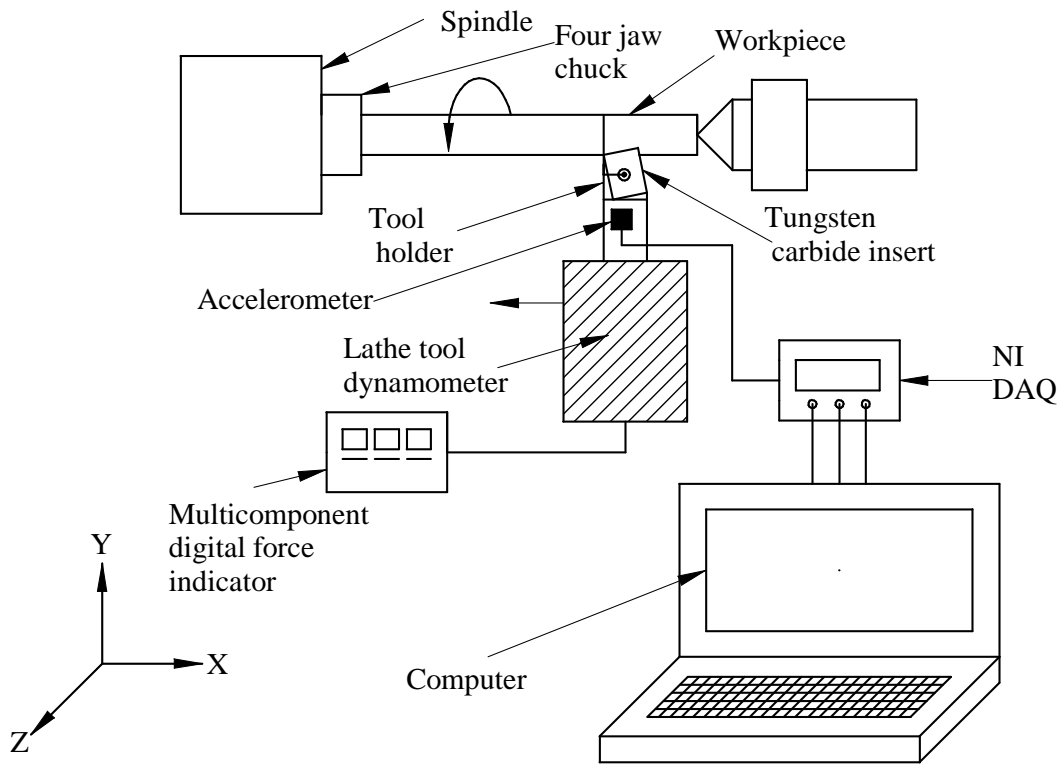


Figure 3.1 Schematic line diagram of experimental setup

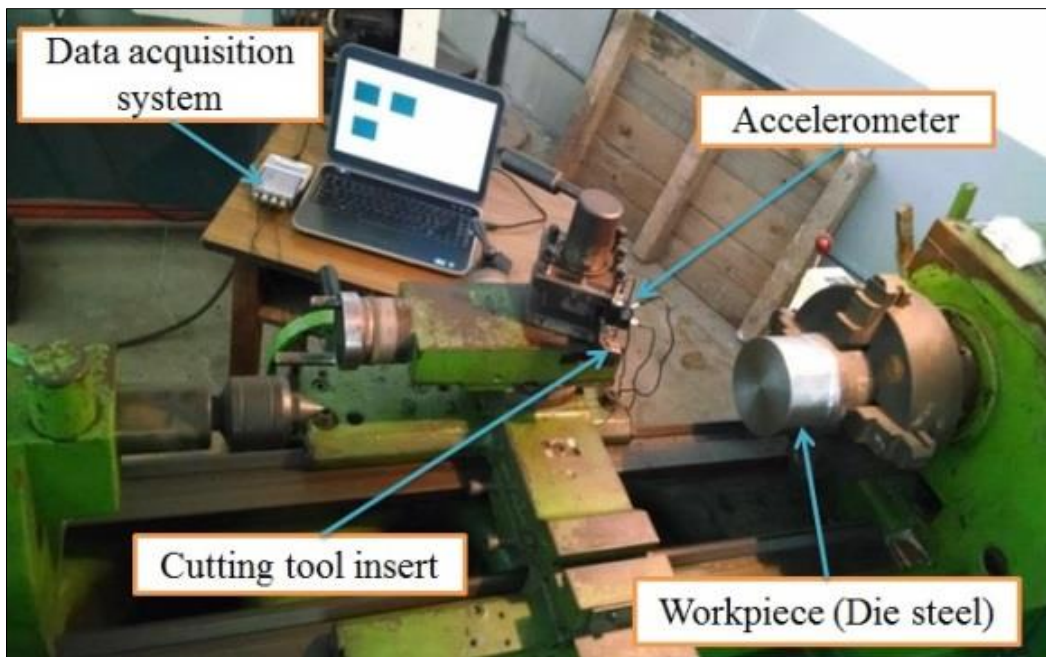


Figure 3.2 Condition monitoring test setup

3.2.1 Work material

AISI H13 die steel have been used in forming dies, plastic moulds, hot forging dies and hot extrusion tooling in many manufacturing industries due to its excellent toughness, good resistance to thermal shock and fatigue, hardenability and high-temperature strength. A work piece of die steel (AISI H13) diameter of 100 mm and length of 150 mm was used in the study and it was heat treated to 800 °C for 4 hours then allowed to cool down upto 600 °C in furnace and followed by air cooled in order to get homogeneous structure. The following sections illustrate the elemental composition of AISI H13 steel and it was tested through energy dispersive x-ray analysis which exists in scanning electron microscopy (modal-JSM-6380LA, JEOL; Operating voltage- 30kV; Magnification range-300000). Work material properties and chemical composition of the workpiece is as shown in table 3.1 and 3.2 respectively.

Table 3.1 Physical and mechanical properties of AISI H13 steel (Taktak 2007)

Work material properties	AISI H13 steel
Density (kg/m ³)	7800
Hardness (HRC)	40-55
Young's modulus (GPa)	210
Poisson's ratio	0.3
Thermal conductivity (W/m K)	24.3

Table 3.2 Chemical compositions of the work material

C	Si	Mn	P	S	Cr	Mo	V
0.32-0.45	0.80-1.20	0.20-0.50	0.03	0.03	4.75-5.50	1.10-1.75	0.80-1.20

3.2.2 Tool material

The tungsten carbide cutting tool insert is a removable type and offered eight squared working edges. Its standard designation is SNMG120408 and it is manufactured by Kennametal India Ltd, Bangalore. The physical and mechanical properties of WC are

summarized in table 3.3. Tool holder is codified as PSBNL 20 mm × 20 mm K12 with a common active part tool geometry described by lead angle ' ψ_r ' = +75°, cutting edge inclination ' λ ' = -6°, rake angle ' γ ' = -6° and clearance angle ' α ' = +6°.

Table 3.3 Physical and mechanical properties of the tungsten carbide tool insert
(Kennametal India Ltd, Bangalore)

Tool material properties	Tungsten carbide (WC)
Density (kg/m ³)	13300
Hardness (HRC)	75
Young's modulus (GPa)	530
Poisson's ratio	0.24
Thermal conductivity (W/m K)	110

3.3 DATA ACQUISITION USING LAB-VIEW

3.3.1 Sensors used in the experiments

3.3.1.1 Accelerometer

Piezoelectric accelerometer (YMC145A100) was mounted on the tool shank with an operating frequency range between 1 to 5000 Hz is used to pick-up vibration signals (magnitude of acceleration with respect to time). Figure 3.3 shows the triaxial accelerometer and specification of the sensor is provided in table 3.4.



Figure 3.3 Piezoelectric triaxial accelerometer

Table 3.4 Specification of the accelerometer

Make	Integrated electronic piezoelectric
Model	YMC145A100
Sensitivity X axis	97.90 mV/g
Sensitivity Y axis	95.65 mV/g
Sensitivity Z axis	104.6 mV/g
Measuring range	± 50 G
Test environment temperature	22 ⁰ C
Temperature range	-41 to 121 ⁰ C
Size	25.4x25.4x14mm

3.3.1.2 Lathe tool dynamometer

Strain gauge type lathe tool dynamometer (621C) was used to measure the cutting forces. The dynamometer was mounted in the tool post. The three components of the cutting forces; feed force (F_x), thrust force (F_y) and tangential force (F_z), schematically shown in figure 3.4, were recorded using a standard dynamometer allowing measurements from 0 to 500 KgF.

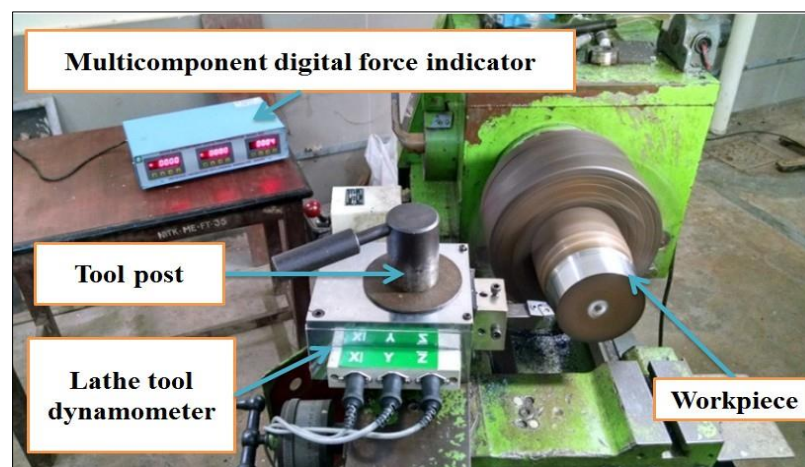


Figure 3.4 Experimental configurations for measuring the components of cutting force

3.3.2 NI-DAQ system

The NI USB-9234, shown in figure 3.5, along with high speed USB carrier is used for acquiring vibration signals. Specifications of NI USB-9234 are shown in table 3.5. The output of accelerometer is connected to NI USB-9234 via Bayonet Neill–Concelman (BNC) cables and from there it is connected to computer. The acquired signals were analyzed using LabVIEW software from National Instruments (NI).

Table 3.5 Specification of NI USB-9234

Parameter	Specification
Number of channels	4 analog input channels
ADC resolution	24 bits
Types of ADC	Delta-Sigma
Sampling mode	Simulations
Sampling frequency	25.6 kS/s
Input voltage	± 5 V

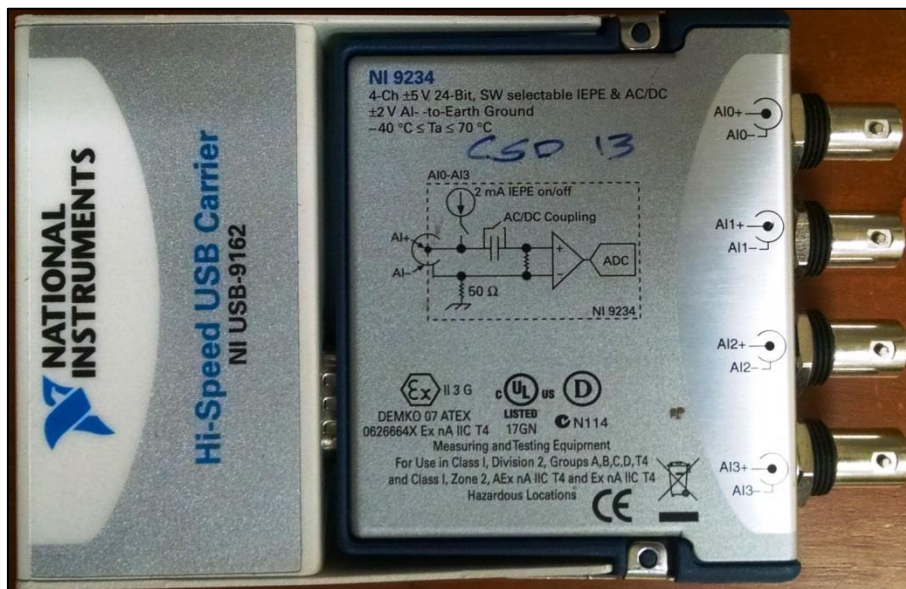


Figure 3.5 NI USB-9234 with NI USB carrier

To prevent aliasing, the signals were sampled at sampling frequency of 25.6 kHz, with 25600 points per 1 sec time interval under controlled testing conditions.

3.3.3 Software interface

A Virtual Instrument (VI) program was developed to acquire and analyze vibration data for these experiments.

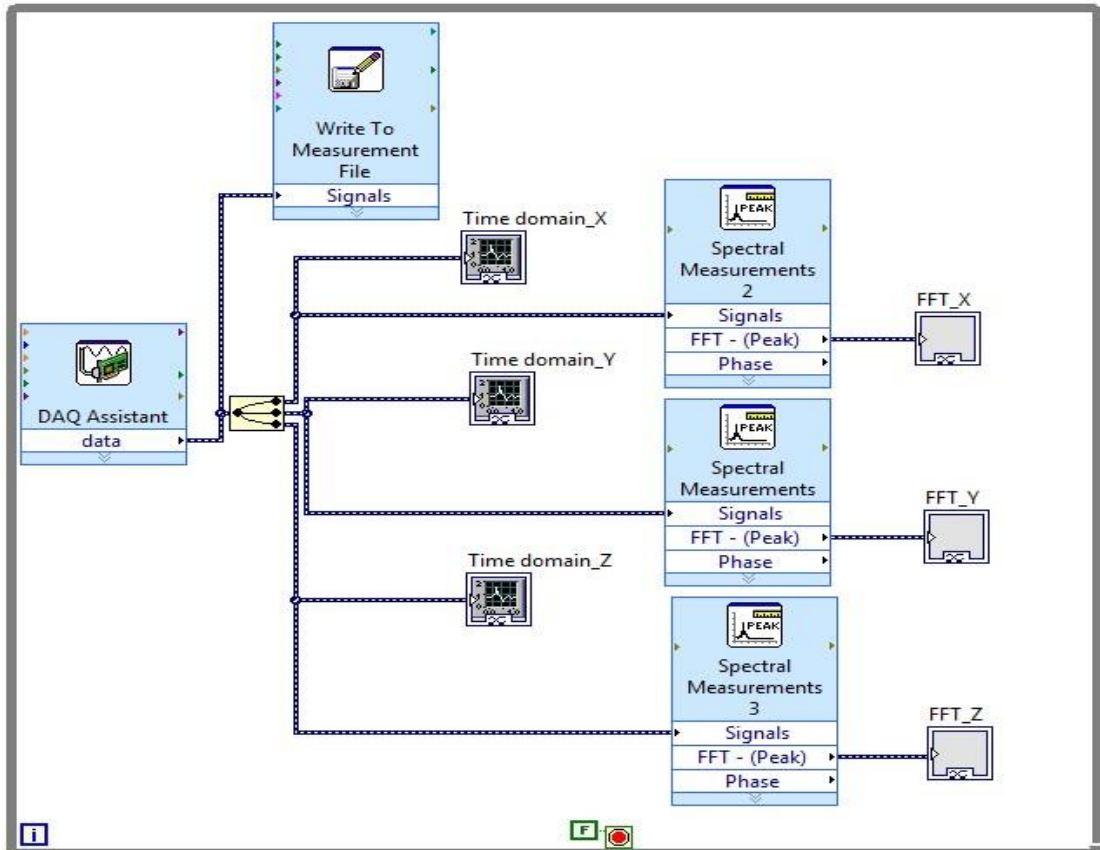


Figure 3.6 VI Block diagram for the data acquisition

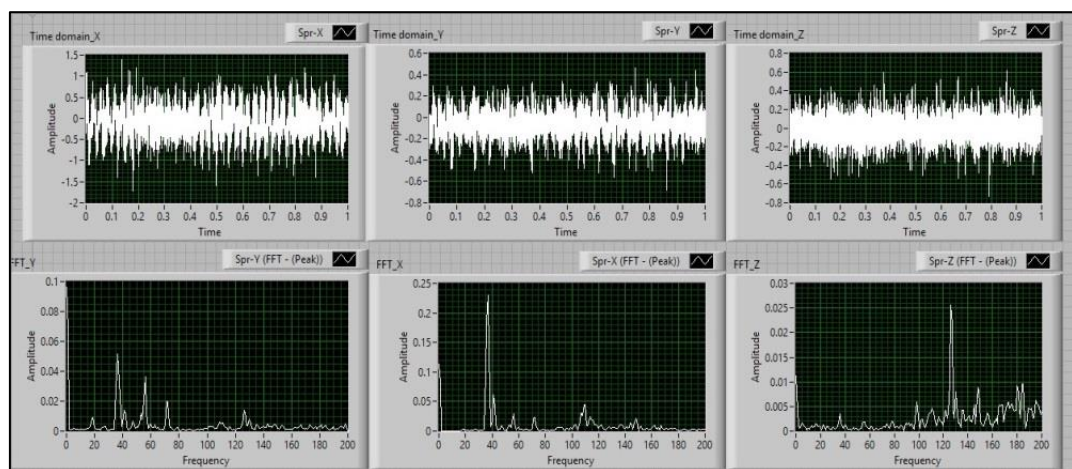


Figure 3.7 Front panel to represent the acquired data

Figure 3.6 shows the graphical block diagram of the VI program. The acquired data were converted into frequency domain by fast Fourier transforms in LabVIEW. Figure 3.7 shows the front panel of the VI program. In order to avoid inconsistency in data acquisition, three trials were performed at the set machining parameters and vibration signal was stored in the data file.

3.4 EXPERIMENTAL PROCEDURE

1. Experiments were carried out on a turning lathe with new and worn out inserts (Industrial practically worn out inserts). Vibration and cutting force signals were acquired from accelerometer and dynamometer while machining, using a new and worn out cutting tool inserts.
2. The cutting conditions used were: cutting speed = 236 m/min; feed rate = 0.1 mm/rev and depth of cut = 0.1 mm.
3. The five different tungsten carbide tool insert conditions shown in figure 3.8 considered in the present study are as follows:
 - The tungsten carbide tool insert is good/healthy/sharp and it is unused.
 - The tungsten carbide tool insert breakage (0.6 mm) condition.
 - The thermally cracked cutting tungsten carbide tool insert (0.3 mm) condition.
 - The cutting tungsten carbide tool insert having notch wear (0.4 mm) condition.
 - Rake face chipping (0.5 mm)

The experimental parameters considered in this present work are summarized in table 3.6.

Table 3.6 Experimental parameters

Lathe	Engine lathe
Workpiece	AISI H13 die steel 100 mm diameter
Tool holder type	PSBNL2020K12
Insert type	Tungsten carbide SNMG120408
Feed rate	0.1 mm/rev
Cutting speed	236 m/min
Depth of cut	0.1 mm

Different tungsten carbide cutting tool insert conditions used in this experiment are shown as in figure 3.8. Combination of different wears specified in the research work for tool condition monitoring is not reported in any of the literature so far, hence this study has been taken for investigation.

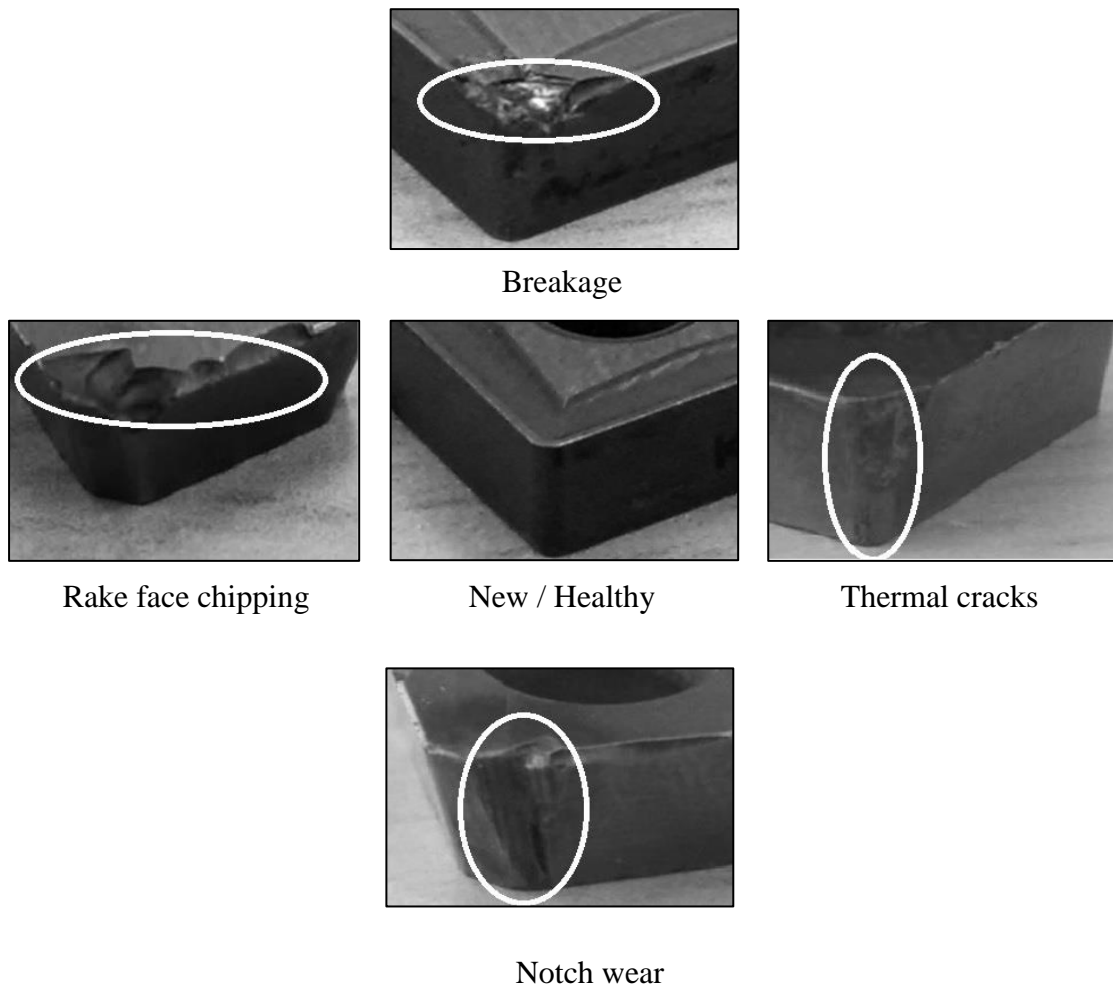


Figure 3.8 Five different tungsten carbide tool insert tip conditions

3.5 METHODOLOGY

The present research work comprises of two stages (1) Online monitoring and (2) Offline monitoring. Flow charts as shown in figure 3.9 and figure 3.10 represent a brief methodology involved in online and offline tool condition monitoring adopted respectively.

3.5.1 Online monitoring

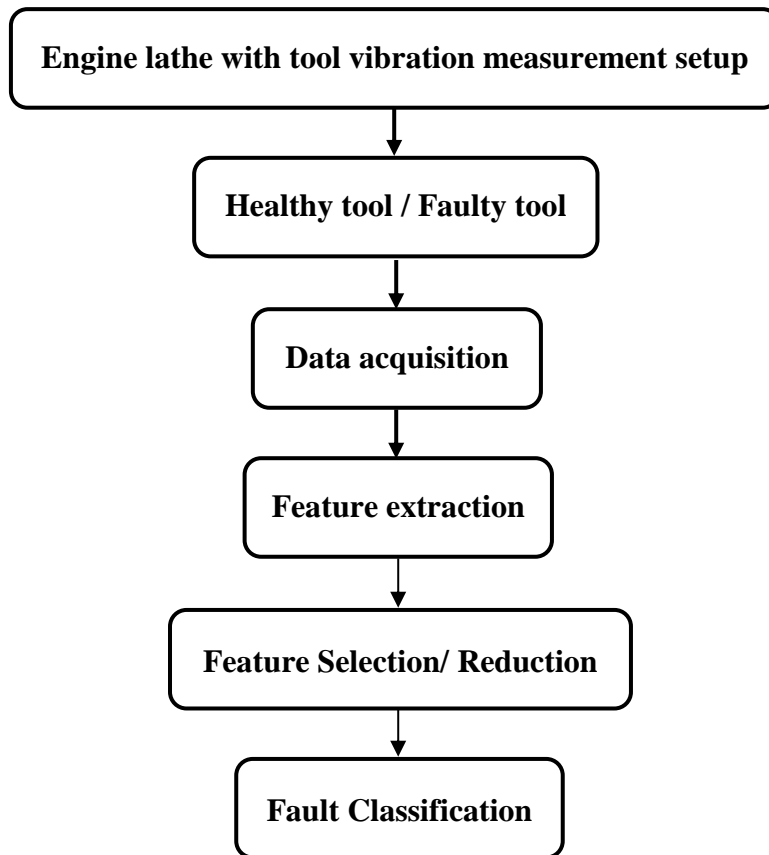


Figure 3.9 Online tool condition monitoring using machine learning approach

3.5.1.1 Vibration measurement setup

Turning operations are carried out in engine lathe with different tool conditions as shown in figure 3.8. Vibration signals were recorded for normal as well as different worn-out conditions of tungsten carbide (WC) tool insert from accelerometer mounted on tool holder. The different worn out conditions of the tool insert considered in the present study are breakage, thermal cracks, notch wear and rake face chipping.

3.5.1.2 Data acquisition

Total 200 samples were collected pertaining to different conditions or classes of tool inserts. Out of which 40 samples were from the normal healthy condition and for each fault condition 40 samples were collected for time interval of 1 s at sampling rate of 25.6 kHz. In order to avoid inconsistency in data acquisition, three trials were

performed at the set machining parameters and vibration signal was stored in the data file.

3.5.1.3 Feature extraction

The features are application dependent and one has to choose a set of good features for better classification on case-by-case basis. The process of computing such measures is called '*feature extraction*'. From the acquired vibration signals, statistical features, histogram features, EMD features and DWT features are extracted from vibration signals. This will be used further for feature selection and classification purpose.

3.5.1.4 Feature selection / reduction

The process of selecting the good features from a pool of features is called '*feature selection*'. The good feature will have feature values with minimum variation within a class and maximum variation between the classes. Many techniques are used for feature selection; among them principal component analysis (PCA) is widely used. For all cases of the study in this thesis, decision tree and PCA has been used for feature selection.

3.5.1.5 Fault classification

Feature classification is the last phase of the machine learning approach. In the classification process, the classification algorithm develops a model with the help of training data and the trained model is used to classify the test data belonging to various classes of faults. There are various classification techniques to classify the cutting tool conditions. Classification can be carried out using many classifiers. Amongst them, ANN, SVM, Bayes net, Naive Bayes, decision tree technique (J48) and K-star are very popular ones. Classifiers such as ANN, SVM, Bayes net, Naive Bayes, K-star algorithm and decision tree have been used for different fault classification from the selected features.

3.5.2 Offline monitoring

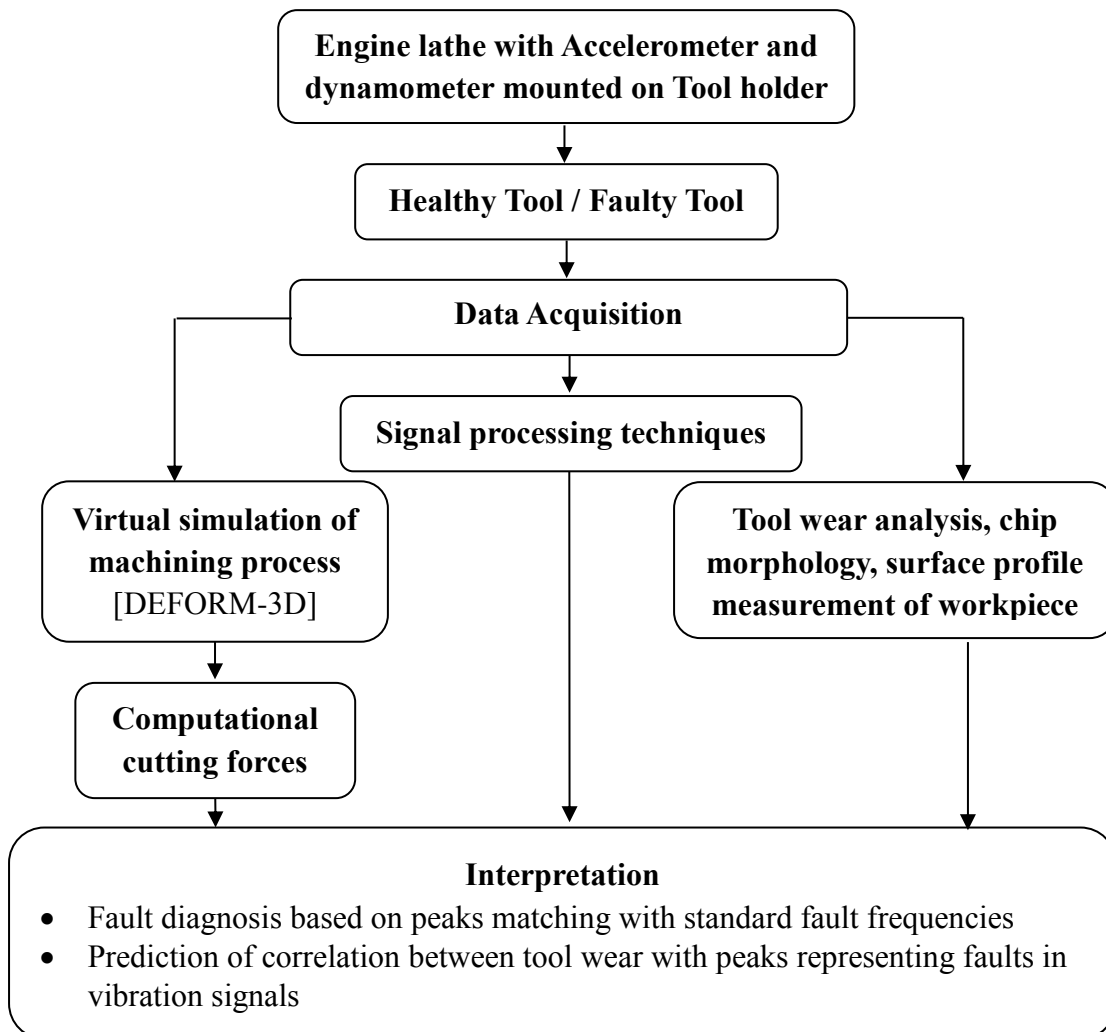


Figure 3.10 Fault diagnosis of cutting tool through offline monitoring techniques

3.5.2.1 Vibration and cutting forces measurement

Along with the 200 samples of vibration signals, cutting force signals were also acquired from normal as well as different worn-out conditions of tungsten carbide (WC) tool insert from accelerometer and dynamometer mounted on tool holder.

3.5.2.2 Data acquisition

Cutting forces were acquired for the different tool conditions using dynamometer. The characteristics of the measured cutting forces with change in depth of cut and cutting speed have been studied for five different condition of tungsten carbide tool insert.

Experiments were repeated with three trails to avoid inconsistency in data at the set machining parameters and cutting forces were recorded.

3.5.2.3 Signal processing techniques

Vibration signal acquired with different tool conditions of cutting tool are used for fault diagnosis using various signal processing techniques. Vibration signal of cutting tool can be analyzed in time and frequency domains. The spectrum may reveal intrinsic characteristics of the frequency components that could be difficult to observe in time domain representation. Cepstrum analysis, wavelet analysis and recurrence quantification analysis are used for fault diagnosis of cutting tool under signal processing techniques.

3.5.2.4 Cutting forces analysis

It has been widely established that variation in the cutting force can be correlated to tool wear. This can largely be attributed to the fact that force becomes important in worn tool conditions as a result of the variations produced due to friction between cutting tool flank and the workpiece. Hence cutting force analysis can be used as offline monitoring technique for fault diagnosis of cutting tools.

3.5.2.5 Machining process simulation with finite element method

Simulation was carried out using Deform 3D Machining V 10.2. Machining parameters such as cutting speed, depth of cut and feed rate were considered as variable to find cutting forces while machining. The cutting force variations with machining parameters are analyzed for the purpose of fault diagnosis.

3.5.2.6 Surface roughness measurement of workpiece

The surface roughness was measured as per Japanese industrial standard (JIS) 2001 by using '*Mitutoyo*' surface roughness tester. The average surface roughness (R_a), are considered for the current study. The surface roughness of the workpiece for different tool conditions were measured at three different locations and the average was taken as the process response.

3.5.2.7 Chip morphology studies

The chips produced during the machining process for different tool conditions were analyzed to understand the chip morphology using optical microscope. The chip formation type does affect the tool wear; the fluctuation of vibration components can effectively describe the chip formation type.

3.5.2.8 Tool wear analysis

The scanning electron microscope (modal- JSM-6380LA, JEOL; Operating voltage- 30 kV; Magnification range-300000) used to capture high resolution images of different wear zone and SEM analysis has been carried out on the worn tungsten carbide insert cutting tools to determine the tool wear mechanisms.

3.6 SUMMARY

This chapter started with discussing about the experimental set up used for research work. Subsequent section describes the data acquisition systems, virtual instrumentation and experimental procedure involved in undertaking the required tests. Later sections provide a conceptual overview of methodology in two major methods. In the subsequent chapter above said methods have been applied to study the condition of the cutting tool.

CHAPTER 4

FAULT DIAGNOSIS USING SIGNAL PROCESSING TECHNIQUES

4.1 INTRODUCTION

Condition monitoring of single point cutting tool based on vibration signal processing is an attractive research area. Vibration signal analysis using signal processing technique is extensively used for condition monitoring of machinery systems (Oppenheim and Schaffer 2004; Badaoui et al. 2001; Randall et al. 2012). Vibration signal of cutting tool can be analyzed in time and frequency domains. The spectrum may reveal intrinsic characteristics of the frequency components that could be difficult to observe in time domain representation. Fast Fourier transform analysis (FFT), cepstrum analysis, wavelet analysis and recurrence quantification analysis are extensively used fault detection techniques. This chapter utilizes vibration signal data from vicinity of lathe cutting tool for fault detection using various signal processing techniques as discussed below.

4.2 TIME AND FREQUENCY DOMAIN ANALYSIS

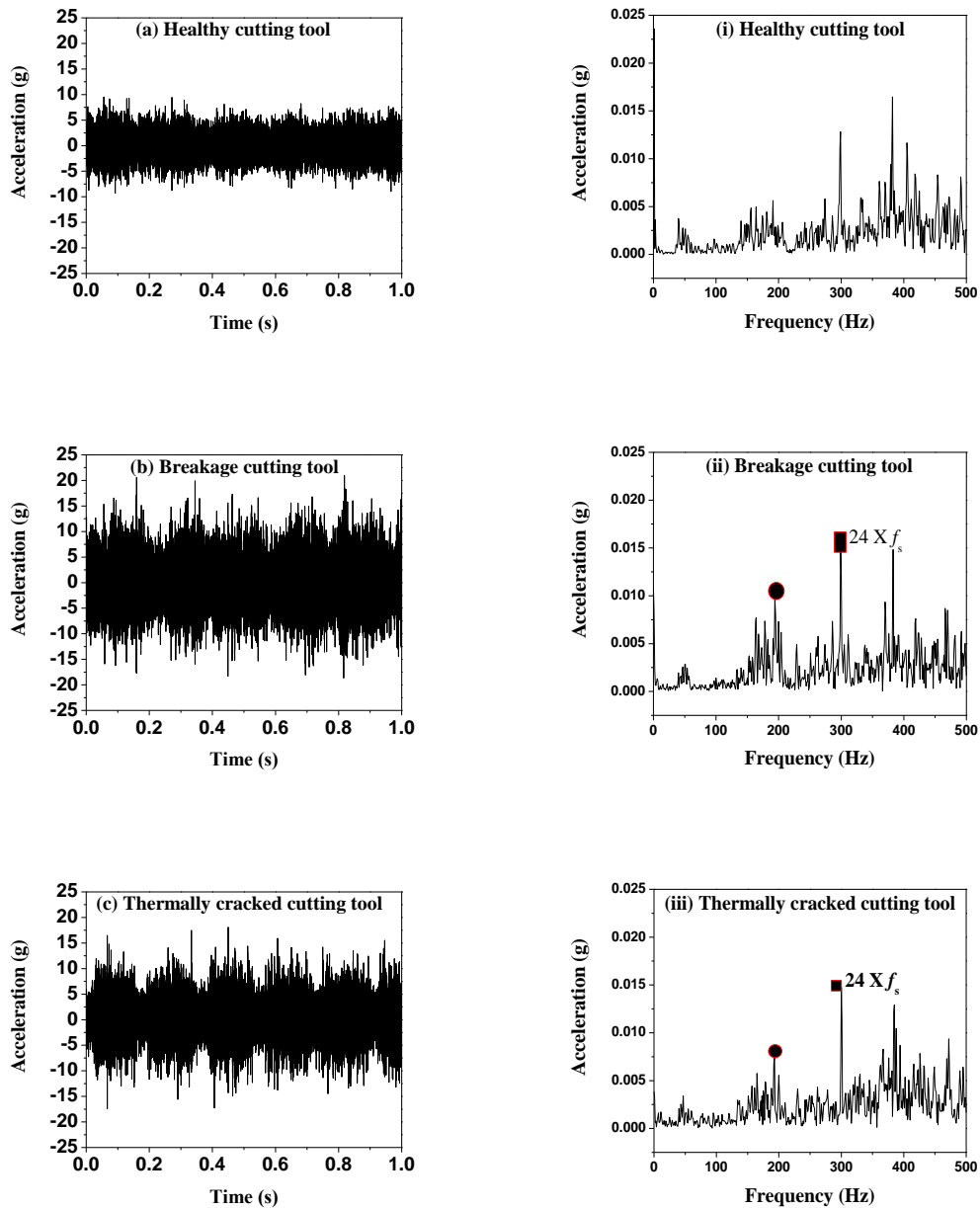
Time domain plot helps to examine the amplitude and phase information of the vibration signal to determine the failure/defect of any rotating machinery system. Fault detection using time series response is difficult task. Fourier transform (FT) is most widely used technique in vibration signal analysis, which converts given signal from time domain to frequency domain. Frequency analysis makes use the Fourier transform pair of equations to convert a signal from the time domain to the frequency domain and vice versa. Fourier's approach is based on the assumption that any waveform can be represented as the superposition of a series of sine and cosine waves at different frequencies. A Fourier series is used for representation of continuous-time periodic signals. For continuous-time aperiodic signal transient signals, the Fourier transform or analysis equation is used (Sujatha 2010). This is defined as

$$X(\omega) = \int_{-\infty}^{+\infty} x(t) e^{-i\omega t} dt \quad (4.1)$$

The inverse Fourier transform or synthesis equation is given by

$$x(t) = \frac{1}{2\pi} \int_{-\infty}^{+\infty} X(\omega) e^{i\omega t} d\omega \quad (4.2)$$

Figure 4.1, shows the time and frequency domain plots of vibration signals recorded for normal as well as different worn-out conditions of tungsten carbide tool insert.



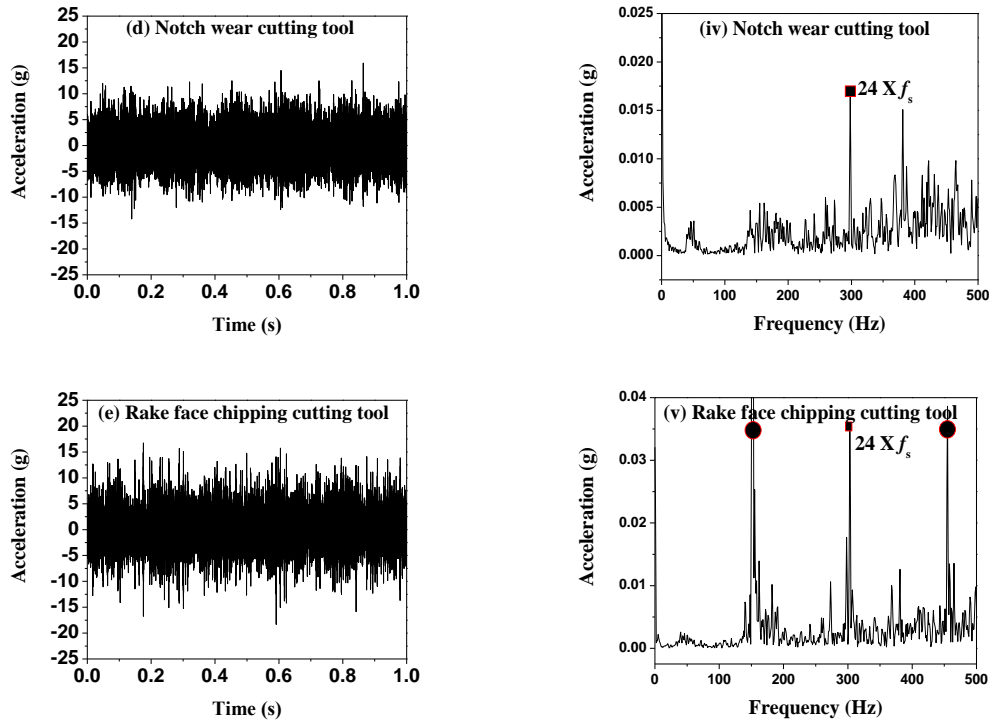


Figure 4.1 Acceleration with healthy and faulty cutting tool inserts in time domain (a-e) and (i) to (v) represents corresponding spectrum

In turning process, the vibration of cutting tool depends on cutting force (Chiou et al. 1998). This cutting force signal is periodic and its variation depends on spindle rotating frequency ' f_s ' and it is defined as,

$$f_s = \frac{n_s}{60} \quad (4.3)$$

Where,

n_s is the spindle speed (in revolutions per minute).

While the presence of peaks at additional frequencies represents the chatter.

Time domain plots (Figure 4.1 (a) to (e)) depict that, as the tool wear progress or the condition of tool changes, the acceleration level increases for all the faulty tool conditions, but it is very difficult to recognize the different condition of the tool. It means that time domain technique for vibration signal analysis gives overall vibration level but do not provide any diagnostic information.

The experimental results of time domain and corresponding spectrum for different tool conditions are as shown in figure 4.1. Figure 4.1 (i) to (v) show the spectrum of healthy and faulty conditions of cutting tool, here 24th multiple of spindle speed frequency (300 Hz) shows the dominance among all other harmonics. Several references are available (Niu et al. 1998) on vibrations in the low frequency range, close to the natural frequency of vibration of spindle work piece (up to 300 Hz). Frequency for the given spindle speed is about 12.5 Hz. It can be noticed from frequency spectrum that, along with spindle speed frequency and its harmonics (1x, 2x, 3x....etc.), few peaks corresponding to chatter are also present. From figures 4.1 (ii) and (iii), observation shows that peak frequency of 200 Hz corresponds to breakage and thermally cracked cutting tool were dominant compare to healthy cutting tool. Peak frequency at 200 Hz, can be due to either breakage or due to thermal cracks in the cutting tool. Further observations from figure 4.1 (v) shows that two peak frequencies corresponding to 150 Hz and 450 Hz are due to rake face chipping of cutting tool. These frequencies information can be used for further based on cepstrum analysis and wavelet analysis to detect the cutting tool fault conditions.

4.3 CEPSTRUM ANALYSIS

A cepstrum is considered as forward Fourier transformation of the logarithm of a spectrum. It is therefore defined as the spectrum of a spectrum. The cepstrum was originally referred as the power spectrum of the logarithmic power spectrum, thus the calculation of cepstrum involves the inverse Fourier transform of the natural logarithm of a spectrum (Randall, 1982). Given a real signal $x(n)$, cepstrum form can be expressed as follows,

The real cepstrum of a signal $x(n)$ (Hasegawa 2000):

$$c(n) = \frac{1}{2\pi} \int_{-\pi}^{\pi} \log |X(e^{j\omega})| e^{j\omega n} d\omega \quad (4.4)$$

Where,

n is cepstral 'log', if $x(n)$ is real, and then $\log |X(e^{j\omega})|$ is even.

Cepstrum reveals the periodicity in frequency domain usually as results of modulation. Figure 4.2 depicts relationship between spectrum and cepstrum.

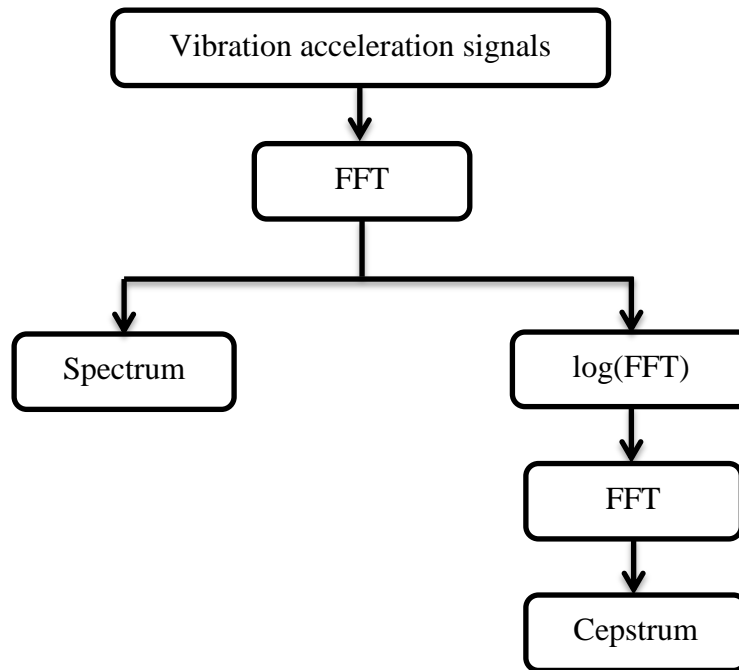


Figure 4.2 Relationship between spectrum and cepstrum

Figure 4.3 (a) to 4.3 (e) shows the vibration responses in quefrequency-domain for different tool conditions. Figures 4.3 (a) represents the vibration response of healthy cutting tool in quefrequency domain. Whereas figure 4.3 (b) to Figure 4.3 (e) represents the vibration response of faulty cutting tools in quefrequency domain.

Comparing the quefrequencies and acceleration of worn out tool conditions with healthy cutting tool. It is observed that there is no significant difference with the quefrequencies and accelerations in case of different tool conditions. Hence, with vibration spectrum/cepstrum analysis is quite challenging for damage detection of a tool (Bediaga et al. 2013).

From the spectrum and cepstrum analyses of turning tool, it can be visualized that even with the presence of defect in the tool, it is quite difficult to identify the particular time at which the defect frequency/quefrequency is being attained and it requires time-frequency domain analysis.

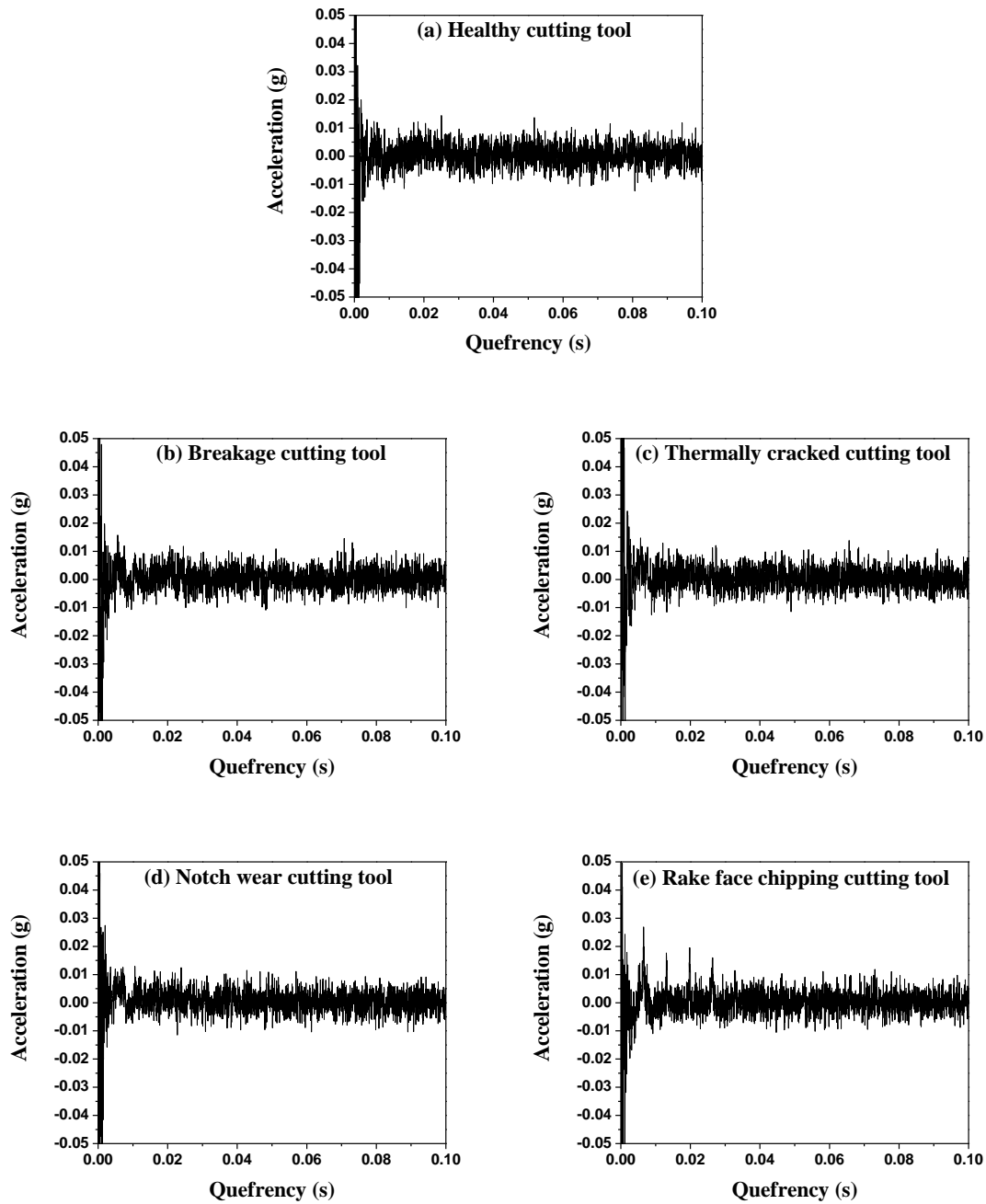


Figure 4.3 Vibration responses in quefrequency-domain for different tool conditions (a-e)

4.4 WAVELET ANALYSIS

The Fourier transform is not suitable for analyzing non-stationary signals, since it fails to reveal the frequency content of a signal at particular time. In signal processing, the limitation of FT led to the introduction of new time-frequency analysis called continuous wavelet transform (CWT).

Generally conventional data processing is computed in time or frequency domain. Wavelet processing combines both time and frequency. Wavelet analysis is one of the ‘time-frequency’ analysis. A wavelet is a basis function characterized by two aspects, first is its shape and amplitude, which is chosen by user. Second is its scale (frequency) and time (location) relative to the signal (Badour et al. 2013).

The continuous wavelet transform (CWT) can be used to generate spectrograms which show the frequency content of signals as a function of time. A continuous-time wavelet transform of $x(t)$ is defined as,

$$CWT X_{\psi}(a, b) = \frac{1}{\sqrt{|a|}} \int_{-\infty}^{\infty} x(t) \psi^* \left(\frac{t-b}{a} \right) dt, \{a, b \in R, a \neq 0\} \quad (4.5)$$

In the above equation 4.5, $\psi(t)$ is a continuous wavelet function in time domain as well as the frequency domain called the mother wavelet and $\psi^*(t)$ indicates complex conjugate of the analyzing wavelet $\psi(t)$. The parameter ‘ a ’ is termed as scaling parameter and ‘ b ’ is the translation parameter. The transformed signal $X_{\psi}(a, b)$ is a function of the translation parameter ‘ b ’ and the scale parameter ‘ a ’. In WT, signal energy is normalized by dividing the wavelet coefficients by $\frac{1}{\sqrt{|a|}}$ at each scale (Peter et al. 2004).

4.4.1 Continuous wavelet transform

The Morlet wavelet transform belongs to CWT family. It is one of the most popular wavelet used in practice and its mother wavelet (Lardies and Gouttebroze 2002) is given by,

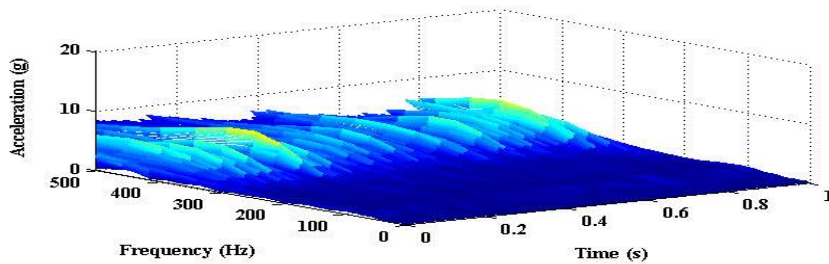
$$\psi(t) = \frac{1}{\sqrt[4]{\pi}} \left(e^{jw_0 t} - e^{-\frac{w_0^2}{2}} \right) e^{-\frac{t^2}{2}} \quad (4.6)$$

In the above equation 4.6, w_0 refers to central frequency of the mother wavelet. The term $e^{-\frac{w_0^2}{2}}$ involved in the equation is used for correcting the non-zero mean of the complex sinusoid and in most of the cases, it can be negligible when $w_0 > 5$.

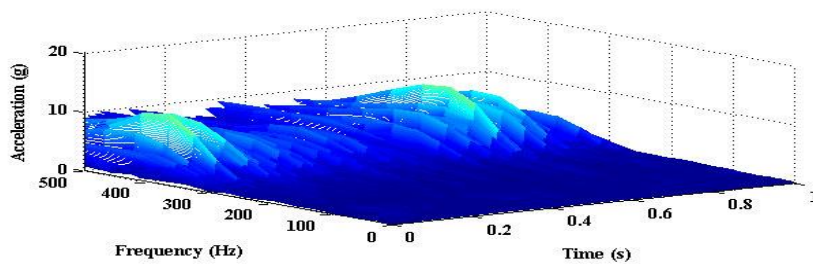
Therefore when the central frequency $w_0 > 5$, the mother wavelet can be redefined as follows;

$$\psi(t) = \frac{1}{\sqrt[4]{\pi}} e^{jw_0 t} * e^{-\frac{t^2}{2}} \quad (4.7)$$

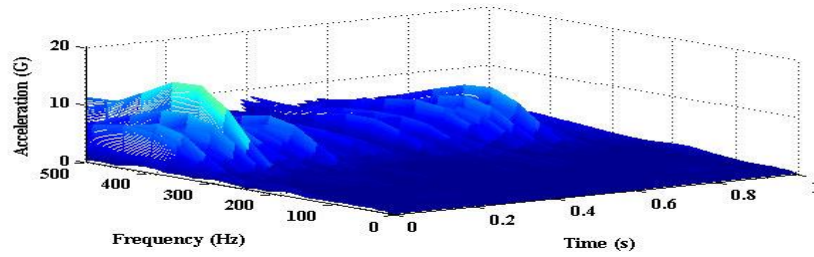
Figure 4.4 illustrates CWT plots of the cutting tool vibration with healthy and fault conditions of cutting tool inserts. Figure 4.4 (a) shows the CWT plot for healthy tool, which depicts the variation of frequency and acceleration with respected to time. From the figure 4.4 (a) for healthy cutting tool the variation of amplitude up to 7 g is observed over the frequency range 500 Hz in the time interval of 1 s. Whereas from the figures 4.4 (b) to figure 4.4 (e) represents CWT plots for the different worn out conditions of cutting tool such as breakage, notch wear, thermal cracks and rake face chipping tool. Variation of acceleration increase in amplitude up to 20 g is observed over the frequency range 500 Hz with the time interval of 1 s for all the worn out tool conditions. This signifies an increase in acceleration can be due the presence in fault in the cutting tool. But it is very difficult to identify the exact time and frequency for each condition of cutting tool. Hence CWT plots are very difficult to analyze the condition of tool (Posenato et al. 2008).



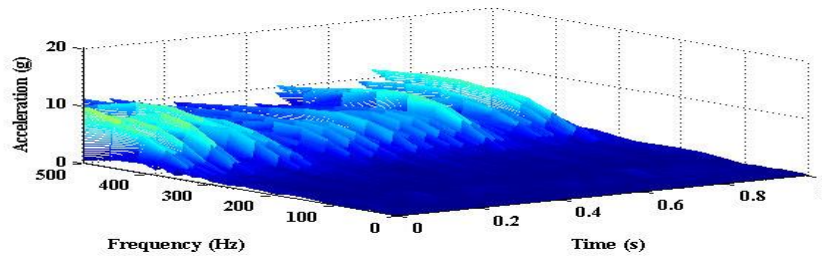
(a) Healthy cutting tool CWT



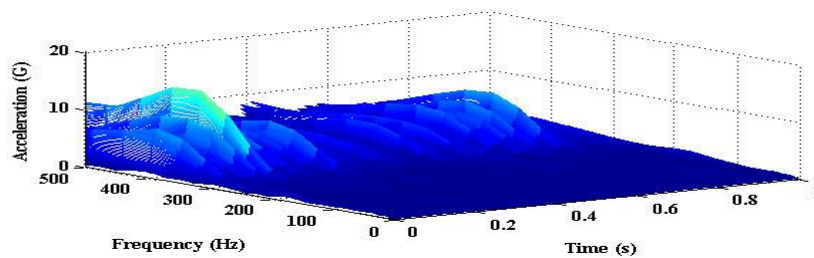
(b) Breakage cutting tool CWT



(c) Thermally cracked cutting tool CWT



(d) Notch wear cutting tool CWT



(e) Rake face chipping cutting tool CWT

Figure 4.4 CWT plots for different tool conditions (a-e)

4.5 DEMERITS OF SPECTRUM, CEPSTRUM AND WAVELET ANALYSIS

Frequency analysis is the most commonly used method for analyzing a vibration signal. The most basic type of frequency analysis is an FFT, or fast Fourier transform, which converts a signal from the time domain into the frequency domain. This is quite useful for analyzing stationary signals whose frequency components do not change over time. Despite its common use, there are many downfalls to just using frequency analysis because its results, such as a power spectrum or total harmonic distortion contain only the frequency information of the signal. They do not contain time information, this means that frequency analysis is not suitable for signals whose

frequencies vary over time. The second limitation of the FFT is that it cannot detect transients or short spikes in the signal. Transients are sudden events that last for a short time in a signal and usually have low energy and a wide frequency band. When transients are transformed into the frequency domain, their energy is spread over a wide range of frequencies. Since transients have low energy, you might not be able to recognize their existence in the frequency domain. While a frequency spectrum or FFT reveals the periodicity of a time domain measurement signal, the cepstrum reveals the periodicity of a spectrum. A cepstrum is often referred to as a spectrum of a spectrum. Cepstrum analysis is especially useful for detecting harmonics. Harmonics are periodic components in a frequency spectrum and are common in machine vibration spectra. Wavelet analysis is appropriate for characterizing machine vibration signatures with narrow band-width frequencies lasting for a short time period. Wavelets have limited bandwidth in the frequency domain and compact bandwidth in the time domain (Loutridis 2004; Bianchini et al. 2011; Li et al. 2009). The technique of recurrence plot (RP) and recurrence quantification analysis (RQA) is well suited for the analysis of nonlinear and chaotic systems and can basically be used for signal processing without denoising (Guhathakurta et al. 2010; Chen 2011; Dia et al. 2012). The technique can reveal quite a lot of information hidden in time series data from a dynamic system about the system characterization. The RQA output useful information from even a short data set, which makes it an attractive feature extraction methodology suitable for deployment in monitoring of real time cutting process.

4.6 RECURRENCE QUANTIFICATION ANALYSIS

Recurrence quantification analysis (RQA), which has its roots in quantifying recurrence plots, is obtained by the phase space reconstruction of vibration signal in time domain. Variation in determinism is one of the variables of the technique and is used as a mean to classify the tool condition. RQA includes time delay and dimensions embedding process so as to reconstruct the time series data of vibration signal, to obtain better information of the changes in nonlinear dynamics underlying in the turning process. The investigation proved that RQA technique has a good potential in classifying the condition of the tool. The RQA parameters such as percent

recurrence, trapping time, percent determinism, percent laminarity, entropy and also the recurrence plots color patterns for different tool condition, can be used in classifying different cutting tool conditions in turning (Webber and Zbilut 2005).

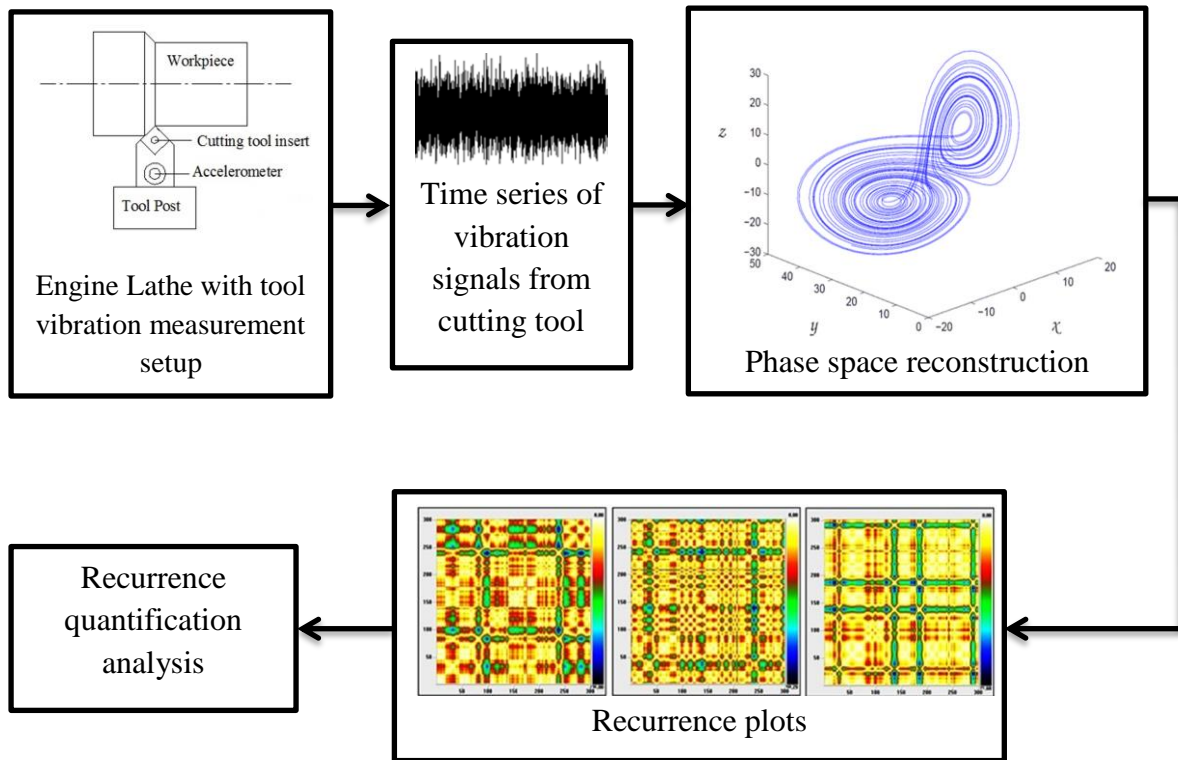


Figure 4.5 Nonlinear recurrence quantification analysis

The research methodology adopted in analyzing the vibration signals using the nonlinear recurrence quantification analysis (RQA) is shown in figure 4.5. The recorded time series data (vibrations signals) is transformed into sequence of points in a higher-dimensional space by applying the Taken's time-delay embedding theorem. This process is called phase space reconstruction. A symmetric distance matrix is then obtained from the trajectory of this attractor. This matrix is represented as color plot called recurrence plot. This plot is quantified using recurrence quantification analysis (RQA). The RQA output measures the number of complexity called RQA variables.

4.6.1 Recurrence plot (RP)

The recurrence plot (RP) approach provides a qualitative interpretation of hidden patterns of dynamical systems (Eckmann et al. 1987). It enables one to investigate the dimensional phase space trajectory by means of two-dimensional (2-D) visualization.

By using recurrence plots, variation patterns of time-series data can be efficiently recognized. Recurrence plots are graphical tools based on phase space reconstruction. The changing state of a dynamic system can be represented by sequences of ‘state vectors’ in the phase space.

Considering an acceleration time series data from a vibration signal:

$$a = \{a(1), a(2), a(3) \dots \dots \dots, a(T)\} \quad (4.8)$$

Where,

‘ T ’ is the length of the time series data

From this one dimensional data vector signal, a family of new vectors called as embedded vectors are to be constructed each having

length $m < T$ which is as given below:

$$A_i = \{a(i), a(i + \tau), \dots \dots \dots, a(i + (m - 1) \tau)\} \quad (4.9)$$

Where,

$i = 1$ to T , τ is the delay time and m is the embedding dimension.

The number of new vectors is given by:

$$N = T - (m - 1) \tau \quad (4.10)$$

Then, the distance between two state vectors A_i and A_j can be defined as follows:

$$D_{ij} = |A_i - A_j| \quad (4.11)$$

The recurrence plots visualizes the relationship between the two state vectors within a 2-D square matrix of size $T \times T$. In this process, a threshold distance ε is generally set for plotting recurrence points, which fall in the neighborhood of a fixed size.

Mathematically it is defined as:

$$r_{ij} = \theta(\varepsilon - \|A_i - A_j\|) \quad (4.12)$$

Where,

r_{ij} an element of the recurrence matrix, ε is the threshold for the distances, $\| \cdot \|$ is a norm and θ is the Heaviside function and is defined as:

$$\begin{aligned}\theta(x) &= 0, \text{ for } x < 0 \\ \theta(x) &= 1, \text{ for } x \geq 0\end{aligned}\tag{4.13}$$

In other words, r_{ij} assumes a value of 1 if (i, j) is recurrent, and a value of 0 otherwise, which are plotted as black and white. Instead of plotting the recurrences in two values (i.e., black and white) by setting a threshold level, the D_{ij} distance matrix can also be used, which helps checking the phase space trajectory of target data.

These distances are given color codes and the recurrence plot occurs as color patterns. With proper values of m and τ this representation is topologically equivalent to the underlying m dimensional system that produces the time series (Zbilut and Webber 1992).

Therefore each unknown point of the phase space at time i is reconstructed by the delayed vector in an n -dimensional space called the reconstructed phase space. There exist a variety of methods for choosing values of m and τ . The optimal delay will produce independent pseudo-state vectors while the optimal dimension will be the smallest one that prevents trajectories in state space from crossing. The most often used methods are the average mutual information (AMI) function for computing the time delay τ , as introduced by Fraser and Swinney (1986) and the false nearest neighbors (FNN) method for the embedding dimension m developed by Kennel et al. (1992). One chooses the first minimum location of the average mutual information function as τ . The percentage false nearest neighbors is computed for each of the m values. The embedding dimension is said to be found for the first percentage of FNN dropping to zero. This percentage never reaches a true zero value because of presence of noise in the signal. Hence optimal m is chosen for minimum value of FNN. The embedding parameters can be found out using the visual recurrence analysis (VRA) V 4.9.

4.6.2 Recurrence quantification analysis parameters

The recurrence plot was able to provide only qualitative visual information. Later in order to quantify the lines in recurrence plots a way of measuring quantitative information has been introduced by Zbilut and Webber (1992).

This provides the means for recurrence quantification analysis. It defines measures of complexity. Following are quantitative parameters of RQA which are defined as:

(a) Percent recurrence (REC):- Percent recurrence measures the percentage of recurrent points in the phase space, excluding the main diagonal. Embedded processes that are periodic will have higher percent recurrence values.

$$REC = \frac{1}{N^2} \sum_{i,j=1}^N r_{ij} \quad (4.14)$$

(b) Percent determinism (DET):- Percent determinism is the percentage of recurrent points that are included in line segments parallel to the upward diagonal and whose length meets or exceeds the minimum length threshold. It allows distinguishing between dispersed recurrent points and those are organized in diagonal patterns, representing strings of vectors (deterministically) repeating themselves.

$$DET = \frac{\sum_{l=l_{min}}^N l \cdot P(l)}{\sum_{i,j=1}^N r_{ij}} \quad (4.15)$$

Where,

l is the length of the diagonal line parallel to the Line of Identity.

$P(l)$ is the frequency distribution of the diagonal lines (that is the histogram of their length l) and

r_{ij} is the recurrence of a state.

(c) Percent laminarity (LAM):- Percent laminarity is the percentage of recurrent points that are included in line segments vertical to the upward diagonal and whose length meets or exceeds the minimum length threshold. It measure chaotic transitions, and is related with the amount of laminar phases in the system (intermittency).

$$LAM = \frac{\sum_{v=v_{min}}^N v \cdot P(v)}{\sum_{v=1}^N v \cdot P(v)} \quad (4.16)$$

Where,

$P(v)$ is the frequency distribution of the lengths v of the vertical lines, which have at least a length of v_{min}

(d) Trapping time (TT):- Trapping time is the average length of vertical line structures. It represents the average time in which the system is "*trapped*" in a specific state

$TT = \text{average length of vertical lines}$

(e) Ratio: - Ratio variable is defined as the quotient of DET divided by REC. It is useful to detect transitions between states. This ratio increases during transitions but settles down when a new quasi-steady state is achieved.

(f) Entropy (ENT):- Entropy variable, is computed as the Shannon entropy of the frequency distribution of the diagonal line lengths distributed over integer bins in a histogram, and quantifies the complexity of recurrence plots. More precisely, the entropy gives a measure of how much information one needs in order to recover the system. A low entropy value indicates that little information is needed to identify the system; in contrast, high entropy indicates that much information is required. Upward line segment lengths are counted and distributed over integer bins of a histogram. Shannon entropy is computed according to the following equation 4.17

$$ENT = - \sum_{l=l_{min}}^N P_l \log_2(P_l) \quad (4.17)$$

(g) Maxline: - The longest line segment measured parallel to the main diagonal. A periodic signal produces long line segments, while short lines indicate chaos.

(h) Trend: - Trend variable is the slope of the least squares regression of local recurrence as a function of the orthogonal displacement from the main diagonal. It represents the measure of the positioning of recurrent points away from the central diagonal. It quantifies the degree of system stationary. In other words it represents the measure of the positioning of recurrent points away from the central diagonal. Low value of trend indicates stationary in the signal and high value of trend either positive or negative indicates drift in the signal.

Figure 4.1 (a-e) shows acceleration-time series plot for healthy insert and different worn out inserts. The times series plots of vibration acceleration for worn tool are

characterized by slightly larger values while the healthy inserts shows shorter amplitude of acceleration. This does not provide clear and distinct method to identify the wear states of the cutting inserts. The acquired time series data are further analyzed to generate threshold recurrence plots.

The procedure followed to get recurrence plots and RQA values are as follows:

- Average mutual information (AMI) analysis was performed to get embedded time delay value.
- False nearest neighbor (FNN) analysis is carried out to determine embedded dimension using previously obtained time delay value. The maximum value for embedded dimension was fixed at 15.
- Recurrence plot without threshold was generated using the available values of embedded time delay and dimension.
- RQA analysis has been carried out using time delay, dimension and threshold radius. The threshold radius of 1.5 was maintained constant throughout the analysis.

As per this procedure AMI and FNN for the time series of healthy insert is estimated. AMI plot (Figure 4.6) demonstrated that the optimal delay (τ) as 2.

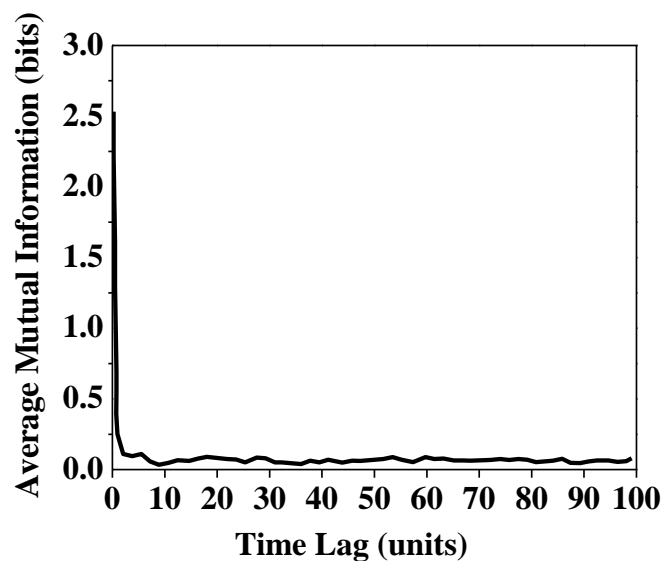


Figure 4.6 AMI plot for healthy insert condition

Thus obtained time delay has been made used in getting the embedding dimension. Figure 4.7 shows the embedding dimension ($m = 2$) obtained from FNN Graph when time delay is 2 for healthy insert condition. The embedding dimension is obtained as first minimum value of FNN plot.

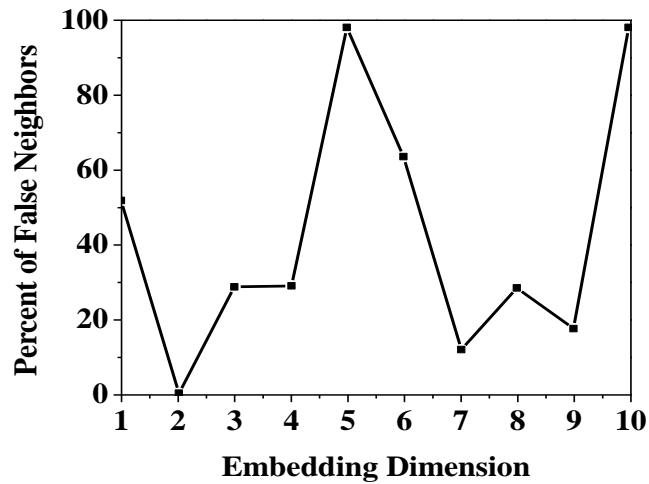


Figure 4.7 FNN plot for healthy insert condition

In this manner AMI and FNN analysis for healthy insert and different worn out inserts were obtained. The corresponding values of embedding dimension and time delay are tabulated as shown in table 4.1.

Table 4.1 Embedding dimension, time delay and threshold radius

Tool Condition	Embedding dimension (m)	Time delay (τ)	Threshold radius (ϵ)
Healthy	2	2	1.5
Breakage	2	2	1.5
Thermal cracks	3	2	1.5
Notch wear	2	2	1.5
Rake face chipping	3	2	1.5

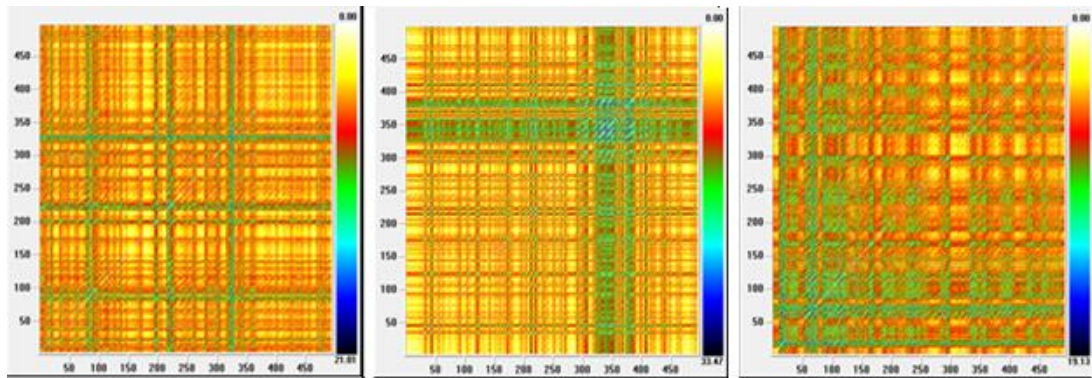
These values provide base for constructing the phase space to reveal the underlying turning dynamics when turning with different worn inserts. Table 4.1 indicates the

values of embedding dimension and time delay, but they are not sufficient to classify the different tool conditions.

4.6.3 Qualitative investigation

Using the results of AMI and FNN, the corresponding recurrence plots (Figure 4.8) have been developed without considering threshold radius for different tool conditions. A clear distinction in the patterns of recurrence plots has been observed. Information about the dynamics of a time series is usually obtained from the line structure and point density in a recurrence plots. A homogeneous recurrence plots with no structure is typical of a stationary or autonomous process such as white noise. Recurrence plots of oscillating systems, on the other hand, have diagonally oriented or periodic recurrent structures (i.e., diagonal lines or checker board patterns). Vertical or horizontal lines in a recurrence plots signify the presence of laminarity or intermittency in the time series, whereas abrupt changes in dynamics as well as extreme events are characterized by white areas or bands.

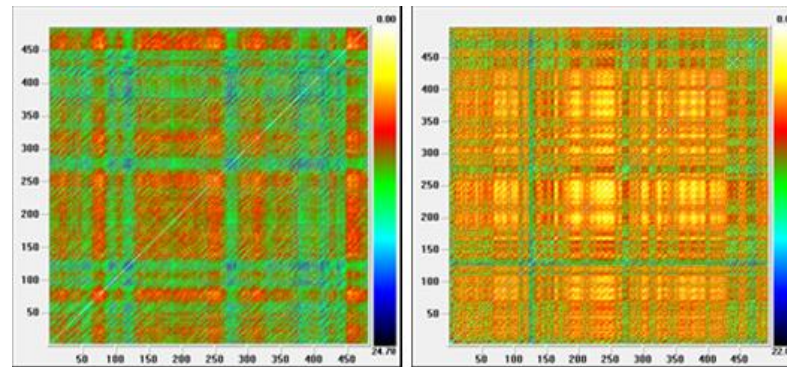
These textures of recurrence plots are required to provide initial visual inspection and in identifying the changes in dynamics of the system. As inserts with different classes of wear while performing cutting operation, the vibration signals will be having different dynamics which are revealed by color or/and texture pattern of recurrence plots. Figure 4.8 reveal the changing recurrence plots patterns for different tool conditions. Figure 4.8 shows lot of diagonal lines which indicates periodicity in turning operation and also shows the presence of more vertical lines for thermal cracks indicating laminarity or intermittency due to increase in wear of cutting tool inserts. Observation from recurrence plots demonstrates that the shorter diagonal lines which are away from the main diagonal line called as line of identity shows lot of discontinuities in them, as compared to healthy and different worn insert recurrence plots. There is clear change in color combinations of the recurrence plots patterns as recurrence plots changes from healthy to worn inserts, illustrating qualitative observation for different tool conditions. As worn out tools produce the instability in turning dynamics, effects have been observed on recurrence plots. The color combination of recurrence plots also changes.



(a) Healthy

(b) Breakage

(c) Thermal crack



(d) Notch wear

(e) Rake face chipping

Figure 4.8 Recurrence plots for different conditions of tool (a-e)

The features described for recurrence plots indicate the characteristics in identifying the different tool condition of turning inserts. In this investigation, the recurrence plots have been able to provide a visual comparison between different tool conditions.

4.6.4 Quantitative investigation

Recurrence plots provide the initial visual comparison between different states of the insert wear condition. The quantitative investigation of recurrence plots will be required to substantiate the qualitative observations. The recurrence plot has to be quantified for which RQA provides the frame work. RQA parameters study has been carried out for different inserts. The embedding dimensions, time delay and threshold radius are indicated in table 4.1 were used in RQA analysis. Euclidian distance has

been considered for determining distance between new vectors. A minimum diagonal length of 2 units was considered as base for RQA analysis. The dimension and delay are fixed based on AMI and FNN analysis. Euclidean distance is chosen for computing the distances between the phase space vectors. The RQA analysis has been carried out for full data after phase space reconstruction i. e. from 1 to 500 which is called as full epoch study. RQA parameters are computed for the full epoch and recorded. The full epoch study is carried out on vibration data of different worn conditions of the turning inserts. This will help in bringing out the influence of insert wear on RQA parameter and also the behavior of RQA parameters as tool condition changes. The summary of RQA parameters is as shown in table 4.2.

Table 4.2 RQA analysis for different tool conditions

RQA Parameters	Tool Condition				
	Healthy	Breakage	Thermal cracks	Notch wear	Rake face chipping
Percent recurrence	6.546	2.626	2.975	3.969	1.564
Percent determinism	20.573	14.954	10.433	15.138	10.469
Percent laminarity	18.406	5.754	12.185	9.608	2.083
Trapping time	2.147	2.055	1.82	1.986	2
Ratio	3.143	5.694	3.507	3.607	6.693
Entropy	1.261	1.129	1.016	1.007	0.987
Maxline	7	3	7	6	4
Trend	4.653	0.862	1.213	2.374	-1.519

4.6.4.1 Influence of different tool conditions on RQA parameters

- a) **Percentage recurrence (REC):** It is observed as the percentage of recurrence for healthy tool having more value as compared with the recurrence values of other faulty tools. Turning with healthy insert is more periodic compared to other faulty inserts; this correlation is well depicted by recurrence values.

- b) Percent determinism (DET):** Percent determinism value decreases with the increase level of fault occurred in the tool. DET values indicate deterministic nature of embedded series. For healthy insert DET value is highest, hence the embedded time series is quite deterministic compared with the fault inserts. When machining dynamics becomes more complex, the embedded time series becomes less deterministic.
- c) Percent laminarity (LAM):** The LAM values indicate laminarity or intermittency in the process. In case of dynamic systems intermittency is the alternation of phases of apparently periodic and chaotic dynamics. The LAM values decreases as the wear values increase in the cutting tool. LAM values for healthy insert are high, they indicating that the extent of intermittency is more than the LAM values of faulty inserts
- d) Trapping time (TT):** The TT values show decreasing trend as wear level increases. TT values represent the average time system that is trapped in specific state. It can be deduced from healthy insert that the system is trapped for more amount of time than the faulty inserts.
- e) Ratio:** Ratio is the indicator of transition between non chaotic to chaotic states. High ratio indicates presence of transition to chaotic state and low ratio represents quasi steady state. It is observed that healthy, thermal cracks and notch wear inserts attain at quasi steady state, whereas rake face chipping and breakage are chaotic state.
- f) Entropy:** Entropy is an indicator of the amount of information required to identify the system. For healthy insert, entropy is high and hence more information is required, whereas for other fault insert less information is required as their entropy values are low.
- g) Maxline:** Maxline also indicates intermittency of the process. High values of maxline indicate that the process is periodic and low values indicate that the process is chaotic. In this cutting condition maxline values of healthy, thermal cracks and notch wear are high, whereas for breakage and rake face chipping maxline values are low i.e. non periodic.
- h) Trend:** Trend indicates the drift or stationarity of the signal. A high value of trend indicates drift in the signal and low value of trend indicates stationarity.

For healthy insert, trend value is high indicating drift in the signal. In the case of breakage and rake face chipping the trend values is indicating stationarity in the process comparatively.

4.7 SUMMARY

This chapter explains about analyzing vibration signals acquired for different tool conditions (healthy and faulty) using the time domain, frequency domain, cepstrum plots, wavelet transform plots, recurrence plots and RQA for detecting the faults. It was found that the time domain signals analysis gives overall vibration level but do not provide any fault diagnostic information. Spectrum analysis is most widely used signal processing technique, but sometimes quite difficult to identify the defect frequency and it requires domain knowledge. Cepstrum analysis is suitable technique to identify and distinguish the fault frequencies. Wavelet analysis is three dimensional time, frequency and amplitude representation of a signal, which is inherently suited to indicate transient events in the signals. Since turning operation generates non-stationary signals and complex signals, fault diagnosis of cutting tool can be effectively monitored using recurrence quantification analysis rather than traditional approaches. Both qualitative and quantitative approaches were carried out in order to classify different conditions of the cutting tool inserts. In the qualitative approach, the recurrence plots demonstrated that it can be used to classify healthy and faulty inserts based on the color patterns. Recurrence plots have been used with parameterization to give RQA parameters. Most of these parameters were able to show definite trend in RQA parameters with different tool conditions. Recurrence plots and RQA have significant feature to distinguish different tool conditions. The detection of fault using these techniques is difficult and it needs a highly skilled and experienced technician who has clear understanding of the techniques used and also thorough knowledge about the machine in which the fault is detected (Dalpiaz et al. 1998). Therefore machine learning approach is a promising tool which can be easily applied for fault diagnosis. In chapter 5 Fault diagnosis using machine learning approach is described for online tool condition monitoring.

CHAPTER 5

FAULT DIAGNOSIS USING MACHINE LEARNING TECHNIQUE

5.1 INTRODUCTION

Machine learning is an area of artificial intelligence involving developing techniques to allow computers to learn. More specifically, machine learning is a method for creating computer programs by the analysis of data sets. Many of the machine learning methods is iterative in nature and they require high speed processors. The aforesaid developments accelerate the application of machine learning methods for solving problems in real time. Fault diagnosis is one of the application areas, where machine learning methods are widely used. This chapter briefly describes the machine learning methods commonly used for fault diagnosis of single point cutting tool.

5.2. NEED FOR MACHINE LEARNING TECHNIQUES

Fault diagnosis of single point cutting tool can be performed in both time domain and frequency domain analysis. Each of these has its own limitations. Spectral analysis mainly depends on fast Fourier transform (FFT) for monitoring the level of some characteristic frequencies. In addition, factors like cutting parameters variations mainly influence the characteristic frequency of the machine. Recurrence quantification analysis (RQA) methodology provides quantitative decision support in condition monitoring of cutting tool. Research efforts addressing the issues of noise and stationarity characteristics of vibration signals and moreover, the computational time demand for the signal RQA feature extraction, which will render a fresh fundamental contribution to the field of nonlinear dynamics. Machine learning methods address most of the problems and are proved to be a stronger method. Researchers have reported the capability of many machine learning techniques to perform fault diagnosis. In general, the fault diagnosis is carried out through three phases namely, feature extraction, feature selection and feature classification. The works reported follow different techniques, further each elaborates one or other of

these phase under different test conditions. Nevertheless, there is a clear need for a uniform and a focused approach.

5.3 MACHINE LEARNING APPROACH

Cutting tool fault diagnosis is a procedure of mapping the information obtained in the measurement space and/or features in the feature space to identify the cutting tool faults in the faults space. The mapping process is also called machine learning or pattern recognition. Traditionally, pattern recognition is done manually with auxiliary graphical tools such as power spectrum graph, phase spectrum graph, cepstrum graph, auto regression (AR) spectrum graph, spectrogram, wavelet scalogram, wavelet phase graph, etc. However, manual pattern recognition requires expertise in the specific area of the diagnostic application. Thus, highly trained and skilled personnel are needed. Therefore, automatic pattern recognition is highly desirable. This can be achieved by classification of signals based on the information and/or features extracted from the signals using machine learning techniques. In the following sub-sections, important machine learning techniques are discussed.

Feature extraction and feature classification are the most important phase in machine learning techniques. For feature extraction, various methods such as statistical features, histogram features, EMD features etc. have been in practice. However, all these methods may not be suitable when the signal is highly non-stationary in nature. Wavelet analysis is the one which can overcome the above problem due to its strong mathematical background and its extreme flexibility. A comprehensive approach is to deal with all significant family of features and to do an exhaustive study of all corresponding classification techniques under identical test conditions.

The methodology followed in the fault diagnosis of single point cutting tool using machine learning approach is illustrated in figure 5.1. In this study, 40 vibration signals from cutting tool were acquired with healthy and practically industrial worn out cutting tools. The different features such as statistical features, discrete wavelet transform (DWT) features, histogram features and empirical mode decomposition (EMD) features were extracted from vibration signals to identify the status of cutting

tool. Decision tree (J48 algorithm) technique or principal component analysis (PCA) has been used for important feature selection/reduction out of extracted features.

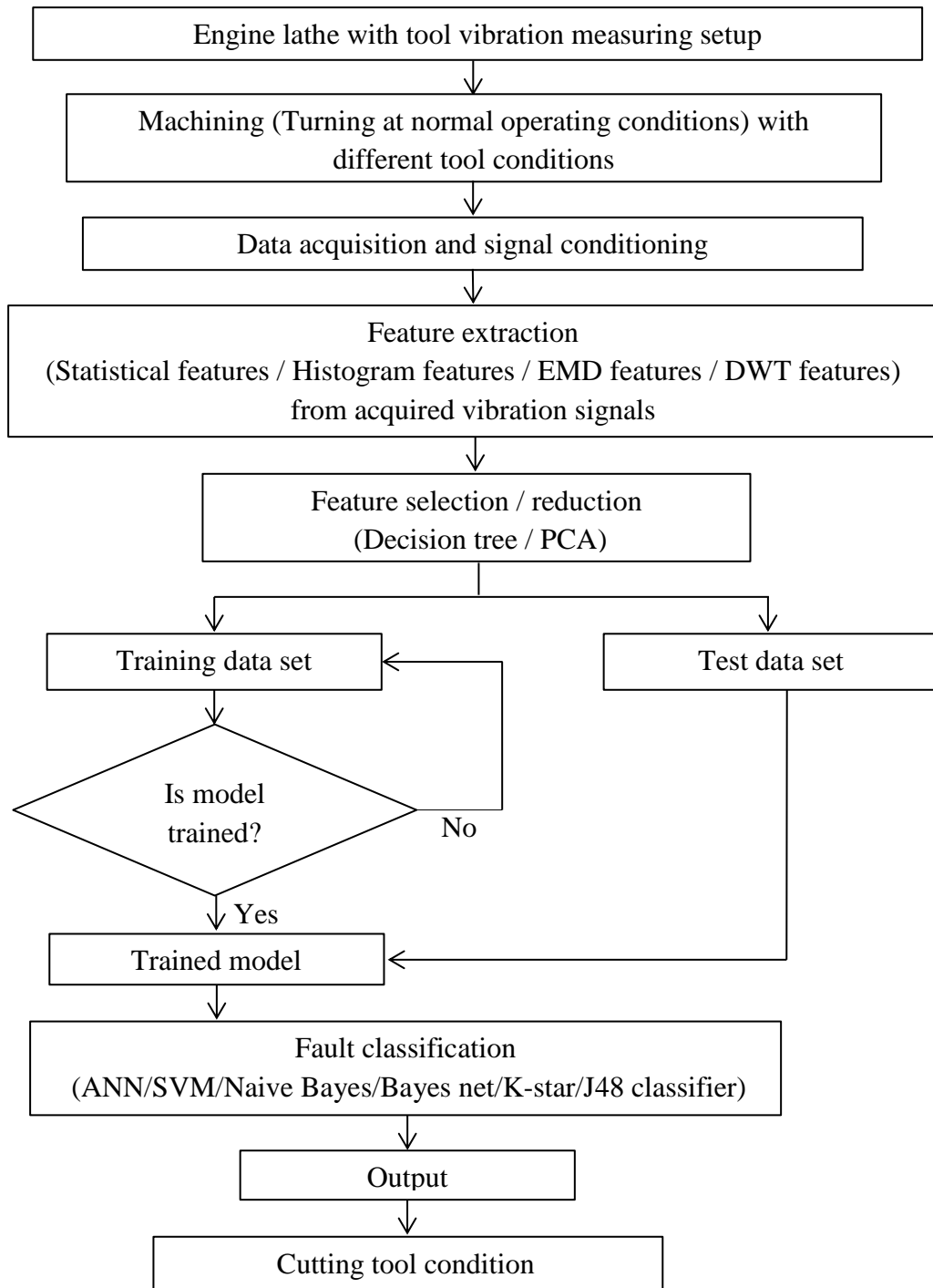


Figure 5.1 Flow chart of fault diagnosis of cutting tool with machine learning approach

Different classification models such as SVM, Naive Bayes, Bayes net, K-star, J48 and ANN have been used as a classifier for fault diagnosis of cutting tools. Machine learning has three important phases, they are discussed in the following sub-sections.

5.4 FEATURE EXTRACTION

Feature extraction constitutes computation of specific measures which characterize the signal. The vibration signals taken from cutting tool at different conditions form the input to the classifier in this study. Classifier is an algorithm which maps the points from input space to the fault space. The fault space has four regions (corresponding to four fault conditions). The input is made up of 25600 points of digitized vibration signal and using each point as an input will require 25600 inputs. If each data point (out of 25600) is considered as an input to the classifier, then most of the classifiers will find it difficult to manage such a large number of input variables. To reduce the number of input variables, researchers use a few measures of the data points instead of the data themselves. These measures are called as '*features*'. The features are application dependent and one has to choose a set of good features for better classification on case-by-case basis. The process of computing such measures is called '*feature extraction*'.

5.4.1 Statistical features

Statistical analysis of vibration signals yields different parameters. Research work reported by Elangovan et al. 2011 use these in combinations to elicit information regarding cutting tool faults. Such procedures use allied logic often based on physical considerations. A fairly wide set of these parameters was selected as a basis for the study. They are mean, standard error, median, mode, standard deviation, sample variance, kurtosis, skewness, range, minimum, maximum, and sum. In this study, these parameters were extracted from vibration signals and used as features.

- a) Standard error: Standard error is a measure of the amount of error in the prediction of y for an individual x in the regression, where \bar{x} and \bar{y} are the sample means and ' n ' is the sample size. The standard error of the prediction,

$$y = \frac{\sigma}{\sqrt{N}} \quad (5.1)$$

- b) Standard deviation: This is a measure of the effective energy or power content of the vibration signal. The following formula was used for computation of standard deviation. Where ‘ \bar{x} ’ is the sample mean and ‘ x_i ’ represents the i^{th} value of the discrete time signal.

$$\sigma = \sqrt{\frac{1}{N} \sum_{i=1}^N (x_i - \bar{x})^2} \quad (5.2)$$

- c) Sample variance: It is the variance of the signal points and the following formula was used for computation of sample variance.

$$\text{Sample Variance} = \sigma^2 \quad (5.3)$$

- d) Kurtosis: Kurtosis indicates the flatness or the spikiness of the signal. Its value is very low for normal condition of the cutting tool and high for the faulty condition of the tool due to the spiky nature of the signal.

Where ‘ n ’ is the sample size.

$$\text{Kurtosis} = \left\{ \frac{n(n+1)}{(n-1)(n-2)(n-3)} \sum \left(\frac{x_i - \bar{x}}{s} \right)^4 \right\} - \frac{3(n-1)^2}{(n-2)(n-3)} \quad (5.4)$$

Where ‘ s ’ is the sample standard deviation.

- e) Skewness: Skewness characterizes the degree of asymmetry of a distribution around its mean. The following formula was used for computation of skewness.

$$\text{Skewness} = \frac{n}{n-1} \sum_{i=1}^n \left(\frac{x_i - \bar{x}}{s} \right)^3 \quad (5.5)$$

- f) Range: It refers to the difference between maximum and minimum signal point values for a given signal.
- g) Minimum value: It refers to the minimum signal point value in a given signal. As the tool gets worn-out, the vibration levels seem to go high. Therefore, it can be used to detect tool wear condition.
- h) Maximum value: It refers to the maximum signal point value in a given signal.

- i) Sum: It is the totality of all feature values for each sample.

5.4.2. Histogram features

Observing the magnitude of the time domain signal, it is found that the range of vibration amplitude varies from class to class. A better graph to show the range of variation is the histogram plot. The information derived from a histogram plot can be used as features in the fault diagnosis. A representative sample from each cutting tool condition (class) is taken and the histogram is plotted. The selection of bin involves two criteria.

- a) The bin range should accommodate the amplitude range of signals obtained from all conditions of cutting tool being analyzed. The vibration amplitude range is divided into set of sub ranges starting from minimum value to maximum value of the vibration signal. The sub-ranges known as bins form the x-axis of the histogram. The number of data points whose vibration amplitude value falls within a particular bin is counted and the count forms the y-axis of the histogram. The histograms for each cutting tool condition are plotted using vibration signals as separate plots. The objective here is to find out the bins whose y-axis values are same for a particular class but different from other classes. These values for a particular condition of the cutting tool may be small, but it may be large for another condition. The bin range selected should accommodate all conditions. i.e., the bin range should start from the minimum of minimum amplitude of different classes and go up to maximum of maximum amplitude of different classes.

The procedure for computing minimum of minimum amplitude is as follows:

- i. Find out the minimum amplitude of each signal in a particular class.
- ii. Repeat step (i) for all classes.
- iii. Find the minimum of those minimum amplitudes.

The procedure for computing the maximum of maximum amplitude is similar to this.

- b) The width of the bin should be fixed such that the height of bins is different for different condition of the cutting tool. It need not be true for all width of bins, but at least a few of them should follow this criterion, so that it can be used as a

feature for distinguishing various conditions (classes). Bin width is a set of limiting values that should be in ascending order so that the program counts the number of data points between the current bin number and the adjoining higher bin, if any. The bin width need not be constant always; however, in this study a constant bin width is used.

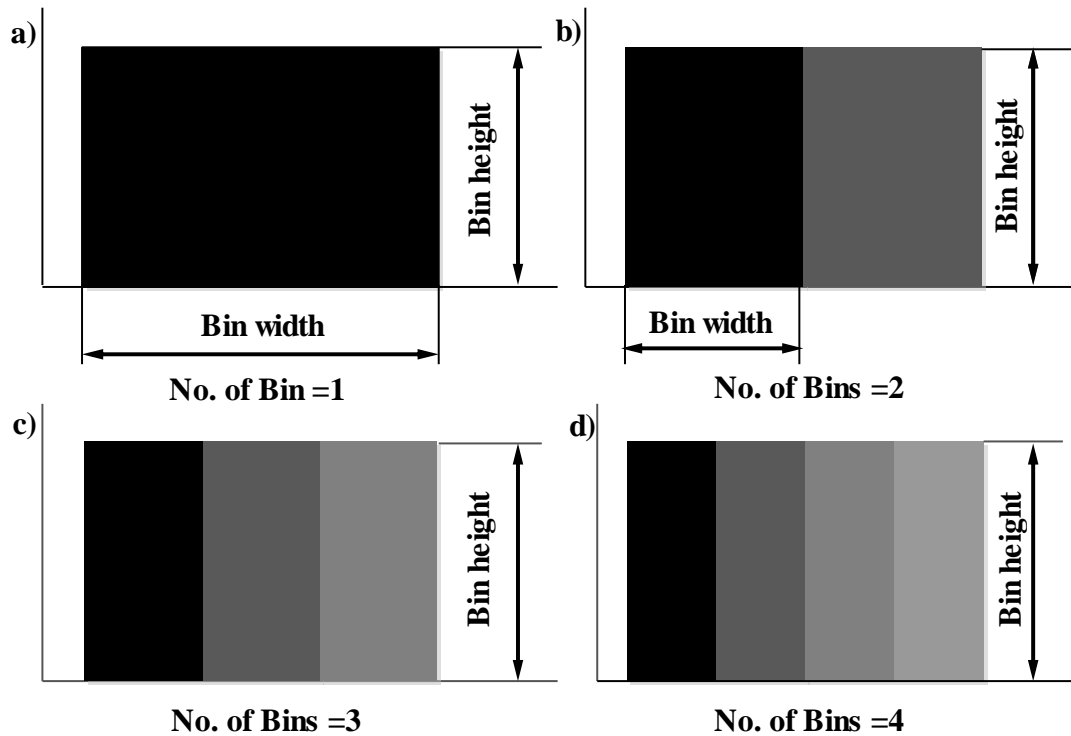


Figure 5.2 Sample histogram of a rectangular distribution

Following the above criteria, the bin width and bin range were selected and histogram has been plotted. Figure 5.2 and 5.3 refers to a typical bin of the histogram plot illustrating the variations in bin width and bin height etc. As it is seen from figure 5.2, there are significant differences in some of the feature values (bin ranges) for different types of faults. Selecting those features is crucial for effective classification; doing it manually demands more expertise; however, the effectiveness of the features is not guaranteed. Selecting the good features through a suitable algorithm can yield better classification results.

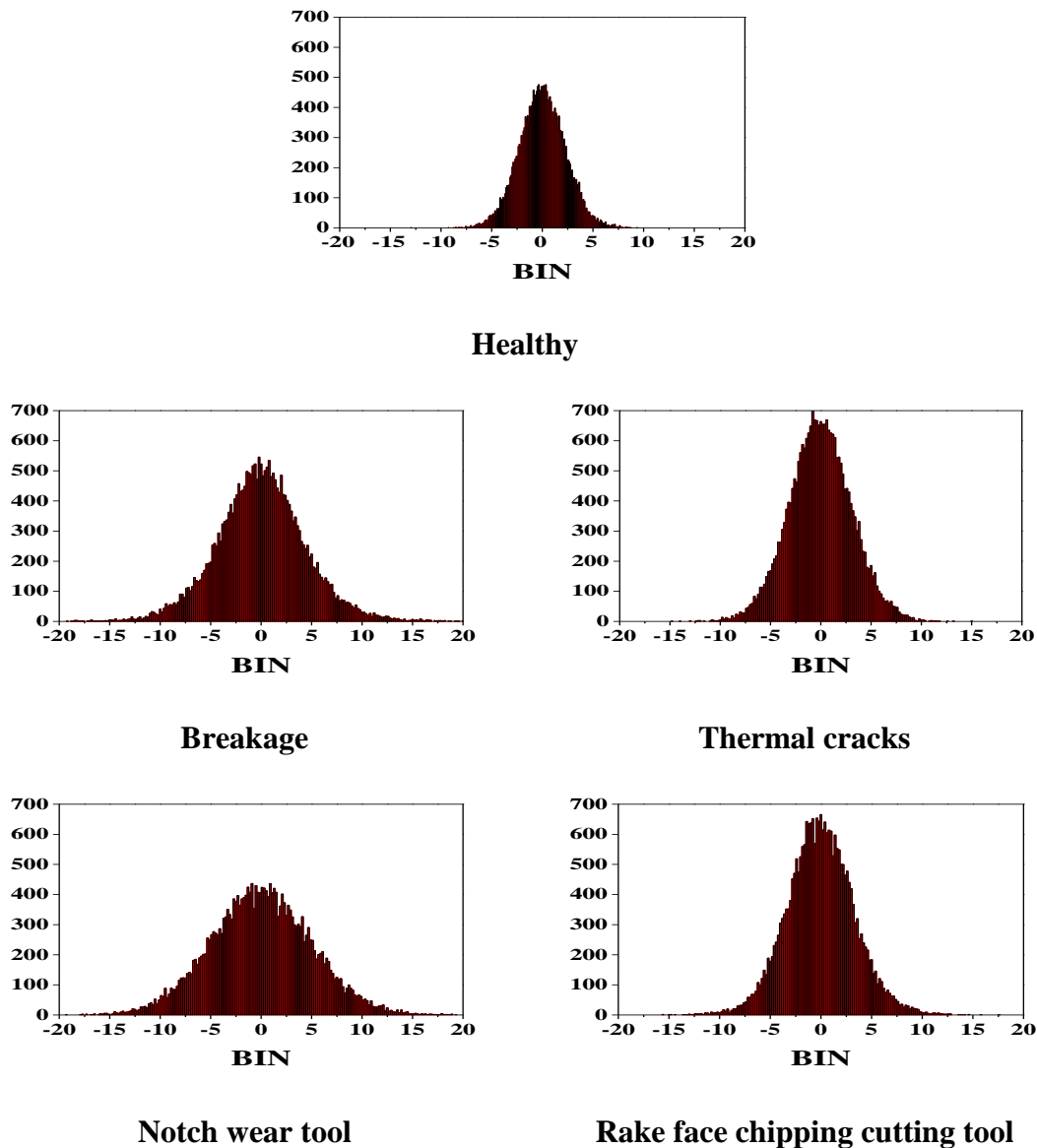


Figure 5.3 Histogram of signals

5.4.3 Discrete wavelet transform features

Wavelet means ‘small wave’. Short duration finite energy $s(t)$ functions are called as wavelets. By definition it is a small wave, $\psi(t)$ hence, it should be time limited. Finite energy functions are those which will represent a phenomenon like a spring oscillation due to an initial stimulus. It exists only for a short duration and releases finite amount of energy. Wavelet transform is defined as the integral of the signal multiplied by scaled, shifted versions of a basic wavelet function - a real-valued function whose Fourier transform satisfies the admissibility criteria:

$$C(a, b) = \int_R S(t) \frac{1}{\sqrt{a}} \psi\left(\frac{t-b}{a}\right) dt$$

$$a \in R^+ - \{0\}, b \in R. \quad (5.6)$$

Where,

C – Continuous wavelet coefficients

t – time

a – scaling parameter

b – time localization parameter

Both ‘a’ and ‘b’ can be continuous or discrete variables. Multiplication of each coefficient by an appropriately scaled and shifted wavelet yields the constituent wavelets of the original signal. For signals of finite energy, continuous wavelet synthesis provides the reconstruction formula:

$$s(t) = \frac{1}{K_\psi} \int_R \int_{R^+} C(a, b) \frac{1}{\sqrt{a}} \psi\left(\frac{t-b}{a}\right) \frac{da}{a^2} db \quad (5.7)$$

Use of Discrete Wavelet Transform (DWT) for analysis retains effectiveness without sacrificing accuracy. In this scheme, ‘a’ and ‘b’ are given by:

$$(j, k) \in Z^2 : a = 2^j, b = k2^j, Z = \{0, \pm 1, \pm 2\}$$

Defining

$$(j, k) \in Z^2: \psi_{jk}(t) = 2^{-j/2} \psi(2^{-j}t - k)$$

$$\phi_{j,k}(t) = 2^{-j/2} \phi(2^{-j}t - k)$$

A wavelet filter with impulse g , plays the role of the ψ wavelet and a scaling filter with impulse response h , plays the role of scaling function ϕ , g and h are defined on a regular grid ΔZ , where Δ is the sampling period (without loss of generality, set $\Delta = 1$). Discrete wavelet analysis yields

$$C(a, b) = c(j, k) = \sum_{n \in Z} s(n) g_{j,k}(n)$$

$$a = 2^j, b = k2^j, j \in N, k \in N \quad (5.8)$$

Corresponding synthesis relation is:

$$s(t) = \sum_{j \in \mathbb{Z}} \sum_{k \in \mathbb{Z}} c(j, k) \psi_{j,k}(t) \quad (5.9)$$

The detail at level j is defined as:

$$D_j(t) = \sum_{k \in \mathbb{Z}} c(j, k) \psi_{j,k}(t) \quad (5.10)$$

And the approximation to $s(t)$ at any level is:

$$A_{j-1} = \sum_{j > J} D_j \quad (5.11)$$

The following equations hold:

$$A_{j-1} = A_j + D_j \quad (5.12)$$

$$s = A_J + \sum_{j \leq J} D_j \quad (5.13)$$

Decomposition is the process of splitting the signal into trend (low frequency component) and detail (high frequency component). In practice, the decomposition can be determined iteratively using wavelets, with successive approximations computed in turn, a signal is decomposed into many lower-resolution components as shown in figure 5.4. This is known as the '*wavelet decomposition tree*'. The discrete wavelet transform (DWT) provides an effective method for generating features. The collection of all such features forms the feature vector. A feature vector is given by

$$v^{dwt} = \{v_1^{dwt}, v_2^{dwt}, \dots, v_{12}^{dwt}\}^T \quad (5.14)$$

A component v_i^{dwt} in the feature vector is related to the individual resolutions by the following equation

$$v_i^{dwt} = \frac{1}{n_i} \sum_{j=1}^{n_i} w_{i,j}^2 ; i = 1, 2, \dots, 12 \quad (5.15)$$

Where,

$$n_1 = 2^{12}, n_2 = 2^{11}, \dots, n_{12} = 2^0.$$

v_i^{dwt} is the i^{th} feature element in a DWT feature vector. n_i is the number of samples in an individual sub-band, $w_{i,j}^2$ is the j^{th} coefficient of the i^{th} sub-band.

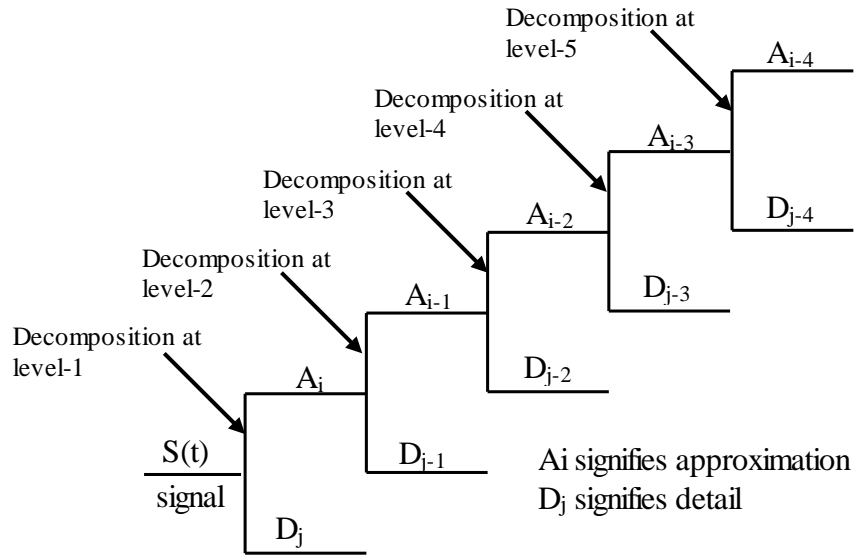


Figure 5.4 Wavelet decomposition tree

5.4.4 Empirical mode decomposition features

The assumption behind the development of EMD algorithm is that any signal consists of different intrinsic modes of oscillations. EMD decomposes a non-stationary signal into different IMFs. An IMF is a function that satisfies the two following definitions:

- The number of IMF extrema (the sum of the maxima and minima) and the number of zero-crossings must either be equal or differ at most by one.
- At any point of an IMF the mean value of the envelope defined by the local maxima and the envelope defined by the local minima shall be zero.

An IMF represents a simple oscillatory mode compared with the simple harmonic function. With the definition, any signal $x(t)$ can be decomposed as follows:

$$x(t) = \sum_{i=1}^n c_i(t) + r_n \quad (5.16)$$

EMD decomposes the given signal into ‘ n ’ empirical modes and a residue ‘ r_n ’ which represents central tendency of signal $x(t)$. The IMFs $c_1(t)$, $c_2(t)$, ..., $c_n(t)$ include different frequency bands ranging from high to low. The frequency components contained in each frequency band are different and they change with the variation of signal $x(t)$.

Each resulting IMFs component consist the local characteristic of the signal. While the cutting tool inserts with different mechanical faults while operating, the amplitude energy of each IMF are obviously different, therefore amplitude energy feature of each IMF component can be used to identify the different fault of single point cutting tool. In order to classify the faults, the amplitude energy feature can be treated as input vector for classifier. The total energy ‘ E_{pi} ’ of the first ‘ n ’ IMFs is calculated as:

$$E_{pi} = \sum_{h=1}^m |c_i(t_h)|^2 \quad (5.17)$$

Where

‘ E_{pi} ’ represents amplitude energy of the i^{th} IMFs, ‘ $h = 1$ to m ’ indicates the discrete data length of the i^{th} IMFs.

A feature vector with the amplitude energy as element is constructed as:

$$T = [E_{p1}, E_{p2}, \dots \dots \dots E_{pn}] \quad (5.18)$$

Where

‘ n ’ represents number of IMFs

Considering the amplitude energy of several IMFs, it may be sometimes very large or very low, in order to avoid attributes in greater numeric ranges which dominate the smaller numeric ranges and also to reduce numerical difficulties during the calculation, normalizing is essential.

‘ T ’ is regulated by normalizing the feature, for the convenience of the following analysis and processing.

Let

$$E = \left(\sum_{i=1}^n |E_{pi}|^2 \right)^{1/2} \quad \text{then,}$$

$$T' = \left[\frac{E_{p1}}{E}, \frac{E_{p2}}{E}, \dots \dots \dots \frac{E_{pn}}{E} \right]$$

$$= [E_1, E_2, \dots \dots \dots E_n] \quad (5.19)$$

Where,

T' represents normalized vector.

This normalised vector T' shall be treated as main input vector of the proposed fault diagnosis model so that cutting tool fault can be distinguished (Chen et al. 2013).

5.5 FEATURE SELECTION

The features can be any measure of data points or the signal; but the relevance of them will depend on how well they help in the process of classification. The process of selecting the good features from a pool of features is called '*feature selection*'. The good feature will have feature values with minimum variation within a class and maximum variation between the classes. Many techniques are used for feature selection; among them principal component analysis (PCA) is widely used. For all cases of the study in this thesis, decision tree and PCA has been used for feature selection. These methods are described in detail below.

5.5.1 Principal component analysis (PCA)

In PCA, the amount of information is measured in terms of variance. The idea of PCA is to rotate the feature axes such that the information (Variance) along one axis is maximum compared to the other. After such a rotation, the feature, which has the maximum variance, is the best feature. The same idea can be extended to multiple features in descending order.

PCA visualization for two-dimensional problem is depicted in figure 5.5. X and Y are the initial positions of the axes and X' and Y' are positions after rotation. The axes X and Y are rotated such that the variance along one axis (here X') is minimum. After

rotation, the axis which has maximum variance, is called '*principal direction*'. The unit vector along the principal direction is called '*eigen-vector*' and upon projecting all data points on to the *eigen-vector* (taking dot product), the value obtained is '*eigen-value*'.

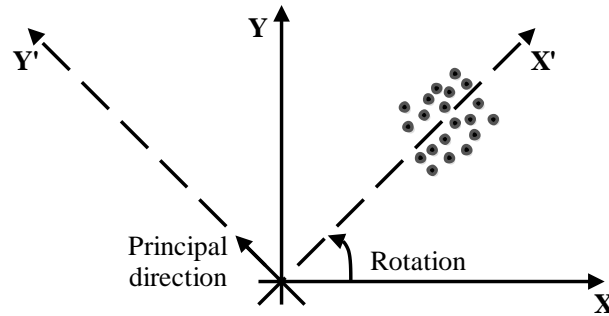


Figure 5.5 PCA visualization

The step-by-step procedure involved is as follows:

Step 1: Find the mean value of the signal. Subtract the mean value from each element of the mean.

Step 2: Calculate the variance matrix.

$$cov(X, Y) = \frac{\sum_{i=1}^n (X_i - \bar{X})(Y_i - \bar{Y})}{(n - 1)} \quad (5.20)$$

Where,

X, Y are columns of a data set

\bar{X}, \bar{Y} are means of X and Y

i is index that varies from 1 to n.

Step 3: Calculate the eigenvectors and eigenvalues of the covariance matrix.

Step 4: Order them by eigenvalue, highest to lowest. This will provide components in order of significance. Ignore the components which are having lesser significance.

5.5.2 Decision tree technique

Decision tree consists of tree structured algorithm which depicts the classification information of the data. The purpose of decision tree is to expose the information contained in the data. It's a predictive machine-learning model. As the name indicates

decision tree follows the pattern of tree, which is constructed using single root, number of branches, number of nodes and leaves. One branch that starts from root to leaf is chain of nodes and each node consists of one attribute. The occurrence of an attribute is the number of times the attribute occurs in the tree, which provides the information about the importance of the associated attribute.

The method of forming the decision tree and exploiting the same for feature selection is given as follows,

- The group of features obtained will be treated as input to the decision tree algorithm.
- The decision tree consists of leaf nodes, which indicates class labels and other nodes accompanied with the classes to be classified.
- Each branch of the tree illustrates each possible value of the feature node from which they generate.
- The decision tree can be used to classify feature vectors by starting at the root to leaf node of the tree, which provides a classification of the instance, is identified.
- At each decision node, one can select the most convenient feature for classification using appropriate estimation criteria. This selection brings about the concepts of entropy reduction and information gain, are discussed in the following subsection (Sugumaran et al. 2007).

5.5.2.1 Information gain and entropy reduction

Information gain is used for measuring association between inputs and outputs. It is a state to state change in information entropy. Entropy is a measure of disorder of data. It is generated from information theory. As the entropy value increases, will get more information content. For feature 'A', information gain (S, A) relative to a collection of examples S, is defined as:

$$Gain(S, A) = Entropy(S) - \sum_{v \in value(A)} \frac{|S_v|}{|S|} Entropy(s_v) \quad (5.21)$$

Where,

A value (A) is the set of all possible values for attribute A.

'S_v' is the subset of S for which feature A has value v.

Entropy is given by,

$$Entropy(S) = \sum_{i=1}^c -P_i \log_2 P_i \quad (5.22)$$

Where,

‘ c ’ represents number of classes.

‘ P_i ’ is probability of class ‘ i ’. Compute it as the proportion of class ‘ i ’ in the set.

In equation 5.22, the negative sign is to make the entropy a positive value as the results of logarithm (of a fraction) in this equation always yields a negative value.

5.6 FAULT CLASSIFICATION METHODS

As defined earlier, classifier is a function which maps a set of inputs from feature space to its corresponding classes. In the present study, from set of extracted features the classifier maps them to the condition of the cutting tool. In practice pattern classification can be carried out using many classifiers. Amongst them, Artificial neural network, Bayes net, Naive Bayes, K-star and Support vector machines are very popular ones. The following sections describe briefly about the commonly used classifiers.

5.6.1 Artificial neural network

Artificial neural network (ANN) is formed based on cells simulating the low level functions of biological neurons. In ANN, knowledge about the problem is distributed in neurons and connection weights links between neurons. The neural network has to be trained to adjust the connection weights and biases in order to produce the desired mapping. At the training stage, the feature vectors are given as input to the network along with known output vector and the network adjusts its variable parameters, the weights and biases, to capture the relationship between the input patterns and outputs. ANN is particularly useful for complex pattern recognition and classification tasks. The capability of learning from examples, the ability to reproduce arbitrary nonlinear functions of input, and the highly parallel and regular structure of ANN make them

especially suitable for pattern classification tasks. ANN is characterized by their topology, weight vector and activation functions. They have three layers namely an input layer, which receives signals from the external world, a hidden layer, which does the processing of the signals and an output layer, which gives the result back to the external world. Each layer is made up of artificial neurons. An artificial neuron is shown in figure 5.6. Various neural network structures are available. The reviews of literature reveals that both supervised learning and unsupervised learning have been applied in similar problems.

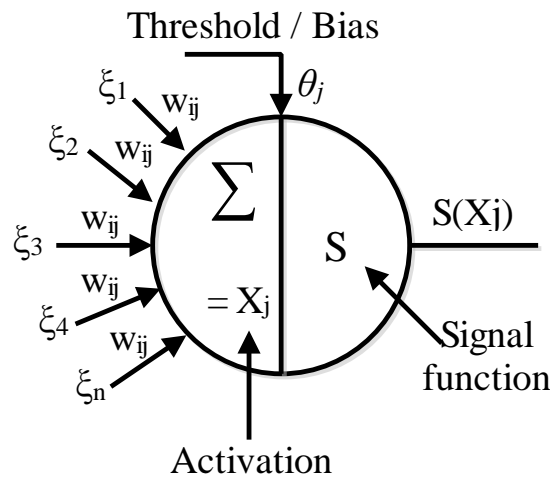


Figure 5.6 Artificial neuron used in the neural network

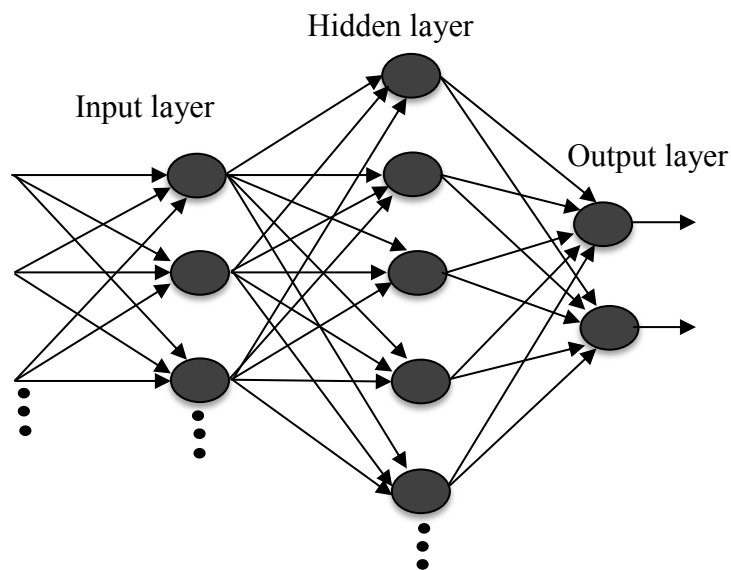


Figure 5.7 Multi-layer network

5.6.1.1 Multi-layer perceptron (MLP)

This is an important class of neural networks, namely the feed forward networks. Typically, the network consists of a set of input parameters that constitute the input layer, one or more hidden layers of computation nodes and an output layer of computation nodes (Figure 5.7).

Each neuron in the hidden and output layer consists of an activation function, which is generally a non-linear function like the logistic function and is given by

$$f(x) = \frac{1}{1 + e^{-x}} \quad (5.23)$$

Where,

$f(x)$ is differentiable and

$$x = \sum_{i=1} W_{ij} \xi_i + \theta_j \quad (5.24)$$

The suffixes i , j and k represent the input layer, the hidden layer and the output layer respectively. W_{ij} is the weight vector connecting the i^{th} neuron of the input layer to the j^{th} neuron of the hidden layer, ξ_i is the input vector and θ_j is the threshold of the j^{th} neuron of the hidden layer. Similarly, W_{ik} is the weight vector connecting j^{th} neuron of the hidden layer with the k^{th} neuron of the output layer. The weights those are important in predicting the processes are unknown. The weights of the network to be determined are initialized to small random values. The choice of initial values selected obviously affects the rate of convergence. The weights are updated through an iterative learning process known as ‘error back propagation (EBP) algorithm’. Error back propagation process consists of two passes through the different layers of the network; a forward pass in which input patterns are presented to the input layer of the network and its effect propagates through the network layer by layer. Finally, a set of outputs is produced as the actual response of the network. During the forward pass the synaptic weights of the networks are all fixed. The error value is then calculated, which is the mean square error (MSE) and is given by

$$E_{tot} = \frac{1}{n} \sum_{n=1}^n E_n \quad (5.25)$$

Where,

$E_n = \frac{1}{2} \sum_{k=1}^m (\xi_k^n - O_k^n)^2$, Where, n is the number of neurons in the output layer,

ξ_k^n is the k^{th} component of the desired or target output vector and

O_k^n is the k^{th} component of the output vector.

The weights in the links connecting the output and the hidden layer W_{jk} are modified as follows:

$$\Delta W_{jk} = \eta(-\partial E / \partial W_{jk}) = \eta \delta_j y_j,$$

Where,

η is the learning rate.

Considering the momentum term (α) $\Delta W_{jk} = \alpha \eta \delta_j y_j$ and $W_{jk}^{old} + \Delta W_{jk}$. Similarly the weights in the links connecting the hidden and input layer W_{ij} are modified as follows:

$$\Delta W_{jk} = \alpha \eta \delta_j \xi_i \quad (5.26)$$

Where,

$$\delta_j = y_j(1 - y_j) \sum_{k=1}^m \delta_k W_{jk} \quad (5.27)$$

$$W_{ij}^{new} = W_{ij}^{old} + \Delta W_{ij} \quad (5.28)$$

$$\delta_k = (\xi_k - O_k) O_k (1 - O_k) \quad (5.29)$$

For output neurons and for hidden neurons

$$\delta_j = y_j(1 - y_j) \sum_{k=1}^m \delta_k W_{jk} \quad (5.30)$$

The training process is carried out until the total error reaches an acceptable level (threshold). If $E_{\text{tot}} < E_{\text{min}}$ the training process is stopped and the final weights are stored, which is used in the testing phase for determining the performance of the developed network.

5.6.2 Naive Bayes classifier

Bayesian decision making refers to choosing the most likely class that is given the value of feature or features. Considering the classification into two classes $C1$ and $C2$ based on a single feature x , from the training sets of the two classes, histograms can be prepared and the respective probabilities are determined. Information extracted there from can be used to carry out classification based on the feature x . Figure 5.8, shows a hypothetical case. The class $C1$ can be assigned for values of x small enough and the alternate class $C2$ assigned for sufficiently large values of x . This leads to the possibility of deciding a classification boundary and a rationale for it. Consider a sample with feature value $x=x_b$ such that

$$P_{c1}(x_b)dx = P_{c2}(x_b)dx \quad (5.31)$$

A sample with feature value $x < x_b$ has $P_{c1}(x_b)dx > P_{c2}(x_b)dx$ It can be classified as belonging to class $C1$. On the other hand a sample with feature value $x > x_b$ has $P_{c1}(x_b)dx < P_{c2}(x_b)dx$. It can be classified as belonging to class $C2$. Thus $x=x_b$ constitutes the classification boundary. The procedure can be directly extended to multiple classes and features (Amarnath et al. 2015).

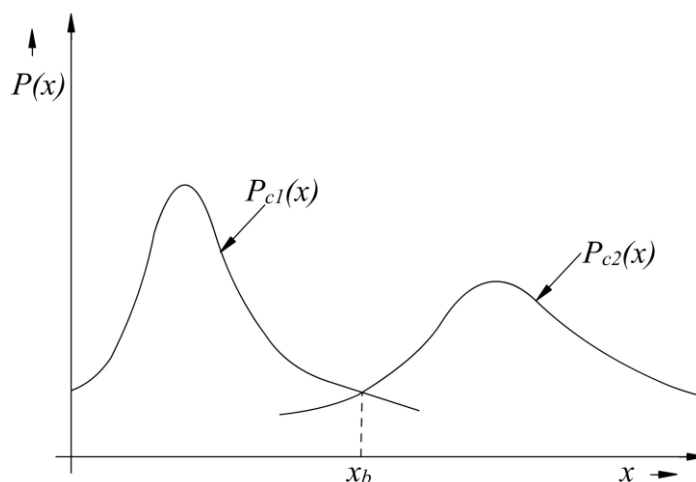


Figure 5.8 Histogram of a hypothetical two-class problem

5.6.3 Bayes net algorithm

A Bayesian network is a probabilistic graphical model. It is a directed acyclic graph (DAG), which implies that it is a network of random variables, which make the node and the nodes to be related with their conditional dependencies.

The Bayesian network consists of a set of variables, $V = \{A_1, A_2, \dots, A_N\}$ and a set of direct edge E between variables, which form a directed acyclic graph (DAG) $G = (V, E)$ where a joint distribution of the variables is represented by the product of conditional distributions of each variable given its parents. Each node, $A_i \in V$ represents a random variable and a directed edge from A_i to A_j , $(A_i, A_j) \in E$, represents the conditional dependency between A_i and A_j . In a Bayesian network, each variable is independent of its non-descendants, given a value of its parents in 'G'. This independence encoded in 'G' reduces the number of parameters which is required to characterize a joint distribution, so that posterior distribution can be efficiently inferred.

In a Bayesian network over $V = \{A_1, A_2, \dots, A_n\}$, the joint distribution $P(V)$ is the product of all conditional distributions specified in the Bayesian network such as

$$P(A_1, A_2, \dots, A_n) = \prod_{i=1}^N P(A_i / Pa_i) \quad (5.32)$$

Where,

$P(A_i/Pa_i)$ is the conditional distribution of A_i , given Pa_i which denotes the parent set of A_i . A conditional distribution for each variable has a parametric form that can be determined by the maximum likelihood estimation.

The Bayesian network has advantages such as avoidance of overfitting data, accommodating missing values.

5.6.4 Support vector machine

Support vector machine (SVM) is one of the supervised learning methods used for classification. It is a discriminative classifier in which training data are separated using Hyper-plane (Cortes and Vapnik 1995). Figure 5.9, shows the standard SVM

classifier, where two different training data points (visually represented as triangles and circles), are linearly classified. SVM performs classification process by separating the training data set into two classes (namely triangles and circles) in such a way that margin is maximized, so that generalization error is minimized. The nearest data points on which margin are defined is referred to as support vectors (Bansal et al. 2013). These points plays important role in the process of creating hyper plane.

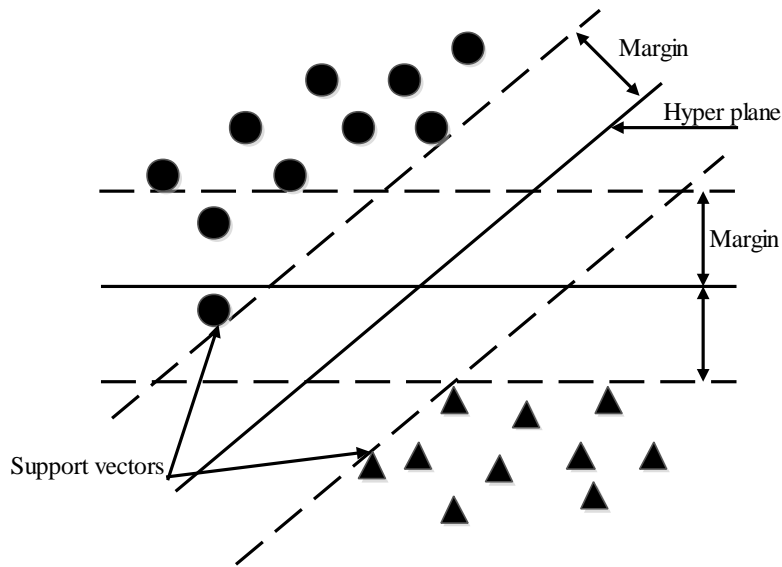


Figure 5.9 Illustration of support vector machine classifier

Considering training data set $\{(x_i, y_i)\}; i=1 \text{ to } L, x_i \in \mathbb{R}^n, y_i \in \{1, -1\}$ where L indicates total number of data points, x_i is the input vector and y_i is indicator vector, it is required to determine the hyper plane which separates the data points linearly into two classes (triangles and circles). $y_i \in \{1, -1\}$ concerned with the two types of classes. For the hyper plane $f(x) = 0$ which separates the given data is obtained as a solution to the following optimization problem.

$$\text{Minimize } \frac{1}{2} \|w\|^2 + C \sum_{i=1}^L \xi_i \quad (5.33)$$

$$\text{Subject to } \begin{cases} y_i (w^T x_i + b) \geq 1 - \xi_i \\ \xi_i \geq 0; i = 1 \text{ to } L \end{cases} \quad (5.34)$$

Where,

‘ ξ ’ is slack variable, ‘ b ’ is the bias, $C > 0$ is the constant representing penalty parameter and ‘ w ’ is weight vector (Kankar et al. 2011).

After training, for any new set of features prediction of its class is possible using the decision function as given below, which is a function of ‘ w ’ and ‘ γ ’. It is called testing.

$$f(x) = \text{sign}(w^T x - \gamma) \quad (5.35)$$

If the value of $f(x)$ is positive then new set of features belongs to class circles; otherwise it belongs to class triangles.

5.6.5 K-star algorithm

K* is an instance-based classifier, that is the class of a test instance and is based upon the class of those training instances similar to it, as determined by some similarity function. It differs from other instance-based learners in that it uses an entropy-based distance function. The K-star algorithm uses entropic measure, based on probability of transforming instance into another by randomly choosing between all possible transformations. A consistency of approach in real, symbolic, missing value attributes makes it important. An instance based algorithm made for symbolic attributes fail in features of real value thus lacking in incorporated theoretical base. Approaches successful in feature of real values are thus in an ad – hoc fashion are made to handle symbolic attributes. Handling of missing values by classifiers results a similar problem. Usually missing values are treated as a separate value and are thought as maximally different and are substitute for average value, otherwise simply to be ignored (Cleary and Trigg 1995).

5.7 RESULTS AND DISCUSSIONS

5.7.1 Classification based on statistical features

From the acquired vibration signal from cutting tool, twelve statistical features were extracted. Table 5.1 depicts extracted statistical features and out of 40 samples only two samples pertaining to each class of defect are shown in this table.

Table 5.1 Extracted statistical features

Class	Sample No.	Values											
		Mean	Standard Error	Median	Mode	Standard Deviation	Sample Variance	Kurtosis	Skewness	Range	Minimum	Maximum	Sum
Healthy	1	0.0055	0.0032	0.0066	0.3321	0.7256	0.5265	0.0442	-0.0121	7.1346	-3.9515	3.1831	0.0055
	2	0.0055	0.0027	0.0071	-0.1165	0.6112	0.3736	0.1088	-0.0183	5.8215	-2.8960	2.9255	0.0055
Breakage	1	-0.0077	0.0278	-0.0509	0.3273	4.4426	19.7371	0.2326	0.0232	40.3391	-21.9223	18.4168	-0.0077
	2	-0.0032	0.0285	-0.0019	2.9243	4.5641	20.8309	0.2861	0.0273	41.4111	-22.6087	18.8024	-0.0032
Thermal cracks	1	0.0008	0.0143	-0.0068	0.8641	2.2906	5.2470	0.2143	0.0231	22.3246	-11.4335	10.8911	21.6735
	2	0.0017	0.0143	0.0055	-0.1668	2.2934	5.2595	0.2873	0.0278	25.1048	-12.5777	12.5271	43.2151
Notch wear	1	0.0002	0.0207	-0.0146	-2.5025	3.3077	10.9410	0.3726	0.0389	32.8081	-14.9869	17.8213	4.6818
	2	0.0046	0.0205	-0.0115	-0.5410	3.2800	10.7587	0.3768	0.0366	31.8735	-16.7361	15.1373	117.5168
Rake face chipping	1	0.0053	0.0044	0.0020	-0.6649	0.9750	0.9505	0.3269	0.0035	12.2095	-5.9494	6.2601	264.0113
	2	0.0057	0.0036	0.0061	0.2973	0.8042	0.6467	0.1983	0.0030	7.6646	-3.8190	3.8456	285.0222

From this table, it can be observed that all features for each class of defect are different to some extent. It becomes difficult work for anyone to distinguish the difference, for fault diagnosis. Therefore important features out of extracted features are selected using decision tree (J48 algorithm) or principal component analysis (PCA).

5.7.2 Feature selection (Statistical features)

All the features need not necessarily reveal the required information. Generally, some features may yield more information than others. The process of selecting such good features which reveal more information for classification is called feature selection. This process is also known as '*dimensionality reduction*', as each feature adds a dimension in feature space and selecting a few features reduces the dimension. The techniques used in the study of feature selection are J48 algorithm or PCA.

5.7.2.1 Principal component analysis (PCA)

PCA transforms the data to a new coordinate system in such a way that the greatest variance by any projection of the data comes to lie on the first coordinate (called the first principal component), the second greatest variance on the second coordinate, and so on. PCA can be used for dimensionality reduction for a dataset while retaining the characteristics of the dataset that contribute most to its variance, by keeping lower-order principal components and ignoring higher-order ones. Such low order components often contain the "most important" aspects (information) of the data. The number of data to be analyzed can be reduced, if the user can tolerate some amount of error in each data. One problem with PCA is that the original data cannot be used as such. The data after transformation will be different from the original data. Hence, some of the researchers will prefer other techniques for selection of higher order features. Twelve features mentioned in section 5.3.1 are the inputs. After processing, PCA yields six features. With these six features, the classification is performed using J48 algorithm and the classification efficiency is found to be 77%. The same data set is used for feature selection and classification using decision tree and classification efficiency found to be of 85%. Observation shows that classification efficiency with

the decision tree higher than that of PCA (about 8%). Above results depicts that, decision tree performs better than the PCA for feature selection. However, it is to be mentioned here that this result cannot be generalized for all data sets and features.

5.7.2.2 Decision tree (J48 algorithm)

Statistical features (which are extracted from acquired vibration signals) will serve as input to J48 decision tree algorithm. Generated decision tree as output from J48 algorithm is as shown in figure 5.10. It is clear from that the top node, which is the best node for classification. The other features in the nodes of decision tree appear in descending order of importance. It is to be stressed here that only features that contribute to the classification appears in the decision tree and others do not. Features, which have less discriminating capability, can be consciously discarded by deciding on the threshold. The algorithm identifies the good features for the purpose of classification from the given training data set, and thus reduces the domain knowledge required to select good features for pattern classification problem.

5.7.2.2.1 Features suggested by J48 algorithm

Dominating features represent the cutting tool condition descriptions. The level of contribution by an individual feature is given by a statistical measure within the parenthesis in the decision tree shown in figure 5.10. The first number in the parenthesis indicates the number of data points that can be classified using that feature set. The second number indicates the number of samples against this action. If the first number is very small compared to the total number of samples, then the corresponding features can be considered as outliers and hence ignored. Figure 5.10 depicts seven dominating features and there significance in order of importance, they are maximum, standard error, range, skewness, kurtosis, mean and median

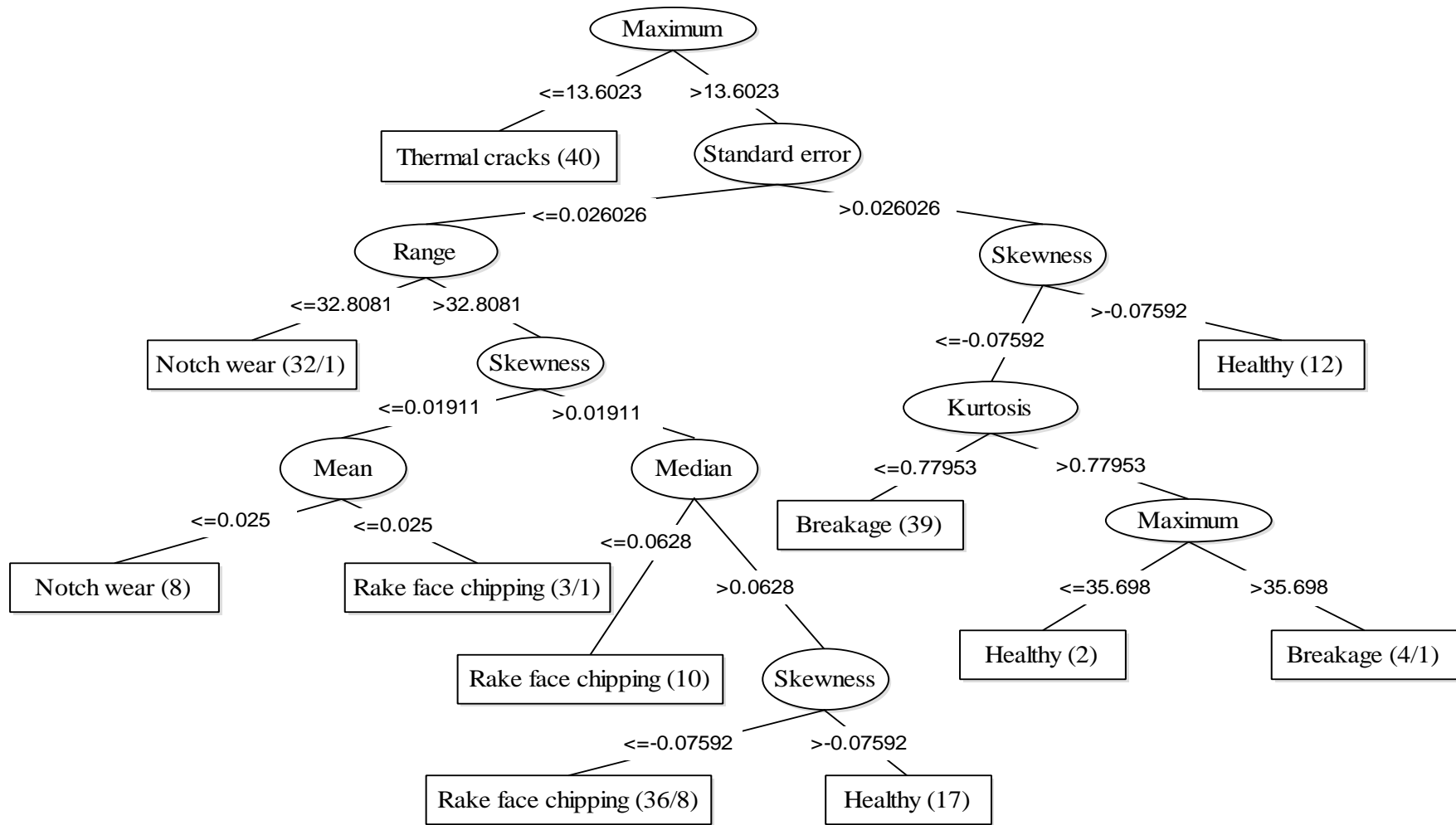


Figure 5.10 Decision tree for statistical features

5.7.3 Classification

Classification is a two-phase process they are (i) training and (ii) testing. Training is the process of learning to label from the samples. Training can be in supervised mode or in unsupervised mode. Unsupervised training is used in situations, where the target class information is not available. In this study, the target class information is available. Hence, supervised mode is used for training. Testing is the process of checking, how well the classifier has learnt to label the unseen samples. The testing results of most of the classifiers used here are presented in the form of the confusion matrix.

5.7.3.1 Artificial neural network

The classification accuracy of ANN with statistical features for cutting tool fault diagnosis application is studied. The ANN results are presented in table 5.2 and table 5.3.

Table 5.2 ANN results with statistical features

Test Parameter	Values
Test mode	10-fold cross-validation
Time taken	0.4 seconds
Total Number of Instances	200
Correctly Classified Instances	167 (83.5%)
Incorrectly Classified Instances	33 (16.5%)

Table 5.3 Confusion matrix of ANN with statistical features

a	b	c	d	e	Class
29	3	0	0	8	a-Healthy
4	34	0	0	2	b- Breakage tool
0	0	39	0	1	c- Thermal cracks
1	1	0	34	4	d- Notch wear
5	2	1	1	31	e- Rake face chipping

The seven statistical features discussed earlier namely maximum, standard error, range, skewness, kurtosis, mean and median were the input nodes, which form the input layer. The conditions of the tungsten carbide cutting tool insert under study namely, healthy cutting tool (Healthy), cutting tool with breakage (Breakage), cutting tool with thermal cracks (Thermal cracks), cutting tool with notch wear (Notch wear) and cutting tool with chipping on rake face (Rake face chipping) were the possible outputs of the ANN.

From the confusion matrix, one can note that 33 samples are misclassified. However, the overall classification accuracy is found to be 83.5%. The instances of misclassification may be due to the weaker signals and improper training of the model.

5.7.3.2 Naive Bayes algorithm

Naive Bayes classifier makes use of condition probability for its classification. Table 5.4 and table 5.5 shows the classification parameters and the confusion matrix respectively.

Table 5.4 Naive Bayes algorithm results with statistical features

Test Parameter	Values
Test mode	10-fold cross-validation
Time taken	0.01 seconds
Total Number of Instances	200
Correctly Classified Instances	121 (60.5%)
Incorrectly Classified Instances	79 (39.5%)

From the confusion matrix, total numbers of misclassification instances are seventy nine. The overall classification efficiency is only 60.5%, which is less than that of ANN. As the classification efficiency is considerably low, Naïve Bayes classifier with statistical features for fault diagnosis of cutting tool is not very attractive.

Table 5.5 Confusion matrix of Naive Bayes algorithm with statistical features

a	b	c	d	e	Class
27	3	0	1	9	a-Healthy
13	3	0	1	23	b- Breakage tool
0	1	39	0	0	c- Thermal cracks
0	2	0	35	3	d- Notch wear
7	1	0	15	17	e- Rake face chipping

5.7.3.3 Bayes net algorithm

Bayes net algorithm works on the same principle as that of the Naïve Bayes classifier with the only difference being that it also uses the search algorithm for classification purpose. Hence, the results vary in comparison with Naïve Bayes algorithm. The parameters of classification and confusion matrix pertaining to the Bayes net are presented in table 5.6 and table 5.7 respectively.

Table 5.6 Bayes net algorithm results with statistical features

Test Parameter	Values
Test mode	10-fold cross-validation
Time taken	0.04 seconds
Total Number of Instances	200
Correctly Classified Instances	171 (85.5%)
Incorrectly Classified Instances	29 (14.5%)

Table 5.7 Confusion matrix of Bayes net algorithm with statistical features

a	b	c	d	e	Class
31	0	0	0	9	a-Healthy
3	36	0	1	0	b- Breakage tool
0	0	40	0	0	c- Thermal cracks
1	0	0	34	5	d- Notch wear
8	0	0	2	30	e- Rake face chipping

Confusion matrix depicts twenty nine misclassifications out of 200 samples. As the classification efficiency (about 85.5%) is considerably low, Bayes net with statistical features for fault diagnosis of cutting tool is not suitable.

5.7.3.4 Support vector machine

The test conditions and the corresponding output values are given in table 5.8 and followed by the confusion matrix in table 5.9. From the confusion matrix, out of 200 instances, 142 have been correctly classified with classification efficiency of 71%. As the classification efficiency is considerably very low, SVM with statistical features for fault diagnosis of cutting tool is not preferable.

Table 5.8 SVM results with statistical features

Test Parameter	Values
Test mode	10-fold cross-validation
Time taken	0.07 seconds
Total Number of Instances	200
Correctly Classified Instances	142 (71%)
Incorrectly Classified Instances	58 (29%)

Table 5.9 Confusion matrix of SVM with statistical features

a	b	c	d	e	Class
19	4	0	3	14	a-Healthy
4	34	0	1	1	b- Breakage tool
0	0	39	0	1	c- Thermal cracks
0	2	0	37	1	d- Notch wear
4	4	1	18	13	e- Rake face chipping

5.7.3.5 K-star algorithm

The seven statistical features of five different cutting tool condition vibration signals were given as an input to the K-star algorithm. The identified classification efficiency and the time taken to complete the process are presented in the table 5.10

Table 5.10 K-star algorithm results with statistical features

Test Parameter	Values
Test mode	10-fold cross-validation
Time taken	0.01 seconds
Total Number of Instances	200
Correctly Classified Instances	169 (84.5%)
Incorrectly Classified Instances	31 (15.5%)

Table 5.11 Confusion matrix of K-star algorithm with statistical features

a	b	c	d	e	Class
30	2	0	0	8	a-Healthy
1	36	0	0	3	b- Breakage tool
0	0	40	0	0	c- Thermal cracks
1	1	0	33	5	d- Notch wear
7	2	0	1	30	e- Rake face chipping

The K-star yields the classification efficiency of 84.5%. Table 5.11 presents the confusion matrix with K-star algorithm as classifier.

5.7.3.6 J48 algorithm

Decision tree algorithm (otherwise referred as J48 algorithm) performs both feature selection and classification simultaneously. Table 5.12 and table 5.13 show the parameters and confusion matrix of decision tree respectively.

Twenty nine instances are misclassified and the overall classification accuracy is about 85.5%, which is considerably high compare to all other algorithms. But still J48 with statistical features for fault diagnosis of cutting tool is not preferable.

Table 5.12 J48 algorithm results with statistical features

Test Parameter	Values
Test mode	10-fold cross-validation
Time taken	0.06 seconds
Total Number of Instances	200
Correctly Classified Instances	171 (85.5%)
Incorrectly Classified Instances	29 (14.5%)

Table 5.13 Confusion matrix of J48 algorithm with statistical features

a	b	c	d	e	Class
30	2	0	0	8	a-Healthy
3	36	1	0	0	b- Breakage tool
0	0	39	1	0	c- Thermal cracks
0	1	0	36	3	d- Notch wear
8	0	0	2	30	e- Rake face chipping

The statistical features are extracted from the acquired vibration signals and feature selection has been performed using PCA and decision tree (J48 algorithm). The procedure led to the selection of seven features. Their performances in fault classification have been presented.

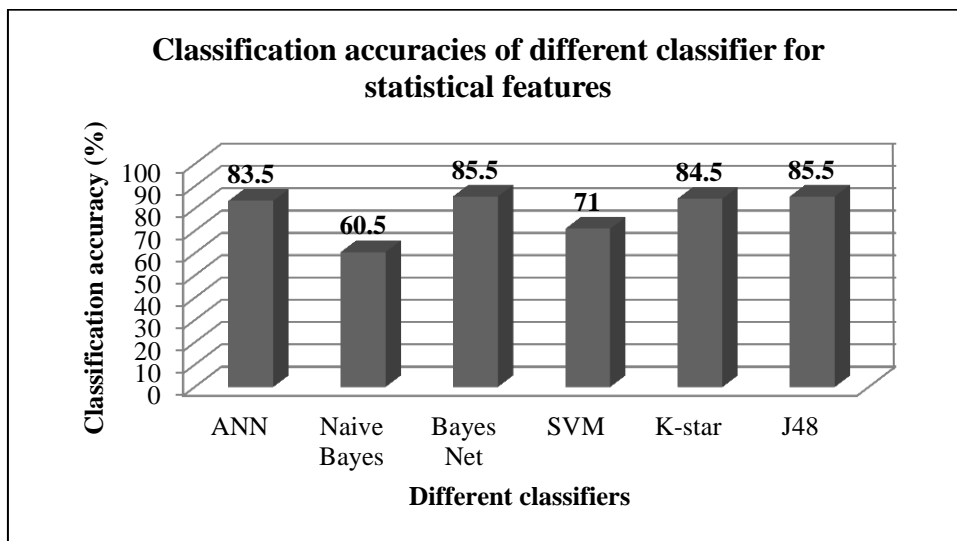


Figure 5.11 Classification efficiencies of different classifiers for statistical features

The summary of classification efficiencies of different classifiers with statistical features is as shown in figure 5.11. Figure 5.11 depicts that Bayes net classifier and decision tree (J48 algorithm) will give highest classification with statistical features.

5.7.4 Classification with discrete wavelet features

The discrete wavelet transform (DWT) is based on sub-band coding. It can be used effectively to analyze the signal as long as the time duration of the wavelet is large compared to the sampling period. This requirement is the same as the sampling theorem put in a different form. DWT is easy to implement and also reduces the computation time. Hence, DWT is taken up for study. From the acquired vibration signals pertaining to five different class or condition of tool, eight discrete wavelet features were extracted using DWT. Table 5.14, depicts extracted features using DWT method, out of 40 samples only two samples pertaining to each class are shown in table 5.14. Amongst these features, a set of good features which will have high discriminating ability is chosen using J48 and PCA algorithm. Fault classification study based on different classifiers is carried out with selected DWT features.

Table 5.14 Extracted features using DWT method

Class	Sample No.	Wavelet coefficient							
		V1	V2	V3	V4	V5	V6	V7	V8
Healthy	1	0.042	0.207	0.912	3.893	5.386	0.594	0.625	2.169
	2	0.040	0.199	0.924	3.674	6.081	0.648	0.819	2.355
Breakage	1	0.042	0.250	1.056	2.219	2.997	2.148	1.234	1.783
	2	0.045	0.256	1.074	2.365	3.295	2.411	1.529	1.700
Thermal cracks	1	0.066	0.261	0.816	2.453	3.774	0.409	0.575	1.636
	2	0.075	0.257	0.771	2.414	3.410	0.443	0.651	1.704
Notch wear	1	0.035	0.190	0.961	2.061	2.564	1.331	0.939	2.026
	2	0.034	0.188	0.871	2.213	2.986	1.448	0.931	1.793
Rake face chipping	1	0.036	0.194	0.871	1.925	1.789	0.697	0.589	2.162
	2	0.035	0.192	0.861	2.008	2.232	0.851	0.580	2.081

5.7.5 Feature selection (DWT features)

Eight features mentioned in table 5.14 are the inputs. After processing, PCA yields four features. With these four features, the classification is performed using J48 algorithm and the classification efficiency is found to be 91.5%.

The same data set is used for feature selection and classification using decision tree and found that the classification efficiency of 93.5%. It can be observed that classification efficiency with the decision tree is about 2% higher than that of PCA. From the above results, it can be noted that decision tree performs better than the PCA for feature selection.

However, it is to be mentioned here that this result cannot be generalized for all data sets and features. Eight DWT features are used as input to J48 algorithm, out of which five features were eliminated at the outset due to their imperceptible contribution to the classification. From figure 5.12, three contributors are identified as dominant features amongst all extracted features, they are V2, V1 and V7.

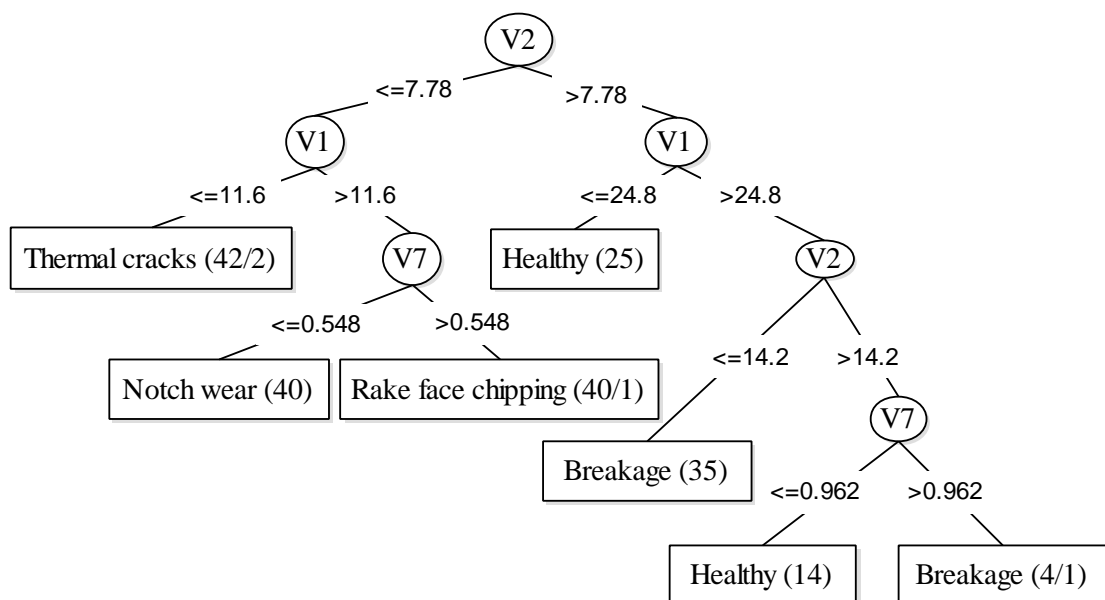


Figure 5.12 Decision tree for DWT features

5.7.6 Classification

Classification efficiencies of DWT features in combination with different classifiers are studied. The classifiers are artificial neural networks (ANN), Naive Bayes, Bayes net, support vector machines (SVM), K-star, and J48 algorithm. The results are reported in the following sub sections.

5.7.6.1 Artificial neural network

The three selected DWT features of five different cutting tool condition vibration signals were given as an input to the ANN. Table 5.15 depicts the classification efficiency and the time taken to complete the process. Table 5.16 shows the confusion matrix of ANN, observation shows that classification efficiency (about 96%) is considerably good, ANN with DWT features for fault diagnosis of cutting tool is attractive.

Table 5.15 ANN results with DWT features

Test Parameter	Values
Test mode	10-fold cross-validation
Time taken	0.3 seconds
Total Number of Instances	200
Correctly Classified Instances	192 (96%)
Incorrectly Classified Instances	8 (4%)

Table 5.16 Confusion matrix of ANN with DWT features

a	b	c	d	e	Class
40	0	0	0	0	a-Healthy
0	38	1	0	1	b- Breakage tool
0	0	40	0	0	c- Thermal cracks
0	1	0	38	1	d- Notch wear
0	0	1	3	36	e- Rake face chipping

5.7.6.2 Naive Bayes algorithm

Table 5.17 and table 5.18 illustrate the test conditions and confusion matrix of the Naïve Bayes classifier respectively. From the confusion matrix, 157 instances are correctly classified with classification efficiency of 78.5%. As the classification efficiency is considerably low, Naive Bayes algorithm with DWT features for fault diagnosis of cutting tool is not very preferable.

Table 5.17 Naive Bayes algorithm results with DWT features

Test Parameter	Values
Test mode	10-fold cross-validation
Time taken	0.01 seconds
Total Number of Instances	200
Correctly Classified Instances	157 (78.5%)
Incorrectly Classified Instances	43 (21.5%)

Table 5.18 Confusion matrix of Naive Bayes algorithm with DWT features

a	b	c	d	e	Class
39	1	0	0	0	a-Healthy
33	5	1	0	1	b- Breakage tool
1	0	39	0	0	c- Thermal cracks
3	0	0	37	0	d- Notch wear
1	0	1	1	37	e- Rake face chipping

5.7.6.3 Bayes net algorithm

The Bayes net yields the classification efficiency of 84.5%. The classification efficiency of Bayes net is higher, when compared to classification efficiency of Naive Bayes classifier. Table 5.19 and table 5.20 show the Bayes net results and confusion matrix.

Table 5.19 Bayes net algorithm results with DWT features

Test Parameter	Values
Test mode	10-fold cross-validation
Time taken	0.03 seconds
Total Number of Instances	200
Correctly Classified Instances	169 (84.5%)
Incorrectly Classified Instances	31 (15.5%)

Table 5.20 Confusion matrix of Bayes net algorithm with DWT features

a	b	c	d	e	Class
25	14	0	1	0	a-Healthy
8	30	1	0	1	b- Breakage tool
0	0	40	0	0	c- Thermal cracks
0	3	0	35	2	d- Notch wear
0	0	1	0	39	e- Rake face chipping

5.7.6.4 Support vector machine

The support vector machine is one of the classification techniques for fault diagnosis. SVM identifies the hyperplane to classify feature data set. The chosen three DWT features were given as an input to the SVM for classification. The classification results are summarized in table 5.21 and table 5.22.

Table 5.21 SVM results with DWT features

Test Parameter	Values
Test mode	10-fold cross-validation
Time taken	0.07 seconds
Total Number of Instances	200
Correctly Classified Instances	148 (74%)
Incorrectly Classified Instances	52 (26%)

Table 5.22 Confusion matrix of SVM with DWT features

a	b	c	d	e	Class
20	1	0	19	0	a-Healthy
3	35	1	0	1	b- Breakage tool
0	0	40	0	0	c- Thermal cracks
0	0	1	39	0	d- Notch wear
0	0	1	25	14	e- Rake face chipping

The time taken to complete the process is 0.07 seconds. The confusion matrix is shown in the table 5.22 which illustrates that the fifty two instances are misclassified. The classification efficiency of classifier is 74%, which indicates that the SVM classifier is not good for fault classifications.

5.7.6.5 K-star algorithm

The parameters of classification and confusion matrix of K-star are presented in table 5.23 and table 5.24 respectively.

From the confusion matrix (table 5.24), only eight instances are misclassified. As the classification efficiency (about 96%) is considerably good, K-star with DWT features for fault diagnosis of cutting tool is preferable.

Table 5.23 K-star algorithm results with DWT features

Test Parameter	Values
Test mode	10-fold cross-validation
Time taken	0.01 seconds
Total Number of Instances	200
Correctly Classified Instances	192 (96%)
Incorrectly Classified Instances	8 (4%)

Table 5.24 Confusion matrix of K-star algorithm with DWT features

a	b	c	d	e	Class
40	0	0	0	0	a-Healthy
2	36	1	0	1	b- Breakage tool
0	0	39	0	1	c- Thermal cracks
0	1	0	39	0	d- Notch wear
0	0	1	1	38	e- Rake face chipping

5.7.6.6 J48 algorithm

J48 algorithm makes use of information gain and entropy for its classification. Its classification parameters and confusion matrix are presented in table 5.25 and table 5.26 respectively.

Table 5.25 J48 algorithm results with DWT features

Test Parameter	Values
Test mode	10-fold cross-validation
Time taken	0.01 seconds
Total Number of Instances	200
Correctly Classified Instances	188 (94%)
Incorrectly Classified Instances	12 (6%)

Table 5.26 Confusion matrix of J48 algorithm with DWT features

a	b	c	d	e	Class
37	3	0	0	0	a-Healthy
2	36	1	0	1	b- Breakage tool
0	2	37	1	0	c- Thermal cracks
0	1	0	39	0	d- Notch wear
0	0	1	0	39	e- Rake face chipping

From the confusion matrix, one can note that there are only twelve misclassifications. The overall classification efficiency is found to be 94%. As the classification efficiency is considerably low when compare to ANN and K-star algorithm, decision tree technique (J48 algorithm) with DWT features for fault diagnosis of cutting tool is not preferable.

The DWT features are extracted from the acquired vibration signals and feature selection has been performed using PCA and decision tree J48 algorithm. The procedure led to the selection of three features. Their performances in classification have been presented. The summary of classification efficiencies of different classifiers is shown in figure 5.13. From the figure 5.13, K-star algorithm with the DWT features gives the highest classification efficiency. ANN and K-star algorithm are the best possible classifiers amongst the classifiers considered with present DWT features.

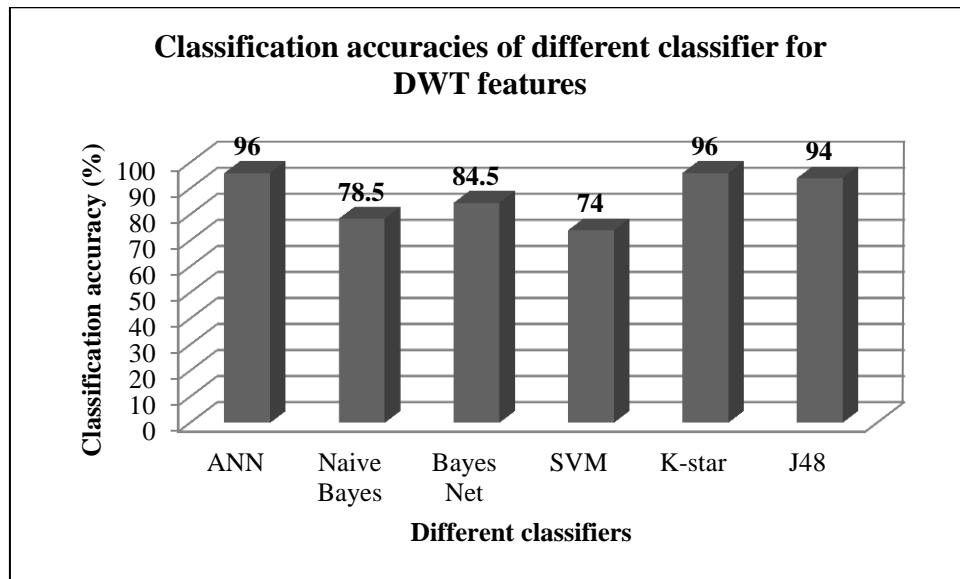


Figure 5.13 Classification efficiencies of different classifiers for DWT features

5.7.7 Classification with EMD features

From the acquired vibration signals pertaining to five different class of the tool, features are decomposed into some IMFs using EMD. The first 8 IMFs contained mainly the dominant fault information's that are used to construct the amplitude energy feature vector to verify the performance of the proposed model. Feature

energy vector T' are obtained according to equation 5.19 and treated as an input vector to decision tree (J48 algorithm). Table 5.27 depicts evaluated energy feature vector (two samples per each class) using EMD method.

Table 5.27 Feature vector based on EMD method

Class	Sample No.	Energy feature vector							
		E ₁	E ₂	E ₃	E ₄	E ₅	E ₆	E ₇	E ₈
Healthy	1	0.9918	0.143	0.9831	0.0404	0.012	0.026	0.076	0.007
	2	0.9907	0.103	0.9861	0.0299	0.010	0.009	0.015	0.004
Breakage	1	0.9887	0.128	0.0321	0.0294	0.016	0.005	0.005	0.004
	2	0.9843	0.123	0.0398	0.0385	0.022	0.013	0.022	0.014
Thermal cracks	1	0.9906	0.101	0.0377	0.0861	0.015	0.011	0.015	0.018
	2	0.9915	0.091	0.9864	0.0778	0.016	0.007	0.006	0.006
Notch wear	1	0.9529	0.138	0.9831	0.0566	0.019	0.005	0.008	0.005
	2	0.9531	0.124	0.1079	0.0393	0.016	0.006	0.003	0.004
Rake face chipping	1	0.9927	0.093	0.0651	0.0819	0.011	0.005	0.004	0.054
	2	0.9917	0.082	0.0640	0.0767	0.019	0.004	0.005	0.016

Figure 5.14 shows the decomposed first eight IMFs for healthy condition using EMD. Cutting passes are clearly visible in IMF c_2 , c_3 , and c_4 . IMF c_1 captures most of the high-frequency disturbances and noise, whose amplitude seems to be modulated by the turning passes, amplitude increases as the metal to metal contact increases between tool and workpiece. IMF c_6 , c_7 , and c_8 capture the low-frequency vibration signals, with harmonic content mainly related to tool condition. The EMDs for two different fault conditions are reported in figure 5.15, which shows intrinsic mode functions of cutting tool vibration signal for the breakage and thermally cracked tool. Figure 5.16 shows intrinsic mode functions of cutting tool vibration signal for the notch wear and rake face chipping tool.

Normal working conditions/ Healthy cutting tool (reference)

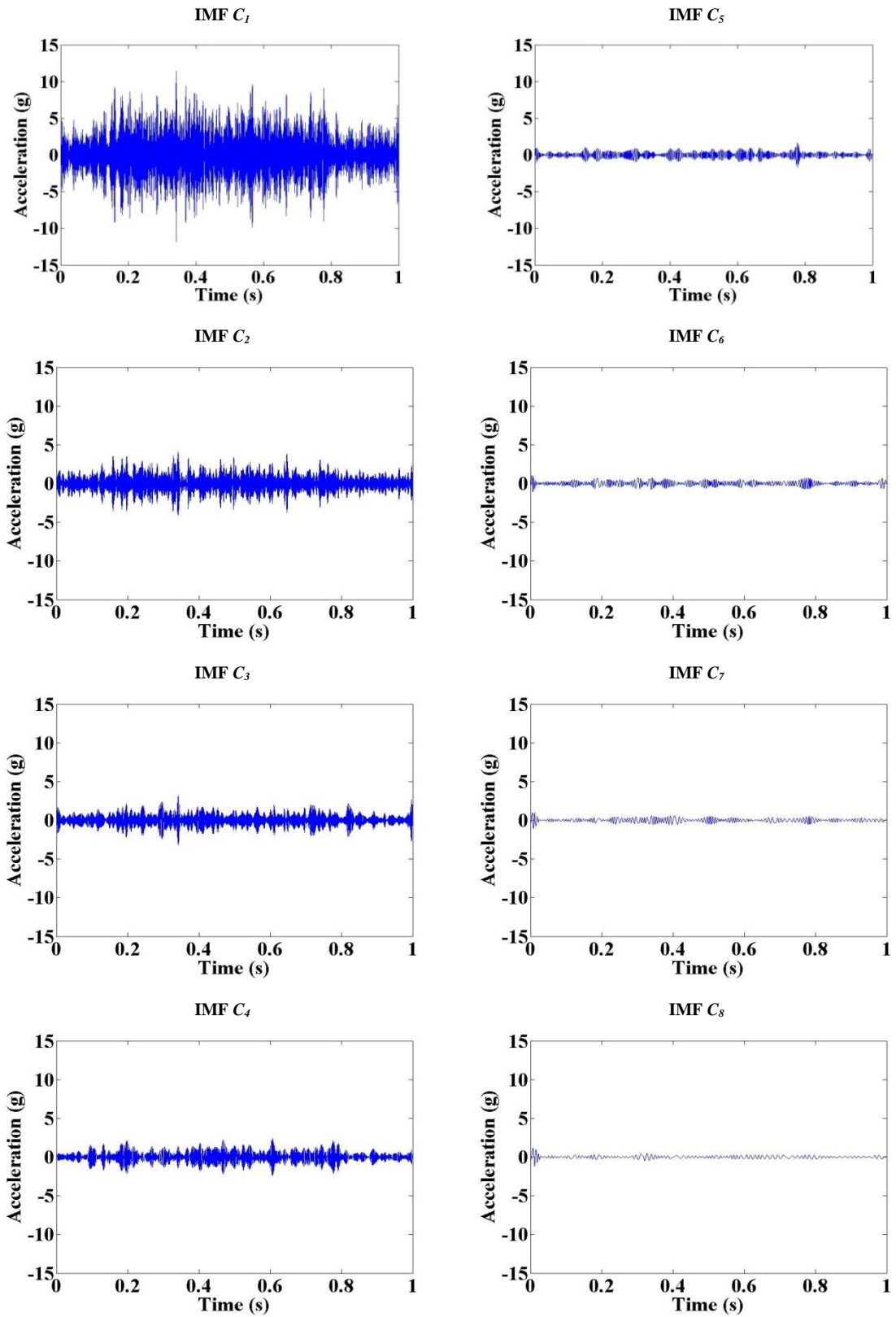
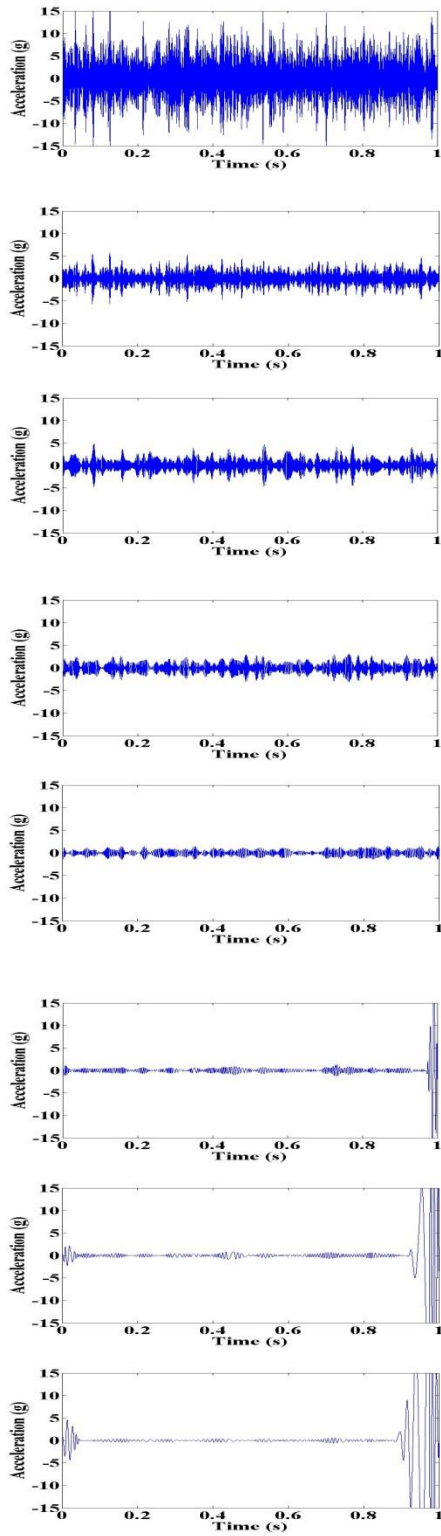


Figure 5.14 Intrinsic mode functions of cutting tool vibration signal with a healthy insert

Breakage tool



Thermally cracked tool

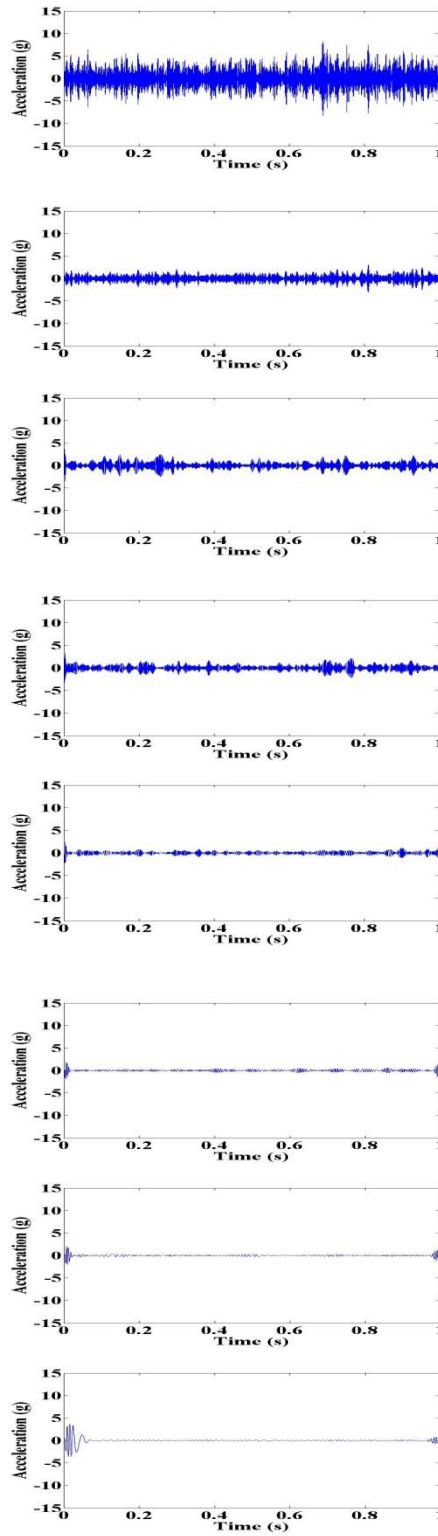
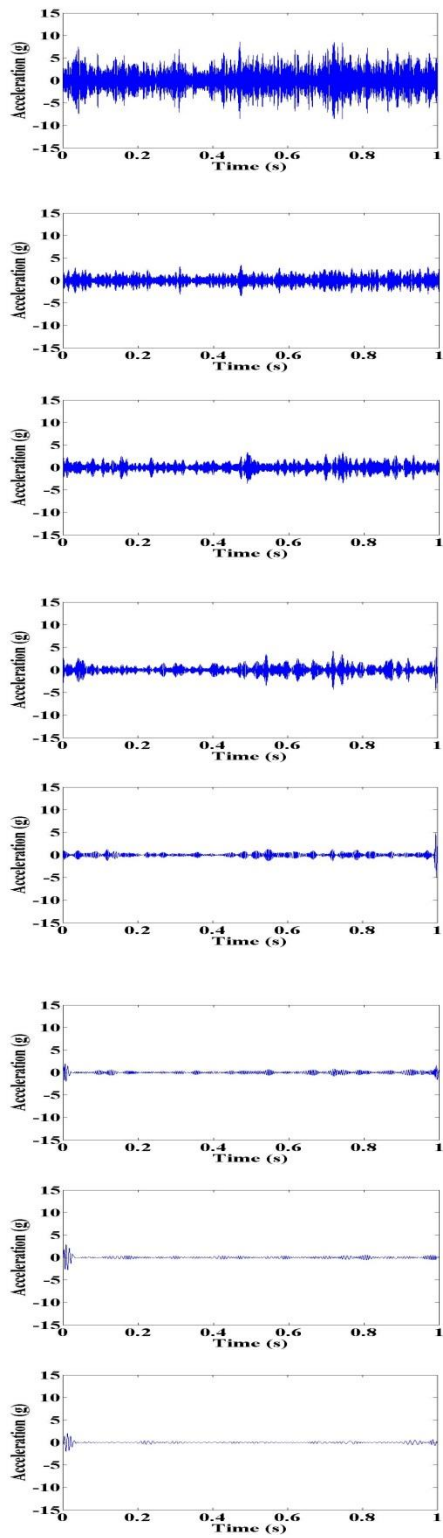


Figure 5.15 Intrinsic mode functions of breakage and thermally cracked tool insert

Notch wear



Rake face chipping tool

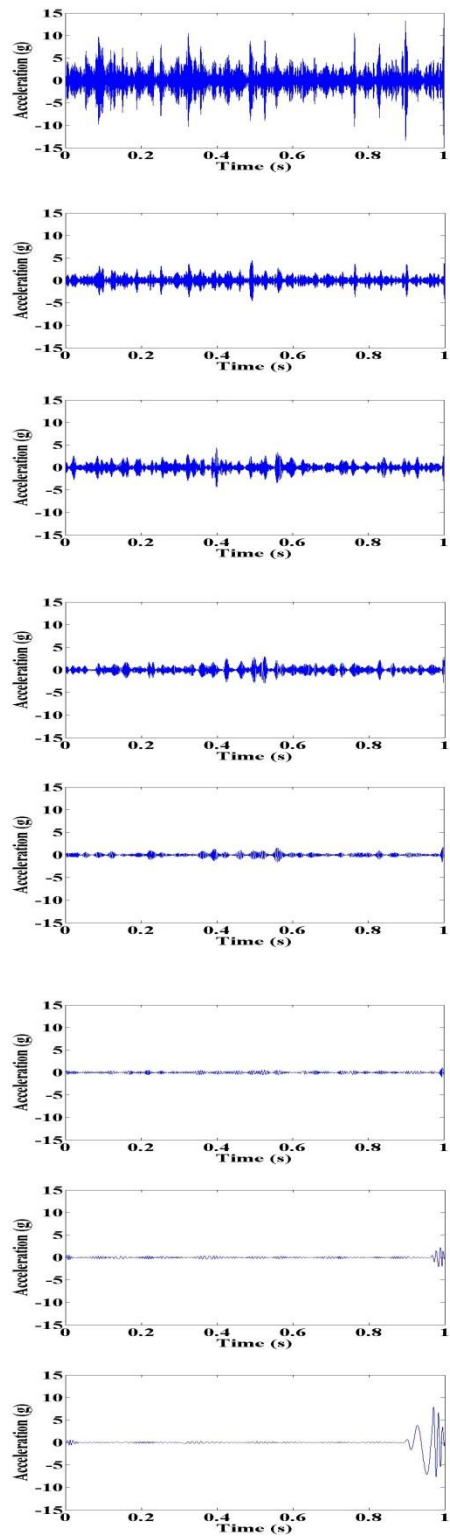


Figure 5.16 Intrinsic mode functions of notch wear and rake face chipping tool insert

5.7.8 Feature selection (EMD features)

Eight features mentioned in table 5.27 are considered as the input to either PCA algorithm or decision tree (J48 algorithm). After processing, PCA yields six features. With these six features, the classification is performed using J48 algorithm and the classification efficiency is found to be 59%. The same data set is used for feature selection and classification using decision tree technique and found that the classification efficiency is 96%. This proves that classification efficiency with the decision tree is about 37% higher than that with PCA. From the above results, it can be concluded that decision tree performs better than the PCA for feature selection. However, it is to be mentioned here that this result cannot be generalized for all data sets and features. Eight EMD features were used as an input to the J48 algorithm out of which five features were eliminated at the outset due to their imperceptible contribution to the classification. From figure 5.17, three contributors are identified as dominant amongst the extracted EMD features, namely E_1 , E_3 and E_4 .

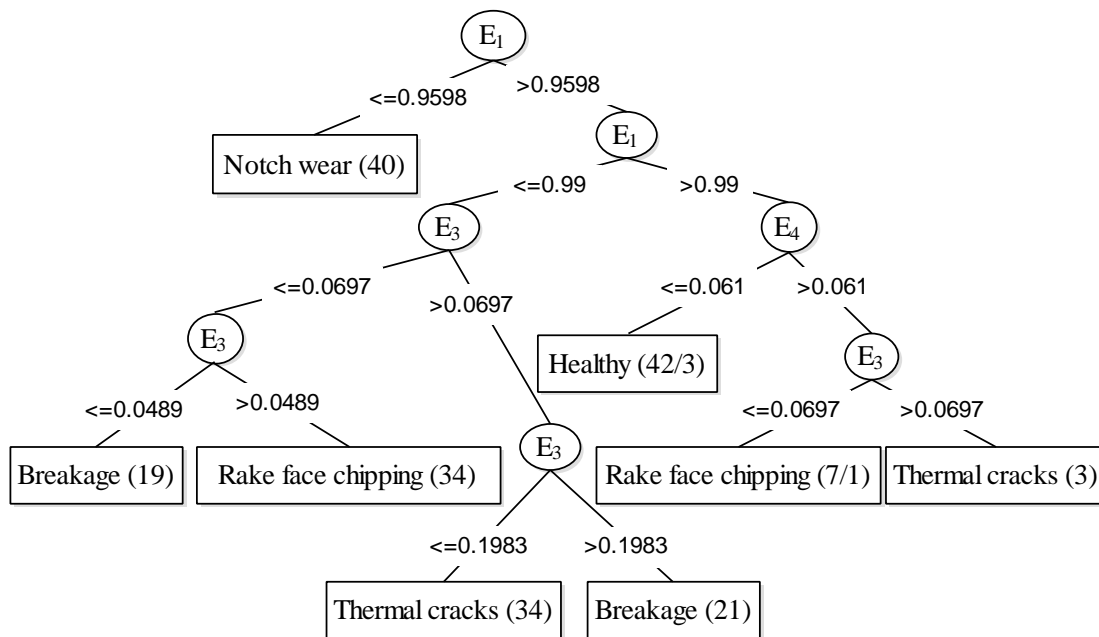


Figure 5.17 Decision tree for EMD features

5.7.9 Classification

Classification efficiency of EMD features in combination with different classifiers have been studied. The classifiers are Artificial Neural Networks (ANN), Naive Bayes, Bayes net, Support Vector Machines (SVM), K-star, and J48 algorithm. The results are reported in the following sub sections.

5.7.9.1 Artificial neural network

The chosen three EMD features are given as an input to the ANN for classification. The classification results are summarized in table 5.28 and table 5.29.

The time taken to complete the process is 0.31 seconds. The confusion matrix is shown in the table 5.29. The classification efficiency of about 82.5% indicates that the ANN is not good enough for fault classifications.

Table 5.28 ANN results with EMD features

Test Parameter	Values
Test mode	10-fold cross-validation
Time taken	0.31 seconds
Total Number of Instances	200
Correctly Classified Instances	165 (82.5%)
Incorrectly Classified Instances	35 (17.5%)

Table 5.29 Confusion matrix of ANN with EMD features

a	b	c	d	e	Class
34	5	0	0	1	a-Healthy
2	29	6	0	3	b- Breakage tool
3	2	31	0	4	c- Thermal cracks
0	0	0	40	0	d- Notch wear
1	6	2	0	31	e- Rake face chipping

5.7.9.2 Naive Bayes algorithm

Table 5.30 and table 5.31 show the parameters of classification and confusion matrix respectively.

Table 5.30 Naive Bayes algorithm results with EMD features

Test Parameter	Values
Test mode	10-fold cross-validation
Time taken	0.01 seconds
Total Number of Instances	200
Correctly Classified Instances	192 (96%)
Incorrectly Classified Instances	8 (4%)

Table 5.31 Confusion matrix of Naive Bayes algorithm with EMD features

a	b	c	d	e	Class
39	0	0	0	1	a-Healthy
6	34	0	0	0	b- Breakage tool
0	0	40	0	0	c- Thermal cracks
0	0	0	40	0	d- Notch wear
0	1	0	0	39	e- Rake face chipping

From the confusion matrix, it can be noted that there are only eight misclassifications. As the classification efficiency 96% is considerably good, Naive Bayes algorithm with EMD features for fault diagnosis of cutting tool is preferable.

5.7.9.3 Bayes net algorithm

Table 5.32 and table 5.33 presents, Bayes net classification parameters and confusion matrix respectively. From the confusion matrix, shown, only three instances are misclassified out of 200 samples. The overall classification efficiency is found to be 98.5%, which is higher than that of all the other classifiers. As the classification efficiency is considerably high, Bayes net classifier with EMD features for fault diagnosis of cutting tool is attractive.

Table 5.32 Bayes net algorithm results with EMD features

Test Parameter	Values
Test mode	10-fold cross-validation
Time taken	0.03 seconds
Total Number of Instances	200
Correctly Classified Instances	197 (98.5%)
Incorrectly Classified Instances	3 (1.5%)

Table 5.33 Confusion matrix of Bayes net algorithm with EMD features

a	b	c	d	e	Class
39	1	0	0	0	a-Healthy
2	38	0	0	0	b- Breakage tool
0	0	40	0	0	c- Thermal cracks
0	0	0	40	0	d- Notch wear
0	0	0	0	40	e- Rake face chipping

5.7.9.4 Support vector machine

The three selected EMD features of five different cutting tool condition vibration signals are given as an input to the SVM. The identified classification efficiency and the time taken to complete the process are presented in the table 5.34

Table 5.34 SVM results with EMD features

Test Parameter	Values
Test mode	10-fold cross-validation
Time taken	0.11 seconds
Total Number of Instances	200
Correctly Classified Instances	136 (68%)
Incorrectly Classified Instances	64 (32%)

Table 5.35 Confusion matrix of SVM with EMD features

a	b	c	d	e	Class
25	0	14	0	1	a-Healthy
14	7	17	0	2	b- Breakage tool
0	0	37	0	3	c- Thermal cracks
0	0	0	40	0	d- Notch wear
0	0	12	1	27	e- Rake face chipping

Table 5.35 presents the confusion matrix of SVM classifier with EMD features. It is found that classification efficiency is of 68%, which is relatively very low in comparison with other classifiers.

5.7.9.5 K-star algorithm

The K-star yields the classification efficiency of 97%. The classification efficiency is higher as compared to the classification efficiency of SVM classifier.

Table 5.36 K-star algorithm results with EMD features

Test Parameter	Values
Test mode	10-fold cross-validation
Time taken	0.01 seconds
Total Number of Instances	200
Correctly Classified Instances	194 (97%)
Incorrectly Classified Instances	6 (3%)

Table 5.37 Confusion matrix of K-star algorithm with EMD features

a	b	c	d	e	Class
39	1	0	0	0	a-Healthy
4	36	0	0	0	b- Breakage tool
0	0	40	0	0	c- Thermal cracks
0	0	0	40	0	d- Notch wear
0	1	0	0	39	e- Rake face chipping

The K-star results are presented in table 5.36 and table 5.37. The overall classification efficiency is 97%, which is high and considerably good.

5.7.9.6 J48 algorithm

The J48 algorithm test conditions and the corresponding output values are given in table 5.38 and followed by the confusion matrix in table 5.39. From the confusion matrix, 193 instances have been correctly classified with classification efficiency of 96.5%. As the classification efficiency is considerably very good, J48 with EMD features for fault diagnosis of cutting tool is very attractive.

Table 5.38 J48 algorithm results with EMD features

Test Parameter	Values
Test mode	10-fold cross-validation
Time taken	0.01 seconds
Total Number of Instances	200
Correctly Classified Instances	193 (96.5%)
Incorrectly Classified Instances	7 (3.5%)

Table 5.39 Confusion matrix of J48 algorithm with EMD features

a	b	c	d	e	Class
39	0	0	0	1	a-Healthy
0	40	0	0	0	b- Breakage tool
3	0	37	0	0	c- Thermal cracks
0	2	0	38	0	d- Notch wear
0	0	1	0	39	e- Rake face chipping

The EMD features are taken from the signals and feature selection is performed using PCA and decision tree J48 algorithm. The procedure led to the selection of three features. Their performances in classification have been presented. The summary of classification efficiencies of different classifiers is shown in the figure 5.18. From the figure 5.18, it can be observed that Bayes net algorithm with the EMD features give

the highest classification efficiency and can be concluded that Bayes net is the best possible classifiers amongst all classifiers with present EMD features.

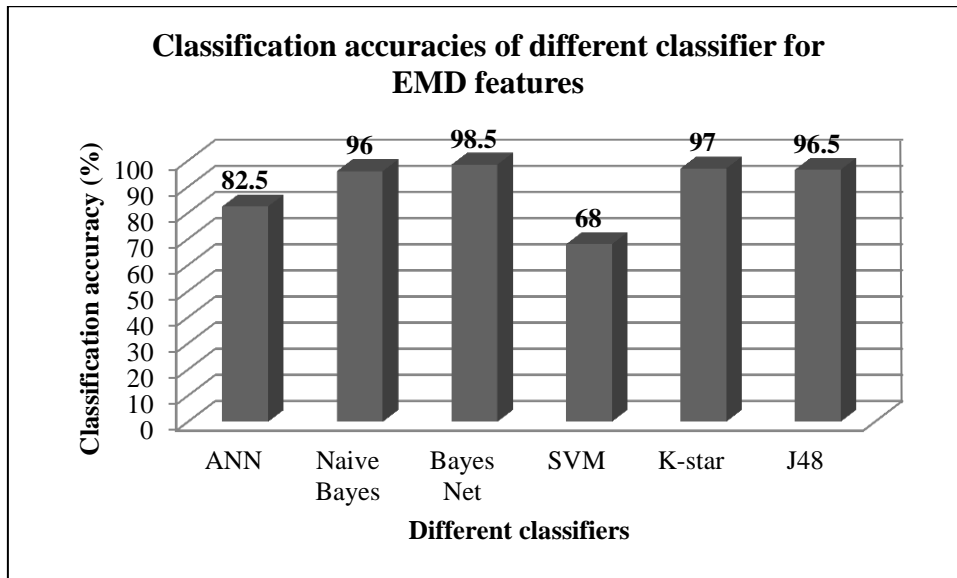


Figure 5.18 Classification efficiencies of different classifiers for EMD features

5.7.10 Classification with histogram features

Histogram is a bar chart, which plots the number of data points that fall within a bin value. Bin value is a series of sub-ranges that span the entire range (from minimum value to maximum value) of data. The height of the bar in the histogram is found to be more or less the same for signals that belong to a particular class; it is significantly different for signals of different classes. Hence the height of the bar can be taken as a feature. (A sample histogram plot is given in figure 5.3) This is called ‘*histogram feature*’ and the same has been used for fault diagnosis of cutting tool. Table 5.40 shows the histogram feature, *f1* to *f15*.

Out of 40 samples only two samples pertaining to each class of tool condition are shown in table 5.40. Amongst these features, a set of good features, which will have high discriminating ability are chosen when using J48 and PCA algorithm. This section presents the results of the study with these features in combination with different classifiers.

Table 5.40 Histogram features extracted from vibration signals for different tool conditions

Class	Sample	Histogram features														
	No.	<i>f1</i>	<i>f2</i>	<i>f3</i>	<i>f4</i>	<i>f5</i>	<i>f6</i>	<i>f7</i>	<i>f8</i>	<i>f9</i>	<i>f10</i>	<i>f11</i>	<i>f12</i>	<i>f13</i>	<i>f14</i>	<i>f15</i>
Healthy	1	0	0	0	0	0	0	599	12965	12036	0	0	0	0	0	0
	2	0	0	0	0	0	0	809	12978	11813	0	0	0	0	0	0
Breakage	1	0	0	0	0	1	37	1507	11260	11220	1518	57	0	0	0	0
	2	0	0	0	0	2	34	1190	11548	11596	1206	24	0	0	0	0
Thermal cracks	1	0	0	0	0	0	0	111	12651	12705	133	0	0	0	0	0
	2	0	0	0	0	0	0	141	12843	12467	149	0	0	0	0	0
Notch wear	1	0	0	0	0	0	2	596	12279	12122	597	4	0	0	0	0
	2	0	0	0	0	0	2	570	12212	12226	589	1	0	0	0	0
Rake face chipping	1	0	0	2	2	1	20	830	11944	11842	935	21	1	1	0	1
	2	0	0	1	3	3	27	897	11865	11813	951	34	5	0	1	0

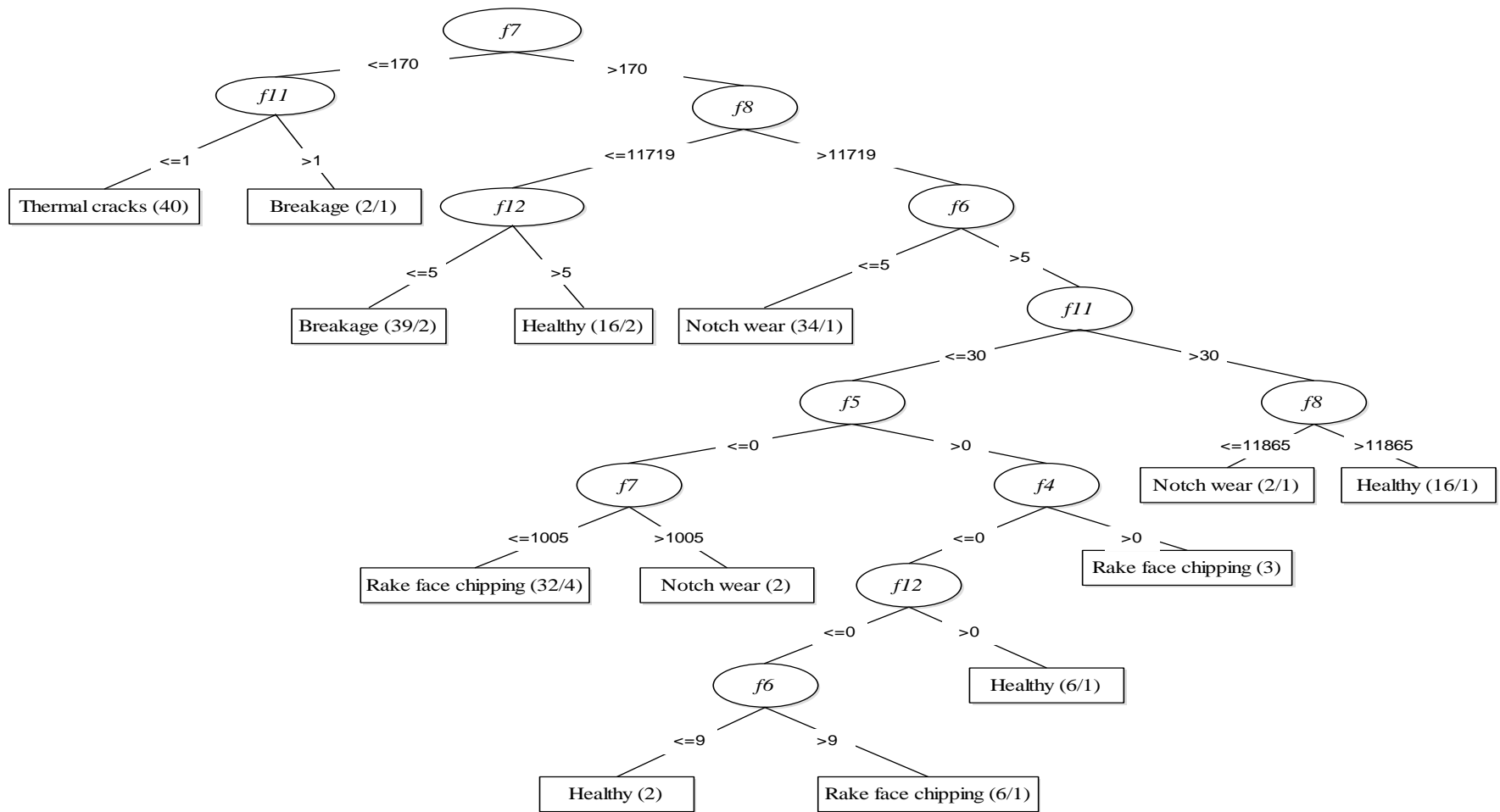


Figure 5.19 Decision tree for histogram features

5.7.11 Feature selection (histogram features)

Fifteen features mentioned in table 5.40 are considered as input to either decision tree technique (J48 algorithm) or PCA algorithm for feature selection. After processing, PCA yields six features. With these six features, the classification is performed using J48 algorithm and the classification efficiency is found to be 78.5%. The same data set is used for feature selection and classification using decision tree technique (J48 algorithm) and found that the classification efficiency is of 82%. It shows that classification efficiency with the decision tree is about 3.5% higher than that with PCA. From the above results, performance of feature selection of decision tree technique (J48 algorithm) is proved to be better than the PCA algorithm. However, it is to be mentioned here that this result cannot be generalized for all data sets and features. Fifteen histogram features were used as input to J48 algorithm, out of which eight features are eliminated at the outset due to their imperceptible contribution to the classification. Referring to the figure 5.19, seven contributors are identified as dominant amongst the extracted histogram features, namely *f7*, *f8*, *f11*, *f12*, *f6*, *f5* and *f4*.

5.7.12 Classification

Classification efficiency of histogram features in combination with different classifiers has been studied. The classifiers are artificial neural networks (ANN), Naive Bayes, Bayes net, support vector machines (SVM), K-star, and J48 algorithm. The results are reported in the following sub sections.

5.7.12.1 Artificial neural network

Classification parameters and confusion matrix of ANN are presented in table 5.41 and table 5.42 respectively. From the confusion matrix, it is observed that there are thirty-three misclassifications. The overall classification efficiency is 83.5%. As the classification efficiency is considerably very low, ANN classifier with histogram features for fault diagnosis of cutting tool is not very attractive.

Table 5.41 ANN results with histogram features

Test Parameter	Values
Test mode	10-fold cross-validation
Time taken	0.37 seconds
Total Number of Instances	200
Correctly Classified Instances	167 (83.5%)
Incorrectly Classified Instances	33 (16.5%)

Table 5.42 Confusion matrix of ANN with histogram features

a	b	c	d	e	Class
31	0	0	0	9	a-Healthy
1	38	1	0	0	b- Breakage tool
0	0	39	1	0	c- Thermal cracks
0	1	0	34	5	d- Notch wear
6	0	2	7	25	e- Rake face chipping

5.7.12.2 Naive Bayes algorithm

The seven selected histogram features of five different cutting tool condition vibration signals are given as input to the Naive Bayes classifier. The identified classification efficiency and the time taken to complete the process are presented in the table 5.43

Table 5.43 Naive Bayes algorithm results with histogram features

Test Parameter	Values
Test mode	10-fold cross-validation
Time taken	0.01 seconds
Total Number of Instances	200
Correctly Classified Instances	123 (61.5%)
Incorrectly Classified Instances	77 (38.5%)

Table 5.44 Confusion matrix of Naive Bayes algorithm with histogram features

a	b	c	d	e	Class
16	5	0	3	16	a-Healthy
28	6	0	1	5	b- Breakage tool
1	0	38	1	0	c- Thermal cracks
0	1	0	35	4	d- Notch wear
0	1	1	10	28	e- Rake face chipping

From the confusion matrix presented in table 5.44, classification efficiency (61.5%) found to be very less. So Naive Bayes algorithm with histogram features for fault diagnosis of cutting tool is preferable.

5.7.12.3 Bayes net algorithm

The Bayes net yields the classification efficiency of 79.5%. The efficiency is improved when compared to efficiency obtained using Naive Bayes classifier.

Table 5.45 Bayes net algorithm results with histogram features

Test Parameter	Values
Test mode	10-fold cross-validation
Time taken	0.03 seconds
Total Number of Instances	200
Correctly Classified Instances	159 (79.5%)
Incorrectly Classified Instances	41 (20.5%)

Table 5.46 Confusion matrix of Bayes net algorithm with histogram features

a	b	c	d	e	Class
15	14	0	0	11	a-Healthy
2	37	0	1	0	b- Breakage tool
0	0	40	0	0	c- Thermal cracks
1	1	0	33	5	d- Notch wear
2	0	1	3	34	e- Rake face chipping

The Bayes net results are presented in table 5.45 and table 5.46. As the classification efficiency is considerably low, Bayes net classifier with histogram features for fault diagnosis of cutting tool is not preferable.

5.7.12.4 Support vector machine

The SVM test conditions and the corresponding output values are given in table 5.47 and followed by the confusion matrix in table 5.48.

From the confusion matrix, 128 instances are correctly classified with classification efficiency of 64%. As the classification efficiency is considerably very low, SVM with histogram features for fault diagnosis of cutting tool is not very attractive.

Table 5.47 SVM results with histogram features

Test Parameter	Values
Test mode	10-fold cross-validation
Time taken	0.1 seconds
Total Number of Instances	200
Correctly Classified Instances	128 (64%)
Incorrectly Classified Instances	72 (36%)

Table 5.48 Confusion matrix of SVM with histogram features

a	b	c	d	e	Class
9	7	0	5	19	a-Healthy
2	37	1	0	0	b- Breakage tool
0	1	39	0	0	c- Thermal cracks
0	1	10	22	7	d- Notch wear
0	0	8	11	21	e- Rake face chipping

5.7.12.5 K-star algorithm

Table 5.49 and table 5.50 shows the parameters of classification and confusion matrix of the K-star classifier respectively. As the classification efficiency (84%) is

considerably low, K-star with histogram features for fault diagnosis of cutting tool is not very attractive.

Table 5.49 K-star algorithm results with histogram features

Test Parameter	Values
Test mode	10-fold cross-validation
Time taken	0.01 seconds
Total Number of Instances	200
Correctly Classified Instances	168 (84%)
Incorrectly Classified Instances	32 (16%)

Table 5.50 Confusion matrix of K-star algorithm with histogram features

a	b	c	d	e	Class
33	1	0	0	6	a-Healthy
1	38	1	0	0	b- Breakage tool
0	0	40	0	0	c- Thermal cracks
2	0	0	33	5	d- Notch wear
11	0	1	4	24	e- Rake face chipping

5.7.12.6 J48 algorithm

The chosen seven histogram features are given as input to the J48 classifier for classification. The classification results are summarized in table 5.51 and table 5.52.

Table 5.51 J48 algorithm results with histogram features

Test Parameter	Values
Test mode	10-fold cross-validation
Time taken	0.01 seconds
Total Number of Instances	200
Correctly Classified Instances	161 (80.5%)
Incorrectly Classified Instances	39 (19.5%)

Table 5.52 Confusion matrix of J48 algorithm with histogram features

a	b	c	d	e	Class
29	3	0	0	8	a-Healthy
8	31	1	0	0	b- Breakage tool
0	0	39	1	0	c- Thermal cracks
2	1	0	32	5	d- Notch wear
7	0	1	2	30	e- Rake face chipping

The time taken to complete the process is 0.01 seconds. The confusion matrix is shown in the table 5.52. The classification efficiency of 80.5% indicates that the J48 is not good classifier for fault classifications.

The histogram features are taken and feature selection has been performed using PCA and decision tree J48 algorithm. The procedure led to the selection of seven features. Their performances in classification have been presented. The summary of classification efficiencies of different classifiers is shown in figure 5.20. From the figure 5.20, it is found that the K-star algorithm with the histogram features give the highest classification efficiency and can be concluded that K-star is the best possible classifiers amongst the classifiers considered with present histogram features.

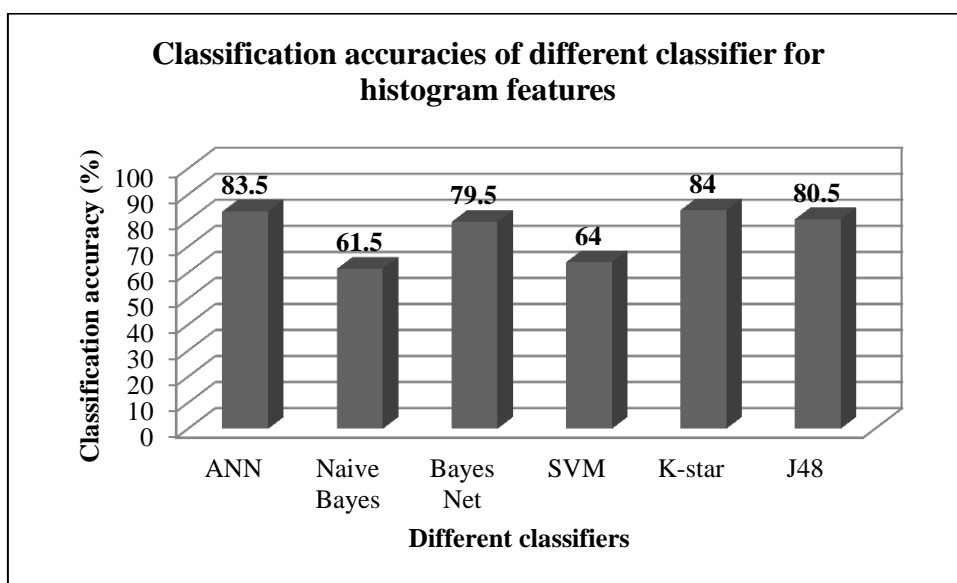


Figure 5.20 Classification efficiencies of different classifiers for histogram features

Table 5.53 Summary of classification accuracies

Features	Classifier	Classification accuracy with PCA feature reduction (%)	Classification accuracy with J48 feature selection (%)
Statistical	ANN	86.0	83.5
	Naive Bayes	63.0	60.5
	Bayes net	82.5	85.5
	SVM	56.0	71.0
	K-star	84.0	84.5
	J48	77.0	85.5
Histogram	ANN	82.5	83.5
	Naive Bayes	62.0	61.5
	Bayes net	78.5	79.5
	SVM	43.5	64.0
	K-star	78.0	84.0
	J48	78.5	80.5
Discrete wavelet transformation	ANN	96.0	96.0
	Naive Bayes	93.5	78.5
	Bayes net	94.0	84.5
	SVM	72.0	74.0
	K-star	98.0	96.0
	J48	91.5	94.0
Empirical mode decomposition	ANN	76.5	82.5
	Naive Bayes	71.0	96.0
	Bayes net	67.5	98.5
	SVM	68.5	68.0
	K-star	68.5	97.0
	J48	59.0	96.5

5.8 SUMMARY

This investigation presents fault diagnosis of cutting tool using machine learning approach based on vibration signals. This methodology involves collecting 200 acceleration vibration signal sample for five different class or condition of tool. From the acquired signals, features were extracted using statistical, histogram, DWT and EMD methods. PCA and J48 algorithm (decision tree) were used for important feature selection. ANN, Naïve Bayes, Bayes net, SVM, K-star and J48 algorithm classifiers have been used to classify the different fault conditions. The detailed classification accuracy with different features and classifiers are as shown in table 5.53. Classification accuracy is found to be reasonably good with J48 feature selection, 6.56% higher when compared to PCA. Based on the results obtained, the proposed methodology with machine learning techniques can be recommended for practical applications and development of on-line fault diagnosis systems for tool condition monitoring.

CHAPTER 6

ANALYSIS OF CUTTING FORCES, SURFACE ROUGHNESS, CHIP MORPHOLOGY AND COMPUTATIONAL APPROACH FOR FAULT DIAGNOSIS OF CUTTING TOOL

6.1 INTRODUCTION

So far, the study of fault diagnosis of tool condition has been devoted to the use of various signal processing techniques and machine learning techniques with a set of features and classifiers for online monitoring of tool condition. The main objective of this study is to find the additional offline monitoring techniques for fault diagnosis of tool conditions. This chapter deals with surface roughness of workpiece, chip morphology studies, predicting cutting forces using computational approach and validation with experimental results. The simulation model has been developed and basic machining parameters were defined, simulations for healthy cutting tool condition have been carried out with the specialized finite element analysis (FEA) technology (Deform 3D Machining V 10.2).

6.2 CUTTING FORCES ANALYSIS

The experiments were conducted with dry cutting on the engine lathe. Figure 3.4 shows an experimental setup for cutting forces measurement. Lathe tool dynamometer has been used for measuring the cutting forces on a lathe machine during turning operations. The dynamometer employs strain gauges for measurement of forces. Individual full bridge strain gauge networks have been installed for each of the three force measurement directions inside the dynamometer. Multicomponent digital force indicator comprises of strain gauge signal conditioning unit along with the three digital displays. The cutting forces were acquired from the single point cutting under normal condition (Healthy) and with four different worn out tungsten carbide tool insert conditions.

6.2.1 Experimental approach

The characteristics of the measured cutting forces (F_y and F_z) with change in depth of cut and cutting speed have been studied for five different tungsten carbide tool insert conditions. It has been found that the presence of tool wear has significant effect on the general trends and characteristics of the measured thrust force and cutting force from the machining tests, when compared with the healthy cutting tool. The typical and representative trends for the experimental thrust force (F_y) and cutting force (F_z) with respect to the process variables are shown in figure 6.1 to 6.4.

Figure 6.1 and figure 6.2 shows the relationship between thrust force and cutting force with variation in cutting speed for different tungsten carbide tool insert conditions at a constant depth of cut of 0.1mm.

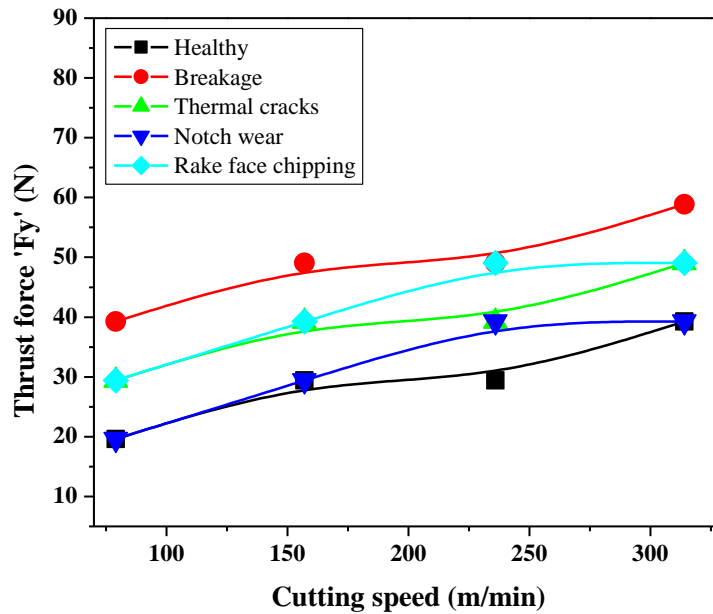


Figure 6.1 Influence of the cutting speed on the thrust force (F_y) for depth of cut ' d '= 0.1mm

Figure 6.1 shows the evolution of the thrust force (F_y) according to the cutting speed. The thrust force increase, when the cutting speed increases. This increase in thrust force

is due to ploughing effect that prevails under the conditions of small feed rate and small depth of cut compared to nose radius and also large negative rake angle. Here in all the cases, the thrust forces are observed very low for healthy tool compared to worn out tools. This observation agrees well with results reported by Huang and Liang, (2005); Chou and Evans (1999). Also, the thrust force was sensitive to the changes of cutting edge geometry and tool wear. In addition, it was affected by cutting speed and tool wear. Moreover, the cutting forces as well as surface roughness are also influenced by the insert cutting edge geometry as it is mentioned by Ozel et al (2005).

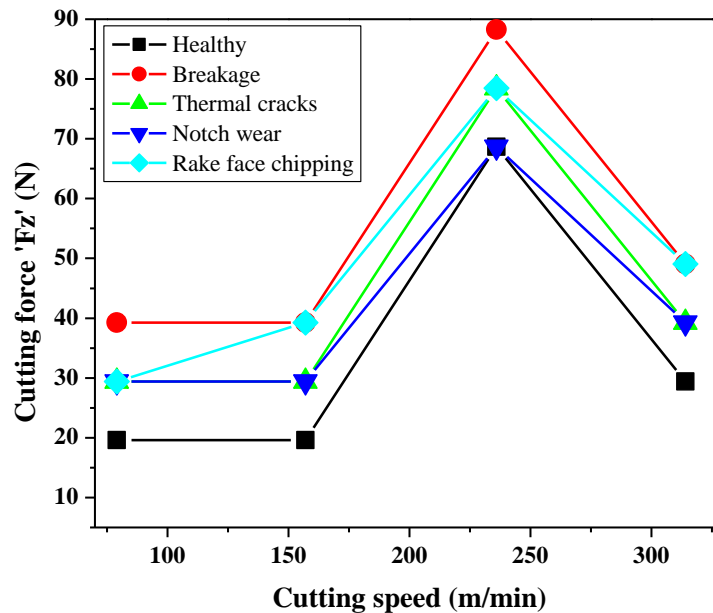


Figure 6.2 Influence of the cutting speed on the cutting force (F_z) for depth of cut $d' = 0.1$ mm

Figure 6.2 depicts the evolution of the cutting force (F_z) according to the cutting speed. The cutting force component decrease with increase in cutting speed. This cutting force decrease is due to the plastic softening of machined material under the effect of the increased machining temperature. This is explained by the effects of the temperature on the tool-chip interface. As cutting speed increases from 236 m/min to 314 m/min results in rise in interface tool-chip temperature. This change in temperature results in softening

of machining material. Consequently, this reduces shearing forces in the shear zone and reduction in contact between tool-chip face. This effect increases the shear angle and decreases in chip thickness, which reduces the contact area between tool-chip, hence cutting force (F_z) decreases beyond 236 m/min.

Figure 6.3 and Figure 6.4 shows the effect of depth of cut on the measured thrust force (F_y) and cutting force (F_z) for different conditions of tungsten carbide tool insert at a constant cutting speed of 236 m/min. It is found that the thrust force (F_y) and cutting force (F_z) increases linearly with an increase in depth of cut. As the depth of cut increase, cutting tool will be subjected to remove more material and hence it will result in increased frictional force and rubbing force on the wear land. Further it leads to change in the basic chip formation.

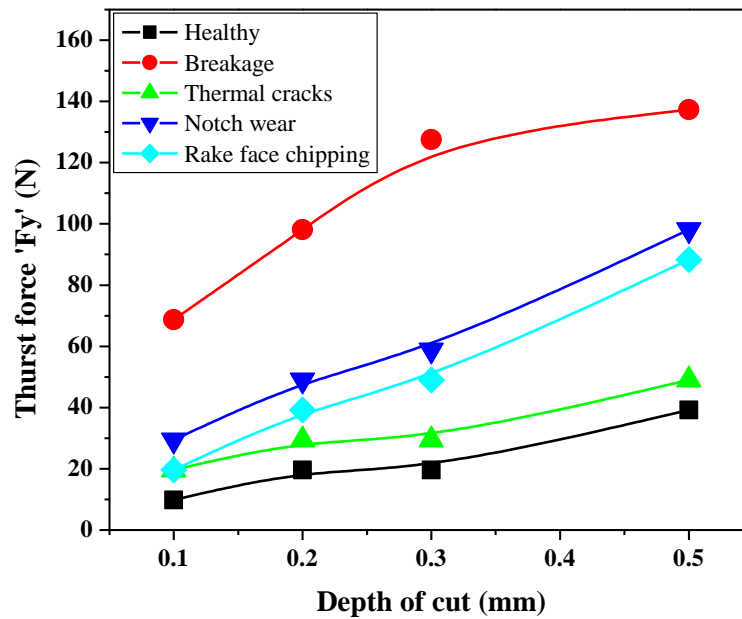


Figure 6.3 Influence of the depth of cut on the thrust force (F_y) for cutting speed ' v ' = 236 m/min

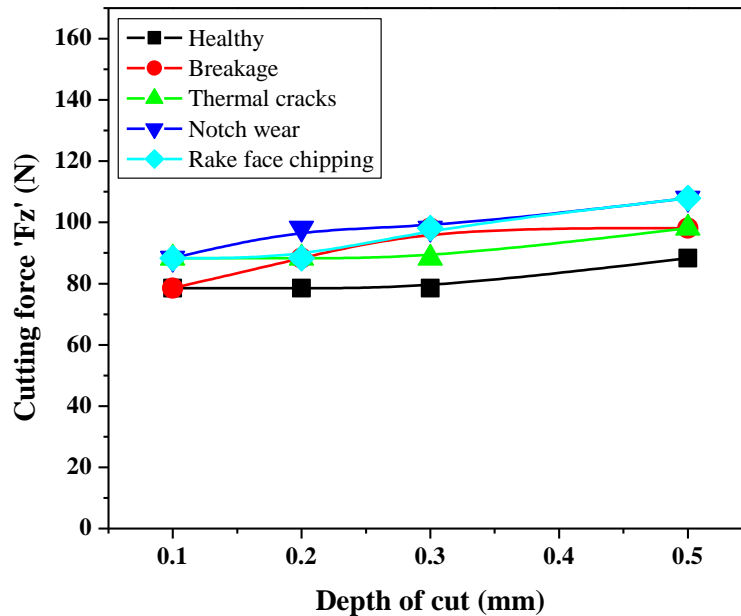


Figure 6.4 Influence of the depth of cut on the cutting force (F_z) for cutting speed

$$v = 236 \text{ m/min}$$

This in turn leads to increase in thrust force and cutting force. Lin and Chen (1995) reported that when depth of cut is increased (i.e. cutting does not take place at nose radius), the cutting force would be larger than the thrust force. From figure 5.15-5.17 energies of the characteristic IMF components vary significantly with tool conditions and from figure 6.1-6.4 tool wear seems to affect the qualitative trends of the cutting forces. This energy of the characteristic IMF components and cutting forces components provides an effective indication for the detection of tool condition, which can be used to monitor tool wear and classify different tool conditions.

Table 6.1 presents experimental results of cutting forces components thrust force (F_y) and cutting force (F_z) for combinations of cutting regime parameters (cutting speed and depth of cut) and different tungsten carbide tool insert conditions.

Table 6.1 Influence of the depth of cut and cutting speed on the cutting forces for different tool conditions

Cutting parameters		Tool conditions									
		Healthy		Breakage		Thermal cracks		Notch wear		Rake face chipping	
Cutting speed 'v'	Depth of cut 'd'	Thrust force 'Fy'	Cutting force 'Fz'	Thrust force 'Fy'	Cutting force 'Fz'	Thrust force 'Fy'	Cutting force 'Fz'	Thrust force 'Fy'	Cutting force 'Fz'	Thrust force 'Fy'	Cutting force 'Fz'
(m/min)	(mm)	(N)	(N)	(N)	(N)	(N)	(N)	(N)	(N)	(N)	(N)
79	0.1	19.62	19.62	39.24	39.24	29.43	29.43	19.62	29.43	29.43	29.43
157	0.1	29.43	19.62	49.05	39.24	39.24	29.43	29.43	29.43	39.24	39.24
236	0.1	29.43	68.67	49.05	88.29	39.24	78.48	39.24	68.67	49.05	78.48
314	0.1	39.24	29.43	58.86	49.05	49.05	39.24	39.24	39.24	49.05	49.05
236	0.1	9.81	78.48	68.67	78.48	19.62	88.29	29.43	88.29	19.62	88.29
236	0.2	19.62	78.48	98.1	88.29	29.43	88.29	49.05	98.1	39.24	88.29
236	0.3	19.62	78.48	127.53	98.1	29.43	88.29	58.86	98.1	49.05	98.1
236	0.5	39.24	88.29	137.34	98.1	49.05	98.1	98.1	107.9	88.29	107.91

The results indicate that the lower cutting forces were registered at the higher cutting speeds. This can be related to the temperature increase in machining zone and leads to the drop of the workpiece yield strength and chip thickness. The results also show that cutting forces increase with increasing depth of cut because chip thickness becomes significant, which causes the growth of the deformed metal volume. Consequently, enormous forces are required to cut the chip. Furthermore, thrust force and cutting force developed for all worn out tool conditions were 76.5% higher than healthy cutting tool. The thrust force and cutting force is larger in worn out tool condition is also reported by Chen (2000). The effect of tool wear on the cutting forces is investigated (figure 6.1 to 6.4), it can be noticed that the thrust force and cutting force increases linearly with the tool wear. This increase may be a result of the rubbing or ploughing force on the wear land, or the change in the basic chip formation process or both.

6.2.2 Computational approach

Finite element simulations in machining process are increasingly used by researchers in the machining field, because of experimental tests are more expensive and time consuming. Another advantage of this method is that, it provides information on cutting forces, deformations, stresses and temperatures that occur during the machining process and also gives chip shape and tool wear rate information.

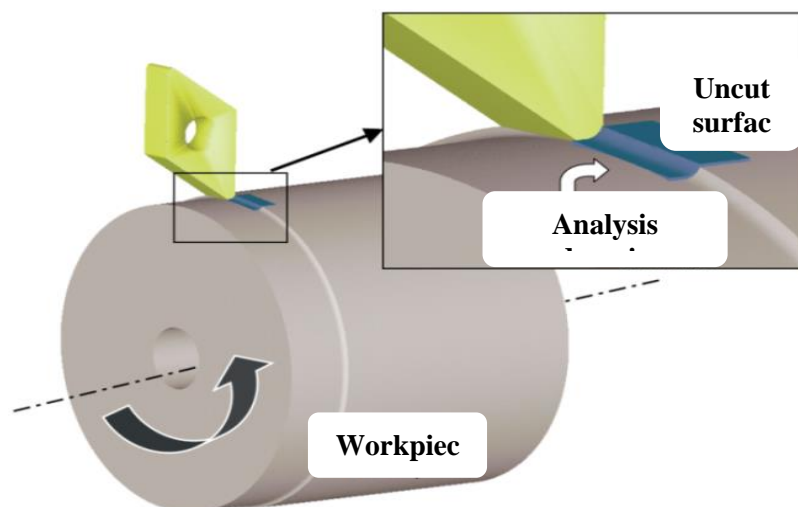


Figure 6.5 Basic components of turning and relation to analysis domain

For turning operations the rotating work piece, cutting tool insert and their relation to the analysis domain are shown in figure 6.5. The engineers can study the effect of machining parameters like, cutting speed, feed rate and depth of cut on the process response.

Typical analysis model generated using the current system is shown in figure 6.6. The cylindrical workpiece is assumed as a rectangular block indicating the feed rate in the direction of its breadth, cutting speed along length and depth of cut along the height of block.

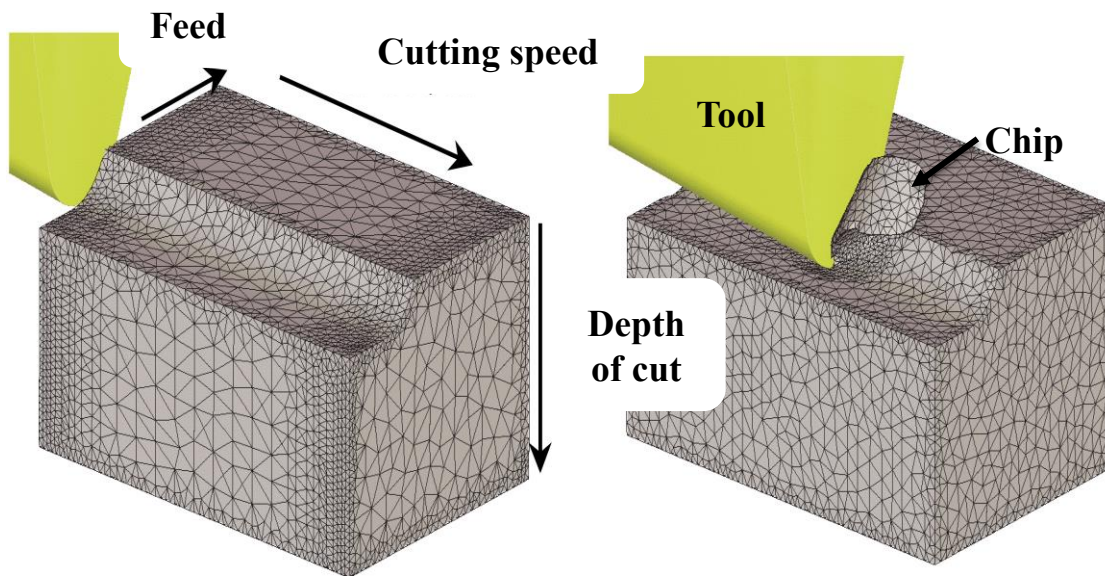


Figure 6.6 Simulation model and basic cutting parameters

Simulation was carried out using Deform 3D Machining V 10.2. Machining parameters like cutting speed and depth of cut were considered as variable.

The tool was considered as a rigid body. The tool mesh has been set to 1500 elements and the cutting material chosen to be as tungsten carbide. The workpiece is considered as a plastic body with a mesh of 3000 elements. AISI H13 die steel material has been chosen for the workpiece material.

6.2.3 Validation of computational cutting forces

In order to verify the computationally predicted cutting forces which are developed while machining, it is necessary to assess the results qualitatively and quantitatively based on experimental results.

Machining test runs were conducted in order to assess the possibility and predictive capability of the computational cutting forces. The experiment will enable comparisons to be made between the predicted cutting forces (F_y and F_z) and experimentally measured forces so that the effects of the machining variables, such as depth of cut and cutting speed, on the predicted forces will be analyzed.

6.2.4 Effect of depth of cut on cutting forces

Qualitative comparisons of the computational predicted forces are drawn by plotting the trends of the predicted forces together with the measured forces with respect to depth of cut variables. Figure 6.7 and 6.8 shows the trends of the predicted thrust force and cutting force with the measured experimental forces.

An increase in the depth of cut increases the cutting area and hence the cutting forces. The increase in the depth of cut increases the heat generation and hence tool wear, which resulted in the higher thrust and cutting force. The increase in the depth of cut also increases the chatter and it produces incomplete machining, which leads to higher cutting forces.

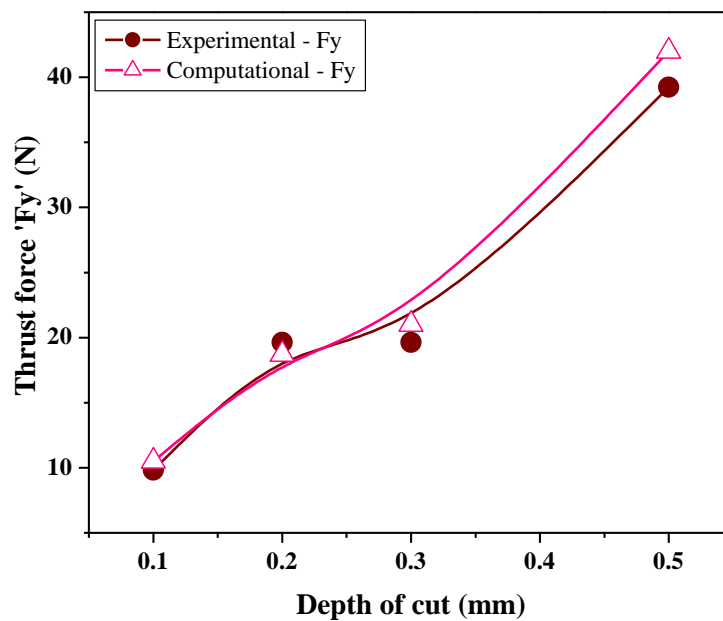


Figure 6.7 Predicted and experimental thrust force (F_y) vs. depth of cut

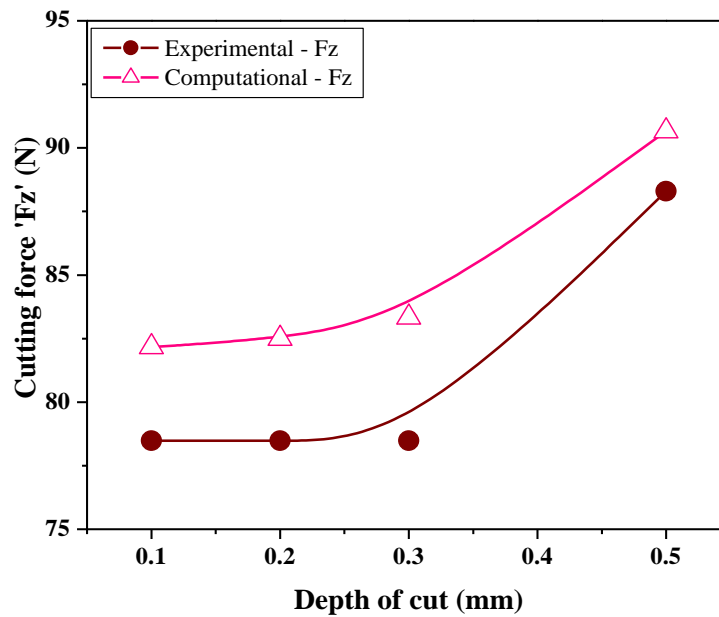


Figure 6.8 Predicted and experimental cutting force (Fz) vs. depth of cut

6.2.5 Effect of cutting speed on cutting forces

The effect of cutting speed on the predicted thrust force and cutting force are drawn in the figure 6.9 and 6.10 for experimental and predicted results. An increase in cutting speed results in slight increase in cutting forces.

In figure 6.10 as the cutting speed increases from 236 m/min to 314 m/min, cutting force (Fz) component tends to decrease. With low cutting speed, the cutting edge tends to plough on the work surface, resulting in higher order cutting force (Fz), but as the cutting speed increases, the machining becomes steadier, with a consequent reduction in the cutting force (Fz) components.

From figure 6.9 and 6.10, it can also be seen that the cutting force is always higher than the thrust force component by a considerable margin. These results are in good agreement with Aouici et al. 2012, and indicate that the material removal has occurred in ductile manner without fracture, thus preventing the occurrence of a brittle material removal.

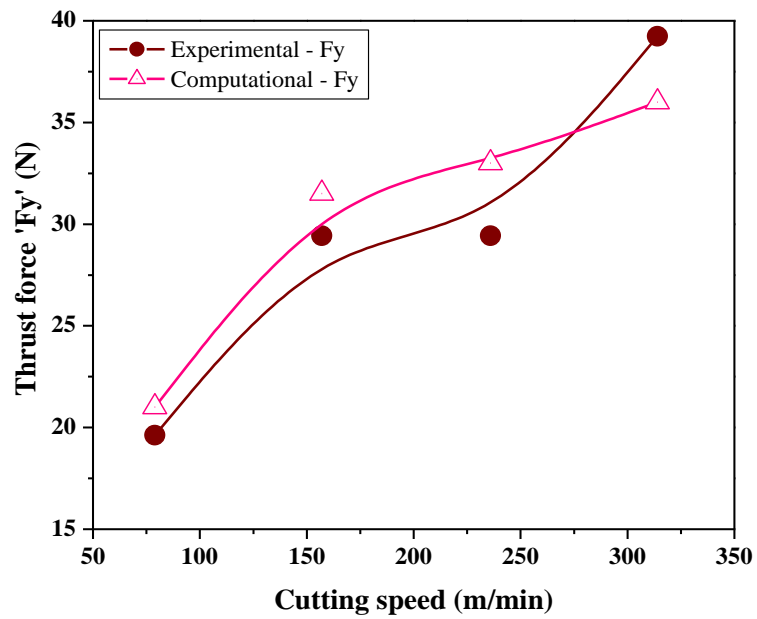


Figure 6.9 Predicted and experimental thrust force (F_y) vs. cutting speed

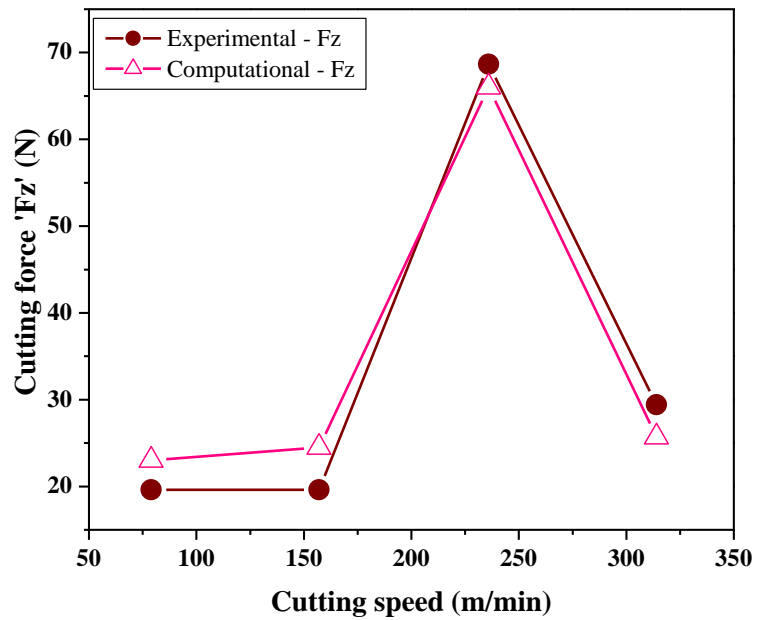


Figure 6.10 Predicted and experimental cutting force (F_z) vs. cutting speed

The Deform-3D has correctly predicted this trend which is consistent with the experimental trends of the cutting forces components. Qualitatively, the measured

experimental forces are in good agreement with predicted values very well under the corresponding machining conditions.

6.3 SURFACE ROUGHNESS (R_a) ANALYSIS

The surface roughness was measured as per Japanese industrial standard (JIS) 2001 by using 'Mitutoyo' surface roughness tester. The average surface roughness (R_a), is considered for the current study. The surface roughness of the workpiece was measured at three different locations and the average was taken as the process response. The cutoff length of 0.8 mm was selected and evaluation length of 4 mm has been used to measure the surface roughness with a stylus speed of 0.25 mm/s. Table 6.2 shows the results of R_a and fluctuation in root mean square (RMS) value of vibration signals

Table 6.2 Surface roughness (R_a), a_x , a_y , and a_z for different tool conditions

Sl. No	Tool condition	Surface roughness 'Ra' (μm)	Root mean square (RMS) of vibration signals (g)		
			a_x	a_y	a_z
1	Healthy	0.74	3.90	3.33	1.14
2	Breakage	4.20	5.84	8.61	3.14
3	Thermal cracks	2.10	4.18	6.44	2.38
4	Notch wear	1.04	4.69	6.81	3.54
5	Rake face chipping	4.74	5.84	9.94	2.36

6.3.1 Surface roughness (R_a) and vibration signal (RMS)

The dry machining tests were conducted to study the effect of different tool conditions on the response of surface characteristics (R_a) and fluctuation in root mean square (RMS) value of vibration signals.

6.3.1.1 Surface roughness (Ra)

The surface roughness of the workpiece increases with increase in tool wear. It may be due to the fact that the amount of heat generation increases with increase in tool wear. Figure 6.11, shows that the surface roughness increases with different worn out tool conditions compare to healthy cutting tool, because the contact area between the tool and workpiece increases with worn conditions, which results in increased chip thickness. The surface roughness decreases with the increasing cutting speed, it is possibly as a result of reduction in chip thickness since the contact area between the tool and workpiece decreases with increasing cutting speed. The surface roughness increases with increasing depth of cut, it is probably because of the amount of heat generation increases with increase in depth of cut, subsequently as the cutting tool has to remove more volume of material from the workpiece.

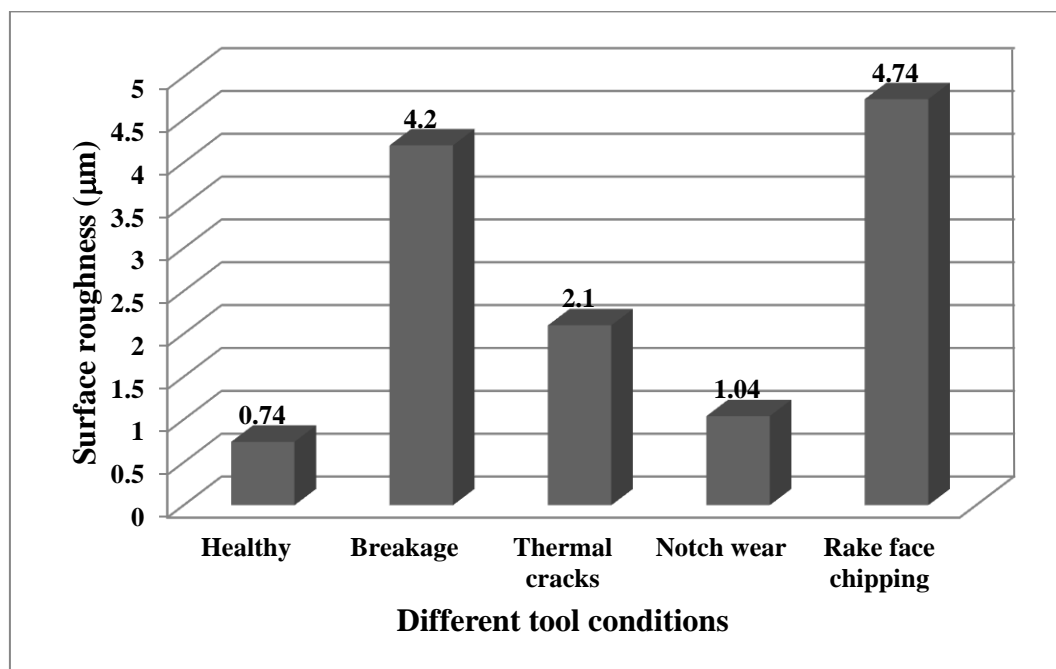


Figure 6.11 Effect of tool condition on surface roughness of the workpiece

Surface roughness is improved by increasing cutting speed. Producing a better surface finish at higher cutting speed is well known in metal cutting. The conventional explanations are related to built-up-edge (BUE) (Bouacha et al. 2010). That is, the formation of BUE is favored in a certain range of cutting speed. By increasing cutting

speed beyond this region, BUE is eliminated and as a result, the surface finish is improved. The deformation velocity influences the properties of the metals. Higher the velocity, the plastic behavior is less significant. The lateral plastic flow of the workpiece material along with the cutting edge direction may increase the peak-to-valley height of the surface irregularity. If the material presents less plasticity by increasing cutting speed and hence deformation velocity, the surface finish can be improved as a result of less significant lateral plastic flow and thus less additional increase in the peak-to-valley height of the machined surface roughness. The damaged tool condition produces a rough surface of the workpiece and thus causes vibration in the system. The investigation of surface roughness is considered being affected by the interference of vibration phenomenon and chip formation occurrences. The plastic deformation of the workpiece is proportional to the amount of heat generation in the workpiece and promotes roughness on the workpiece surface (Arsecularatne et al. 2006; Gaitonde et al. 2009). This phenomenon can be explained by the following three mechanisms (Uehara et al. 1983).

- Decreasing of chatter vibrations with the decrease in cutting forces
- Changing of the mechanism of chip formation from discontinuous type to continuous type
- Absence of built-up edge (BUE) formation.

Machining with worn-out cutting tool increases cutting forces and it decreases effective rake angle. Worn out tool also increase the tendency for BUE formation, which leads to poor surface finish and effect surface residual stresses. Further it leads to tearing or cracking of the machined surface due to severe surface deformation and the heat generated by the worn out tool tip rubbing against this surface. The types of chips produced are important, because the type of chip significantly influences the surface finish produced as well as the overall machining operation. For example, continuous chips are generally associated with good surface finish. Built-up-edge chips usually result in poor surface finish. Serrated chips and discontinuous chips may result in poor surface finish and possibly lead to chatter.

6.3.1.2 Vibration signal (RMS)

Machining with a worn tool increases the fluctuation of forces on the cutting tool. This is attributed to the friction between the flank face of the cutting tool and the workpiece, and also the internal fractures of the tool. Due to these force fluctuations, vibrations occur in the system. Figure 6.12, shows the fluctuation of vibration signal components at different tool conditions, observations shows increase in acceleration (RMS) level for faulty tool conditions.

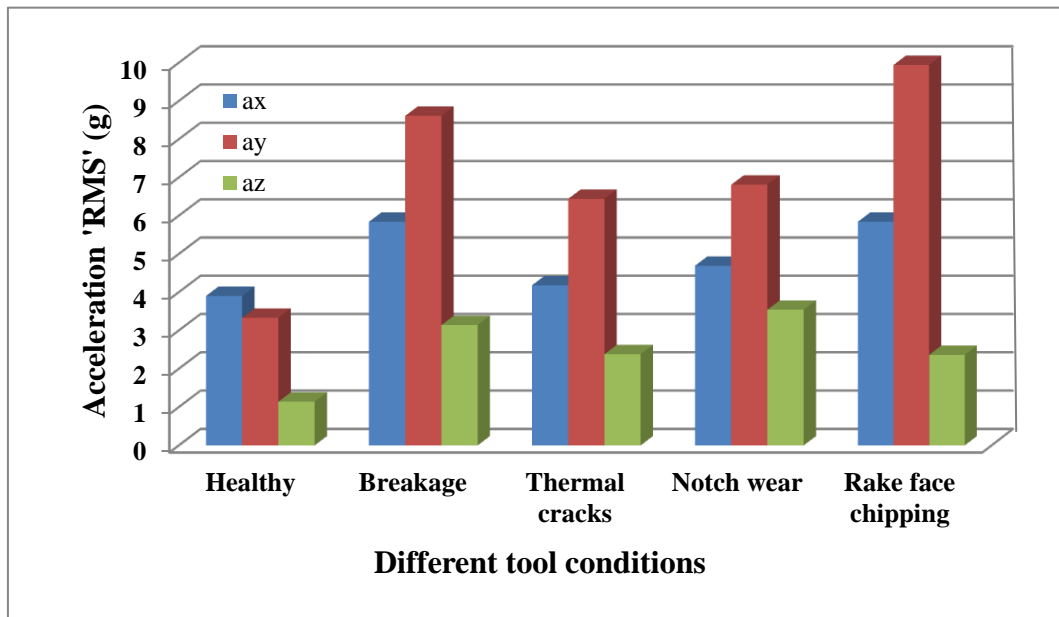


Figure 6.12 Fluctuation of vibration signal (RMS) components at different tool conditions

All the vibration components along the feed ' a_x ', radius ' a_y ' and tangent ' a_z ' directions were found having similar types of pattern in their frequencies (Bhuiyan et al. 2014). The low amplitude signals were most possibly due to the vibration of different machine tool and the machine as a whole; whereas, the different occurrences in turning were the source of high amplitude pattern of signals. The change in surface roughness, the variation in machining conditions, change in level of the tool wear, types of chip formation, tool-chip collision during metal removal and the disturbance in smooth progression of the process, etc. were the major causes of high amplitude frequencies of vibration signal produced in turning. The fluctuation of vibration

components was observed to be very mixed; no specific trend/relationship was observed between the amplitude of vibration components and the chip formation and surface roughness of the workpiece. However, the RMS amplitude of ' a_y ' component was always found to be the significant with tool wear, surface roughness and chip formation type (Barry and Byrne 2002). Tool condition monitoring for different tungsten carbide tool insert conditions based on vibration signal RMS has been performed well to test the effectiveness of the proposed technique.

Figure 6.12, depicts vibration (RMS) component of ' a_y ' and is predominate as compared to other two components. Thus surface roughness and tool condition can be easily monitored by the using vibration signal component ' a_y '. Figure 6.13, illustrates the comparisons of surface roughness of the workpiece and vibration signal component ' a_y ' at different tool conditions, it is clearly shows that vibration signals (RMS) have high influence on surface roughness of the workpiece with different tool conditions.

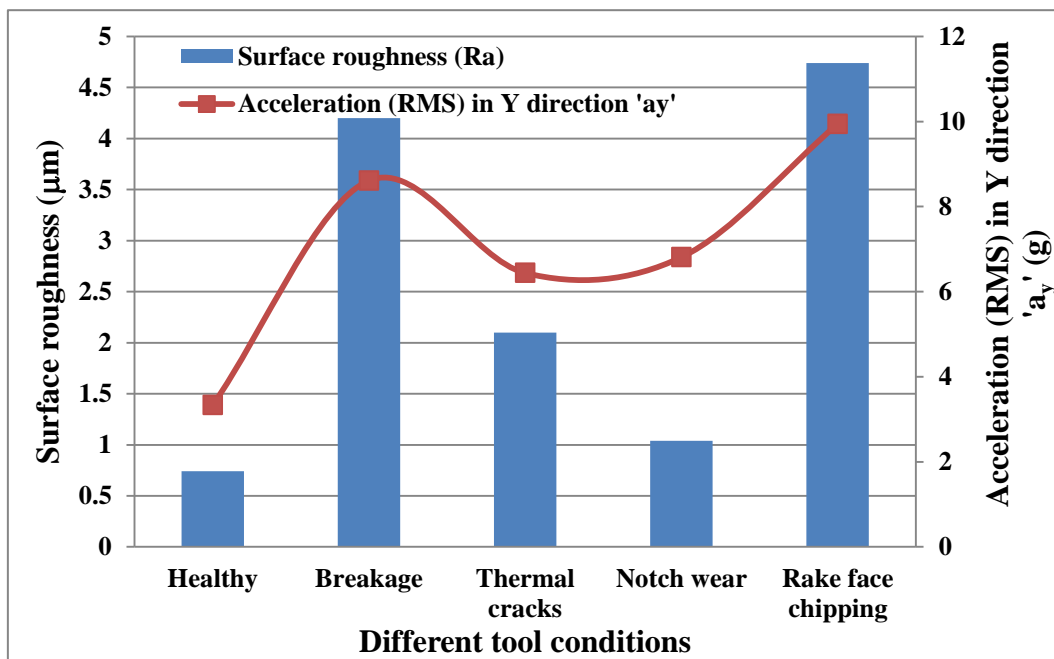


Figure 6.13 Variation in surface roughness of workpiece and vibration signal (RMS) component ' a_y ' at different tool conditions

The vibration (RMS) of ' a_y ' was observed to be considerably high for different tool wear conditions and which were found to be the least for the healthy cutting tool condition. The surface roughness values were found to follow blindly a similar trend like the vibration (RMS) along with the cutting tool conditions. The chip formation type was found to transform gradually from short spiral, conical, straight ribbon, broken and then followed by the long spiral chip formation while machining with healthy, notch wear, thermal cracks, rake face chipping and breakage cutting tool conditions respectively. From table 4.2 high ratios indicates presence of transition to chaotic state and low ratio represents quasi steady state. It is observed that healthy, thermal cracks and notch wear inserts attain at quasi steady state, whereas rake face chipping and breakage attained chaotic state so poor surface finish and increased acceleration (RMS) are observed in case of breakage and rake face chipping tool conditions compared to other tool conditions.

6.4 CHIP MORPHOLOGY STUDIES

The chips produced during the machining process for different tool conditions were analyzed to understand the chip morphology using optical microscope. After material is removed from the workpiece, it flows out in the form of chips. During chip formation, the chip curls either naturally or through contact with the obstacles. If the material strain exceeds the material breaking strain, the chip will break. The chip formation type does affect the tool wear. The fluctuation of vibration components can effectively describe the chip formation type.

6.4.1 Chip morphology

This study aims for better understanding of chip morphology and its evolution through a systematic study via turning of die steels with tungsten carbide inserts. Besides better understanding towards chip formation mechanisms, the chip morphology can be a good and convenient indicator of tool condition in turning operation. The type and form of the chip producing during machining is a critical aspect in any machining process, which strongly influences the machining process stability: long chips can interfere with the machine tool, workpiece and tool, which have harmful impacts upon the material removal process and the product quality

(Barry and Byrne 2002). Small and broken chips are much simpler to handle, transfer, storage and recycle, which yields positive environmental impacts on the manufacturing operations (Byrne et al. 2003; Kim et al. 2005; Viharos et al. 2003).

Table 6.3 Chips formed while machining at different tool conditions


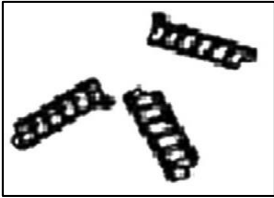
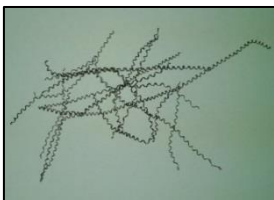
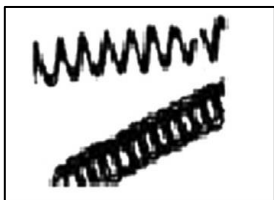
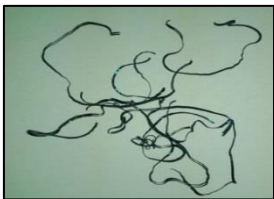
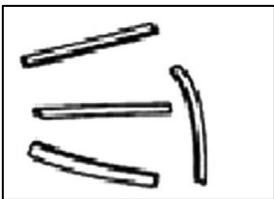




Sl. No	Tool condition	Collected chips from experiment	Chip formation type (Segreto et al. 2014)
1	Healthy	Short spiral chips	
			
2	Breakage	Long spiral chips	
			
3	Thermal cracks	Straight ribbon chips	
			
4	Notch wear	Naturally broken chips	
			
5	Rake face chipping	Conical chips	
			

Table 6.3, shows the different types of chips formed during machining with different tool conditions. While machining with healthy tool, short spiral type chips are formed, which are favorable type of chips. Whereas machining with worn-out inserts such as rake face chipping and breakage tool results in conical chips and long spiral chips respectively, which are unfavorable chips. However during machining with thermally cracked tool insert, results in straight ribbon type chips and finally with notch wear tool, broken chips were observed. From figure 4.1 (a-e) the time series plots of vibration acceleration for worn tool are characterized by slightly larger values while the healthy inserts shows shorter amplitude of acceleration the increase in vibration level, possibly due to the tangling of the chips. The tool–chip contact length is important because it provides an indication of the contact area between the chip and the tool, and therefore, represents the frictional interface that controls heat generation at the secondary deformation zone of the chip during machining (Iqbal et al. 2009). This heat plays an important role during chip formation. The localized shear bands, which are characteristic of the primary and secondary deformation zones in the chip are believed to form by dynamic recrystallization or phase change when the rate of thermal softening exceeds the rate of strain hardening.

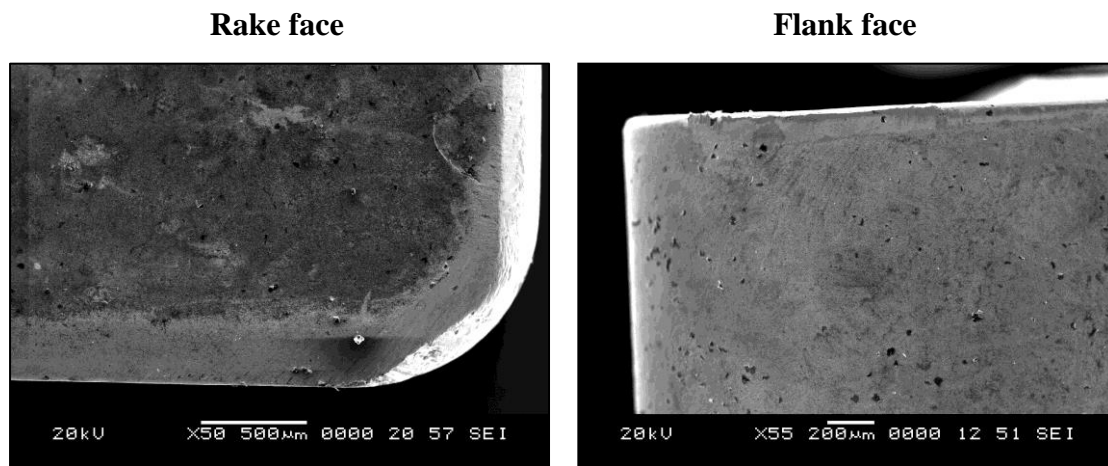
The angle of the primary shear zone is also related to thermal softening and flow stress and is known to increase with increasing cutting speed (increasing heat), which provides unchanged tool geometry. The tool–chip contact length has important implications on chip morphology and length. A shorter tool–chip contact length produces chips with a smaller radius of curvature. If chip is short enough, then it can prevent contact with mechanical chip breakers whereas increase in tool-chip length contact with worn out tool conditions results in increase friction and formation of unfavorable chips.

Although chip morphology cannot be directly related to tool life, it remains a very important practical consideration in machining because smaller chips are less likely to damage tools or the work piece, less hazardous to machine operators and are more convenient to dispose. In the course of a metal cutting operation, process condition modifications arising from tool wear development, irregularity in work material properties, interface temperature related issues, etc., can generate significant

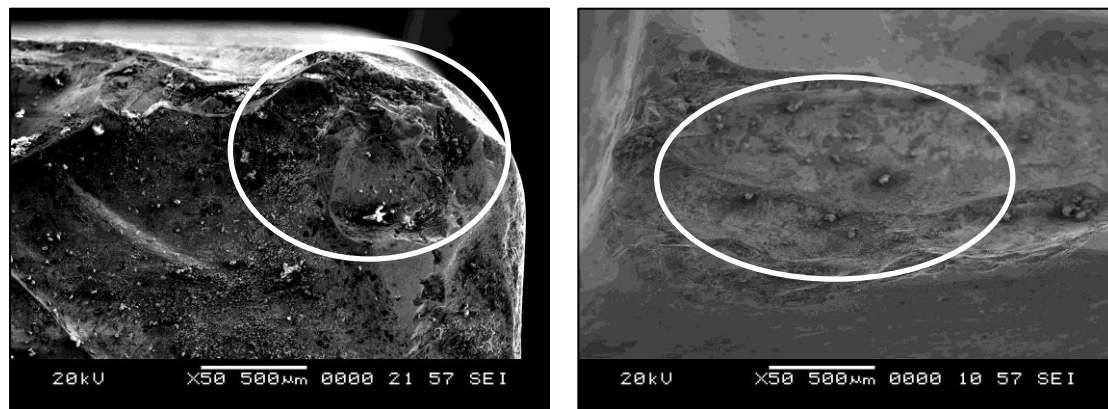
alterations of the chip type and form with detrimental consequences on the manufacturing of the product. Accordingly, to prevent the formation of unfavorable chip types and damages to the machine, the tooling and the workpiece, sensor monitoring methods and chip form control are highly desirable (Segreto et al. 2009).

6.5 SEM micrographs of tool wear

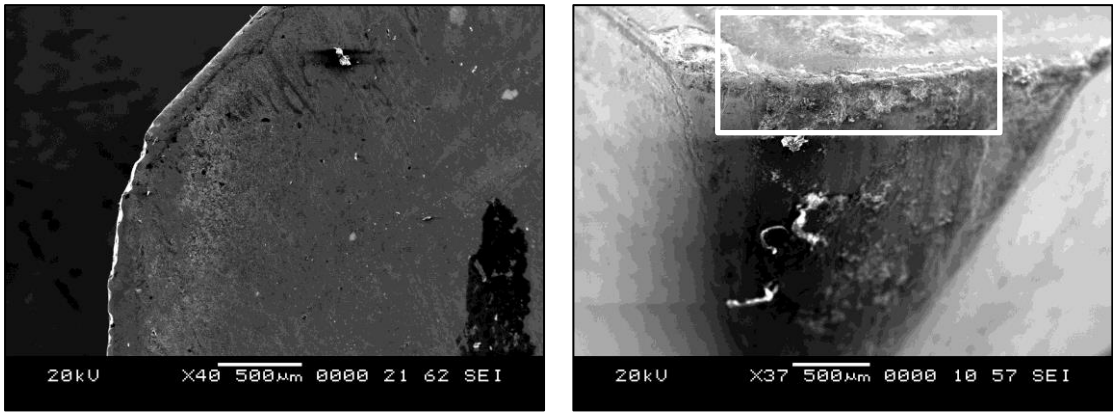
Scanning electron microscopy (modal-JSM-6380LA, JEOL; Operating voltage-30kV; Magnification range-300000) (SEM) micrographs of all five cutting tool inserts were considered to study the tool insert wear characteristics. Figure 6.14, shows the SEM micrographs of rake face and flank face for different tungsten carbide tool insert conditions.



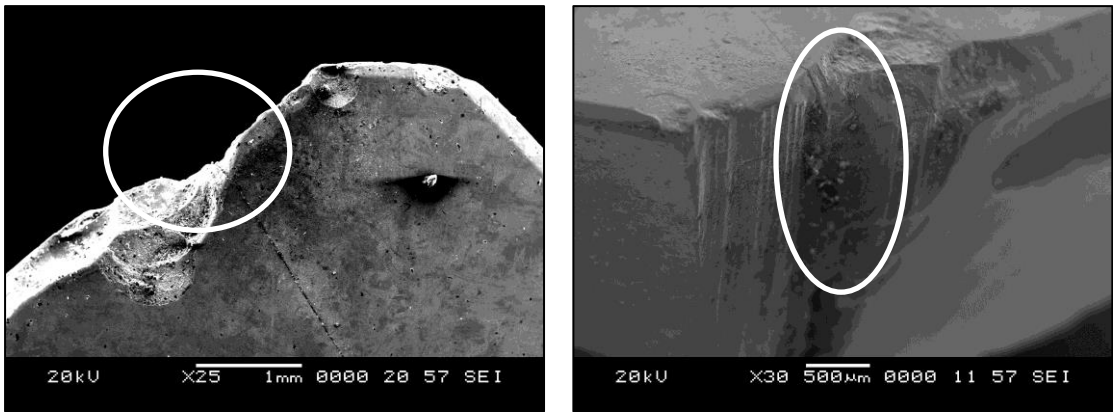
(a) Healthy tool



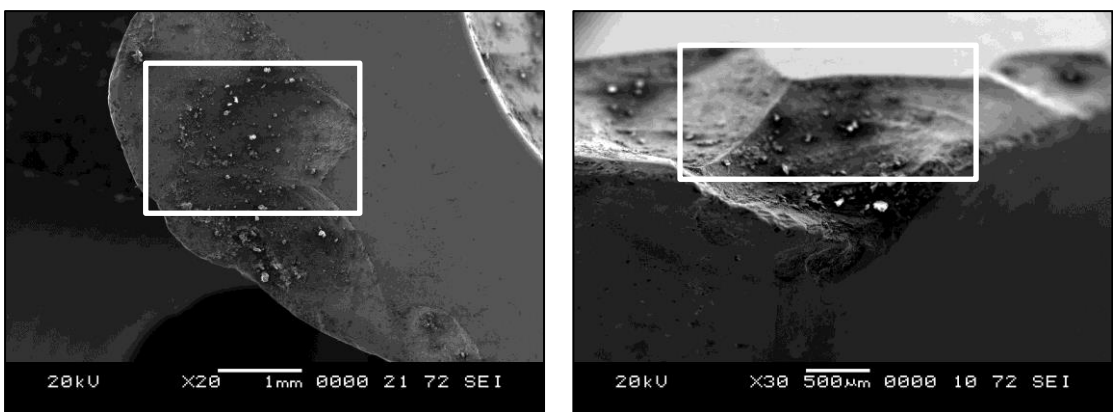
(b) Breakage



(c) Thermal cracks



(d) Notch wear



(e) Rake face chipping

Figure 6.14 SEM micrographs of healthy insert and different worn out inserts (a-e) after machining AISI H13 steel (die steel) under dry condition

The temperature at the tool chip contact zone (secondary shear zone) is proportional to the cutting speed. Therefore, higher cutting speeds results in higher temperature. The results of Gu et al. (1999) agreed with this finding. Higher stresses and temperature on the cutting edge causes the chipping process to take place on the cutting edge. Excessive chipping of the cutting edge was observed as shown in figure 6.14 (e), which may be due to the increase in vibration level, possibly due to the tangling of the chips. From the examination of the wear characteristics that are shown in figure 6.14 (a) to (e), it is observed that the performance of the tungsten carbide tool material can be attributed to the exceptional wear-resistance, high strength and resistance to deformation. These properties are adequate to endure the thermal and mechanical stresses produced in machining die steel at relatively low cutting speed.

There are several types of wear mechanisms that can influence the tool wear and subsequently the tool life of tungsten carbide tool while machining with die steel. Tool wear analysis has been carried out on the worn tools to find the tool wear mechanisms. The observed wear mechanisms were adhesion, abrasion, attrition and thermal fatigue. The temperature generated within the primary and secondary shear zones affects the wear rate of tool materials. Hence, high machining temperature often results in severe tool wear. Figure 6.15 (a) and (b) show the edge chipping and micro-thermal cracks at higher and lower scale.

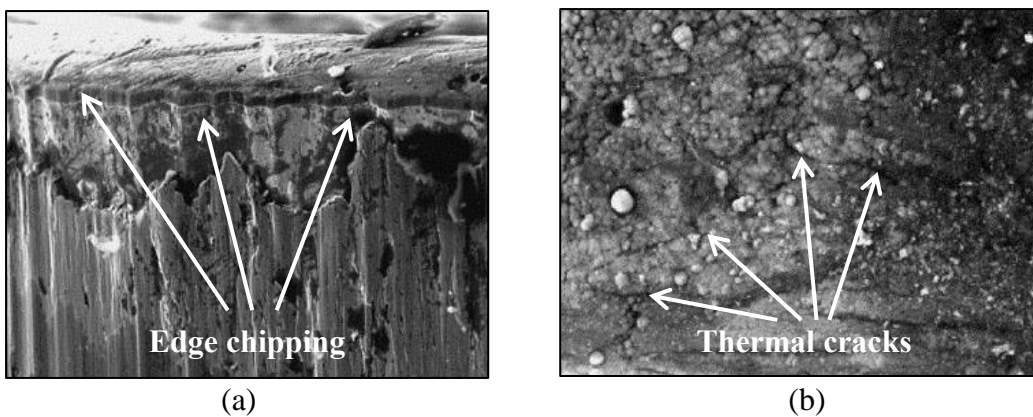


Figure 6.15 SEM image showing (a) edge chipping (b) micro-thermal cracks

Figure 6.16 (a) shows the micrograph, which exhibits massive metal adhesion resembling a build up edge (BUE) structure. However, this is not a stable kind of BUE since not many inserts exhibited this phenomenon. Karagoz and Fischmeister (1996) reported similar observations in their work. Figure 6.16 (b) shows micro-abrasion wear indicated by fine grooves. This is due to high temperatures resulted from high cutting speeds, which weaken the cutting tool by decreasing its hardness.

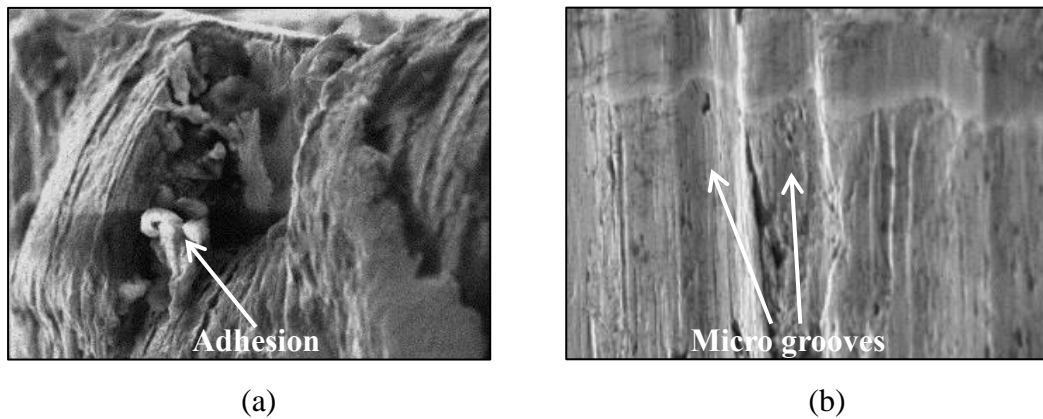


Figure 6.16 SEM image showing (a) adhesion (b) micro-abrasion

At higher cutting speed micro thermal-fatigue and micro-attrition wear started appearing as shown in figure 6.17 (a) and figure 6.17 (b). It is believed that the strongly adhering chip plucks away thin portions of the tool, as it moves over the tool surface (Trent 1988; Lim et al. 2000).

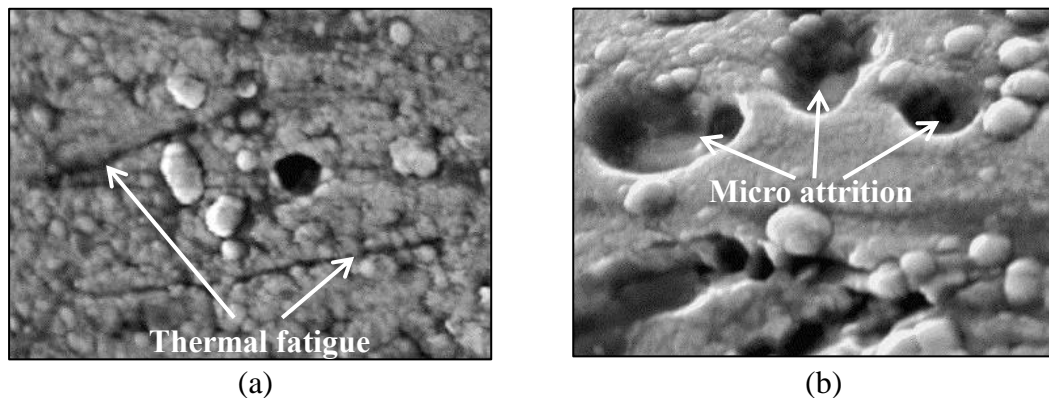


Figure 6.17 SEM image showing (a) micro-thermal-fatigue. (b) micro-attrition

6.6 SUMMARY

This chapter presented the results of investigations undertaken to find suitability of vibration signals and cutting forces to detect the condition of single point tungsten carbide cutting tool insert, surface roughness and type of chip formation. Tests were carried out while turning die steel (AISI H13) using tungsten carbide inserts for regular intervals of time with different tungsten carbide insert tool conditions such as healthy, rake face chipping, notch wear, breakage and thermal cracks. Vibration signals and cutting forces were acquired, while machining with different tool condition. Measurements of surface roughness of the workpiece and chip morphological studies were carried out at different tool conditions for the analysis. Experimental results show that there is an increase in the level of acceleration and cutting forces at faulty tool condition as compared with the healthy condition of the tool. Based on this finding, cutting tool acceleration and cutting forces can be used to predict the tool condition, surface roughness and chip formation type. Qualitative comparisons of the computational predicted forces are drawn by plotting the trends of the predicted forces together with the measured forces. The Deform-3D has correctly predicted this trend which is consistent with the experimental trends of the cutting forces components. Tool wear analysis has been carried out on the worn tungsten carbide insert cutting tools to find the tool wear mechanisms. Based on SEM micrographs of worn surface of the cutting tool, micro-abrasion, micro-attrition, adhesion and micro-fatigue behaviors are identified as the dominant kinds of wear mechanisms.

CHAPTER 7

CONCLUSION AND SCOPE FOR FUTURE WORK

7.1 CONCLUSION

Analysing of cutting tool vibration signals along with cutting forces for fault diagnosis of cutting tool forms is the main theme of this thesis. To perform the same, turning operation has been taken for the study. The research work concerns with fault diagnosis of single point cutting tool by using both online and offline condition monitoring techniques in conjunction with advanced signal processing approaches. The present research work is organized in three phases.

The first part of investigations aim for fault detection of cutting tool using signal processing techniques such as time domain analysis, spectrum analysis, cepstrum analysis, continuous wavelet transform analysis and recurrence quantification analysis. Based on results of this phase of investigation following conclusions are drawn.

1. Time domain technique for vibration signal analysis gives overall vibration level but do not provide any fault diagnostic information.
2. Turning operations mostly provides non-stationary and complex vibration signatures for which the spectral analysis, cepstrum analysis and continuous wavelet transform analysis approach are found to be insignificant.
3. Recurrence plots and recurrence quantification analysis had significant features to distinguish the worn states of the inserts. Recurrence plots based on color pattern and texture were able to distinguish cutting tool conditions through visualization in the qualitative investigation.
4. In quantitative investigation for different cutting tool conditions, the percent recurrence (REC), percent determinism (DET), percent laminarity (LAM), trapping time (TT) and entropy values decrease with the worn out cutting tool compare to healthy cutting tool.

The second phase of studies focused on building an online monitoring system for fault diagnosis of cutting tool using machine learning techniques. Various features such as discrete wavelet transform features, statistical features, histogram features and empirical mode decomposition features were extracted from the acquired vibration signals pertaining to all class of fault category. Decision tree technique and principal component analysis were used for important feature selection and used different classifiers such as SVM, Naïve Bayes, Bayes net, K-star, J48 and ANN to distinguish the healthy as well as different condition of cutting tool inserts. Based on the investigation, following conclusions are listed below,

1. Based on the information provided in table 5.53, fault classification accuracies with K-star algorithm and Bayes net algorithm are found to be 98% and 98.5% with discrete wavelet transform features and empirical mode decomposition features respectively. These machine learning methods gives more accuracy to correctly predict the condition of cutting tool and it can be recommended for practical applications and development of on-line fault diagnosis systems for tool condition monitoring.
2. Decision tree technique is found to be more effective than principal component analysis for feature selection in machine learning technique to improve classification efficiencies.

The third phase of investigation deals with cutting forces analysis, surface roughness studies, chip morphology studies and computational approach for fault diagnosis of cutting tool. Following conclusions are drawn based on the results,

1. Thrust force (F_y) and cutting force (F_z) for all worn out tool conditions are 76.5% higher than healthy tool, this is due to ploughing effect that prevails under the worn out tool conditions and may be due to the fact that the friction between the tool-workpiece contacts increases with increase in tool wear.
2. The Deform-3D has correctly predicted the trend of cutting forces, which is consistent with the experimental trends of the cutting forces components.
3. Surface roughness (R_a) of workpiece and tool condition can be easily monitored by observing the level of vibration signal (RMS) component ' a_y '.

4. Machining with healthy tool resulted in formation of short spiral type chips, which are favorable chip type, whereas machining with worn-out inserts resulted in formation of unfavorable chip types. The fluctuation of vibration components can effectively describe the chip formation type.
5. Based on SEM micrographs of worn surface of the cutting tool, micro-abrasion, micro-attrition, adhesion and micro-fatigue behaviors are identified as the dominant kinds of wear mechanisms.

7.2 SCOPE FOR FUTURE WORK

Although the fault diagnosis of single point cutting tool monitored through various online and offline techniques, still there is much scope exists for further investigations, the following suggestion may be useful for future work:

- Microcontroller based portable hardware kit can be fabricated using best feature-classifier for the automated fault diagnosis.
- Machine learning process can be tried with feature fusion or decision fusion of sound and vibration signals.
- Acoustic emission (AE) technique, Ultrasonic technique, Motor current signature analysis etc. can be used to predict tool wear.
- Cutting fluids analysis and additional tribological studies can be carried out to explore the additional information for developing efficient tool condition monitoring systems.

7.3 KEY CONTRIBUTIONS

The main contributions of this study are the followings,

1. Many researchers reported on fault diagnosis either online monitoring or offline monitoring, but this research work considers fault diagnosis of single point cutting tool by using both online and offline condition monitoring techniques in conjunction with advanced signal processing approaches.
2. In this present work, attempt has been made to exploit the new technique recurrence quantification analysis (RQA) to classify the different tungsten carbide cutting tool insert conditions in turning operation.

3. In the present study combinations of different types of industrial practical worn out inserts are considered for fault diagnosis of single point cutting tool inserts.
4. The monitoring strategy proposed in the research work includes many of the methods investigated in other recent studies. Further large number of features generated and investigated is also a contribution with regard to the literatures.

REFERENCES

- Abouelatta, O. B. and Madl, J. (2001). "Surface roughness prediction based on cutting parameters and tool vibrations in turning operations." *Journal of Materials Processing Technology*, 118(1), 269-277.
- Abu-Zahra, N. H. and Yu, G. (2003). "Gradual wear monitoring of turning inserts using wavelet analysis of ultrasound waves." *International Journal of Machine Tools and Manufacture*, 43(4), 337-343.
- Acuna-González, N., García-Ochoa, E. and González-Sánchez, J. (2008). "Assessment of the dynamics of corrosion fatigue crack initiation applying recurrence plots to the analysis of electrochemical noise data." *International Journal of Fatigue*, 30(7), 1211-1219.
- Addin, O., Sapuan, S. M., Mahdi, E. and Othman, M. (2007). "A Naïve-Bayes classifier for damage detection in engineering materials." *Materials and Design*, 28(8), 2379-2386.
- Addin, O., Sapuan, S. M., Othman, M. and Ali, B. A. (2011). "Comparison of Naïve Bayes classifier with back propagation neural network classifier based on f-folds feature extraction algorithm for ball bearing fault diagnostic system." *International Journal of the Physical Sciences*, 6(13), 3181-3188.
- Ali, J. B., Fnaiech, N., Saidi, L., Chebel-Morello, B. and Fnaiech, F. (2015). "Application of empirical mode decomposition and artificial neural network for automatic bearing fault diagnosis based on vibration signals." *Applied Acoustics*, 89, 16-27.
- Amarnath, M., Jain, D., Sugumaran, V. and Kumar, H. (2015). "Fault diagnosis of helical gear box using Naïve Bayes and Bayes net." *International Journal of Decision Support Systems*, 1(1), 4-17.

Amarnath, M., Sugumaran, V. and Kumar, H. (2013). "Exploiting sound signals for fault diagnosis of bearings using decision tree." *Measurement*, 46(3), 1250-1256.

Amarnath, M., Sujatha, C. and Swarnamani, S. (2009). "Experimental studies on the effects of reduction in gear tooth stiffness and lubricant film thickness in a spur geared system." *Tribology International*, 42(2), 340-352.

Amiri, G. G. and Darvishan, E. (2015). "Damage detection of moment frames using ensemble empirical mode decomposition and clustering techniques." *KSCE Journal of Civil Engineering*, 1-10.

Aouici, H., Yallese, M. A., Chaoui, K., Mabrouki, T. and Rigal, J. F. (2012). "Analysis of surface roughness and cutting force components in hard turning with CBN tool: prediction model and cutting conditions optimization." *Measurement*, 45(3), 344-353.

Arsecularatne, J. A., Zhang, L. C. and Montross, C. (2006). "Wear and tool life of tungsten carbide, PCBN and PCD cutting tools." *International Journal of Machine Tools and Manufacture*, 46(5), 482-491.

Asilturk, I. and Akkuş, H. (2011). "Determining the effect of cutting parameters on surface roughness in hard turning using the Taguchi method." *Measurement*, 44(9), 1697-1704.

Azouzi, R. and Guillot, M. (1997). "On-line prediction of surface finish and dimensional deviation in turning using neural network based sensor fusion." *International Journal of Machine Tools and Manufacture*, 37(9), 1201-1217.

Badaoui, M., Antoni, J., Guillet, F., Daniere, J. and Velez, P. (2001). "Use of the moving cepstrum integral to detect and localise tooth spalls in gears." *Mechanical Systems and Signal Processing*, 15(5), 873-885.

Badour, F., Sunar, M. and Cheded, L. (2013). “Vibration analysis of rotating machinery using time–frequency analysis and wavelet techniques.” *Mechanical Systems and Signal Processing*, 25(6), 2083-2101.

Bakker, O. J., Gibson, C., Wilson, P., Lohse, N. and Popov, A. A. (2015). “Linear friction weld process monitoring of fixture cassette deformations using empirical mode decomposition.” *Mechanical Systems and Signal Processing*, 62, 395-414.

Bansal, S., Sahoo, S., Tiwari, R. and Bordoloi, D. J. (2013). “Multiclass fault diagnosis in gears using support vector machine algorithms based on frequency domain data.” *Measurement*, 46(9), 3469-3481.

Barry, J. and Byrne, G. (2002). “Chip formation, acoustic emission and surface white layers in hard machining.” *CIRP Annals-Manufacturing Technology*, 51(1), 65-70.

Bediaga, I., Mendizabal, X., Arnaiz, A. and Munoa, J. (2013). “Ball bearing damage detection using traditional signal processing algorithms.” *Instrumentation and Measurement Magazine, IEEE*, 16(2), 20-25.

Benardos, P. G. and Vosniakos, G. C. (2003). “Predicting surface roughness in machining: a review.” *International Journal of Machine Tools and Manufacture*, 43(8), 833-844.

Bhuiyan, M. S. H., Choudhury, I. A. and Dahari, M. (2014). “Monitoring the tool wear, surface roughness and chip formation occurrences using multiple sensors in turning.” *Journal of Manufacturing Systems*, 33(4), 476-487.

Bianchini, C., Immovilli, F., Cocconcelli, M., Rubini, R. and Bellini, A. (2011). “Fault detection of linear bearings in brushless AC linear motors by vibration analysis.” *Industrial Electronics, IEEE Transactions on*, 58(5), 1684-1694.

Bin, G. F., Gao, J. J., Li, X. J. and Dhillon, B. S. (2012). “Early fault diagnosis of rotating machinery based on wavelet packets—empirical mode decomposition

feature extraction and neural network.” *Mechanical Systems and Signal Processing*, 27, 696-711.

Bonifacio, M. E. R. and Diniz, A. E. (1994). “Correlating tool wear, tool life, surface roughness and tool vibration in finish turning with coated carbide tools.” *Wear*, 173(1), 137-144.

Boothroyd, G. (1988). “*Fundamentals of Metal Machining and Machine Tools*.” CRC Press.

Borghesani, P., Pennacchi, P., Randall, R. B., Sawalhi, N. and Ricci, R. (2013). “Application of cepstrum pre-whitening for the diagnosis of bearing faults under variable speed conditions.” *Mechanical Systems and Signal Processing*, 36(2), 370-384.

Bouacha, K., Yallese, M. A., Mabrouki, T. and Rigal, J. F. (2010). “Statistical analysis of surface roughness and cutting forces using response surface methodology in hard turning of AISI 52100 bearing steel with CBN tool.” *International Journal of Refractory Metals and Hard Materials*, 28(3), 349-361.

Bradley, C. and Wong, Y. S. (2001). “Surface texture indicators of tool wear—a machine vision approach.” *The International Journal of Advanced Manufacturing Technology*, 17(6), 435-443.

Braun, W. J., Miller, M. H. and Schultze, J. F. (1999). “The development of machine-tool force reconstruction for wear identification.” *Society of Photo-Optical Instrumentation Engineers Proceedings Series*, 94-98.

Byrne, G., Dornfeld, D. and Denkena, B. (2003). “Advancing cutting technology.” *CIRP Annals-Manufacturing Technology*, 52(2), 483-507.

Byrne, G., Dornfeld, D., Inasaki, I., Ketteler, G., König, W. and Teti, R. (1995). “Tool condition monitoring (TCM)—the status of research and industrial application.” *CIRP Annals-Manufacturing Technology*, 44(2), 541-567.

Cao, H., Zhou, K. and Chen, X. (2015). "Chatter identification in end milling process based on EEMD and nonlinear dimensionless indicators." *International Journal of Machine Tools and Manufacture*, 92, 52-59.

Cao, L. J., Chua, K. S., Chong, W. K., Lee, H. P. and Gu, Q. M. (2003). "A comparison of PCA, KPCA and ICA for dimensionality reduction in support vector machine." *Neurocomputing*, 55(1), 321-336.

Ceretti, E., Fallböhmer, P., Wu, W. T. and Altan, T. (1996). "Application of 2D FEM to chip formation in orthogonal cutting." *Journal of Materials Processing Technology*, 59(1), 169-180.

Chen, F., Tang, B. and Chen, R. (2013). "A novel fault diagnosis model for gearbox based on wavelet support vector machine with immune genetic algorithm." *Measurement*, 46(1), 220-232.

Chen, W. (2000). "Cutting forces and surface finish when machining medium hardness steel using CBN tools." *International Journal of Machine Tools and Manufacture*, 40(3), 455-466.

Chen, W. S. (2011). "Use of recurrence plot and recurrence quantification analysis in Taiwan unemployment rate time series." *Physica A: Statistical Mechanics and its Applications*, 390(7), 1332-1342.

Chen, X., Cheng, K. and Wang, C. (2014). "Design of a smart turning tool with application to in-process cutting force measurement in ultraprecision and micro cutting." *Manufacturing Letters*, 2(4), 112-117.

Chiou, R. Y. and Liang, S. Y. (1998). "Chatter stability of a slender cutting tool in turning with tool wear effect." *International Journal of Machine Tools and Manufacture*, 38(4), 315-327.

Choi, D., Kwon, W. T. and Chu, C. N. (1999). "Real-time monitoring of tool fracture in turning using sensor fusion." *The International Journal of Advanced Manufacturing Technology*, 15(5), 305-310.

Chou, Y. K. and Evans, C. J. (1997). "Tool wear mechanism in continuous cutting of hardened tool steels." *Wear*, 212(1), 59-65.

Chou, Y. K. and Evans, C. J. (1999). "White layers and thermal modeling of hard turned surfaces." *International Journal of Machine Tools and Manufacture*, 39(12), 1863-1881.

Cleary, J. G. and Trigg, L. E. (1995). "K*: An instance-based learner using an entropic distance measure." In *Proceedings of the 12th International Conference on Machine learning*, 5, 108-114.

Coker, S. A. and Shin, Y. C. (1996). "In-process control of surface roughness due to tool wear using a new ultrasonic system." *International Journal of Machine Tools and Manufacture*, 36(3), 411-422.

Cortes, C. and Vapnik, V. (1995). "Support-vector networks." *Machine learning*, 20(3), 273-297.

Dalpiaz, G., Rivola, A. and Rubini, R. (1998). "Gear fault monitoring: Comparison of vibration analysis techniques." In *Proceedings of the 3rd International Conference on Acoustical and Vibratory Surveillance Methods and Diagnostic Techniques*, 1-10.

Devillez, A., Lesko, S. and Mozer, W. (2004). "Cutting tool crater wear measurement with white light interferometry." *Wear*, 256(1), 56-65.

Dia, S., Fontaine, S. and Renner, M. (2012). "Using Recurrence Plots for Determinism Analysis of Blade-Disk Tribometer." *Experimental Techniques*, 36(1), 26-33.

Dimla, D. E. (1999). "Application of perceptron neural networks to tool-state classification in a metal-turning operation." *Engineering Applications of Artificial Intelligence*, 12(4), 471-477.

Dimla, D. E. (2000). "Sensor signals for tool-wear monitoring in metal cutting operations—a review of methods." *International Journal of Machine Tools and Manufacture*, 40(8), 1073-1098.

Dimla, D. E., Lister, P. M. and Leighton, N. J. (1998). "Automatic tool state identification in a metal turning operation using MLP neural networks and multivariate process parameters." *International Journal of Machine Tools and Manufacture*, 38(4), 343-352.

Dos Santos, A. L. B., Duarte, M. A. V., Abrao, A. M. and Machado, A. R. (1999). "An optimisation procedure to determine the coefficients of the extended Taylor's equation in machining." *International Journal of Machine Tools and Manufacture*, 39(1), 17-31.

Eckmann, J. P., Kamphorst, S. O. and Ruelle, D. (1987). "Recurrence plots of dynamical systems." *EPL Europhysics Letters*, 4(9), 973.

Elangovan, M., Devasenapati, S. B., Sakthivel, N. R. and Ramachandran, K. I. (2011). "Evaluation of expert system for condition monitoring of a single point cutting tool using principle component analysis and decision tree algorithm." *Expert Systems with Applications*, 38(4), 4450-4459.

Elangovan, M., Sugumaran, V., Ramachandran, K. I. and Ravikumar, S. (2011). "Effect of SVM kernel functions on classification of vibration signals of a single point cutting tool." *Expert Systems with Applications*, 38(12), 15202-15207.

Elwakil, A. S. and Soliman, A. M. (1999). "Mathematical models of the twin-t, wien-bridge and family of minimum component electronic chaos generators with demonstrative recurrence plots." *Chaos, Solitons and Fractals*, 10(8), 1399-1412.

Ertunc, H. M., Loparo, K. A. and Ocak, H. (2001). "Tool wear condition monitoring in drilling operations using hidden Markov models (HMMs)." *International Journal of Machine Tools and Manufacture*, 41(9), 1363-1384.

Ezugwu, E. O., Olajire, K. A. and Bonney, J. (2001). "Modelling of tool wear based on component forces." *Tribology Letters*, 11(1), 55-60.

Filice, L., Micari, F., Settineri, L. and Umbrello, D. (2007). "Wear modelling in mild steel orthogonal cutting when using uncoated carbide tools." *Wear*, 262(5), 545-554.

Fnides, B., Yallese, M. A., Mabrouki, T. and Rigal, J. F. (2011). "Application of response surface methodology for determining cutting force model in turning hardened AISI H11 hot work tool steel." *Sadhana*, 36(1), 109-123.

Franco-Gasca, L. A., Herrera-Ruiz, G., Peniche-Vera, R., de Jesús Romero-Troncoso, R. and Leal-Tafolla, W. (2006). "Sensorless tool failure monitoring system for drilling machines." *International Journal of Machine Tools and Manufacture*, 46(3), 381-386.

Fraser, A. M. and Swinney, H. L. (1986). "Independent coordinates for strange attractors from mutual information." *Physical Review A*, 33(2), 1134.

Gaitonde, V. N., Karnik, S. R., Figueira, L. and Davim, J. P. (2009). "Machinability investigations in hard turning of AISI D2 cold work tool steel with conventional and wiper ceramic inserts." *International Journal of Refractory Metals and Hard Materials*, 27(4), 754-763.

Georgoulas, G., Tsoumas, I. P., Antonino-Daviu, J. A., Climente-Alarcon, V., Stylios, C. D., Mitronikas, E. D. and Safacas, A. N. (2014). "Automatic pattern identification based on the complex empirical mode decomposition of the startup current for the diagnosis of rotor asymmetries in asynchronous machines." *Industrial Electronics, IEEE Transactions on*, 61(9), 4937-4946.

Girish Kumar M, Hemantha, K. Gangadhar, N., Hemantha Kumar and Prasad K. (2014). "Fault Diagnosis of welded joints through Vibration signals using Naïve Bayes Algorithm." *Procedia Materials Science*, 5, 1922-1928.

Gong, W., Li, W., Shirakashi, T. and Obikawa, T. (2004). "An active method of monitoring tool wear states by impact diagnostic excitation." *International Journal of Machine Tools and Manufacture*, 44(7), 847-854.

Grabec, I., Govekar, E., Susič, E. and Antolovič, B. (1998). "Monitoring manufacturing processes by utilizing empirical modeling." *Ultrasonics*, 36(1), 263-271.

Grasso, M., Pennacchi, P. and Colosimo, B. M. (2014). "Empirical mode decomposition of pressure signal for health condition monitoring in waterjet cutting." *The International Journal of Advanced Manufacturing Technology*, 72(1-4), 347-364.

Groover, M. P. (2007). "*Fundamentals of Modern Manufacturing: Materials Processes, and Systems*." John Wiley and Sons.

Grzesik, W. (2008). "Influence of tool wear on surface roughness in hard turning using differently shaped ceramic tools." *Wear*, 265(3), 327-335.

Gu, J., Tung, S. C. and Barber, G. C. (1998). "Wear mechanisms of milling inserts: dry and wet cutting." *In Wear Processes in Manufacturing. ASTM International*. 31-47.

Guhathakurta, K., Bhattacharya, B. and Chowdhury, A. R. (2010). "Using recurrence plot analysis to distinguish between endogenous and exogenous stock market crashes." *Physica A: Statistical Mechanics and its Applications*, 389(9), 1874-1882.

Gupta, M. and Gill, S. K. (2012). "Prediction of cutting force in turning of UD-GFRP using mathematical model and simulated annealing." *Frontiers of Mechanical Engineering*, 7(4), 417-426.

Haddag, B., Makich, H., Nouari, M. and Dhers, J. (2014). "Tribological behaviour and tool wear analyses in rough turning of large-scale parts of nuclear power plants using grooved coated insert." *Tribology International*, 80, 58-70.

Huang, Y. and Liang, S. Y. (2005). "Modeling of cutting forces under hard turning conditions considering tool wear effect." *Journal of Manufacturing Science and Engineering*, 127(2), 262-270.

Huda, M., Yamada, K., Hosokawa, A. and Ueda, T. (2002). "Investigation of temperature at tool-chip interface in turning using two-color pyrometer." *Journal of Manufacturing Science and Engineering*, 124(2), 200-207.

Indira, V., Vasanthakumari, R., Sakthivel, N. R. and Sugumaran, V. (2011). "A method for calculation of optimum data size and bin size of histogram features in fault diagnosis of mono-block centrifugal pump." *Expert Systems with Applications*, 38(6), 7708-7717.

Iqbal, S. A., Mativenga, P. T. and Sheikh, M. A. (2009). "A comparative study of the tool-chip contact length in turning of two engineering alloys for a wide range of cutting speeds." *The International Journal of Advanced Manufacturing Technology*, 42(1-2), 30-40.

Jaharah, A. G., Wahid, S. W., Hassan, C. C., Nuawi, M. Z. and Nizam, A. M. (2009). "The effect of uncoated carbide tool geometries in turning AISI 1045 using finite element analysis." *European Journal of Scientific Research*, 28(2), 271-277.

Jang, D. Y., Choi, Y. G., Kim, H. G. and Hsiao, A. (1996). "Study of the correlation between surface roughness and cutting vibrations to develop an on-line roughness measuring technique in hard turning." *International Journal of Machine Tools and Manufacture*, 36(4), 453-464.

Jantunen, E. (2002). "A summary of methods applied to tool condition monitoring in drilling." *International Journal of Machine Tools and Manufacture*, 42(9), 997-1010.

Jardine, A. K., Lin, D. and Banjevic, D. (2006). "A review on machinery diagnostics and prognostics implementing condition-based maintenance." *Mechanical Systems and Signal Processing*, 20(7), 1483-1510.

Jawahir, I. S., Dillon Jr, O. W., Balajj, A. K., Redetzky, M. and Fang, N. (1998). "Predictive modeling of machining performance in turning operations." *Machining Science and Technology*, 2(2), 253-276.

Jegadeeshwaran, R. and Sugumaran, V. (2013). "Comparative study of decision tree classifier and best first tree classifier for fault diagnosis of automobile hydraulic brake system using statistical features." *Measurement*, 46(9), 3247-3260.

Jegadeeshwaran, R. and Sugumaran, V. (2015). "Brake fault diagnosis using Clonal Selection Classification Algorithm (CSCA)—A statistical learning approach." *Engineering Science and Technology, an International Journal*, 18(1), 14-23.

Jemielniak, K. and Otman, O. (1998). "Tool failure detection based on analysis of acoustic emission signals." *Journal of Materials Processing Technology*, 76(1), 192-197.

Jemielniak, K., Urbański, T., Kossakowska, J. and Bombiński, S. (2012). "Tool condition monitoring based on numerous signal features." *The International Journal of Advanced Manufacturing Technology*, 59(1-4), 73-81.

Jessy, K., Dinakaran, D. and Kumar, S. S. (2015). "Investigating the fluctuations in tool vibration during GFRP drilling through recurrence quantification analysis." *Journal of Mechanical Science and Technology*, 29(3), 1265-1272.

Junsheng, C., Dejie, Y. and Yu, Y. (2006). "A fault diagnosis approach for roller bearings based on EMD method and AR model." *Mechanical Systems and Signal Processing*, 20(2), 350-362.

Jurkovic, J., Korosec, M. and Kopac, J. (2005). "New approach in tool wear measuring technique using CCD vision system." *International Journal of Machine Tools and Manufacture*, 45(9), 1023-1030.

Kankar, P. K., Sharma, S. C. and Harsha, S. P. (2011). "Fault diagnosis of ball bearings using machine learning methods." *Expert Systems with Applications*, 38(3), 1876-1886.

Karagoz, S. and Fischmeister, H. F. (1996). "Metallographic observations on the wear process of TiN-coated cutting tools." *Surface and Coatings Technology*, 81(2), 190-200.

Karandikar, J. M., Abbas, A. E. and Schmitz, T. L. (2014). "Tool life prediction using Bayesian updating. Part 1: Milling tool life model using a discrete grid method." *Precision Engineering*, 38(1), 9-17.

Karim, Z., Nuawi, M. Z., Ghani, J. A. Azrulhisham, E. A., and Abdullah, S. (2013). "Development of machining condition monitoring system using piezoelectric sensor analyzed by I-kaz multilevel method." *World Applied Sciences Journal*, 21(2), 264-268.

Karthik, A., Chandra, S., Ramamoorthy, B. and Das, S. (1997). "3D tool wear measurement and visualisation using stereo imaging." *International Journal of Machine Tools and Manufacture*, 37(11), 1573-1581.

Kassim, A. A., Mannan, M. A. and Jing, M. (2000). "Machine tool condition monitoring using workpiece surface texture analysis." *Machine Vision and Applications*, 11(5), 257-263.

Kaymakci, M., Kilic, Z. M. and Altintas, Y. (2012). "Unified cutting force model for turning, boring, drilling and milling operations." *International Journal of Machine Tools and Manufacture*, 54, 34-45.

Kennel, M. B., Brown, R. and Abarbanel, H. D. (1992). "Determining embedding dimension for phase-space reconstruction using a geometrical construction." *Physical Review A*, 45(6), 3403.

- Kerr, D., Pengilley, J. and Garwood, R. (2006). "Assessment and visualisation of machine tool wear using computer vision." *The International Journal of Advanced Manufacturing Technology*, 28(7-8), 781-791.
- Kilundu, B., Dehombreux, P. and Chiementin, X. (2011). "Tool wear monitoring by machine learning techniques and singular spectrum analysis." *Mechanical Systems and Signal Processing*, 25(1), 400-415.
- Kim, J. H., Chang, H. K., Han, D. C., Jang, D. Y. and Oh, S. I. (2005). "Cutting force estimation by measuring spindle displacement in milling process." *CIRP Annals-Manufacturing Technology*, 54(1), 67-70.
- Kovac, P. and Sidjanin, L. (1997). "Investigation of chip formation during milling." *International Journal of Production Economics*, 51(1), 149-153.
- Kumar, H., Ranjit Kumar, T. A., Amarnath, M. and Sugumaran, V. (2014). "Fault diagnosis of bearings through vibration signal using Bayes classifiers." *International Journal of Computer Aided Engineering and Technology*, 6(1), 14-28.
- Kumar, M., Shankar Mukherjee, P. and Mohan Misra, N. (2013). "Advancement and current status of wear debris analysis for machine condition monitoring: a review." *Industrial Lubrication and Tribology*, 65(1), 3-11.
- Kumar, S. A., Ravindra, H. V. and Srinivasa, Y. G. (1997). "In-process tool wear monitoring through time series modelling and pattern recognition." *International Journal of Production Research*, 35(3), 739-751.
- Kurada, S. and Bradley, C. (1997). "A review of machine vision sensors for tool condition monitoring." *Computers in Industry*, 34(1), 55-72.
- Lalbondre, R., Krishna, P. and Mohankumar, G. C. (2014). "An Experimental Investigation on Machinability Studies of Steels by Face Turning." *Procedia Materials Science*, 6, 1386-1395.

Lalwani, D. I., Mehta, N. K. and Jain, P. K. (2008). "Experimental investigations of cutting parameters influence on cutting forces and surface roughness in finish hard turning of MDN250 steel." *Journal of Materials Processing Technology*, 206(1), 167-179.

Lardies, J. and Gouttebroze, S. (2002). "Identification of modal parameters using the wavelet transforms." *International Journal of Mechanical Sciences*, 44(11), 2263-2283.

Lee, J. H., Kim, D. E. and Lee, S. J. (1998). "Statistical analysis of cutting force ratios for flank-wear monitoring." *Journal of Materials Processing Technology*, 74(1), 104-114.

Lee, K. J., Lee, T. M. and Yang, M. Y. (2007). "Tool wear monitoring system for CNC end milling using a hybrid approach to cutting force regulation." *The International Journal of Advanced Manufacturing Technology*, 32(1-2), 8-17.

Leshock, C. E. and Shin, Y. C. (1997). "Investigation on cutting temperature in turning by a tool-work thermocouple technique." *Journal of Manufacturing Science and Engineering*, 119(4), 502-508.

Lever, P. J., Marefat, M. M. and Ruwani, T. (1997). "A machine learning approach to tool wear behavior operational zones." *Industry Applications, IEEE Transactions on*, 33(1), 264-273.

Li, H., Fu, L. and Li, Z. (2009). "Fault detection and diagnosis of gear wear based on teager-huang transform." *In Artificial Intelligence*, 663-666).

Li, X. (2002). "A brief review: acoustic emission method for tool wear monitoring during turning." *International Journal of Machine Tools and Manufacture*, 42(2), 157-165.

Liang, B., Iwnicki, S. D. and Zhao, Y. (2013). "Application of power spectrum, cepstrum, higher order spectrum and neural network analyses for induction motor fault diagnosis." *Mechanical Systems and Signal Processing*, 39(1), 342-360.

- Lim, C. Y. H., Lim, S. C. and Lee, K. S. (2000). "Crater wear mechanisms of TiN coated high speed steel tools." *Surface engineering*, 16(3), 253-256.
- Lim, G. H. (1995). "Tool-wear monitoring in machine turning." *Journal of Materials Processing Technology*, 51(1), 25-36.
- Lin, Z. C. and Chen, D. Y. (1995). "A study of cutting with a CBN tool." *Journal of Materials Processing Technology*, 49(1), 149-164.
- Litak, G., Gajewski, J., Syta, A. and Jonak, J. (2008). "Quantitative estimation of the tool wear effects in a ripping head by recurrence plots." *Journal of Theoretical and Applied Mechanics*, 46, 521-530.
- Liu, K., Li, X. P., Rahman, M. and Liu, X. D. (2003). "CBN tool wear in ductile cutting of tungsten carbide." *Wear*, 255(7), 1344-1351.
- Liu, Z., Chai, T., Yu, W. and Tang, J. (2015). "Multi-frequency signal modeling using empirical mode decomposition and PCA with application to mill load estimation." *Neurocomputing*, 169, 392-402.
- Loutridis, S. J. (2004). "Damage detection in gear systems using empirical mode decomposition." *Engineering Structures*, 26(12), 1833-1841.
- Lungu, N. and Borzan, M. (2012). "Effect of cutting speed and feed rate on tool geometry, temperature and cutting forces in machining AISI 1045 carbon steel using FEM simulation." *Proceedings in Manufacturing Systems*, 7(4), 245-252.
- Luo, S. Y., Liao, Y. S. and Tsai, Y. Y. (1999). "Wear characteristics in turning high hardness alloy steel by ceramic and CBN tools." *Journal of Materials Processing Technology*, 88(1), 114-121.
- Luo, X., Cheng, K., Holt, R. and Liu, X. (2005). "Modeling flank wear of carbide tool insert in metal cutting." *Wear*, 259(7), 1235-1240.

Makadia, A. J. and Nanavati, J. I. (2013). "Optimisation of machining parameters for turning operations based on response surface methodology." *Measurement*, 46(4), 1521-1529.

Masugi, M. (2006). "Recurrence plot-based approach to the analysis of IP-network traffic in terms of assessing nonstationary transitions over time." *Circuits and Systems I: Regular Papers*, IEEE Transactions on, 53(10), 2318-2326.

Matassini, L. and Manfredi, C. (2002). "Software corrections of vocal disorders." *Computer Methods and Programs in Biomedicine*, 68(2), 135-145.

Mori, K., Kasashima, N., Yoshioka, T. and Ueno, Y. (1996). "Prediction of spalling on a ball bearing by applying the discrete wavelet transform to vibration signals." *Wear*, 195(1), 162-168.

Morsy, M. and Achtenová, G. (2014). "Vehicle gearbox fault diagnosis based on cepstrum analysis." *World Academy of Science, Engineering and Technology, International Journal of Mechanical, Aerospace, Industrial, Mechatronic and Manufacturing Engineering*, 8(9), 1568-1574.

Muralidharan, V. and Sugumaran, V. (2012). "A comparative study of Naïve Bayes classifier and Bayes net classifier for fault diagnosis of monoblock centrifugal pump using wavelet analysis." *Applied Soft Computing*, 12(8), 2023-2029.

Murata, M., Kurokawa, S., Ohnishi, O., Uneda, M. and Doi, T. (2012). "Real-time evaluation of tool flank wear by in-process contact resistance measurement in face milling." *Journal of Advanced Mechanical Design, Systems, and Manufacturing*, 6(6), 958-970.

Nayfeh, T. H., Eyada, O. K. and Duke, J. C. (1995). "An integrated ultrasonic sensor for monitoring gradual wear on-line during turning operations." *International Journal of Machine Tools and Manufacture*, 35(10), 1385-1395.

Nichols, J. M., Trickey, S. T. and Seaver, M. (2006). "Damage detection using multivariate recurrence quantification analysis." *Mechanical Systems and Signal Processing*, 20(2), 421-437.

Ning, L., Veldhuis, S. C. and Yamamoto, K. (2008). "Investigation of wear behavior and chip formation for cutting tools with nano-multilayered TiAlCrN/NbN PVD coating." *International Journal of Machine Tools and Manufacture*, 48(6), 656-665.

Ning, Y., Rahman, M. and Wong, Y. S. (2001). "Investigation of chip formation in high speed end milling." *Journal of Materials Processing Technology*, 113(1), 360-367.

Niu, Y. M., Wong, Y. S. and Hong, G. S. (1998). "An intelligent sensor system approach for reliable tool flank wear recognition." *The International Journal of Advanced Manufacturing Technology*, 14(2), 77-84.

Norouzi, H. R., Tahmasebpoor, M., Zarghami, R. and Mostoufi, N. (2015). "Multi-scale analysis of flow structures in fluidized beds with immersed tubes." *Particuology*, 21, 99-106.

Nouri, M., Fussell, B. K., Ziniti, B. L. and Linder, E. (2015). "Real-time tool wear monitoring in milling using a cutting condition independent method." *International Journal of Machine Tools and Manufacture*, 89, 1-13.

Oppenheim, A. V. and Schafer, R. W. (2004). "From frequency to quefrequency: A history of the cepstrum." *Signal Processing Magazine, IEEE*, 21(5), 95-106.

Ozel, T. and Karpat, Y. (2005). "Predictive modeling of surface roughness and tool wear in hard turning using regression and neural networks." *International Journal of Machine Tools and Manufacture*, 45(4), 467-479.

Ozel, T., Karpat, Y., Figueira, L. and Davim, J. P. (2007). "Modelling of surface finish and tool flank wear in turning of AISI D2 steel with ceramic wiper inserts." *Journal of Materials Processing Technology*, 189(1), 192-198.

Pal, S., Heyns, P. S., Freyer, B. H., Theron, N. J. and Pal, S. K. (2011). "Tool wear monitoring and selection of optimum cutting conditions with progressive tool wear effect and input uncertainties." *Journal of Intelligent Manufacturing*, 22(4), 491-504.

Park, C. S., Choi, Y. C. and Kim, Y. H. (2013). "Early fault detection in automotive ball bearings using the minimum variance cepstrum." *Mechanical Systems and Signal Processing*, 38(2), 534-548.

Patra, K., Pal, S. K. and Bhattacharyya, K. (2010). "Fuzzy radial basis function (FRBF) network based tool condition monitoring system using vibration signals." *Machining Science and Technology*, 14(2), 280-300.

Peng, Y. (2006). "Empirical model decomposition based time-frequency analysis for the effective detection of tool breakage." *Journal of Manufacturing Science and Engineering*, 128(1), 154-166.

Peter, W. T., Yang, W. X. and Tam, H. Y. (2004). "Machine fault diagnosis through an effective exact wavelet analysis." *Journal of Sound and Vibration*, 277(4), 1005-1024.

Pfeifer, T. and Thrum, H. (1996). "Open systems link sensors and measurement applications to machine tool control units." *Measurement*, 19(2), 113-121.

Posenato, D., Lanata, F., Inaudi, D. and Smith, I. F. (2008). "Model-free data interpretation for continuous monitoring of complex structures." *Advanced Engineering Informatics*, 22(1), 135-144.

Prakash, M. and Kanthababu, M. (2013). "In-process tool condition monitoring using acoustic emission sensor in microendmilling." *Machining Science and Technology*, 17(2), 209-227.

Rafal, R., Pawel, L., Krzysztof, K., Bogdan, K. and Jerzy, W. (2015). "Chatter identification methods on the basis of time series measured during titanium superalloy milling." *International Journal of Mechanical Sciences*, 99, 196-207.

Ramesh, K. and Siong, L. B. (2011). "Extraction of flank wear growth models that correlates cutting edge integrity of ball nose end mills while machining titanium." *The International Journal of Advanced Manufacturing Technology*, 52(5-8), 443-450.

Randall, R. B. (1982). "Cepstrum analysis and gearbox fault-diagnosis." *Maintenance Management International*, 3(3), 183-208.

Randall, R. B., Peeters, B., Antoni, J., and Manzato, S. (2012). "New cepstral methods of signal pre-processing for operational modal analysis." *In Proceedings of ISMA*, 755-764.

Rao, K. V., Murthy, B. S. N. and Rao, N. M. (2013). "Cutting tool condition monitoring by analyzing surface roughness, work piece vibration and volume of metal removed for AISI 1040 steel in boring." *Measurement*, 46(10), 4075-4084.

Rao, S. B. (1986). "Tool wear monitoring through the dynamics of stable turning." *Journal of Manufacturing Science and Engineering*, 108(3), 183-190.

Ravikumar, S., Ramachandran, K. I. and Sugumaran, V. (2011). "Machine learning approach for automated visual inspection of machine components." *Expert Systems with Applications*, 38(4), 3260-3266.

Ravindra, H. V., Srinivasa, Y. G. and Krishnamurthy, R. (1993). "Modelling of tool wear based on cutting forces in turning." *Wear*, 169(1), 25-32.

Rehorn, A. G., Jiang, J. and Orban, P. E. (2005). "State-of-the-art methods and results in tool condition monitoring: a review." *The International Journal of Advanced Manufacturing Technology*, 26(7-8), 693-710.

Ren, Q., Balazinski, M., Baron, L., Jemielniak, K., Botez, R. and Achiche, S. (2014). "Type-2 fuzzy tool condition monitoring system based on acoustic emission in micromilling." *Information Sciences*, 255, 121-134.

Risbood, K. A., Dixit, U. S. and Sahasrabudhe, A. D. (2003). "Prediction of surface roughness and dimensional deviation by measuring cutting forces and

vibrations in turning process.” *Journal of Materials Processing Technology*, 132(1), 203-214.

Saglam, H. and Unuvar, A. (2003). “Tool condition monitoring in milling based on cutting forces by a neural network.” *International Journal of Production Research*, 41(7), 1519-1532.

Saimurugan, M., Ramachandran, K. I., Sugumaran, V. and Sakthivel, N. R. (2011). “Multi component fault diagnosis of rotational mechanical system based on decision tree and support vector machine.” *Expert Systems with Applications*, 38(4), 3819-3826.

Saini, S., Ahuja, I. S. and Sharma, V. S. (2012). “Influence of cutting parameters on tool wear and surface roughness in hard turning of AISI H11 tool steel using ceramic tools.” *International Journal of Precision Engineering and Manufacturing*, 13(8), 1295-1302.

Sakthivel, N. R., Sugumaran, V. and Babudevasenapati, S. (2010). “Vibration based fault diagnosis of monoblock centrifugal pump using decision tree.” *Expert Systems with Applications*, 37(6), 4040-4049.

Sakthivel, N.R., Indira, V., Nair, B.B. and Sugumaran, V. (2011). “Use of histogram features for decision tree-based fault diagnosis of monoblock centrifugal pump.” *International Journal of Granular Computing, Rough Sets and Intelligent Systems*, 2 (1), 23–36.

Samanta, B. and Al-Balushi, K. R. (2003). “Artificial neural network based fault diagnostics of rolling element bearings using time-domain features.” *Mechanical Systems and Signal Processing*, 17(2), 317-328.

Saravanan, N., Siddabattuni, V. K. and Ramachandran, K. I. (2008). “A comparative study on classification of features by SVM and PSVM extracted using Morlet wavelet for fault diagnosis of spur bevel gear box.” *Expert Systems with Applications*, 35(3), 1351-1366.

Scandiffio, I., Diniz, A. E. and De Souza, A. F. (2015). "Evaluating surface roughness, tool life, and machining force when milling free-form shapes on hardened AISI D6 steel." *The International Journal of Advanced Manufacturing Technology*, 1-12.

Scheffer, C. and Heyns, P. S. (2001). "Wear monitoring in turning operations using vibration and strain measurements." *Mechanical Systems and Signal Processing*, 15(6), 1185-1202.

Scheffer, C., Engelbrecht, H. and Heyns, P. S. (2005). "A comparative evaluation of neural networks and hidden Markov models for monitoring turning tool wear." *Neural Computing and Applications*, 14(4), 325-336.

Segreto, T., Simeone, A. and Teti, R. (2014). "Principal component analysis for feature extraction and NN pattern recognition in sensor monitoring of chip form during turning." *CIRP Journal of Manufacturing Science and Technology*, 7(3), 202-209.

Segreto, T., Teti, R., Neugebauer, R. and Schmidt, G. (2009). "Shape Memory Alloy Machining Evaluation through Cutting Force Sensor Monitoring." 5th I* PROMS NoE Virtual Int. In *Conf. on Innovative Production Machines and Systems-IPROMS*, 6-17.

Sen, A. K., Longwic, R., Litak, G. and Górski, K. (2008). "Analysis of cycle-to-cycle pressure oscillations in a diesel engine." *Mechanical Systems and Signal Processing*, 22(2), 362-373.

Sevilla-Camacho, P. Y., Robles-Ocampo, J. B., Jauregui-Correa, J. C. and Jimenez-Villalobos, D. (2015). "FPGA-based reconfigurable system for tool condition monitoring in high-speed machining process." *Measurement*, 64, 81-88.

Sharma, R. K., Sugumaran, V., Kumar, H. and Amarnath, M. (2015). "A comparative study of Naïve Bayes classifier and Bayes net classifier for fault diagnosis of roller bearing using sound signal." *International Journal of Decision Support Systems*, 1(1), 115-129.

Sikdar, S. K. and Chen, M. (2002). "Relationship between tool flank wear area and component forces in single point turning." *Journal of Materials Processing Technology*, 128(1), 210-215.

Silva, R. G., Reuben, R. L., Baker, K. J. and Wilcox, S. J. (1998). "Tool wear monitoring of turning operations by neural network and expert system classification of a feature set generated from multiple sensors." *Mechanical Systems and Signal Processing*, 12(2), 319-332.

Souza, J. V. C., Nono, M. C. A., Ribeiro, M. V., Machado, J. P. B. and Silva, O. M. M. (2009). "Cutting forces in turning of gray cast iron using silicon nitride based cutting tool." *Materials and Design*, 30(7), 2715-2720.

Stoney, R., O'Donnell, G. E. and Geraghty, D. (2013). "Dynamic wireless passive strain measurement in CNC turning using surface acoustic wave sensors." *The International Journal of Advanced Manufacturing Technology*, 69(5-8), 1421-1430.

Sugumaran, V. and Ramachandran, K. I. (2007). "Automatic rule learning using decision tree for fuzzy classifier in fault diagnosis of roller bearing." *Mechanical Systems and Signal Processing*, 21(5), 2237-2247.

Sugumaran, V. and Ramachandran, K. I. (2011). "Fault diagnosis of roller bearing using fuzzy classifier and histogram features with focus on automatic rule learning." *Expert Systems with Applications*, 38 (5), 4901-4907.

Sugumaran, V., Muralidharan, V. and Ramachandran, K. I. (2007). "Feature selection using decision tree and classification through proximal support vector machine for fault diagnostics of roller bearing." *Mechanical Systems and Signal Processing*, 21(2), 930-942.

Sujatha, C. (2010). "*Vibration and Acoustics*." Tata McGraw-Hill Education.

Sullivan, D. and Cotterell, M. (2001). "Temperature measurement in single point turning." *Journal of Materials Processing Technology*, 118(1), 301-308.

Sun, J., Hong, G. S., Wong, Y. S., Rahman, M. and Wang, Z. G. (2006). "Effective training data selection in tool condition monitoring system." *International Journal of Machine Tools and Manufacture*, 46(2), 218-224.

Sun, W., Chen, J. and Li, J. (2007). "Decision tree and PCA-based fault diagnosis of rotating machinery." *Mechanical Systems and Signal Processing*, 21(3), 1300-1317.

Tahmasebpour, M., Zarghami, R., Sotudeh-Gharebagh, R. and Mostoufi, N. (2015). "Characterization of fluidized beds hydrodynamics by recurrence quantification analysis and wavelet transform." *International Journal of Multiphase Flow*, 69, 31-41.

Teti, R., Jemielniak, K., O'Donnell, G. and Dornfeld, D. (2010). "Advanced monitoring of machining operations." *CIRP Annals-Manufacturing Technology*, 59(2), 717-739.

Thomas, M., Beauchamp, Y., Youssef, A. Y. and Masounave, J. (1996). "Effect of tool vibrations on surface roughness during lathe dry turning process." *Computers and Industrial Engineering*, 31(3), 637-644.

Trent E. M. (1988). "Metal cutting and the tribology of seizure: I seizure in metal cutting." *Wear*, 128(1), 29-45.

Uehara, K., Sakurai, M. and Takeshita, H. (1983). "Cutting performance of coated carbides in electric hot machining of low machinability metals." *CIRP Annals-Manufacturing Technology*, 32(1), 97-100.

Vagnorius, Z., Rausand, M. and Sørby, K. (2010). "Determining optimal replacement time for metal cutting tools." *European Journal of Operational Research*, 206(2), 407-416.

Vernekar, K., Kumar, H. and Gangadharan, K. V. (2014). "Gear fault detection using vibration analysis and continuous wavelet transform." *Procedia Materials Science*, 5, 1846-1852.

Viharos, Z. J., Markos, S. and Szekeres, C. (2003). "ANN-based chip-form classification in turning." In *Proceedings of the XVII. IMEKO World Congress—Metrology in the 3rd Millennium*, 1469-1473.

Villumsen, M. F. and Fauerholdt, T. G. (2008). "prediction of cutting forces in metal cutting, using the finite element method, a Lagrangian approach." In *Proceedings of the 7th German LS-DYNA Forum*, 8(3), 1-16.

Wang, C., Xie, Y., Zheng, L., Qin, Z., Tang, D. and Song, Y. (2014). "Research on the chip formation mechanism during the high-speed milling of hardened steel." *International Journal of Machine Tools and Manufacture*, 79, 31-48.

Wang, H., Li, R., Tang, G., Yuan, H., Zhao, Q. and Cao, X. (2014). "A compound fault diagnosis for rolling bearings method based on blind source separation and ensemble empirical mode decomposition." *Plos One*, 9(10), 109-166.

Wang, W. H., Hong, G. S., Wong, Y. S. and Zhu, K. P. (2007). "Sensor fusion for online tool condition monitoring in milling." *International Journal of Production Research*, 45(21), 5095-5116.

Wang, Y., Yan, X., Li, B. and Tu, G. (2012). "The study on the chip formation and wear behavior for drilling forged steel S48CS1V with TiAlN-coated gun drill." *International Journal of Refractory Metals and Hard Materials*, 30(1), 200-207.

Wanigarathne, P. C., Kardekar, A. D., Dillon, O. W., Poulachon, G. and Jawahir, I. S. (2005). "Progressive tool-wear in machining with coated grooved tools and its correlation with cutting temperature." *Wear*, 259(7), 1215-1224.

Webber Jr, C. L. and Zbilut, J. P. (2005). "Recurrence quantification analysis of nonlinear dynamical systems." *Tutorials in Contemporary Nonlinear Methods for the Behavioral Sciences*, 26-94.

Widodo, A. and Yang, B. S. (2007). "Support vector machine in machine condition monitoring and fault diagnosis." *Mechanical Systems and Signal Processing*, 21(6), 2560-2574.

Wilkinson, P., Reuben, R. L., Jones, J. D. C., Barton, J. S., Hand, D. P., Carolan, T. A. and Kidd, S. R. (1997). "Surface finish parameters as diagnostics of tool wear in face milling." *Wear*, 205(1), 47-54.

Wong, Y. S., Nee, A. Y. C., Li, X. Q. and Reisdorf, C. (1997). "Tool condition monitoring using laser scatter pattern." *Journal of Materials Processing Technology*, 63(1), 205-210.

Xie, J., Luo, M. J., Wu, K. K., Yang, L. F. and Li, D. H. (2013). "Experimental study on cutting temperature and cutting force in dry turning of titanium alloy using a non-coated micro-grooved tool." *International Journal of Machine Tools and Manufacture*, 73, 25-36.

Xu, J., Yamada, K., Seikiya, K., Tanaka, R. and Yamane, Y. (2014). "Comparison of applying static and dynamic features for drill wear prediction." *Journal of Advanced Mechanical Design, Systems, and Manufacturing*, 8(4), 56-63.

Yaldız, S. and Unsaçar, F. (2006). "Design, development and testing of a turning dynamometer for cutting force measurement." *Materials and Design*, 27(10), 839-846.

Yang, W., Court, R., Tavner, P. J. and Crabtree, C. J. (2011). "Bivariate empirical mode decomposition and its contribution to wind turbine condition monitoring." *Journal of Sound and Vibration*, 330(15), 3766-3782.

Yang, Z., Merrild, U. C., Runge, M. T., Pedersen, G. K. and Borsting, H. (2009). "A study of rolling-element bearing fault diagnosis using motor's vibration and current signatures." In *The 7th IFAC International Symposium on Fault Detection, Supervision and Safety of Technical Processes*, 354-359.

Yen, Y. C., Söhner, J., Weule, H., Schmidt, J. and Altan, T. (2002). "Estimation of tool wear of carbide tool in orthogonal cutting using FEM simulation." *Machining Science and Technology*, 6(3), 467-486.

Yeo, S. H., Khoo, L. P. and Neo, S. S. (2000). "Tool condition monitoring using reflectance of chip surface and neural network." *Journal of Intelligent Manufacturing*, 11(6), 507-514.

Yu, Y. and Junsheng, C. (2006). "A roller bearing fault diagnosis method based on EMD energy entropy and ANN." *Journal of Sound and Vibration*, 294(1), 269-277.

Zbilut, J. P. and Webber, C. L. (1992). "Embeddings and delays as derived from quantification of recurrence plots." *Physics Letters A*, 171(3), 199-203.

Zhang, G., To, S. and Xiao, G. (2014). "Novel tool wear monitoring method in ultra-precision raster milling using cutting chips." *Precision Engineering*, 38(3), 555-560.

Zhou, J. M., Andersson, M. and Stahl, J. E. (2003). "The monitoring of flank wear on the CBN tool in the hard turning process." *The International Journal of Advanced Manufacturing Technology*, 22(9-10), 697-702.

List of Publications based on Ph.D Research Work

Sl. No.	Title of the Paper	Authors (In the same order as in the paper, underline the Research Scholar's name)	Name of the Journal / Conference / Symposium, Vol., No., Pages	Month & Year of Publication	Category *
1	Fault Diagnosis of Single Point Cutting Tool through Discrete Wavelet Features of Vibration Signals using Decision Tree Technique and Multilayer Perceptron	<u>N. Gangadhar</u> , Kiran Vernekar, Hemantha Kumar and S. Narendranath	Journal of Vibration Engineering and Technologies, Vol. 5, No. 2.	April, 2017	1
2	Recurrence Quantification Analysis to Classify the Tool Condition of Tungsten Carbide while Machining Die Steel	<u>N. Gangadhar</u> , Madhusudana C. K, Hemantha Kumar and S. Narendranath.	International Journal of Condition Monitoring, Vol. 6, No. 1, pp. 02-08	March, 2016	1
3	Condition Monitoring of Single Point Cutting Tool through Vibration Signals using Decision Tree Algorithm	<u>Gangadhar N.</u> , Kumar, H., and Narendranath, S	Journal of Vibration Analysis, Measurement, and Control, Vol.3, No.1, pp. 34-43.	June, 2015	1
4	Fault Diagnosis of Single Point Cutting Tool through Vibration Signal Using Decision Tree Algorithm	<u>Gangadhar N.</u> , Kumar, H., Narendranath, S., and Sugumaran, V	Procedia Materials Science, Vol. 5, pp. 1434-1441.	September, 2014	1
5	Effect of cutting speed and feed rate on temperature and cutting force in machining of Hardened steel AISI H13 using computational approach	<u>N. Gangadhar</u> , Hemantha Kumar, S. Narendranath	CALM-2014, SRM University, CHENNAI	December, 2014	3

* Category: 1 : Journal paper, full paper reviewed
 2 : Journal paper, Abstract reviewed
 3 : Conference/Symposium paper, full paper reviewed
 4 : Conference/Symposium paper, abstract reviewed
 5 : others (including papers in Workshops, NITK Research Bulletins, Short notes etc.)
 (If the paper has been accepted for publication but yet to be published, the supporting documents must be attached.)

List of communicated papers

N. Gangadhar, Hemantha Kumar, and S. Narendranath, “Machine Learning Approach for Condition Monitoring of Single Point Cutting Tool based on Histogram Features.” *International Journal of Acoustics and Vibration*

Status: Under review

N. Gangadhar, Hemantha Kumar and S. Narendranath, “Use of Empirical Mode Decomposition Method, Principal Component Analysis and K-Star Algorithm for Fault Diagnosis of Single Point Cutting Tool through Machine Learning Approach.” *International Journal of Systems Assurance Engineering and Management*

Status: Under review

BIO-DATA

1. **Name** : Gangadhar N.
2. **Father's Name** : Nanjundaiah
3. **Date of Birth** : 10/04/1986
4. **Nationality** : Indian
5. **Marital Status** :Married
6. **Address** :

Permanent Address

S/o. Nanjundaiah
Hondarabalu,
Madhuvanahalli Post,
Kollegal Taluk, Chamarajanagar
Pin-571440, Karnataka, India

Present Address

Assistant Professor,
Department of Mechanical Engineering
Ambedkar Institute of Technology, Near Jnana
Bharathi Campus, Mallathalli, Bangalore
Pin-560056 Karnataka, India

7. **Mobile Number** : +91-9900783626
8. **E-mail id.** :ngangadhar4@gmail.com
9. **Educational Qualification** :

Qualification	College/school	University/Board	Year of Passing	Performance
Ph.D. in Mechanical Engineering	National Institute of Technology Karnataka	National Institute of Technology Karnataka	Pursuing	-----
M.Tech in Manufacturing Technology	National Institute of Technology Calicut	National Institute of Technology Calicut	2010	7.1 (CGPA)
B.E in Mechanical Engineering	Dr. Ambedkar Institute of Technology Bangalore	Visvesvaraya Technological University	2008	62.42%

10. **Work Experience** :

Name of the Organization	Duration	Position
Dr. Ambedkar Institute of Technology Bangalore	Aug 2010 to Dec 2012	Assistant Professor

I declare that above information is true and correct to best of my knowledge and belief.

(Gangadhar N.)